A methodology to quantify the groundwater impacts of mega-tailings dams for the gold mining industry, South Africa

AAJ Naudé

21633878

Dissertation submitted in fulfilment of the requirements for the degree Magister Scientiae in Environmental Sciences (specializing in Hydrology and Geohydrology) at the Potchefstroom Campus of the North-West University

Supervisor: Prof I Dennis

September 2016

Declaration

I Abraham Albertus Jacobus Naudé, hereby declare that this dissertation submitted by me for the completion of the Master of Science Degree at the North West University, Potchefstroom, is my own independent work and has not been submitted by me at another university. I further more cede copyright of the dissertation to the North West University.

Abraham Albertus Jacobus Naudé

(Student number: 21633878)

Summary

The recovery of base and precious metals (gold, silver, copper, platinum etc.) often entails the removal of a large quantity of rock strata by means of deep shaft and opencast mining practices. The crushing and milling of ore results in a waste product that ranges from sand to clay sized particles, referred to as tailings. Tailings are deposited as slurry and stored in purpose built impoundments known as Tailings Storage Facilities (TSFs), where it will remain for the duration of the mine and well after mining has ceased. One of the most significant impact of gold mine tailings is the seepage of contaminated water from these impoundments into the surrounding groundwater and surface water bodies.

As a result of diminishing ore reserves and increasing pressure on mining houses to rehabilitate old mining sites, the focus has shifted to the reclamation of dormant TSFs. This development has given rise to new deposition strategies, with increased stability, resulting in larger TSFs. These “new” TSFs have also given designers the opportunity to correct previous design errors that have resulted in serious environmental impacts in the past.

The aims of this dissertation will attempt to combine the findings from previous studies that focused on the impacts of decommissioned TSFs so as to develop a workable methodology for contamination prediction, utilising an effective water balance as a basis and ultimately evaluating the extent of groundwater contamination by means of numerical models.

The established methodology is tested in order to evaluate the effectiveness thereof. The case study was also used to determine the extent of groundwater contamination through seepage from the mega tailings facility. Focus was placed on the geotechnical properties of specifically gold tailings material in order to establish the hydrological character of water movement through the TSF. The chemical properties of gold tailings were also investigated by means of a literature study to establish major contaminants associated with the ore. Natural aquifer parameters where obtained during field investigations.

The seep/W modelling package was used to determine seepages from the base of the mega tailings using an operational and post operational water balance applied as a flux on top of the TSF. Seepage fluxes from seep/W were applied to a numerical groundwater model PMWIN so as to evaluate the extent of contaminant migration from the base of the TSF through the natural aquifer system.

During the operational phase of the TSF, increased seepage fluxes result in an elevated phreatic surface which causes a localised groundwater mound situation. Once deposition ceases, there is a rapid decrease in the phreatic surface and subsequent decrease in seepage

fluxes as natural rainfall becomes the only source of water to the TSF. The increased contaminant loads from the gold TSFs raise the overall contaminant loads found in the natural groundwater system surrounding these facilities. Predictive modelling revealed that there is a large contaminant plume moving in a downstream direction eventually contributing to a major South African river.

Key words

Gold, Groundwater, Contamination, Numerical Modelling, Pollution Plume, Mega Tailings Facility

Acknowledgements

I would like to take this opportunity to thank the Lord for giving me the ability and opportunity to complete this dissertation, all merit is due to Divine guidance.

To Prof. Ingrid Dennis, thank you, for the useful comments and guidance throughout the project as well as the farmer Mr Nikolaas Maree for conducting the field studies on his farm.

And a special thank you to my parents Braam and Leslie Naude for all their love and support, without which this dissertation would have not been completed.

Lastly I would like to thank the plant manager Mr Johnny Botha for the understanding and time given off from work to attend to my project.

Table of Contents

List of Figures

LIST OF ABBREVIATIONS

ΔS	Water stored within a TSF
$\Delta S_{overflow}$	Infiltration Rate of overflow material per day
$\Delta S_{underflow}$	Infiltration Rate of under flow material per day
$2NaAu(CN)_2$	Sodium Aurocyanide
2NaOH	Sodium Hydroxide
2D	Two dimensional
3D	Three dimensional
A	Area of the Control Plane
AMD	Acid Mine Drainage
$A_{overflow}$	Total Area covered by overflow material
As	Arsenic
$A_{undeflow}$	Total Area covered by underflow material
b’	Aquitard thickness
C	Contaminant Concentration
Ca	Calcuim
$Ca(CN)_2$	Calcium Cyanide
Cd	Cadmium
C_F	Flux Averaged Contaminant Concentration
CIP	Carbon In Pulp
Cl	Chloride
CN	Cyanide
Co	Cobalt
CoAsS	Cobaltite
Cu	Copper
d	Length of the borehole screen
D	Saturated Thickness
DEM	Digital Elevation Model
dh	Change in Water Level

dt	Change in time
EC	Electrical Conductivity
ERGO	East Rand Gold and Uranium
Fe^{2+}	Ferrous Iron
FeAsS	Arsenopyrite
g	Gram
GIS	Geographical Information System
GPS	Global Positioning System
h_0	Head at t = 0
H_2SO_4	Sulphuric Acid
HCl	Hydrochloric Acid
HCO_3	Bicarbonate
h_t	Head at $t > t_0$
i	Mass flux
i	Hydraulic Gradient
ICP-MS	Inductively Coupled Plasma Mass Spectrometry
J	Mass Flux
J	Spatially variable contaminant flux
J_c	Time Averaged Contaminant Mass Flux
K	Hydraulic Conductivity
KOSH	Klerksdorp – Orkney – Stilfontein – Hartbeesfontein
K_{sat}	Saturated Hydraulic Conductivity
m/d	Metres per Day
$M/t/m^2$	Mass per Time per specific Area
m^3/d	Cubic Metre per Day
m^3/y	Cubic Metre per Year
mamsl	Metres Above Mean Sea Level
mamsl	Metres Above Mean Sea Level
MAP	Mean Annual Precipitation
mbgl	Metres Below Ground Level

mbgl	Metres Below Ground Level
M_d	Mass Discharge
M_d	Mass Discharge
M_{dA}	Mass Discharge at Transect A
mg/l	Milligrams per Litre
mm/y	Millimetre per Year
Mn	Manganese
MODFLOW	Modular Three – Dimensional Finite – Difference Groundwater Flow Model
MT3DMS	Modular Three Dimensional Multispecies Transport Model Simulator
MT3DMS	Modular Three Dimensional Multispecies Transport Model for Simulation
n	Porosity
Na	Sodium
$Na_2Zn(CN)_4$	Sodium Zincate
NaCN	Sodium Cyanide
NGA	National Groundwater Archive
Ni	Nickel
NWU	North West University
O/F	Overflow
P	Precipitation as a flux per day
Pb	Lead
PbS	Galena
PM5	Processing Modflow
PMWIN	Processing Modflow for Windows
ppq	Parts Per Quadrillion
PSD	Particle Size Distribution
Q	Volumetric Flow Rate
q_0	Groundwater Flux
q_0	Specific Discharge
r	Radial distance to the pumping borehole
r^2	Correlation Coefficient

r_c	Radius of the Unscreened Borehole Section
R_e	Radial Distance
r_w	Distance from Borehole to Static Water Level
RWD	Return Water Dam
S	Storativity
S_{beach}	Water stored in beach section of a TSF
SEEP/W	Finite Element Groundwater Seepage analyses software
SO_4^{2-}	Sulphate
S_{pool}	Water stored in pool section of a TSF
Sq.km	Square Kilometre
SRTM	Shuttle Radar Topography Mission
$S_{saturated\ zone}$	Water stored in saturated section of a TSF
$S_{side\ slope}$	Water stored in side slope section of a TSF
SWCC	Soil Water Characteristic Curve
T	Transmissivity
t	Time
t/m^3	Tons per cubic metre
TDS	Total Dissolved Solids
TLC	Temperature, Level, Conductivity
tpm	Tons Per Month
TSF	Tailings Storage Facility
U	Uranium
U/F	Underflow
UO_2	Uranium Dioxide
$UO_3Ti_2O_4$	Brannerite
USCS	United Soil Classification System
USGS	United States Geological Survey
Vdi	Diabase
Vhd	Residual Weathered Andesite
Vm	Dolomite
VWC	Volumetric Water Content

W(u)	Well function
WRC	Water Research Commission

Chapter 1: Introduction

1.1 Preamble

The mining and processing of ore for the recovery of metals has been one of the biggest contributor to environmental related issues in recent times, especially untreated and discarded tailings impoundments leaching contaminants into fresh-water bodies in close proximity of the facilities (Winde et al., 2004).

The recovery and extraction of metals entails a large quantity of rock strata being removed during deep shaft mining or opencast operations. The ore is moved, crushed and pulverised to fine particles in order to remove the precious metals found within the rock structure. This process produces waste material ranging in particle size, from coarse mine waste to fine clays containing chemical precipitates added during the extraction process (Ritcey, 2005).

Tailings management at a mining operation includes numerous components such as: crushing of ore in the milling process, followed by addition and treatment of the metal-rich slurry with chemicals and flocculants to ease the extraction process and provide total removal of the metallurgic species e.g. gold, copper, silver etc. Once the plant process is completed the slurry is transported to the tailings impoundment where it is left for re-mining or rehabilitation by the mining company responsible for the impoundment (Ritcey, 1988).

One of the most significant impacts of gold tailings is the seepage of contaminated water from these dumps into the surrounding groundwater and surface water bodies within the mining area.

Seepage from most Tailings Storage Facilities (TSFs) in the South African gold mining industry is associated with the formation of acidic groundwater conditions as a result of the oxidation of pyrite that would lead to the acidification of natural occurring groundwater (Winde et al., 2004).

Often water discharged from the mining industry contains high levels of dissolved salts. In addition to the elevated salt loads it is found that water from the gold and coal mining industry can also have high levels of ferrous iron (Fe^{2+}) and sulphates. Surface water bodies affected by the contamination are characteristically coated with a reddish brown gel as a result of the oxidation and precipitation of Fe^{2+} to ferric iron (Fe^{3+}). Heavy metals in combination with high salt loads can often toxic to aquatic life (GDACE, 2008).

A study by Winde et al. (2004) on the threats of post mining closure have found that elevated uranium (U) levels in the alluvial groundwater is as a direct result of the dissolution and transportation of uranium within the gold tailings.

The acidic nature of Acid Mine Drainage (AMD) has the ability to dissolve most heavy metals discarded as waste. The seepage from tailings impoundments enters the natural groundwater system, inevitably contributing to streams and rivers as baseflow, spreading the contamination downstream, ultimately increasing the Total Dissolved Solid (TDS) concentration in the water.

Most commonly noted by Winde et al. (2004) is the formation of salt crusts in areas where evaporation would favour crystallisation. These crusts can contain extremely high concentrations of heavy metals. High evaporation rates and surface impingement of the elevated water table on the sides of the tailings impoundments have also led to the formation of heavy metal laden salts around the perimeter of these TSFs. These crusts are of particular concern as rain water runoff can dissolve these salts resulting in a metal rich surface runoff that can flow along the topography toward nearby streams.

The Water Research Commission (WRC) completed a study in the 1980s and concluded that the main contributor to the elevated TDS values in the Vaal River are the many active and inactive TSFs that are strewn across the greater Johannesburg area. The study also identified that rain water had percolated through the facilities, creating groundwater contamination plumes emerging at surface streams as baseflow, thereby actively contributing to a rivers overall dissolved solid load.

The literature has identified some key characteristics of sites contaminated with AMD and they are (Naicker et al., 2003; Jones et al., 1988; Winde et al., 2004):

- Highly acidified topsoil contaminated with typical heavy metals, most notably cobalt (Co), nickel (Ni), Fe^{2+}, Fe^{3+} , and large quantities of U
- Groundwater with low pH and high redox potential during all seasons. The pH is generally below 6 with extremely high concentrations of sulphate.
- Reddish brown leachate as a result of high concentrations of iron (iii) oxide-hydroxide $Fe(OH)_3$ precipitates (limonite) due to the oxidation of Fe^{2+} to Fe^{3+} when exposed to oxygenated water.
- Salt crusts at the banks of surface water bodies. These salt crusts have many varying colours depending on the dominant metal contained within the salt e.g. green salts are most commonly copper rich and brown salts are uranium rich.

1.2 Motivation for Project

There are many studies in the literature that deal with contamination from decommissioned and dormant TSFs. The understanding of the processes of contaminant migration from these TSFs are well established. Some operational TSFs are mainly focused on production, resulting in rudimentary water balances that only account for water that can be recovered and is most often metered volumes. Losses and subsequent impacts are not accounted for in these cases and are unknown for most of the operational life of a TSF (Yibas et al., 2011).

As mineable ore becomes less and environmental pressure increases on the mining houses to rehabilitate old mining sites, the focus has shifted toward reclamation of TSFs. This development has given rise to new deposition strategies, with increased stability, resulting larger TSFs. The reclamation and construction of “new” facilities also give designers and decision makers the opportunity to correct previous design errors.

The outcome of this dissertation will attempt to combine the findings from previous studies that focussed on the impacts of decommissioned TSFs and new TSFs from reclamation projects so as to develop a workable methodology for contaminant prediction. The methodology will attempt to gain a better understanding of operational and post operational water and mass balances in order to predict the potential extent of groundwater contamination; ultimately evaluating the effects of such operations on the natural groundwater system.

1.3 Aims of Dissertation

The objective of this dissertation is to investigate the hydrological characteristics of a gold mega tailings facility constructed from older reclaimed tailings facilities as well as the effects that such a facility will have on the surrounding groundwater; with reference to determining a methodology to investigate the groundwater contamination plume and contaminant migration emanating from the facility, mainly as seepage.

A literature study was conducted to establish the geotechnical characteristics of typical gold tailings material and its chemical composition so as gain insight regarding the hydrological mechanisms responsible for contaminant migration within and to the surrounding environment. Literature will also be consulted to investigate and establish a workable methodology to quantify the impact that a facility of such magnitude will have on the regional groundwater. Once a clear methodology has been established from the literature, it is possible to carry out a basic field analysis, collect site specific data that will be used for conceptualising the study area. Using the conceptual model as a basis, groundwater modelling is conducted to determine the extent of the contamination emanating from the mega tailings facility.

This study aims at establishing a methodology to determine the extent of the groundwater contamination plume emanating from a typical mega tailings facility. The effectiveness of the methodology will be tested using a case study. The study is to be used as a model for understanding:

a) The hydrological characteristics of the tailings facility.
b) Estimation of seepage rates using a depositional and post depositional water balance.
c) The expected extent of seepage from the tailings facility to the surrounding aquifers and the associated quality thereof.
d) Its potential effect on the surface water bodies recharged by groundwater, using a contaminant mass balance approach.
e) Possible mitigation measures as to reduce the impact of the facility on the environment.

1.4 Layout of Document

Chapter 1: Introduction

Chapter 2: Literature Review – Review of current methodologies and studies focused on the contaminant estimation of both active and inactive TSFs. Short comings are also identified in established methodologies.

Chapter 3: Methodology – Formulation of a workable methodology based on the findings and short comings identified during the literature review.

Chapter 5: Mega-tailings investigation – Seepage estimation and contaminant modelling using the methodology established from the literature review.

Chapter 5: Discussion – Results presented and discussed from the mega tailings investigation. Successes of possible mitigation strategies are discussed.

Chapter 6: Conclusions – Overview of the results from the mega tailings investigation.

Chapter 2: Literature Review

2.1 Construction and Design of Gold Mine Tailings

2.1.1 Background

Tailings material is essentially the crushed by product of the original host rock once the metallurgical extraction process has removed the economically valuable portion thereof, in this case gold. The characteristics of a said tailings material is therefore a function of the host rock. The constituents that make up tailings dictate the construction characteristic of the material and environmental liability as a contaminator (Robinson, 2009; Stanley, 1987; Vermeulen, 2001).

Tailings are defined as fine grained slurry resulting from the crushing and pulverizing of raw base-metal ore. During the early part of the 1800s, the mining industry made use of the mercury-gold amalgam extraction process to recover base metals from raw ore. This "primitive" method had a relatively low recovery rate which meant that mines only targeted and removed the highest grade ore. A relatively small amount of waste product behind was left behind, when compared to current mining practices. During this time, it was common practise to discard the waste in nearby streams and rivers. It was only in the 1930s that the dangers of mercury became a serious issue. Coupled with the declining number of rich deposits the industry was forced to look at new methods of extraction. The advances in technology made the Carbon-In-Pulp (CIP) process a viable option utilising cyanide (Sodium cyanide (NaCN)), Calcium cyanide (CaCN) and carbon as the active ingredients, thereby effectively replacing mercury in the metallurgical extraction (Stanley, 1987; Vermeulen, 2001). Cyanidation had a much better recovery rate, creating an opportunity for mines to move toward low grade, high volume mining practices. Not only does sodium cyanide have a better recovery than mercury, it also has a smaller impact on the environment. Although highly toxic during the extraction, once exposed to oxygen and sunlight, sodium/calcium cyanide is broken down into cyanide salts that are stable under natural conditions and non-toxic.

As cyanidation opened the doors to low grade ores being mined, so too did the amount of mining waste produced increase exponentially. Large volumes of ore was run through the process to extract profitable amounts of gold, some ore as low as 2g of gold per ton of ore were treated (Ripley et. al., 1982; Vermeulen, 2001). South African mines were producing in excess of 250 million tons of mine waste annually in 1987, with a typical mining operation generating approximately 100 000 tons of tailings per month (Penman, 1994).

2.1.2 Metallurgical Extraction

The metallurgical extraction process involves the concentration and refinement of a precious metal in a quantity that is profitable to sell as a commodity. The two most significant processes known in the gold mining industry is mercury-gold amalgamation and cyanidation.

a.) **Amalgamation**: Once mechanical pulverisation of ore has taken place, the gold within the pulp is brought into direct contact with mercury, as mercury has the ability to absorb gold, thus establishing the amalgam between mercury and gold. Once the amalgam is achieved, the mixture is washed and pressed through canvas to remove any abundant mercury. The separation of gold and mercury is known as retorting and the retorted gold produced in this step has a typical spongy appearance (Stanley, 1987). Retorted gold is heated to its melting point along with a flux to release the gold from the mercury, producing the end product that is poured from a kiln into bullion bars. This process has large environmental and health hazards as a result of mercury's toxic vapours released during the retorting process (Stanley, 1987; Vermeulen, 2001).

b.) **Cyanidation**: During the more modern cyanidation process, gold is recovered by leaching the pulp with soluble cyanide salts (mainly CaCN and NaCN) as illustrated in the equation below:

$$2Au + 4NaCN + \frac{1}{2}O_2 + H_2O \rightarrow 2NaAu(CN)_2 + 2NaOH$$

The pulp is prevented from sedimentation by continuously agitating the mixture using compressed air. The cyanide extraction method has a gold recovery rate of 98%. It is this outstanding recovery rate and relatively low health hazards that has made cyanidation the standard extraction process in the gold mining industry.

Cyanide leaching produces ionic metal complexes with cyanide and gold. Extracting gold from the newly formed cyanide salt can be conducted by one of two methods (Stanley, 1987):

- Zinc precipitation
- CIP

Zinc precipitation: Soluble lead nitrate is added to the cyanide-gold leachate where zinc precipitates the gold in an emulsifier tank. Zinc has the ability to precipitate gold because of the high electro-ionic bond between the zinc and gold particles. This reaction is explained in the equation:

$$2NaAu(CN)_2 + Zn \rightarrow Na_2Zn(CN)_4 + 2Au$$

CIP: Activated carbon is used to absorb and recover the gold directly from the cyanide leachate. The carbon (usually bigger in grain size) is brought into contact with the leachate by

gravity flow through a series of tanks and screens. Screens ensure that the carbon remains in the tanks as the fluid pulp moves through the screen. The pulp loses gold as it passes through a number of screens and tanks to where it reaches the final tank where the barren pulp is collected. The carbon found in the screen is cleared out and washed with an HCl (hydrochloric acid) solution to remove any remaining debris and pulp. The final step in the process is to liberate the gold from the carbon using caustic soda and recovering the gold by electro winning (Vermeulen, 2001).

2.2 Hydrology of TSFs

The management of water distributed as mine residue is mostly focused in the reclamation of water for use back at the metallurgical plant. The water management is approached from a water balance perspective, however most often these balances are rudimentary and do not account for losses that are intangible and difficult to quantify (Yibas et al., 2011).

These shortfalls in the operational water balance are acceptable as the focus of such a balance is toward dam levels for safety purposes. For contamination prediction and contaminant migration studies these inaccuracies seriously hinder the ability of researchers and decision makers to make accurate predictions with regards to operational and post-closure contamination (Yibas et al., 2010).

2.2.1 Occurrence of water in TSFs

A TSF consists both of saturated and unsaturated conditions with varying porosity throughout its lifetime. As there is a continual deposition of oversaturated tailings slurry in the operational phase, there exists a saturated portion deep within the facility resulting from the continual vertical percolation of supernatant water. The saturated conditions are only evident at its highest elevation located at the centre of the facility where a constant pool of water remains (Winde & Sandham, 2004; Tutu et al., 2008; Yibas et al., 2011). This saturated zone decreases toward the embankment where it will eventually merge with the natural groundwater, contributing to the regional aquifer as seepage (located at the toe area, see Figure 1) (Tutu et al., 2011). The contact between the saturated and unsaturated zones is termed the phreatic surface; this surface is fundamentally the same as its natural counterpart, the water table albeit at an elevated position (Bezuidenthoud & Vermaak, 2010). The position of the saturated zone is dependent on the deposition cycle, Particle Size Distribution (PSD) of the tailings material, slurry density and precipitation. This zone will decrease and dissipate completely under dormant conditions as most of the water from deposition ceases to exist (Yibas et al., 2011).

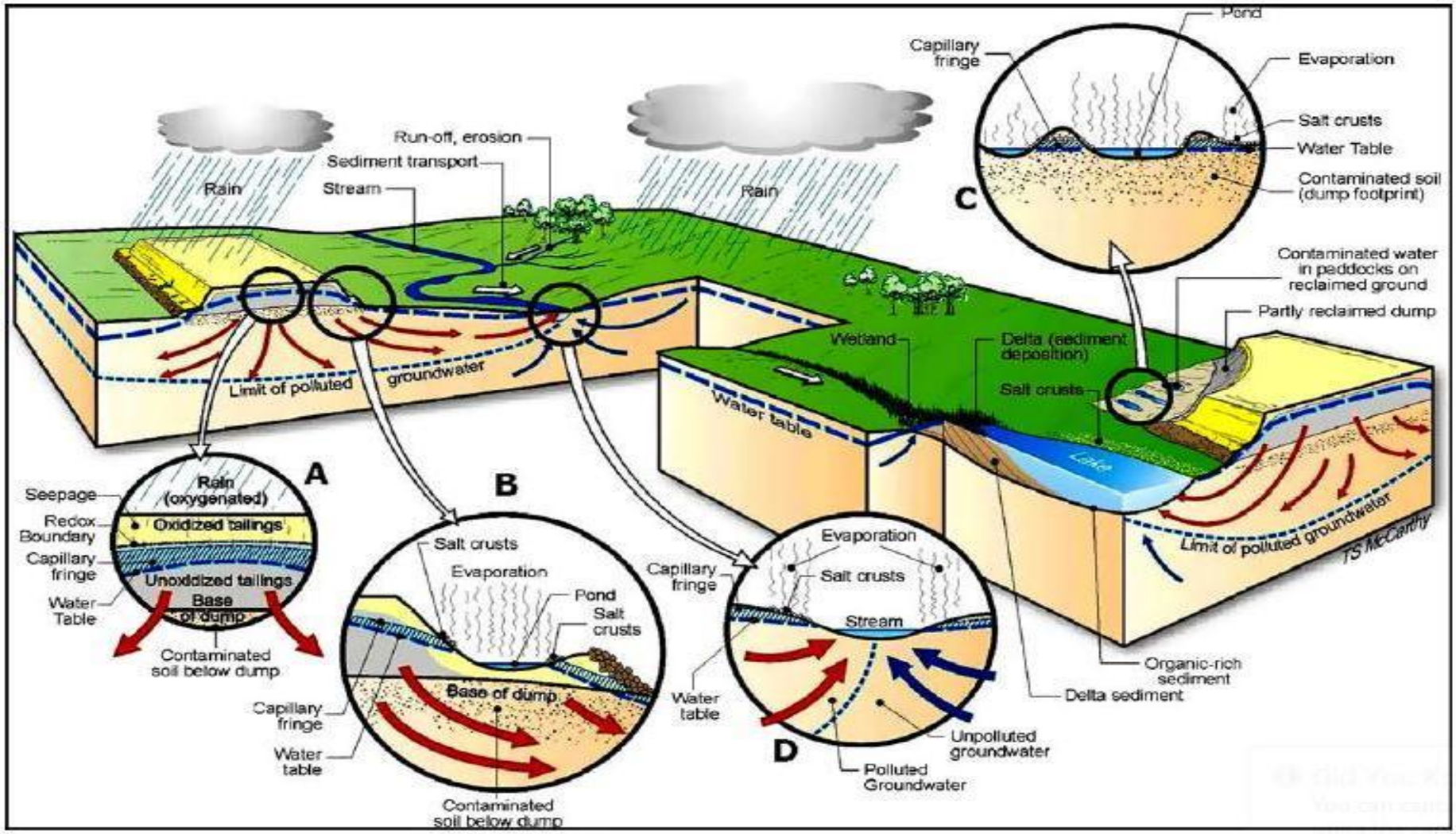

Figure 1: A schematic diagram showing various aspects and dispersal of AMD around gold tailings sites. (A) acid generation within the tailings facility, (B) at the feet of the facility, (C) seepage into paddocks of the impoundment, and (D) baseflow into nearby streams (Tutu et al., 2008)

Surface-groundwater interaction

Contaminants are dissolved and transported through seepage at the base of the TSF where it is in direct contact with the ground surface. However, lined TSFs do not allow water to enter the groundwater. Seepage from the TSF is a contributor to groundwater recharge to local aquifers (Brixel et al., 2012).

Understanding the pathway that contaminants would follow in a groundwater regime requires the understanding the connections between surface water and the aquifer. Identifying the major aquifer types according to their geologic character would explain how groundwater is transferred within the subsurface. Primarily water from TSFs are introduced to the natural aquifer through the embankments and base, therefore the transport of contaminants from the base of the TSF onward is largely dependent on the regional hydrological characteristics that are specific to the aquifers upon which deposition takes place.

Groundwater mound

Rösner (1999) found that the increasing seepage from the continual deposition of supersaturated slurry will cause a wetting front to migrate from the pond at the centre of the TSF toward the saturated zone (see Figure 2) i.e. natural water table. This phenomenon is called a localised groundwater mound due to the elevated state of the saturated zone linking up with the artificial saturation from the TSF above, as displayed in Figure 3 and Figure 4. However Rösner (1999) and Martin & Koerner (1984) describe this process as having four distinctive phases that develops throughout the life of a TSF. These phases are:

Phase 1: The continued saturation from slurry deposition creates a wetting front that advances downward from the base of the TSF toward the saturated zone as shown in Figure 2.

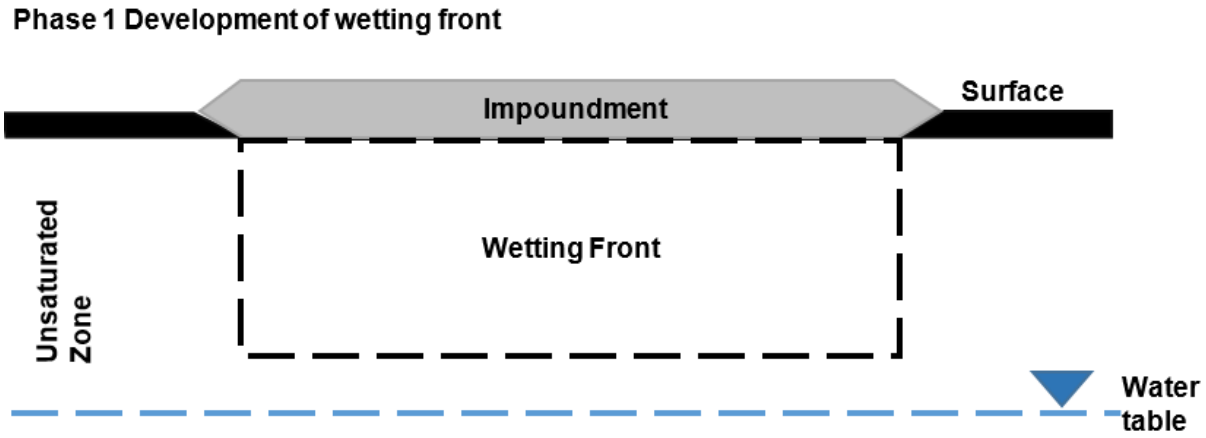

Figure 2: Phase 1 the formation of a wetting front (Martin & Koerner, 1984)

Phase 2: The formation of a positive pressure mound that rises above the topography. Should the wetting front become completely saturated a positive pressure wave moves toward the negative pressure at the saturated zone, resulting in a suction effect (see Figure 3).

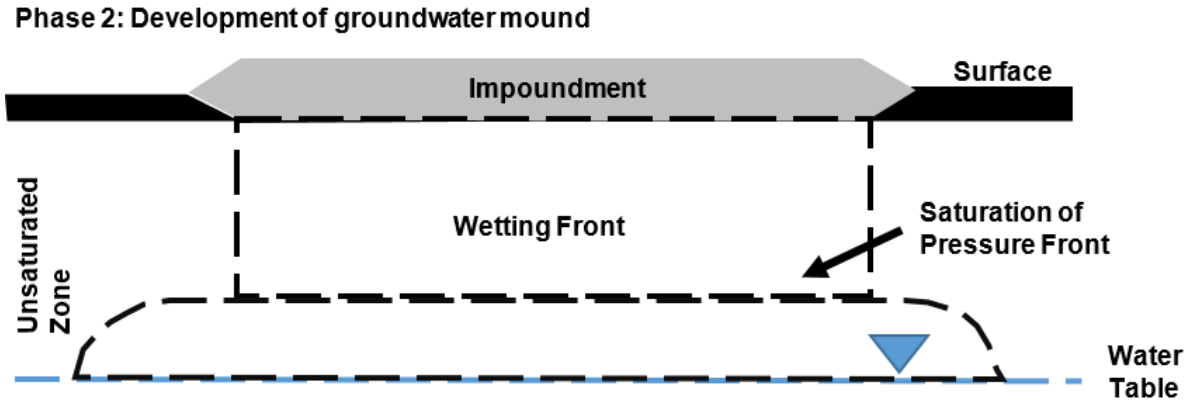

Figure 3: Phase 2 Development of groundwater mound and suction effect (Martin & Koerner, 1984)

Phase 3: This occurs when continual seepage saturates the subsurface to the point of a localised groundwater mound. The natural groundwater is in full contact with the artificial saturation and recharge from the TSF is directly linked to groundwater (see Figure 4).

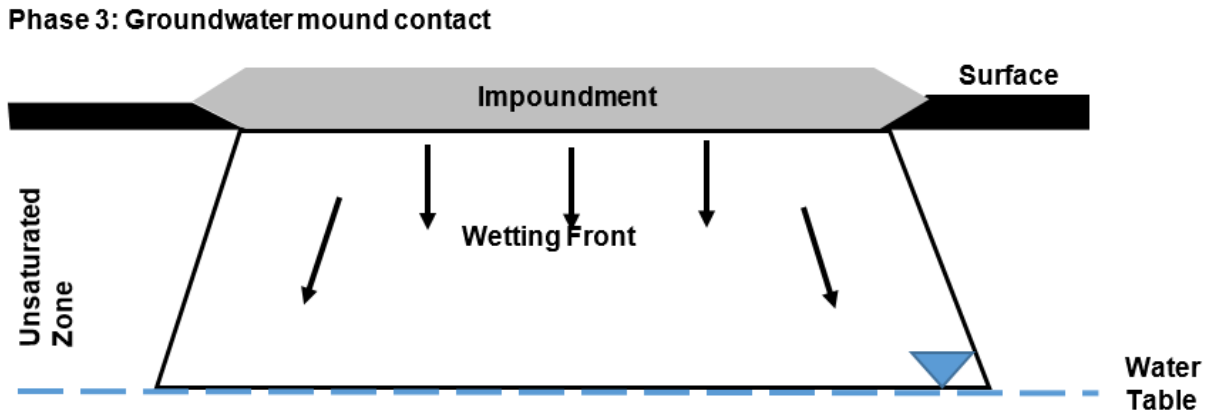

Figure 4: Phase 3 established groundwater mound and recharge from TSF (Martin & Koerner, 1984)

Phase 4: Once closure occurs and the facility moves into a dormant state a resultant desaturation of the facility will cause a recession of the groundwater mound (see Figure 5).

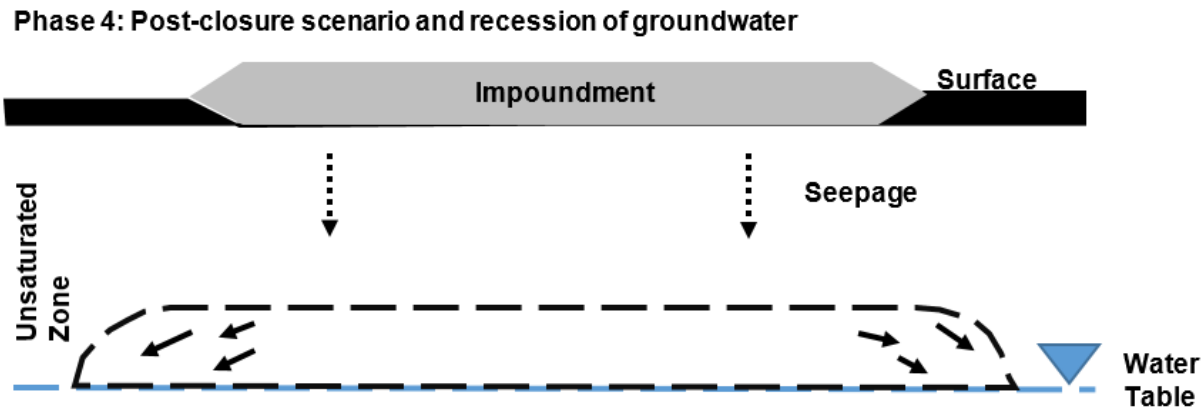

Figure 5: Phase 4 desaturation of the TSF and the regression of the saturated zone (Martin & Koerner, 1984)

2.2.2 Natural aquifers

Primary aquifers

Primary aquifers are defined in the South African Groundwater Dictionary (2011) as an aquifer that transmits and stores water within the original interstices of the geological formation. Aquifers classified according to this definition are mainly of a granular nature e.g. gravels and sandstones (sedimentary rock) where the original interstices have not been destroyed by compaction and subsequent cementation. Matrix porosity is the primary storage mechanisms for these aquifers. These rocks are found at near surface conditions; usually younger geological formations as tectonic and geological events have not destroyed most of the rock matrix. Groundwater movement also depends on the connectivity of pore within the rock matrix i.e. effective porosity (Kresić, 2007).

Flow through the porous rock is diffuse of nature. These aquifers can also be capable of storing and transporting much larger volumes of water than the secondary fractured aquifer types.

Fractured aquifers

Groundwater flow in hard rock aquifers is controlled by the governing hydraulic gradient. However, the rocks ability to store and transport groundwater is determined by the structural properties of the fractures within the matrix of the rock as well as the presence of unconformities such as dykes and sills which originate from younger intrusive magmatic events. Termed secondary aquifers, these aquifers only display permeability by the fracture aperture, connectivity and frequency of the fractures. A fractured rock aquifer is defined by the South African Groundwater Dictionary (2011) as a formation that contains sufficient fissures, fractures, cracks, joints and faults that yields economic quantities of water to boreholes and springs. The orientation of dykes and sills also play an important role as vast differences in

geologic properties create contact zones that can create preferential flow paths for groundwater.

Recharge in hard rock aquifers occurs mostly from vertically orientated fractures that are open and in direct contact with the soils receiving water.

Due to the heterogeneity of fractures and the complexity of fractured aquifer networks it is almost impossible to accurately account for all fractures contributing to groundwater transport and storage. Therefore, borehole testing during aquifer studies would only render an average hydraulic conductivity (Oxtobee & Novakowski, 2002).

Dolomitic aquifers

Dolomite under natural conditions forms large solution cavities as a result of the dissolution/neutralisation reaction of acidic rainwater infiltrating the subsurface. Rainwater becomes more enriched with carbon dioxide once infiltration takes place as it is found that "soil air" can contain up to 90 times more carbon dioxide than in the atmosphere. As a result, groundwater forms weak carbonic acid (H_2CO_3) that will further dissolve carbonate rocks upon contact (Morgan & Brink, 1984):

$$H_2O + CO_2 = H_2CO_3$$

Highly developed network of joints and tension fractures present in some dolomitic areas mean that groundwater could easily percolate through the rock matrix; further widening fractures and joints. Acidic groundwater reacts with the surrounding lithology to form bicarbonates (Morgan & Brink, 1984):

$$3CaCO_3.2MgCO_{3(dolomite)} + 5H_2CO_{3(carbonic\ acid)} = 3Ca(HCO_3)_{2(calcium\ bicarbonate)}$$

Unaffected groundwater within the dolomitic aquifers is typically Ca-Mg-HCO_3 dominated as a result of natural dissolution of carbonate rock and rain containing weak carbonic acid. These dissolution cavities, referred to karst structures are associated with groundwater storage and movement in dolomitic aquifers (Abiye et al., 2011; Hattingh et al., 2003).

Dolomite aquifers are classified as a unique entity due to the presence of both fractures and solution cavities that contribute to its ability to transport and store groundwater. Well-developed karst aquifers have characteristic structural features such as (Abiye et al., 2011)

- Caves
- Sinkholes
- Karst springs

As a result, Taylor & Greene (2008) noted that dolomitic aquifers also have unique groundwater transport mechanisms:

1. Recharge of surface runoff is predominantly through sinkholes and fracture zones with open fissures and dissolution cavities.
2. Rapid moving turbulent flow of groundwater within the channel or conduit structures.
3. Discharge from karst aquifers occurs as perennial springs or baseflow to larger streams.

Just as in the case with a fractured rock aquifer, the movement of groundwater is controlled by the orientation, aperture and frequency of conduits within the rock matrix. The most distinctive feature of the dolomite karsts is the dendritic pattern of conduits that occur across various bedding planes and the increase in aperture size in a downstream direction as dissolution and erosion increases in this direction (Palmer, 1991; Taylor & Greene, 2008). Conduit growth is described in the following steps:

Conduit formation (fracturing) ⟶ Enhanced dissolution and erosion ⟶ Additional conduit growth/enlargement Increased ⟶ Hydraulic capacity and Conductivity ⟶ Subsurface piracy of flows from adjacent aquifers.

Increased flow toward the dolomites would result in the formation of springs and non-perennial streams during high rainfall events. It is for this reason that dolomite aquifers are classified as sensitive, not only from a structural point of view but a contamination point of view as well (Taylor & Greene, 2008).

Aquifers in South African context

The major shallow aquifer units to the south of the gold-mining industry of South Africa are classified under the fractured rocks from the upper Karoo Supergroup (Figure 6). There is a wide spread karstified dolomite/chert combination of the Transvaal Supergroup toward the north, Malmani sequence (Abiye, 2011). Dolomites are in most cases the receivers of acid mine water, especially in the west rand mining areas of Johannesburg (Figure 7) and Carletonville and Klerksdorp-Stilfontein (Abiye et al., 2011). The presence of geological structures such as faults and volcanic events (dykes/sills) according to Duane et al. (1997) play a pivotal role in groundwater recharge. Abiye et al. (2011) also concluded that these structures form the main conduits for groundwater transfer in between different basins during tracer studies using tritium.

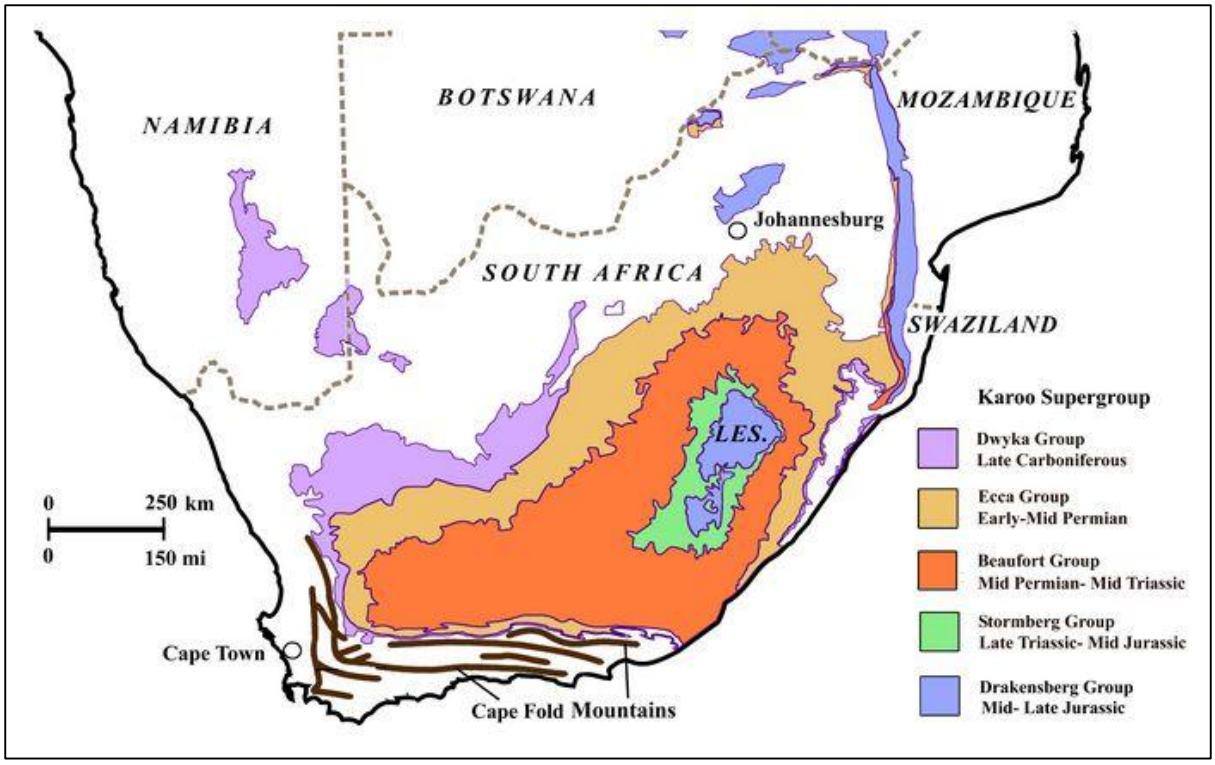

Figure 6: Location of the main Karoo basin, South Africa (Rubridge, 1995)

Research on the Far West Rand dolomites by Morgan & Brink (1984) concluded that groundwater movement is characterised by individual groundwater compartments separated by magmatic intrusions (dykes and sills). The compartments also display vastly varying hydrological characters. During the dewatering of the Venterspost compartment for mining purposes, Enslin & Kriel (1968) calculated storativity values by means of a water balance. They concluded that there is a decrease in storage with a subsequent increase in depth due to the lack of fractures at depth. A large variance in storativity was found from 9.1% at 61 meters to 1.3% at 146 meters. Transmissivity ranges from impervious at 10 m^2/d to 29 000 m^2/d depending on the amount of dissolution and the presence of fractures (see Figure 8).

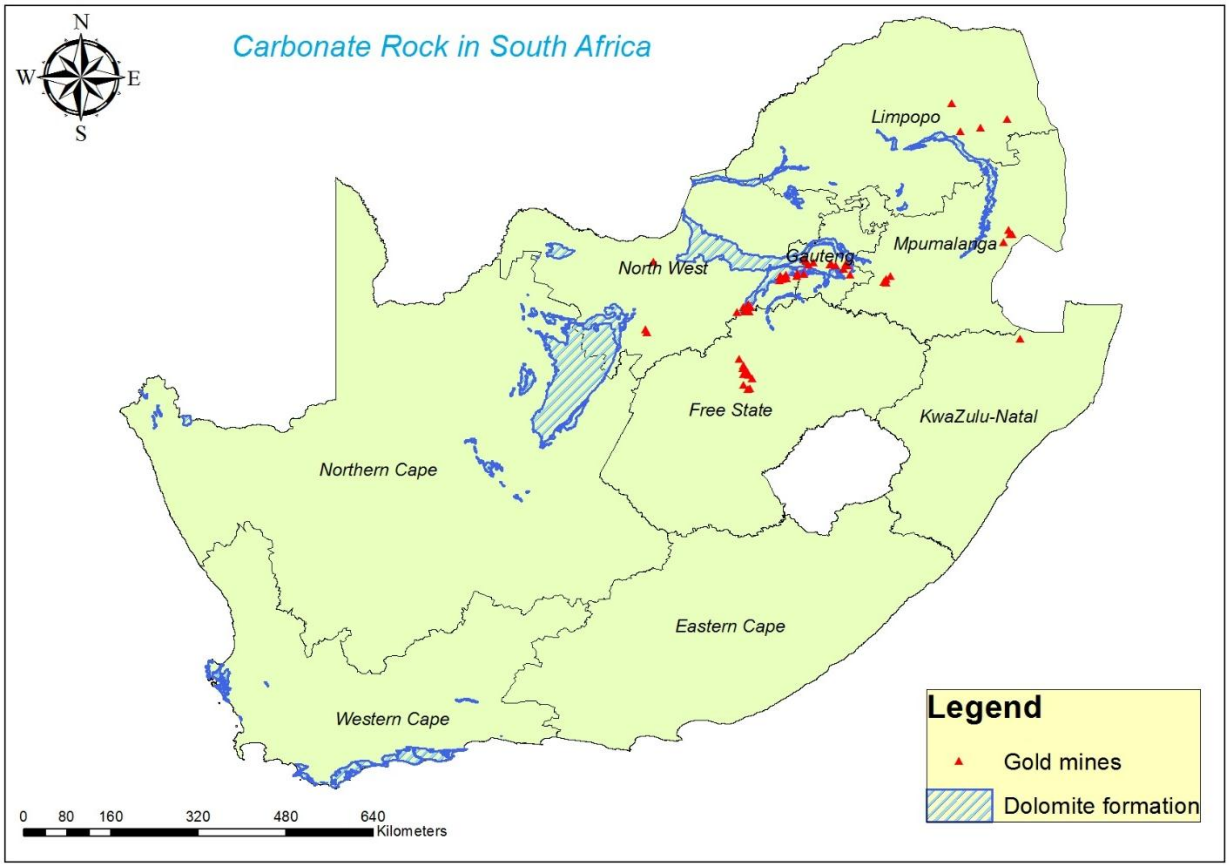

Figure 7: Location of carbonate rocks in South Africa (GCS, 2014)

Hattingh et al. (2003) found that dolomitic aquifers in close proximity to tailings footprints had elevated salt loads and trace elements of As, Cd, Co, Fe, Mn, Ni and CN. Abiye (no date) identified dolomitic water affected by acidic mine water to predominantly consist of Ca-Mg-SO_4, and concluded that SO_4 ions can only have been added from the neutralisation of sulphuric acid water coming into contact with the alkaline carbonate rock strata as natural dolomite does not contain SO_4. Abiye (no date) then used Fe/SO_4 as well as Ca/Cl to identify groundwater affected by acid mine drainage. Groundwater quality improved with an increase in distance down gradient of TSFs as a result of dilution with uncontaminated groundwater.

Coetzee et al. (2013) confirmed the presence of elevated iron and sulphate levels in water during column leach testing, using dolomite pebbles and a weak sulphuric acid iron mixture so as to replicate the interaction between AMD and natural dolomites. It is found that the alkaline rocks initially neutralised the acidic water mixture to the point where the raised pH will cause the precipitation of ferric oxides. The precipitation will create a coating around the carbonate rocks, effectively reducing further neutralisation resulting in a drop in overall pH. Coetzee et al., (2013) noted that even during neutralisation, the carbonate rocks had not reduced the dissolved sulphate load.

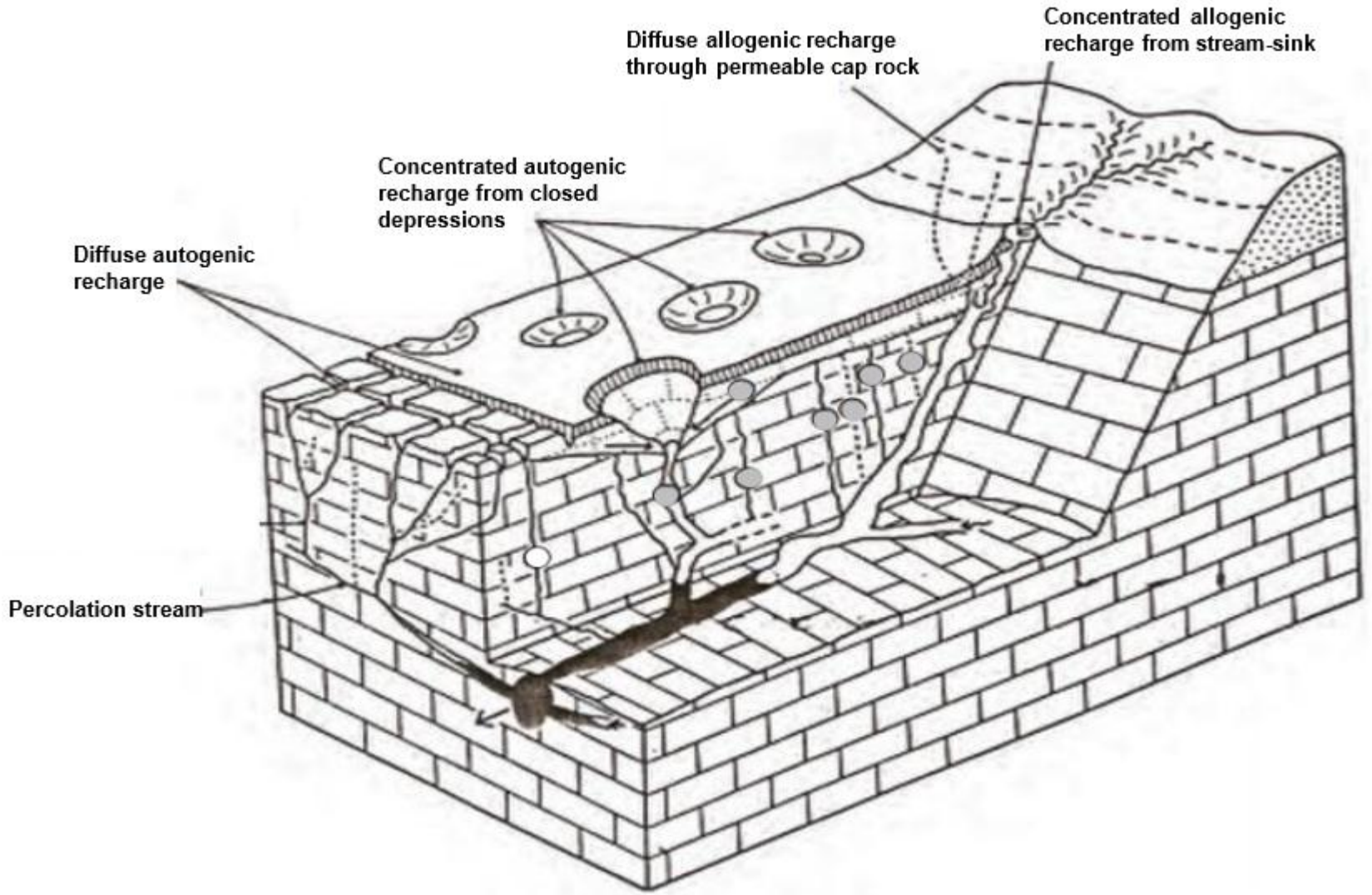

Figure 8: Cross-section of karst aquifer system illustrating the various groundwater transport mechanisms (Taylor & Greene, 2008; Gunn, 1983)

Rösner (1999) concluded that the Malmani dolomites in the greater Johannesburg were the controlling factor in the natural groundwater chemistry. As a result of the natural dissolution of carbonates the groundwater has elevated levels of Ca-Mg-HCO_3 present. However closer to mining activities it was noted that there was a significant increase in Total Dissolved Solids (TDS) values as well as a change in chemical character from Ca-Mg-HCO_3 dominant to Ca-Mg-SO_4. This change in chemistry was attributed to the neutralisation reaction between the alkaline groundwater and sulphate rich acidic water from the TSFs.

2.2.3 Surface water

Streams and rivers

Downstream of mining areas unpolluted groundwater can discharge into natural streams; the volume of water a natural stream receives from a groundwater source is also known as the groundwater contribution to baseflow. Most common natural streams and rivers receive a large volume of water as baseflow and are termed influent gaining streams. The runoff generated by baseflow in an influent gaining stream is mainly dependant on the amount of water available from the groundwater source (Tutu et al. 2008).

Contaminated groundwater from tailings facilities will discharge into an influent stream and dilution of the toxic mine water will lower the danger posed by contaminants entering the river system, however streams close to and/or directly between mine workings do not have enough clean water from uncontaminated sources and can lead to total contamination of the water body (Winde & Sandham, 2004).

Seasonality of contamination

Tutu et al. (2008) discovered that at the end of the wet season the analysis showed elevated EC and a subsequent decrease in pH from samples collected in the dry winter months located in the central parts of South Africa. It was decided that the escalation in values is due to the fact that higher volumes of surface runoff will lead to the dissolution of salt crusts formed during the dry months although this event will only be a short-lived one and only noticeable in the very beginning of the rain season.

Wetlands

Wetlands are commonly found in mining areas, especially around Return Water Dams (RWDs), these are constructed by the mining companies for water retention and supply during the dry winter season. These areas are commonly vegetated by Phragmites and Typha reeds. The sediments of these wetlands and RWDs are usually contaminated with heavy metals, as these precipitate out of solution when anaerobic conditions are dominant (base of wetlands

have minimal amounts of oxygen) and are trapped at the base of wetlands. Higher dissolved oxygen is found at the top and sides of the wetland and oxidation is found. As a result of the precipitation of metals and the biological uptake of these metals within the reeds, wetlands are seen as a contamination sink where contaminants are trapped as long as the water level remains high enough to maintain anaerobic conditions at the base of the wetland (Winde & Sandham, 2004).

2.3 Expected contamination from gold tailings

The Witwatersrand Basin is a pre-cambian sedimentological deposition that consists mainly of rounded quartz pebbles along with phyllosilicates that is typical of river transport and deposition setting. According to Feather & Koen (1975) the Witwatersrand conglomerates has a mineralogical composition of:

- Quarts (70-90%)
- Phyllosilicates (10-30%)
- Secondary minerals (3-5%) include Uraninite (UO_2), Brannerite ($UO_3Ti_2O_4$), Arsenopyrite (FeAsS), Cobaltite (CoAsS), Galena (PbS) and Pyrrotite (FeS).

Contaminants from gold tailings are notoriously associated with sulphates and heavy metals found in the gold bearing ore body. Milled and deposited on TSFs, these large entities are major sources of groundwater contamination. Aquifers surrounding mining areas have been found to have concentrations of salts, sulphates and trace elements of As, Cd, Co, Fe, Mn, Ni and CN that far exceed drinking water standards (Hattingh et al., 2003; Feather & Koen, 1975; Winde, 2001). Heavy metals are found in most cases only to become mobile once a drop pH to below 4.5 had occurred. Acid conditions have been attributed to sulphate oxidation which in turn will mobilise heavy metals in seepage water, resulting in large scale heavy metal contamination of groundwater resources.

Acid Mine Drainage

The oxidation of minor minerals such as pyrite causes a drop in pH of the water found in the slimes solution. Tailings dams are left exposed to oxygenated rainwater that results in the oxidation of the secondary minerals left in the “slimes”. The percolation of rainwater through the highly permeable matrix of the tailings facilities allows the sulphate minerals to oxidise to produce mainly iron as Fe^{2+} and H_2SO_4.

Marsden (1986), Naicker et al. (2003) and Hattingh et al. (2003) found that the depth at which oxidation and leaching of contaminants is at its highest is within the first 2m, oxidation still continues past 2m, up to an average depth of 5m depending on the age of the TSF and

exposure to oxygen. The remaining core of the structure has no oxygen present; therefore, no AMD originates from the inner core of a tailings facility. From geochemical modelling Hattingh et al. (2003) revealed that the groundwater percolating through exposed tailings material is directly affected by the material resulting in a subsequent rise in the dissolved solid load.

Tailings footprints, if left un-rehabilitated showed a drop in pH, indicative of acid production as a result of the continual oxidation of sulphate minerals. Along with acid conditions, a continuous flow of salts associated with SO_4 persisted for periods up to 50 years after dormancy (Blowes et al., 1998; Marsden, 1986). Long-term contamination is also greater on tailings as it is exposed on surface long after the mine is closed down (Johnson & Hallberg, 2005; Hattingh et al., 2003).

Hattingh et al. (2003) observed that especially sulphate loads remained at elevated levels in groundwater surrounding tailings facilities, indicating an accumulation of salt loads within the seepage water. Most noticeable is that variations in sulphate concentrations are attributed to the dissolution and precipitation of mineral species related to the sulphate group minerals e.g. alunite, gypsum and anhydrite.

Significance of Fe(II) and Fe(III)

In the majority of circumstances, atmospheric oxygen acts as the oxidant. However, the oxidation of pyrite can continue with limited oxygen available as ferric iron (Fe^{3+}) can become the oxidant of pyrite as well. The oxidation of pyrite can be up to three orders of magnitude faster than oxidation by oxygen only as ferric iron (Fe^{3+}) acts as a catalyst to pyrite oxidation. The reaction (Figure 9) indicates the three step lifecycle of pyrite oxidation and the production of Fe^{2+} and Fe^{3+} as a result.

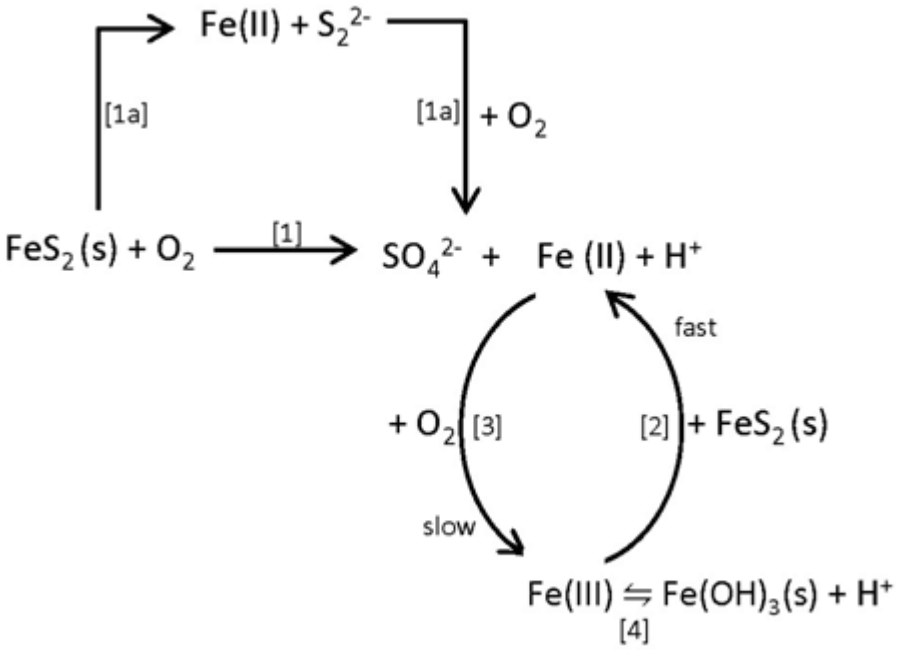

Figure 9: The simplified oxidation model for pyrite (Stumm & Morgan, 1981).

There is however a misconception that AMD reactions will continue to produce acid infinitely as ferric iron takes over as the oxidizing agent in the absence of oxygen, yet reaction 3 in Figure 9 shows that some oxygen is needed to generate ferric iron from ferrous iron in the first place. Therefore, reactions 2 and 3 run hand in hand, as the oxidation of ferrous iron (reaction 3) by oxygen is required to generate and replenish the ferric iron required for reaction 2 to take place (INAP, 2009).

The release of abundant H^+ ions during the formation of $Fe(OH_3)$ will result in acidic conditions. The continual production of H^+ causes the acidic conditions seen in AMD. An effect of AMD is metal leaching as a result of acidic conditions. Trace metals that are commonly associated with AMD are typically Fe and Al with concentrations ranging from 1000 up to 10 000 mg/L. Trace metals such as Cu, Pb, Zn, Cd, Mn, Co, and Ni can also reach elevated concentrations as a result of low pH conditions. Trace metals remobilize into solution at pH lower than four (INAP, 2009).

The production and persistence of acidic conditions depends on the nature of the sulphide mineral that is oxidized and the mechanisms driving the acid producing reaction i.e. oxygen vs. ferric iron as oxidizing agents as well as the presence of acid buffering minerals.

pH and Eh relationship with heavy metal solubility

Studies conducted by Naicker et al. (2003) on contaminated seepage in the Kwazulu Natal Province, South Africa found that there is a steady drop in pH along with a rise in sulphate and metal concentrations in the affected stream, possibly as a result of increased salt loads from contaminated seepage. It is concluded that the drop in pH is as a result of acidic groundwater inflow from the nearby tailings dam. Dilution of acidic seepage downstream has increased the pH; concentrations of Ni and Fe decreased by 50% and 70% respectively. The drop in Fe concentrations was further augmented by the presence of orange limonite and hematite (Iron hydroxide) that had accumulated on rocks found in the stream bed as the precipitation of $Fe(OH_3)$ had taken place.

The Eh-pH diagram suggested by Pourbaix (1988) (see Figure 10) for the Fe-S-H_2O system illustrates that higher pH conditions will favour the formation of hematite ($Fe(OH)_3$), iron hydroxide precipitate. At lower pH conditions iron becomes soluble favouring free Fe^{3+} ions.

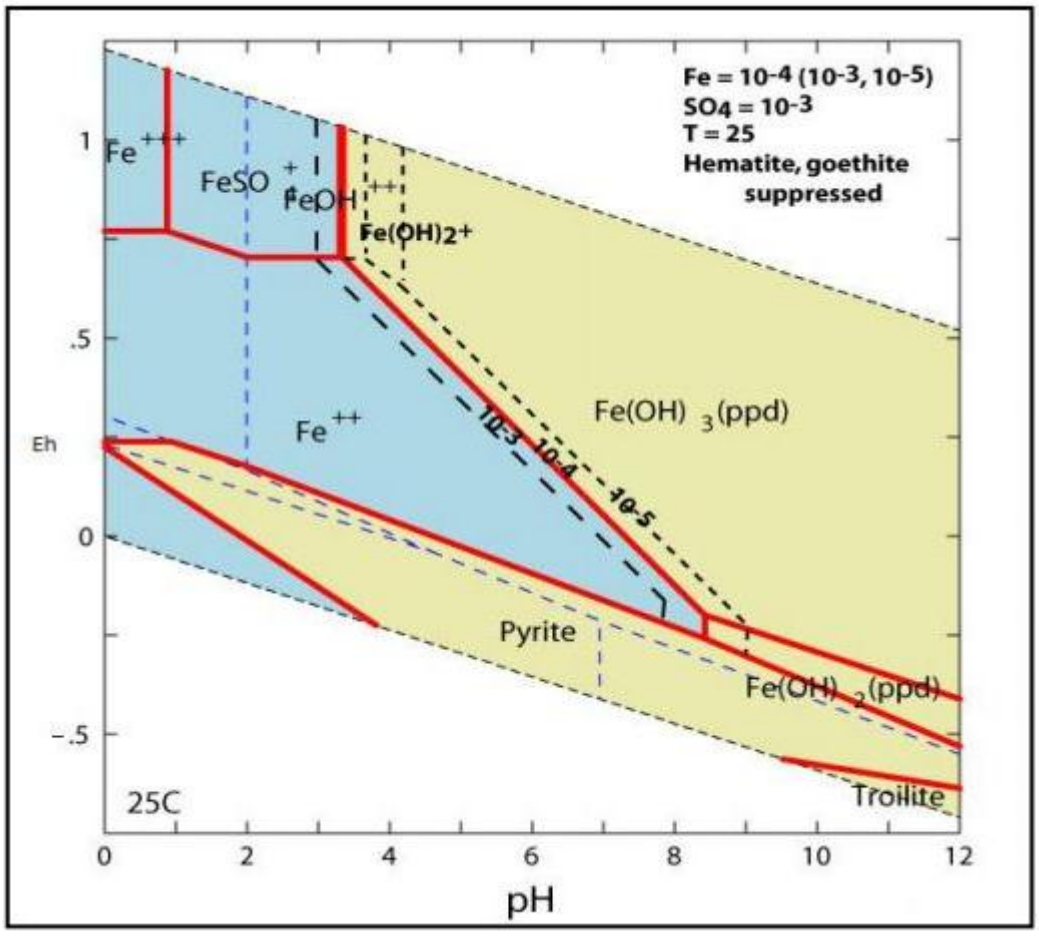

Figure 10: The Pourbaix diagram illustrating the solubility of iron in the Fe-S-H_2O system (Rose, 2010)

Interaction of AMD with sensitive aquifers (Dolomite)

The most common heavy metals liberated by sulphuric acid in gold mine tailings are Mn, Al, Fe, Ni, Zn, Cu, and U that is associated minerals of the ore, which in the South African mining context is the Witwatersrand conglomerates. Seepages from WRDs and TSFs is usually acidic, resulting in a neutralisation reaction once it comes into contact with an alkaline rock such as dolomite or limestone.

Even though dolomite has the ability to neutralize AMD Coetzee et al. (2013) concluded from column leaching that the initial reactions between the AMD and alkaline dolomite produced precipitates on the surface of the dolomite rock itself causing an armouring effect. This armouring would prevent further neutralisation reactions from occurring, thus limiting the natural attenuation of AMD to the extent that acidic conditions could result at a later stage, spreading further downstream of the TSFs.

Risks of Uranium in AMD

Uranium enters the subsurface aquifers by means of seepage from the tailings facilities. The U sorption potential depends on the particular soil properties i.e. pH, redox-potential, soil matrix porosity, particle size and the amount of available water. Previous studies have concluded that the sorption rate of a soil with high clay content is generally greater, therefore Uranium seldom migrates in soils that have high clay content (Shappard et al., 1987). However, soils that lack clay content do not have this sorption ability, therefore uranium retention within the soil is very limited.

The migration of heavy metals stretches from the tailings facility, following topography, finally entering adjacent streams where dilution takes place (Hearne & Bush, 1996; Winde, 2001).

Studies by Winde et al. (2001) on U concentration in the Koekemoer Spruit revealed that the elevated concentrations of U in the groundwater samples suggest that dissolved U is transported from the adjacent tailings dam found in close proximity of the Koekemoer Spruit. The elevated U concentration in the groundwater is due to the fact that the soil in the area, lacks any clay or organic material to absorb U, thus heavy metal contamination from tailings stretches for long distances, often kilometres from the original point of contamination (Winde et al., 2001).

2.3 Quantification of impacts of tailings facilities on groundwater and surface water resources

2.3.1 Introduction

The type of waste material, potential for seepage generation and the vulnerability of the surrounding aquifers are unknown aspects prior to predictive modelling that must be addressed before an acceptable assessment of impacts from a TSF can be made. The chemistry of the tailings material and hydrogeological data of both the natural aquifer and the TSF is translated into a conceptual site model. Conceptual models are subsequently used as a basis for appropriate data collection, keeping the study concise.

Govender et al. (2009) described a TSF as a source-term. Distinct zones within such facility are also identified that had unique hydrological characteristics as a result of particle segregation during deposition. Contaminant seepage flows are limited to the base and outer embankments of the TSFwhere it enters the natural groundwater regime.

The impact of TSFs on natural water bodies (groundwater, surface water) is directly related to the quality and quantity of water leaving the facility as seepage. Additional water from natural rainfall is also affected once it infiltrates the TSF. Wagener et al. (1997) and Brixel et al. (2012) indicate that the most important factors to consider when determining the impacts of TSFs on the natural groundwater regime are:

- Hydrogeological conditions of the impoundment foundation;
- Hydraulic conductivity of the tailings material;
- Hydraulic conductivity of the foundation;
- Geometry of the impoundment wall;
- Surface-water flows and water quality.
- Phreatic levels in embankments.
- Seepage flow rates and water quality of underdrains.
- Groundwater quality.

2.3.2 Conceptual modelling

Conceptual modelling is used in understanding and developing diagrams so as to simplify the complex physical system. The process identifies major sources, sinks and how these two are linked. Conceptual models will form the basis upon which data will be collected and numerical models constructed. Therefore, it is critical to have a good understanding of the problem and all aspects relating to the area before deciding on an appropriate numerical model (Spitz & Moreno, 1996; Labuschagne & Human, 2009).

Brixel et al. (2012) and Labuschagne & Human (2009) note that there are three different conceptual models that are formulated for projects involving the modelling of seepage from TSFs:

- Baseline, pre-depositional conditions. In other words, the natural groundwater system.
- Operational phase model. Once the TSF is already constructed and deposition is an on-going process.
- Dormant or post-closure model. Artificial deposition of water and tailings material has ceased.

The conceptual model should also indicate whether the system can be approximated using steady state or transient modelling conditions. Modelling of pre-depositional conditions will most often require steady state modelling conditions as changes to the system are a rarity; however transient conditions may prevail when determining future impacts once deposition of tailings occurs.

Understanding the sources

An effective conceptual model is one that describes all major groundwater transport mechanisms in the simplest way possible. For the purpose of contaminant modelling of a tailings facility the following key aspects are identified:

- The tailings facilities act as sources of contamination.
- Precipitation and process water deposited on TSFs will transport dissolved contaminants to the receiving groundwater systems.
- Substrata will form the foundation of the facility and can act as a contaminant pathway. Groundwater movement is dictated by natural structures within the rock e.g. fractures, solution cavities, pore spaces etc.
- Receivers of contamination are can be boreholes used for abstraction and surface water bodies such as rivers that are recharged by baseflow.

Understanding the pathways

Understanding pathways that contaminants will follow creates the link between sources and sinks. The natural aquifer system and associated groundwater flow will dictate how contaminants are transported. Therefore, this part of the investigation should identify which geological and hydrogeological data should be gathered that would best describe groundwater movement in the specific study area. The following list is used by Labuschagne & Human (2009) to enable a better understanding of pathway systems:

- Assessment of geographical settings and maps to obtain understanding for the regional environment.
- Assessment of the available geological and hydrogeological data.
- Gap analyses to identify aspects that field work must address.
- Field assessments and data collection to overcome data gaps.

The end deliverable of the pathway identification and understanding process is the setup of cross-sectional diagrams describing the flow system as illustrated in Figure 11. These diagrams will serve as the basis for numerical modelling.

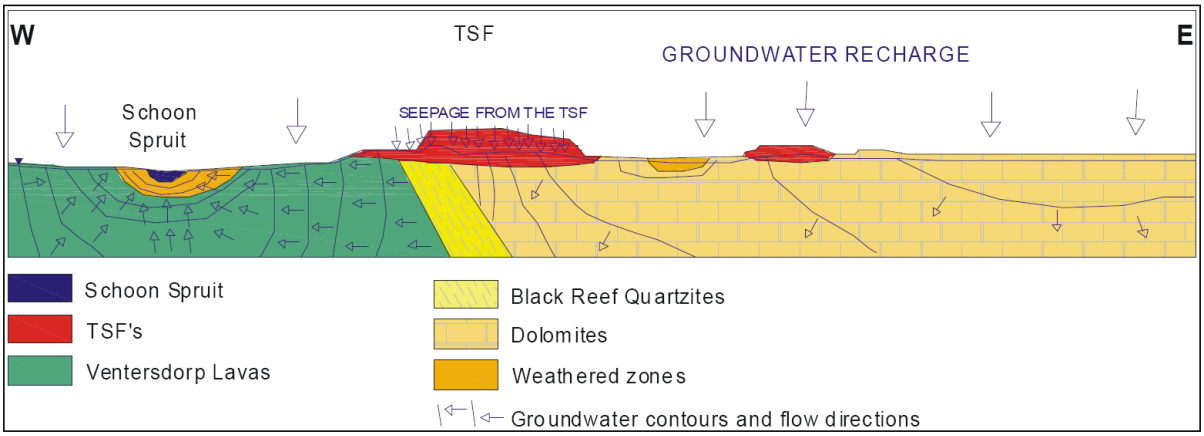

Figure 11: Example of a typical conceptual model indicating major pathways for groundwater flow (Labuschagne & Human, 2009)

2.3.3 Field surveys (Describing physical elements of the conceptual model)

Field surveys is the next phase following conceptual modelling. Field surveys in seepage investigations from TSFs should focus on:

1. Physical hydrological components of both sources, pathways and sinks; these include permeabilities of the tailings material, hydraulic conductivities of the underlying aquifer and possible seepages to rivers or streams (sinks).
2. Chemical characterisation (groundwater quality) of the natural groundwater and seepages from tailings.

Hydrological character of gold tailings

Tailings produced from hard rock mining are milled to a consistency that resembles fine sand or silt sized particles. Before deposition the D_{10} particles vary between 0.001 and 0.004mm whilst the D_{60} particles are between 0.01 and 0.05mm in diameter. Therefore, tailings are generally classified as a uniformly graded soil. The coefficient of uniformity C_u can vary between 8 and 18. The United Soil Classification System (USCS) classifies tailings as silt with low plasticity or silty sands (see Figure 12).

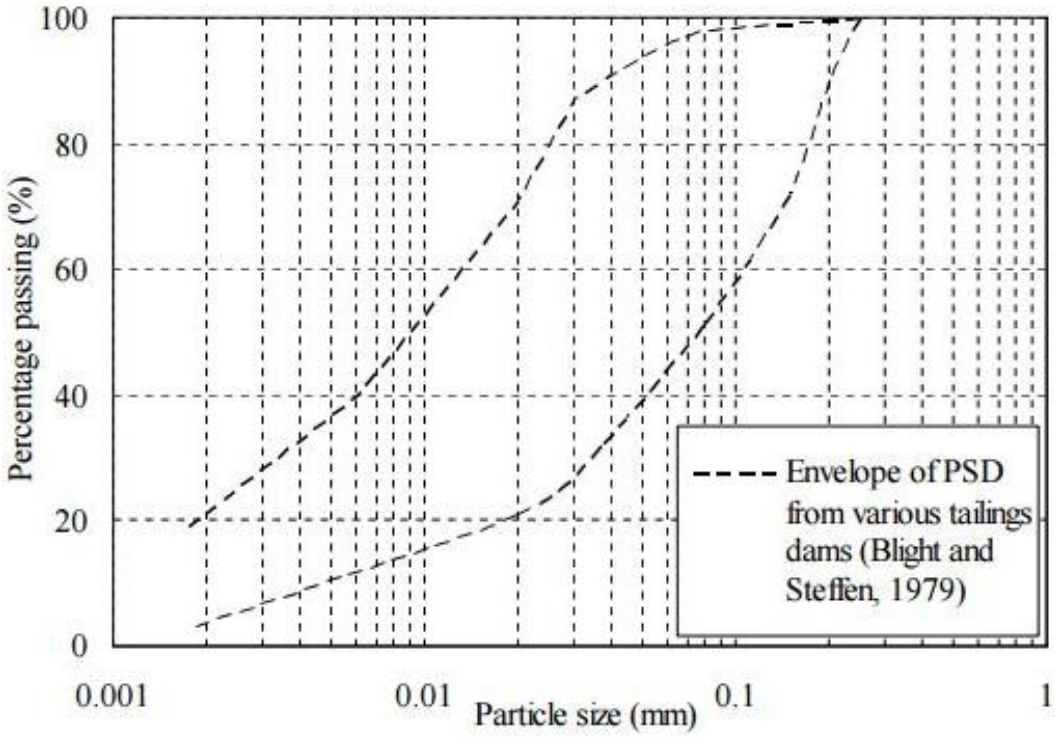

Figure 12: Typical PSD envelope for tailings material (Blight & Steffen, 1979)

Tailings material shares a close relationship with natural soils. Therefore, determination of the hydrological properties of tailings borrows methodologies from geotechnical studies to determine hydraulic conductivity, porosity, shear strength, permeability and water storage. All these properties are considered in the design and construction of TSFs.

The empirical determination of hydraulic conductivity through PSD of soil material has long been studied by Krumbein & Monk (1942) and Hazen (1893). Studies have shown that finer particles play a significant role in the hydraulic conductivity of a soil, therefore it is suggested to select a central tendency value based on fine grain diameters (Mahmoud et al., 1993). Hazen (1893) selected the D_{10} particle size at the effective diameter in saturated hydraulic conductivity calculations.

A geotechnical investigation of tailings is focused on PSD curves and Soil - Water Characteristic Curves (SWCC). The SWCC for a soil illustrates the relationship between water content and soil suction. The water content can be defined as the amount of water that is stored between the pores of a soil. This is usually referred to as the Volumetric Water Content (VWC) or degree of saturation of a soil. This parameter plays a significant role in the conductivity of a soil as water can only be transmitted through a porous medium through pores that are saturated with water, therefore the conductivity of a soil is in part dependent on the degree of saturation of a soil.

However, soils just as tailings material is not always completely saturated with water and there exists an unsaturated state where hydraulic conductivity varies and is very difficult to determine. The unsaturated conductivity of soils is in most cases empirically determined using a SWCC to estimate a hydraulic conductivity curve that describes both saturated and unsaturated hydraulic conductivity for a soil (Fredlund et al., 1997).

Seepage investigation

Fredlund et al., (1997) simulated a drought situation to determine the time it would take to de-saturate a tailings facility located in Papua, New Guinea. The simulation involved both the transient and steady state seepage analyses of the TSF. Steady state simulations where done to determine the head distribution within the TSF after which a transient state simulation was run to determine the desaturation of the TSF.

The volume-mass properties and the PSD of the tailings and foundation soils were used to determine a SWCC and hydraulic conductivity curve for both the tailings and the natural soils so as to perform a seepage analysis. An algorithm from the SoilVision software package developed by Fredlund et al., (1997) was used to estimate a SWCC from volume-mass properties and PSD's. The algorithm predicts the points on a graph of VWC versus matric suction using a best fit practice. The van Genuchten equation was used to fit the predicted points of the SWCC (see Figure 13).

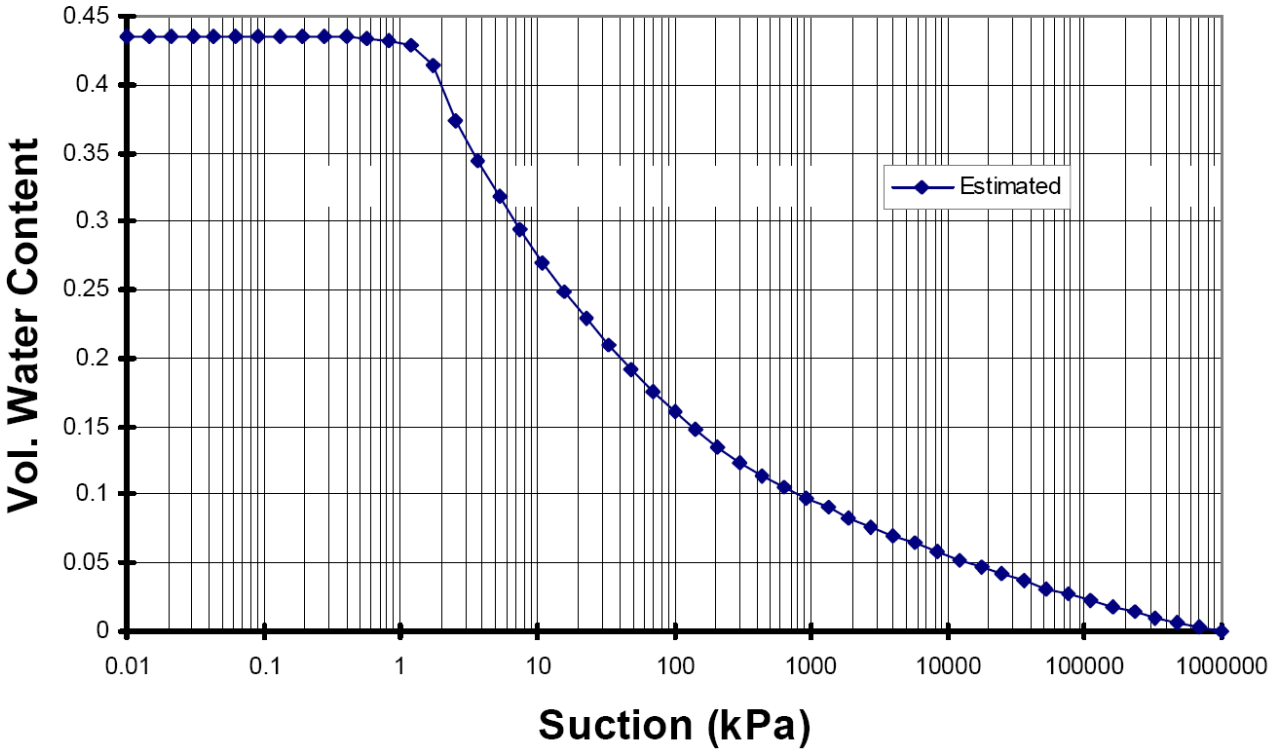

Figure 13: Estimated SWCC for the TSF material Fredlund *et al*. 1997

Once unsaturated conditions were determined, the saturated conductivity of the tailings and soil were predicted. Hazen's equation and the Kozeny – Carmen equation were used to determine the saturated hydraulic conductivity.

Once saturated hydraulic conductivity values were estimated, the entire hydraulic conductivity curve can be estimated based on the SWCC and saturated hydraulic conductivity. A combined graph of the hydraulic conductivity curve for the mine tailings is illustrated in Figure 14.

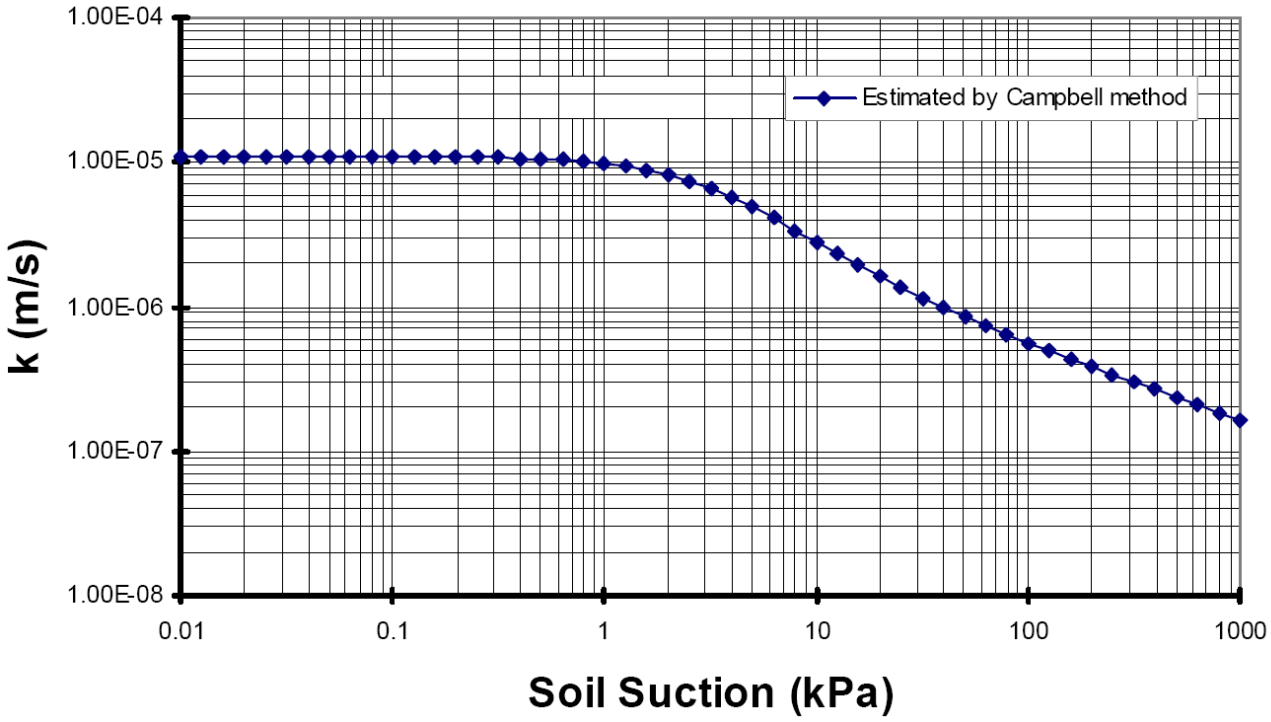

Figure 14: Combined hydraulic conductivity curve for a TSF (Fredlund *et al*. 1997)

These soil property functions were used as input to the Seep/W modelling software package where the steady state and transient state modelling was performed to simulate the desaturation of a TSF. The geotechnical investigation methodology utilised by Fredlund et al. (1997) is summarized in the following steps:

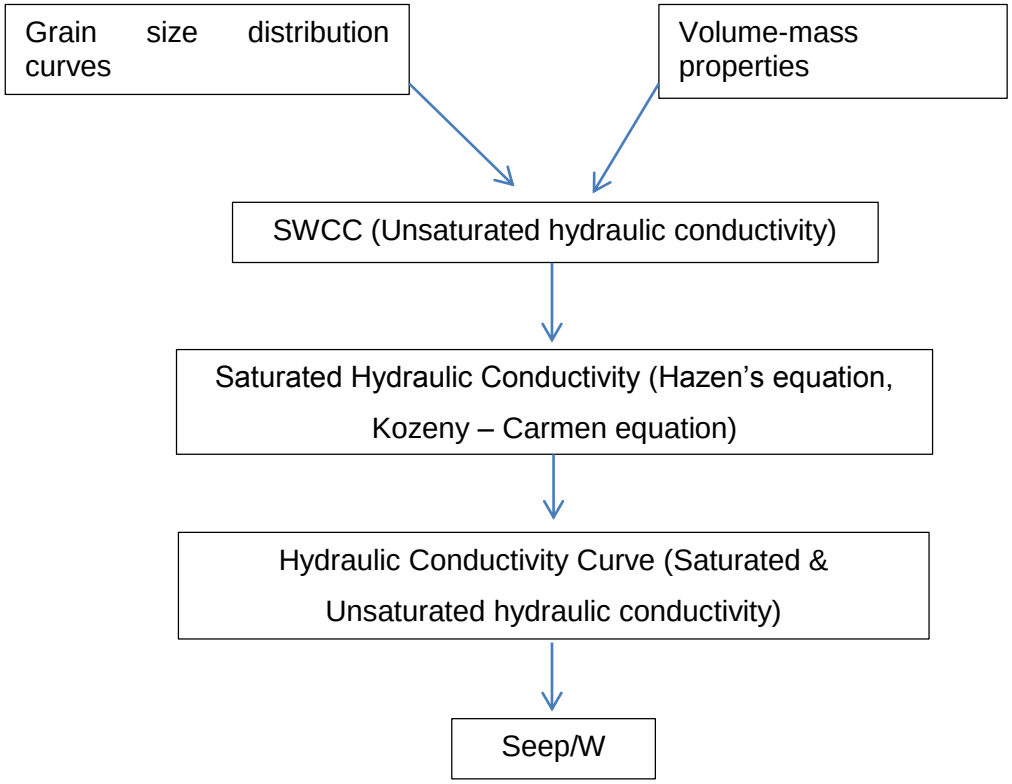

Borehole testing and analyses of the natural aquifer

Field surveys and borehole testing is one of the fundamental methods of obtaining accurate estimates on hydraulic parameters such as hydraulic conductivity, transmissivity and storativity. Common methods of borehole testing are pump tests and slug tests, both of which requires a known volume of groundwater to be displaced and the aquifer response to the change is measured against time.

Pump testing – The purpose of conducting a pump testing is to determine the hydraulic properties of an aquifer. The spatial limitations of an aquifer can also be determined by means of a pump test. Pump testing induces a change in head whilst recording the induced change (see Figure 15). The change is referred to as the drawdown/recovery of head within the pumping borehole (single borehole testing) or, if possible, an observation borehole.

Pump testing requires a suitable pump linked to a system capable of measuring flow rate as well as the displacement of head within the borehole (Rosberg, 2010).

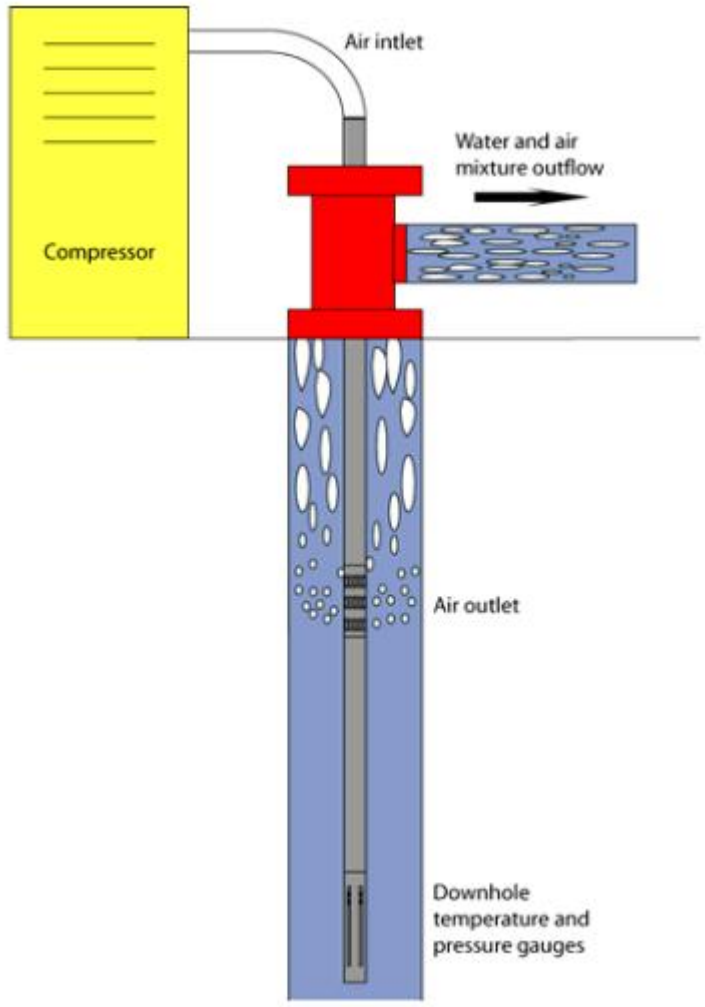

Figure 15: Typical setup of an airlift pump using a compressor to remove water from the borehole (Rosberg, 2010)

Observation boreholes are recommended if the purpose of the aquifer testing is to determine storativity. However, the scarcity of boreholes and the cost associated with drilling monitoring boreholes does not always make it a viable option.

Several solutions have been developed for analysing the raw data captured from pump testing; many of these solutions are included in aquifer testing software and utilise a curve-fitting technique. The objective of any curve fit, whether it is conducted manually or by computer aided software, is to fit a theoretical drawdown curve to the observed data set as closely and accurately as possible; in the process evaluating a set of corresponding physical parameters that is described by the theoretical curve (Cobb et al., 1982). All theoretical curves are based on mathematical equations used to describe certain physical parameters that are specific to an aquifer type or situation, thus each solution or equation comes with its own set of limitations and assumptions. The most common recovery solutions used are (Rosberg, 2010):

- Theis (1935).
- Cooper & Jacob (1946).
- Hantush & Jacob (1955).

The details of the above-mentioned solutions are documented in Appendix A.

Slug testing - The slug test requires that a small volume (slug) of water is rapidly removed or added to the borehole instantaneously disturbing (lowering or rising) the water table at equilibrium. Once the static water level in the borehole is disturbed the recovery is measured. From the Head vs. Time measurements during the recovery period one can determine transmissivity or hydraulic conductivity.

In order to determine the hydraulic conductivity from a slug test in unconfined aquifer conditions, Bouwer & Rice (1976) presented a method illustrated below:

$$Q = 2\pi K d \frac{h_t}{\ln(\frac{R_e}{r_w})}$$

The head's rate of rise, dh/dt, can be expressed as:

$$\frac{dh}{dt} = -\frac{Q}{\pi r_c^2}$$

The two equations are then combined to determine K:

$$K = \frac{r_c^2 \ln\left(\frac{R_e}{r_w}\right)}{2d} \frac{1}{t} \ln \frac{h_0}{h_t}$$

Where (see Figure 16):

r_c = Radius of the unscreened part of the borehole where the disturbance in static head occurred.

r_w = Horizontal distance from the borehole centre to the undisturbed aquifer

r_c = Radius of the casing where the change in head is measured

$\frac{dh}{dt}$ = Rate of rise of the water level in the borehole

R_e = Radial distance over which the difference in head, h_0, is dissipated.

d = Length of the borehole screen

h_0 = Head in the borehole at t = 0

h_t = Head in the borehole at t > t_0

D = Length of the saturated portion of the aquifer

Q = Volume rate of flow into the borehole

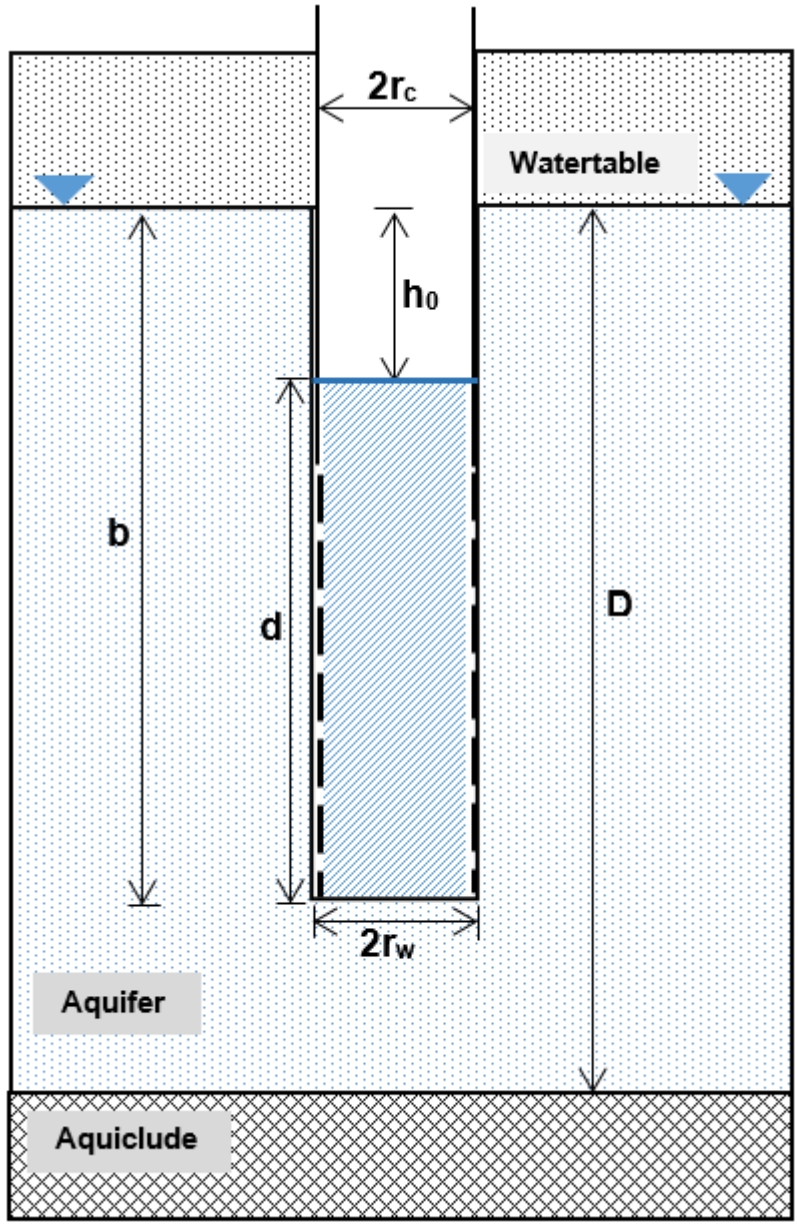

Figure 16: Partially penetrating borehole in an unconfined aquifer where a slug test is performed (Kruseman & de Ridder, 1994)

The values for R_e were determined by Bouwer & Rice (1976) during bench tests, using a resistance network analogue using various values of r_w, d, b, and D. From these values they derived two empirical equations to evaluate R_e for various aquifer systems with differing geometries, in terms of a dimensionless ration of $\ln(R_e/r_w)$. The data from a slug test could be fitted into one of two equations, the first case where b<D (partially penetrating borehole) and the second, where b = D (fully penetrating borehole). As the boreholes in the study are only partially penetrating, the first equation the where $L_w < H$ is defined by equation below for R_e:

$$\ln\frac{R_e}{r_w} = \left[\frac{1.1}{ln\left(\frac{b}{r_w}\right)} + \frac{A + B\ln\left[\frac{(D-b)}{r_w}\right]}{\frac{d}{r_w}}\right]^{-1}$$

Where the values for A and B is a function of d/r_w. Figure 17 indicates the Bouwer and Rice (1976) curves relationship for parameters A,B,C and d/r_w

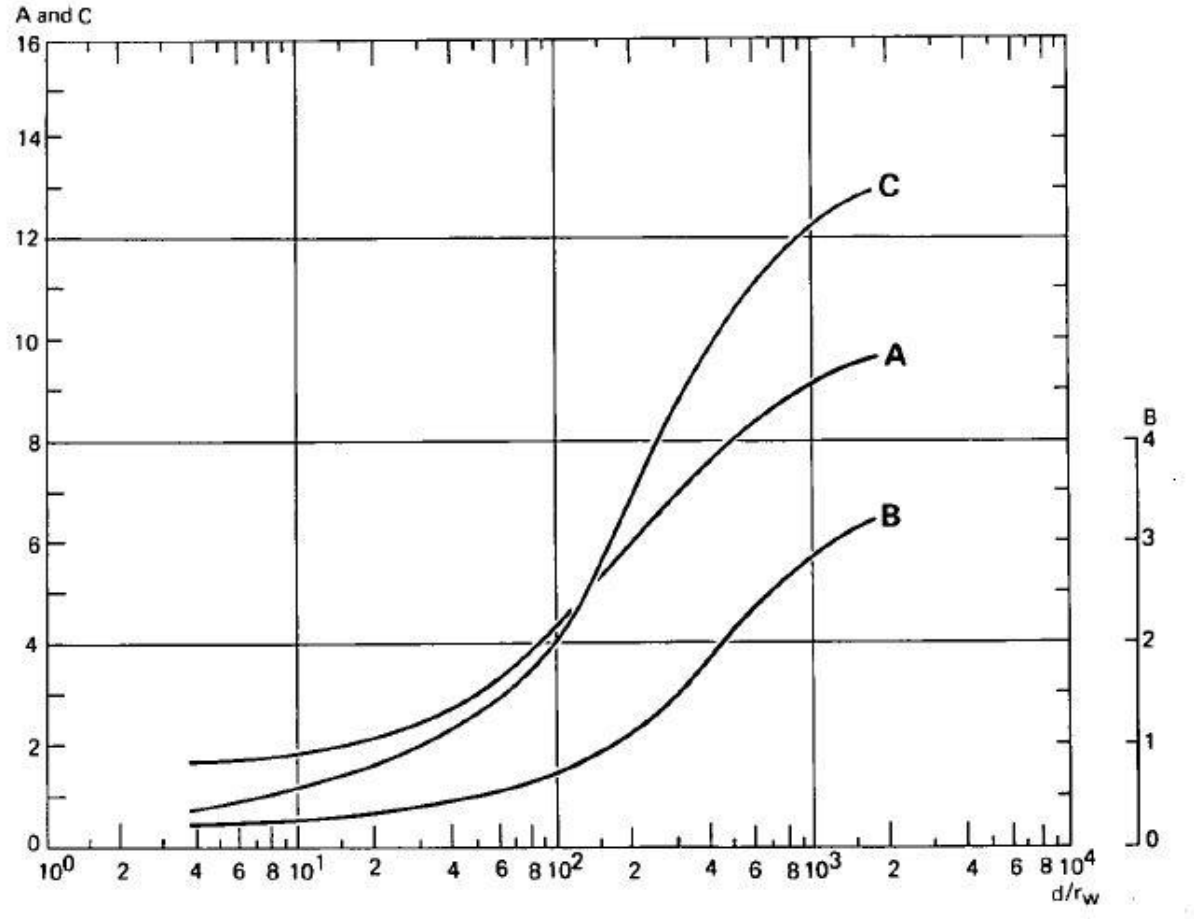

Figure 17: Curves used by Bouwer & Rice (1976) to determine the relationship for parameters A,B,C and d/r_w

K, r_e,r_w,R_c, and d in the first equation are constants. $(1/t)\ln(h_0/h_t)$ is a function of the values for h_t vs t is plotted on a semi-log graph rendering a straight line. Using the straight line,

$(1/t)\ln(h_0/h_t)$ can be calculated for any arbitrary value of t and its corresponding h_t. Knowing the d/r_w ratio, the values for A and B (used for partially penetrating boreholes) can be determined using the Bouwer & Rice curves. Once the numerical values of A,B,b,d and r_w is known; $\ln(R_e/r_w)$ can be calculated using the above mentioned equation. Finally all known values for $\ln(R_e/r_w)$, $(1/t)\ln(h_0/h_t)$, r_c and d, are substituted in the first equation to render K for the aquifer.

Slug tests have obvious advantages, however there are some limitations. Slug tests are only estimates for transmissivity as only a small volume of water is displaced in the direct vicinity of the borehole used to conduct the test (Fisher, 1983). Estimates are therefore not a true representation of the entire aquifer and will require more than one borehole test in the same aquifer unit.

Slug tests are also very sensitive to near borehole conditions and what is called the "skin effect" (the skin effect refers to the mechanical damage or alteration of the aquifer close to the borehole, most often as a result of drilling the borehole). Conductivity estimates can be a few orders of magnitude lower than that of the average hydraulic conductivity of the entire aquifer (Fisher, 1983 and Fabbri et al., 2012).

2.3.4 Water balance

A TSF is an entity which has variable portions of saturated and unsaturated zones. Establishing effective water balances for a TSF is largely dependent of the position of the saturated zone within the tailings. Yibas et al., (2011) states that the hydrological system for operational and non-operational tailings facilities differs conceptually and should be studied differently, Table 1 summarises the conceptual differences that must be considered when calculating a water balance.

Table 1: Key components of a TSF water balance

Operational TSF	Decommissioned TSF
Consistent addition of water	Rainfall is the only addition of water
Presence of saturated zone	Varying unsaturated zones
Pool water level used to calculate changes in dam storage (ΔS_{pool} – Volume of water stored within the pool region of the TSF)	Unsaturated flow principles describe flow
	Rate of drop in phreatic surface to be considered.

Using a water balance approach to quantify specific volumes of water deposited, stored and leaving a TSF requires a full understanding of the hydrological processes listed (Yibas et al., 2011):

- Physical parameters governing flow and storage e.g. design and deposition strategy.

- Hydraulic conductivity of tailings material.
- PSD is the controlling factor when studying unsaturated flow processes in porous mediums.
- Position of the phreatic surface.
- Facility specific factors such as bedding planes and preferential flow paths.

Labuchagne & Human (2009) used a simplified conceptual model developed by Pulles et al. (2002) for TSFs so as to identify four zones that would act as water pathways as illustrated in the Figure 18. The identified pathways were used in an overall water balance to evaluate the quantities of water seeping to the environment. These zones are:

- Zone 1 – The unsaturated zone.
- Zone 2 – The saturated zone.
- Zone 3 – The slope zone (assumed unsaturated).
- Zone 4 – The mixing zone for geochemical modelling.

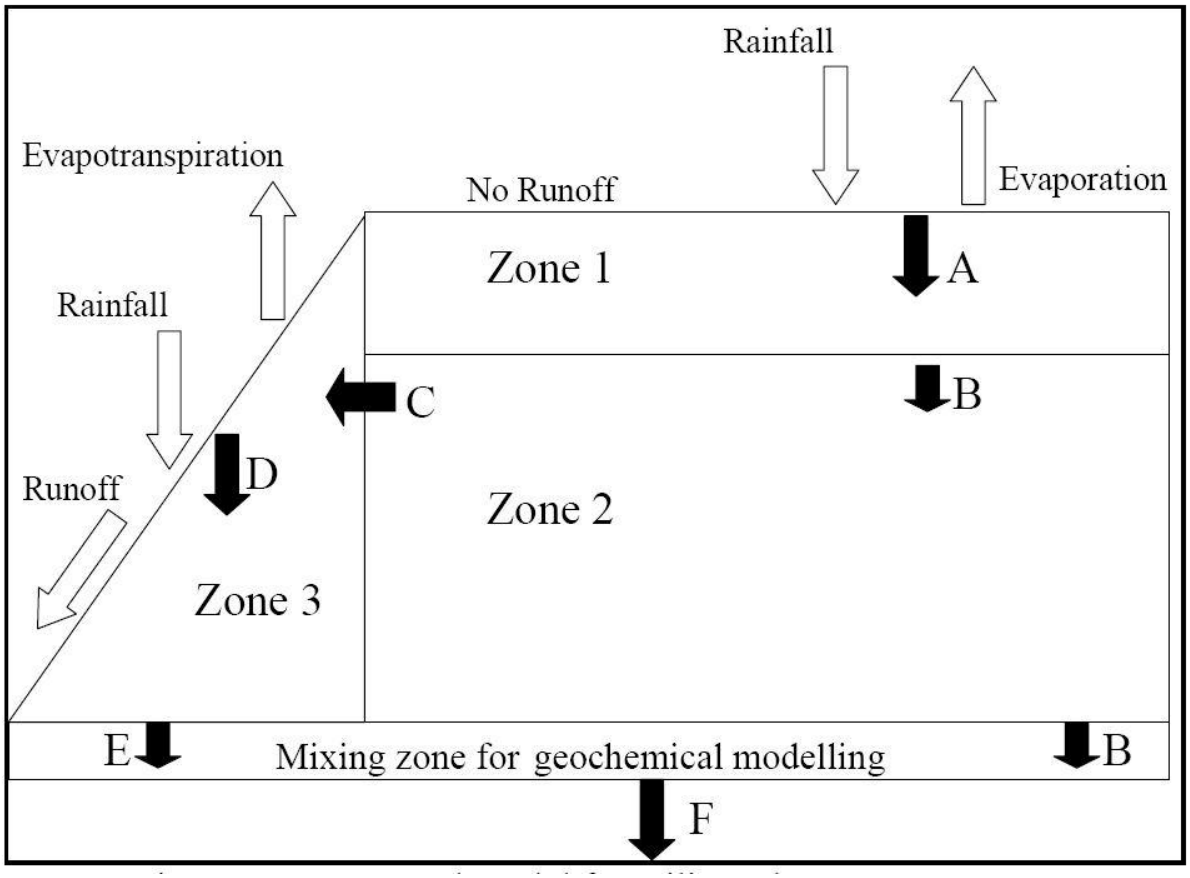

Figure 18: Conceptual model of TSF water pathways from Pulles et al., 2002

During active deposition, the rate at which slurry water is discharged onto the facility accounts for the bulk inflows. In the setup of a water balance the volume of water that reaches the

foundation of the TSF has to be evaluated. This volume is dependent on the physical properties of the tailings material (Yibas et al., 2011; Pulles et al., 2002):

- Slurry solid content
- Tonnage deposited
- Specific gravity of tailings and density of slurry water

Effective water balances attempt to quantify losses from the TSF to the environment and should be integrated into numerical models to assess the interaction between the TSF and its surrounding environment. Results from numerical models are then used as input for geochemical modelling so as to fully assess the impacts of TSFs both from a groundwater quantity and quality perspective. Once these aspects are assessed effective contaminant prediction can be made (Yibas et al., 2011).

Water balances for operational TSFs are characterised by a constant pool located roughly at the centre of the facility, where excess water is decanted for recovery. The monitoring of the pool size and level is used to calculate the tailings storage volume (Yibas et al., 2011).

Yibas et al. (2011) proposed a water balance approach for the quantification of seepage from TSFs as a basis for contamination prediction. The balance equation formulated is illustrated below (*S* is defined as the total volume of water stored in a specific region or time period within a TSF):

$$\Delta S = S_{end\ of\ period} - S_{beginning\ of\ period}$$

The general water balance equation indicates that a negative value for ΔS means that there is a decline in overall storage, therefore positive values would be an increase in storage. As there are clear differences in hydrological variation between different zones in a TSF, these must be treated as individual entities or smaller water balances that would make up the total balance for the entire facility. These different zones, inflows and outflows are described by Yibas et al. (2011) using a diagrammatical sketch (Figure 19).

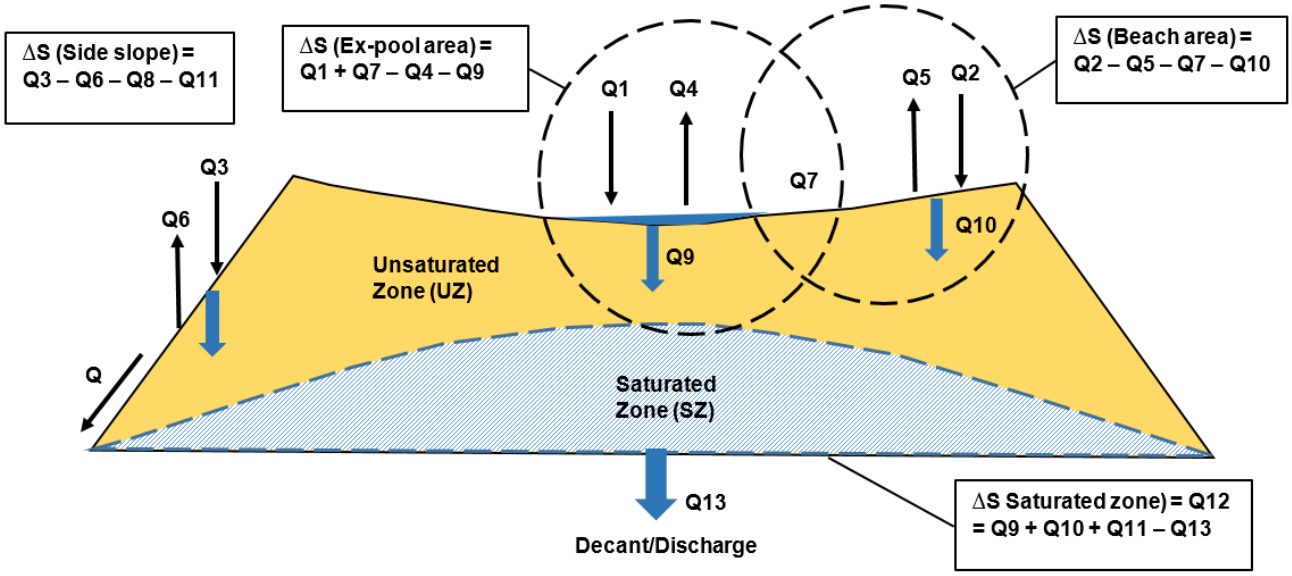

Figure 19: Diagrammatic sketch of a proposed water balance for a TSF (Yibas *et al*. 2011)

The various entities should be calculated individually and incorporated into the entire water balance. The entities identified by Yibas et al. (2011) are listed below:

$\Delta S_{pool} = Q1 + Q7 - Q4 - Q9$

$\Delta S_{beach} = Q2 - Q5 - Q7 - Q10$

$\Delta S_{side\ slope} = Q3 - Q6 - Q8 - Q11$

$\Delta S_{saturated\ zone} = Q12 = Q9 + Q10 + Q11 - Q13$

The combined water balance for the entire TSF is as follows:

$Q13 = Q1 + Q2 + Q3 - Q4 - Q5 - Q6 - Q8 - Q12 - \Delta S_{pool}$

Where:

ΔS = Volume of water stored within a region of the TSF

Q1 = Volume of precipitation from falling on the pool

Q2 = Volume of water from precipitation falling on the beach area

Q3 = Volume of water from precipitation falling on the side slope area

Q4 = Volume of evaporation from the pool area

Q5 = Volume of evaporation from the beach area

Q6 = Volume of evaporation from the side slope area

Q7 = Volume of runoff from the beach area

Q8 = Volume of runoff from the side slope area

Q9 = Volume of infiltration from the pool area

Q10 = Volume of infiltration from the beach area

Q11 = Volume of infiltration from the side slope area

Q12 = Volume of water released from the saturated zone

Q13 = Total volume of discharge/decant/seepage from TSF

General rules used when calculating a water balance (Yibas et al., 2011):

- Runoff = 0.17 * Rainfall, except vegetated areas.
- Evaporation = 0.69 * Rainfall.
- Percolation = 0.17 * Rainfall.

2.3.5 Numerical modelling approach

Numerical modelling is an accepted practice today and is used to predict and assess an aquifer's response to changing environmental conditions, usually as a result of human activities e.g. industrial development, agricultural development, etc. (Fetter, 2001).

Designing a groundwater model, the model user tries to replicate the natural elements so as to simulate and access the aquifers response to induced changes (scenarios). These components according to Spitz & Moreno (1996) are:

- Natural system for which the model is designed
- Mathematical model representing controlling mechanisms in mathematical terms
- Solution of the mathematical problem
- Calibration of the solution by adjusting simulated to observed responses of the natural system
- Validation of the accuracy of model predictions
- Simulations based on the calibrated solution of the conceptual model

Regardless of the variety and complexity of numerical modelling approaches Spitz & Moreno (1996) have identified the main components of any numerical model and listed them in chronological order:

- Compiling and interpreting field data
- Understanding the natural system
- Conceptualizing the groundwater system
- Selecting the numerical model
- Calibrating and validating the model
- Applying the model
- Presenting the results

Seepage modelling

Most TSFs are predominantly under unsaturated conditions, thus hydrological modelling of seepages and contaminant transport requires determination of the unsaturated soil properties

(Fredlund et al., 1994). Soil parameters used in unsaturated flow modelling are derived from nonlinear equations established from known laboratory test data. These equations are referred to as the Hydraulic Conductivity Function (HCF) and SWCC that represents the relationship between the VWC and pore pressure of a particular soil type. To model seepage flux through an unsaturated pile these functions are required for each material in the flow path (Fredlund et al., 1994). Figure 20 is an example of a SWCC.

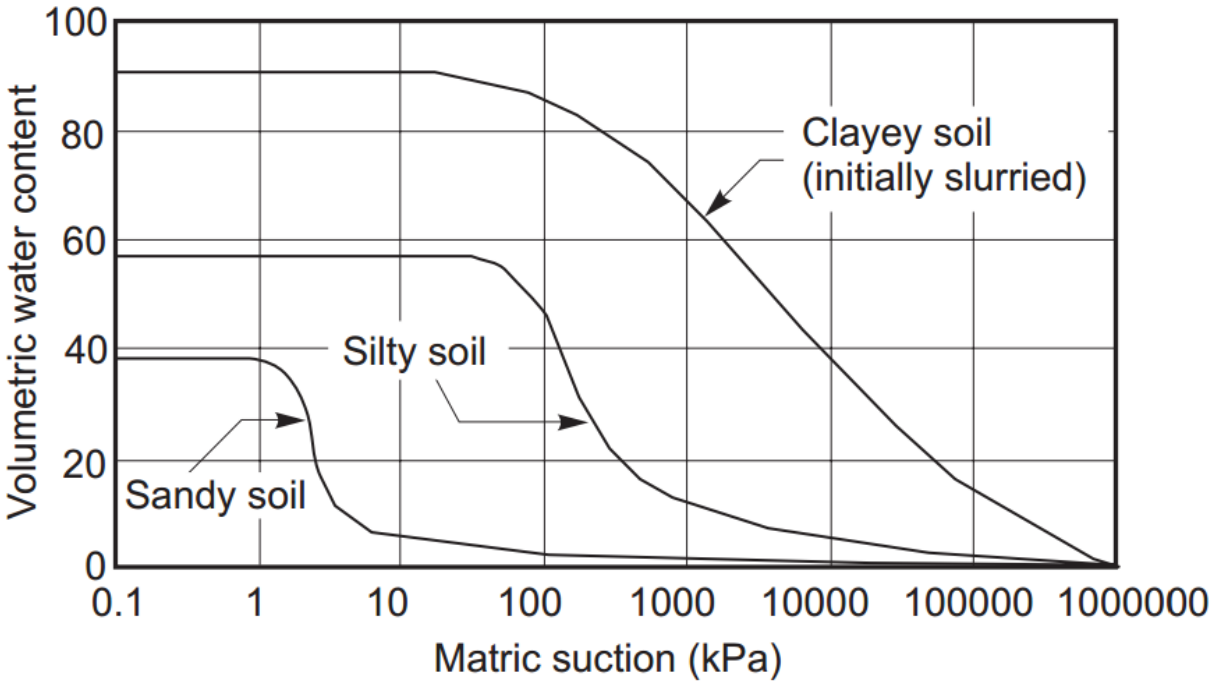

Figure 20: SWCC for sand, silt and clay soils (Fredlund *et al*. 1994)

The SWCC is used to determine the storage function of a soil. In simple terms the SWCC relates to the change in water content of a soil in relation to changes in soil pore pressures and suction. As the pore pressure becomes more negative, larger soil pores are drained and can no longer conduct water, thus reducing hydraulic conductivity (Marino & Luthin, 1982).

The HCF represents the ability of a soil like material to conduct water through its matrix at various states of saturation. The HCF can be estimated using methods established by Fredlund et al. (1994), van Genuchten (1980), Cambel (1973) as well as Brooks & Corey (1964) to describe a soils reaction to various degrees of saturation as a result of pore pressure changes.

The saturated hydraulic conductivity of a soil is the boundary for unsaturated flow conditions. Multiple methods exist to measure or estimate the Saturated Hydraulic Conductivity (SHC) indirectly. This requires the use of formulas that relate hydraulic conductivity to the grain size distribution of the material. Methods from Kozeny (1927) and Hazen (1892) are used.

Detailed simulations of the phreatic surface (saturated conditions) and dam seepage rely on more complex 2-D modelling approaches. These simulations require a cross-section of the entire TSF (see Figure 21), that is representative of the various zones i.e. embankment, beach and pool. Two dimensional models are useful as they enable both the vertical and horizontal components of flow associated with infiltration and percolation through and under tailings embankments. The delineation of component materials that make up the dam core and walls is greatly simplified when only considered in two dimensions, rendering an accurate geometry without demanding an excessive number of grid nodes.

Seepage modelling requires the simulation of saturated and unsaturated flow through soils under a unit of hydraulic gradient. There are three main components to numerical analyses (Geoslope, 2012):

- *Numerical domain*: The first step of modelling deals with the selection of an appropriate geometry and discretized mesh specifying nodes for the calculation of flows across the matrix.
- *Specification of properties*: This requires the specification of material properties. It is during this phase of the project where the physical samples taken during field studies are entered into the modelling domain. These properties are typically hydraulic conductivity, transmissivity; in the case of saturated/unsaturated flows within soils volumetric water content functions and conductivity functions are used to describe flow through the matrix.
- *Specification of boundary conditions*: boundary conditions are the driving force behind any numerical modelling practice. The modelling output is a direct response to the boundary conditions applied. In seepage flow problems the total head difference between two points is used to calculate the flow rate between these specified points. Constant heads and specified inflows are examples of boundary conditions applied to numerical models.

Flows calculated from seepage modelling are applied as a recharge flux to a groundwater model so as to evaluate the natural aquifer response to the added inflow from anthropogenic structures such as earth dams. The inflows are also used as a basis for contaminant transport and contamination prediction in the case of TSFs.

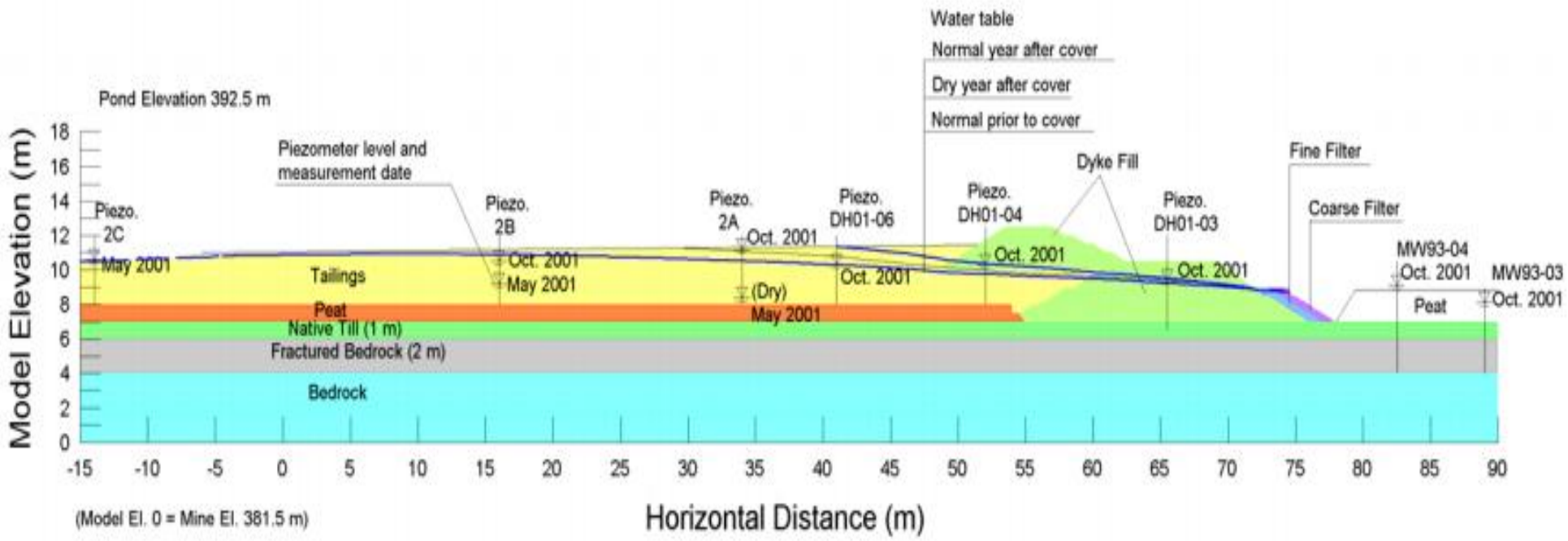

Figure 21: Two dimensional cross section of a typical seepage model for a TSF using the SEEP/W software (Wang & Murry, 2011).

Software codes such as Geostudio SEEP/W and VADOSE/W, Soil Vision and FEFLOW make construction of such models relatively easy, utilising only material design specifications and data from standard geotechnical soil property testing. The cross-sectional interface when assigning geometry to the TSF makes it compatible with conceptual models.

Vertical flows into and out of a TSF are the key components of hydraulics between a TSF and its functioning in the environment. Garrick et al. (2014) concluded that numerical modelling of TSFs will always require a degree of simplification; therefore, software should be selected that reflects key processes of the flow system, whilst being computationally efficient. Many TSF design problems may be appropriately represented by a 2-D vertical flow profile which captures key flows associated with infiltration of water into, through and out of a soil like material with unique geotechnical characteristics that govern flow. Infiltration volumes applied to the specific section is derived water balance calculations that account from water added to the system by slurry deposition and natural precipitation.

2.3.7 Contaminant Mass balance (Mass discharge/flux calculation)

Mass discharge and mass flux estimates are valuable in understanding and managing contaminant plumes. These concepts are the basis for understanding existing groundwater fate and transport phenomena (Hemond & Fechner – Levy, 2000). Mass discharge / flux estimates are used to evaluate a contaminant's impact on down gradient receptors such as water supply boreholes and surface water bodies (ITRC, 2010).

Mass flux (J) is expressed as a mass over time over a specific area ($M/t/m^2$). Therefore, mass flux is a rate measurement specific to a defined area, which is normally a subset of a plume cross-section. Mass flux combines two features of a contaminant plume:

- How much contaminant is moving in the groundwater
- How fast it is moving through a defined section

Mass discharge is an integrated mass flux estimate and is representative of the total mass of any solute conveyed by groundwater through an entire plane in which the majority of the contaminant is moving, Figure 22 illustrates the difference between the concepts of mass flux (J) and mass discharge (M_d).

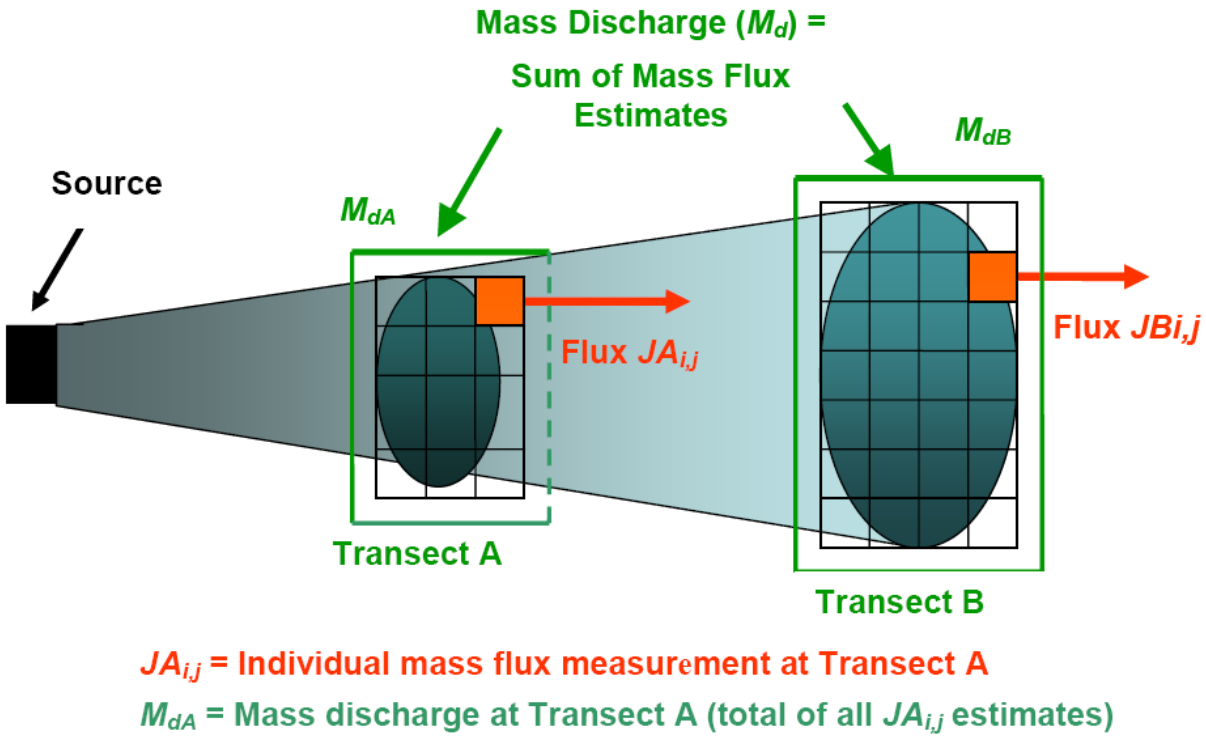

Figure 22: Concepts of Mass flux (*J*) and Mass discharge (M_d) (ITRC, 2010)

Basic concepts

Flux is defined as the flow through a medium. Flux rate therefore is a measurement of the flow across a defined area during a defined time. Mass flux represents a specific area that is sampled and is usually small when compared to the overall contaminant plume dimensions. The critical issue in most contaminant transport investigations in not the mass flux across a particular length or area of the groundwater, but the total contaminant mass conveyed to some point along its length. Mathematically, contaminant mass flux is the product of the concentration of a contaminant in the groundwater and the groundwater flux. Thus the contaminant flux can be calculated as follows (ITRC, 2010):

$$J = q_0 C = KiC$$

Where:

J = Mass Flux ($M/t/m^2$)

q_0 = Groundwater flux ($L^3/L^2/t$)

K = Hydraulic conductivity (m/d)

i = Hydraulic gradient, dimentionless (m/m)

C = Contaminant concentration (M/L^3)

Mass discharge is conceptually similar to the groundwater discharge (Q). Mass discharges is the product of groundwater discharge multiplied by the average contaminant concentration. Contaminant mass discharge in the overall integration of the contaminant mass fluxes over a selected transect, thus mass discharge is calculated as follows (ITRC, 2010):

$$M_d = \int J dA$$

Where:

M_d = Mass discharge (M/t)

J = Spatially variable contaminant flux ($M/t/m^2$)

A = Area of the control plane (L^2)

The ITRC, (2010) identified five basic methods most commonly for the calculation of mass flux and discharge of contaminants in groundwater studies:

1. Transect methods
2. Well capture
3. Passive flux
4. Transects based on contours
5. Solute transport modelling

Transect Methods: Estimates of groundwater contaminant concentration and groundwater velocity are calculated using a series of monitoring points across a contaminant plume. The transect method utilises a control plane (Figure 23) across the plume that is sampled for contaminant concentration and specific discharge to provide flow data.

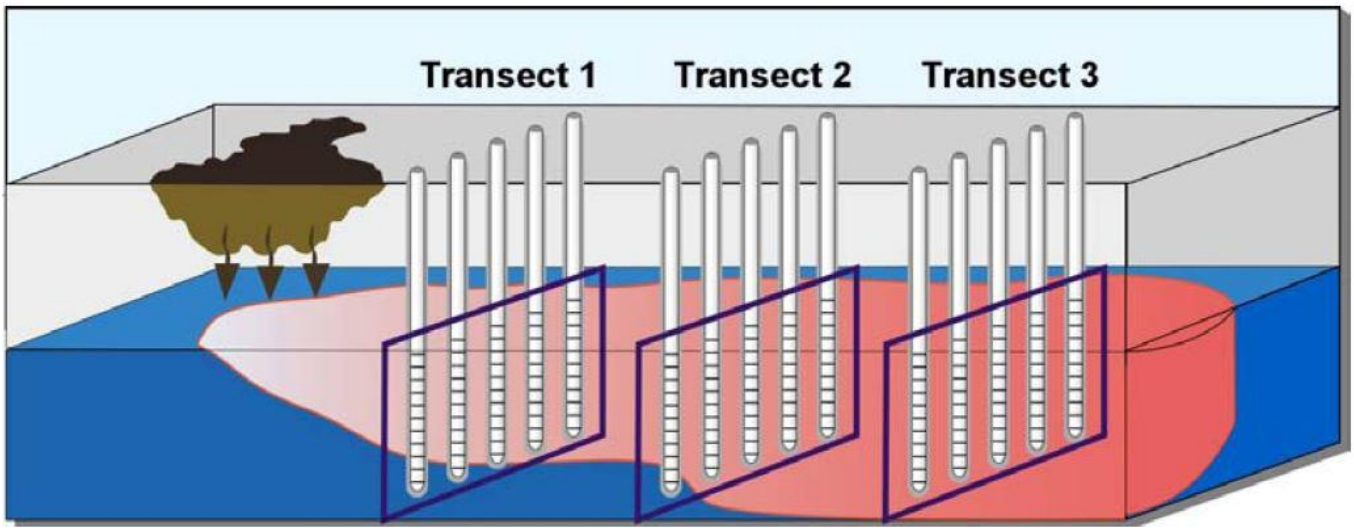

Figure 23: Example of multiple transects intersecting an MtBE plume (Nichols & Roth, 2004)

Well capturing: By measuring the concentration of contaminants and flow from a single well, the mass discharge (unit per time) can be calculated. This approach however assumes that the well selected from abstraction fully captures the horizontal and vertical extent of the contaminant plume. Calculation is done according the following (Nichols & Roth, 2004):

$$M_d = QC$$

Where:

M_d = Mass discharge (M/t)

Q = Water flow (L^3/t)

C = Concentration of contaminant (M/L^3)

Passive Flux Meters (PFM): PFM have been developed to measure the cumulative fluxes of both groundwater and contaminants within the saturated portion of an aquifer. PFM are devices that are placed within a monitoring borehole where it intercepts groundwater, and dissolved contaminants are sorbed to a sorbent inside the PFM; simultaneously the PFM leaches a soluble tracer into the groundwater. Measurements of contaminants and the residual tracer can then be used to estimate groundwater and contaminant flux. Calculations are conducted based on equations established by Hatfield et al. (2002).

$$J_c = q_0 C_F$$

Where:

J_c = Time averaged contaminant mass flux ($M/L^2/t$)

C_F = Flux averaged concentration of contaminant (*M/L*)

q_0 = Specific discharge of the aquifer (*L/t*)

Transects based on contours: This approach uses transects that are not located in borehole networks. Monitoring points that are available in the study area are used to construct a contour map of groundwater concentrations (see Figure 24), either by hand or computer aided software. This method may have a high level of uncertainty than compared to high-density multilevel transect methods (ITRC, 2010).

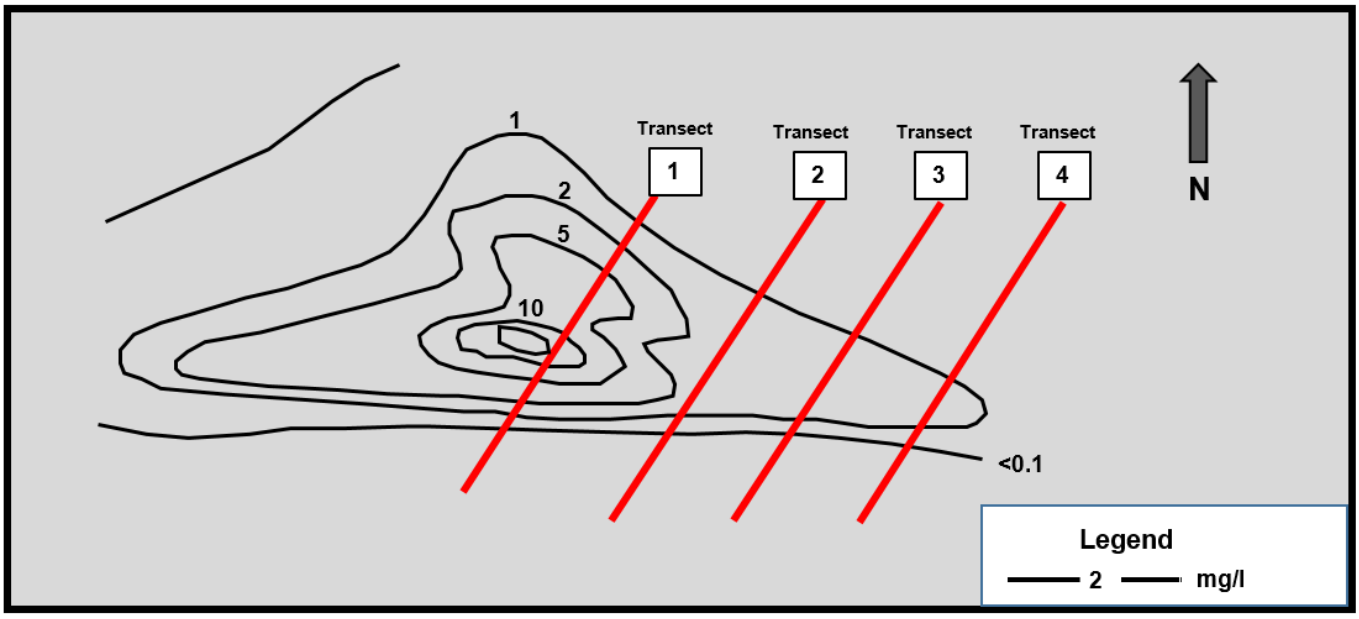

Figure 24: Example of transect based on contour lines (Einarson, 2001)

Solute transport models: These models make use of both groundwater flow data and contaminant data used as an input to the model where it would be processed utilising established groundwater modelling codes to produce and output. Solute transport modelling based on numerical and analytical methods are a more cost effective and popular method especially when confronted with a site that has constraints that cannot accommodate the above mentioned methods.

Rösner (1999) focused on the quantities of SO_4 leaching from dormant TSFs as this was the main driving factor for the production of acidic water and subsequent dissolution of heavy metals associated with the Witwatersrand conglomerates. The annual rainfall and natural recharge values (12.5% of annual precipitation) of the dolomites were used and converted to an area size after Hölting (1996).

Load estimation from Rösner (1999):

1. 80mm recharge/year to 2.563 l/(s.km^2)
2. Conversion from seconds per km^2 to year per km^2

$$2.563 \quad \frac{l}{s.km^2} = 79.97x10^6 \frac{l}{year.km^2}$$

3. Multiplication of recharge value with relevant size of area covered

$$79.97x10^6 \frac{l}{year.km^2} \text{ X } 13km^2 = 1.0397x\ 10^3 \frac{Ml}{year}$$

Seepage analyses on various TSF sites revealed an average SO_4 load of between 1006 mg/l to 4760 mg/l.

Different approaches are based on different calculations and so to calculation techniques. Each technique should consider the outcomes of the study. Analytical approaches make use of simplifying assumptions such as one-dimensional flow fields and simple source characteristics. Numerical models are usually applied when detailed mass flux data is simulated to evaluate the effectiveness of some remedial design at a large scale site. However, the accuracy of mass flux data based numerical modelling practices is dependent on the accuracy on the input data for flow and contaminant concentrations (ITRC, 2010).

Chapter 3: Methodology

3.1 Introduction

The investigation utilised data from previous literature on the contamination from similar Witwatersrand tailings facilities. Site specific data were collected during field investigations and analysed in order to generate usable input data for the numerical modelling phase of the study. A methodology was developed to assess the impact of tailings facilities on groundwater and surface water. The methodology is illustrated by means of a case study.

3.2 Pre-fieldwork (Desk study)

3.2.1 Pre-fieldwork

A detailed literature review and the collection of various records entailed the bulk of the office work that was conducted during the initial phases of the study. The literature review contained studies from both national and international sources with specific reference to the impacts of the mining industry on the environment. From the literature it was evident that the following points need to be addressed in order to delineate and model contamination:

- Literature review focusing on specific rainfall and recharge estimates of the local area as well as principles of groundwater and contaminant modelling. Reports on the area are also consulted to gain insight to the problem.
- A conceptual model is necessary to identify the key driving factors to both groundwater flow and contamination.
- A hydro-census is necessary to obtain information from boreholes on site. Aquifer tests can be conducted during the field work phase. Only relevant boreholes are used for testing and data gathering purposes.
- Site visits are important, where locational and elevation data (GPS Coordinates) is recorded.
- Digital Terrain Model (DTM) must be generated from field data and existing databases.
- Additional site visits will be made to measure groundwater levels, sampling of groundwater for chemical analyses and borehole testing.
- Groundwater level maps will serve as the initial hydraulic head in the models. These maps are created from measured head from the site boreholes and interpolated.
- An operational and decommissioned water balance is to be calculated based on the findings from Yibas et al., (2011) so as to quantify seepage volumes from the TSF that will be applied as a recharge flux.

- Seepage modelling values calculated from the operational and decommissioned water balances will be used as an input to the SEEP/W modelling package. This process will model the TSFs reaction to the volumes of water added during deposition as well as post-deposition. The modelling will determine a seepage flux at the base of the TSF that can be applied to the natural groundwater system.
- Modflow will be used for numerical modelling.

An inventory of all of the available records on boreholes in a regional study provided the necessary background information on the groundwater levels, borehole yields, depth to bedrock as well as the lithological units dominating the surficial aquifers. These data sets were used to understand the processes controlling groundwater storage and movement. Borehole information was obtained from the NGA (National Groundwater Archive) database.

3.2 Preparation of Conceptual Model

The conceptual model for a TSF consists of three distinct zones (embankment, beach and pool) that should be considered in the water balance calculation (Yibas et al., 2011). The hydraulic conductivity of these zones differ therefore the amount of seepage contribution from these zones will differ when combined into an overall water balance. Deposition tonnage and density is the primary factor to consider during the calculation of a water balance during a TSFs operational life (see Figure 25). Once deposition ceases the only water added to the TSF would be that of natural rainfall.

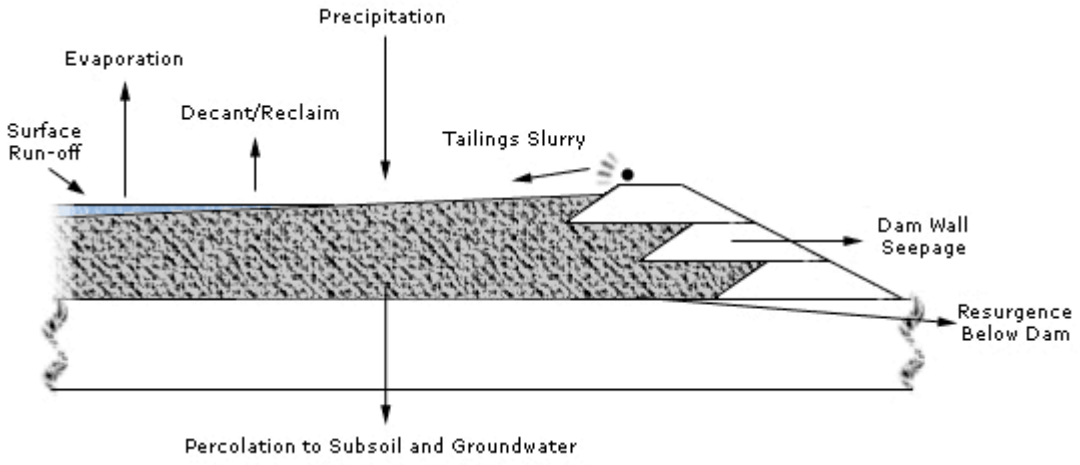

Figure 25: Typical conceptual model for a TSF illustration various components of a TSF water balance (Vick, 1990)

3.3 Field Work

The methods used during the field work were identified during the literature study and adapted accordingly so as to remain focused on the research objectives.

3.3.1 Hydro-census

A hydro-census in the surrounding area was conducted for additional boreholes for the purpose of field surveys and borehole testing.

3.3.2 Elevation data

Topographical elevation for the study area was extracted from the SRTM 90 DEM data. Groundwater elevation data was obtained in the field using GPS in conjunction with a level logger. Groundwater levels were obtained using a Solinst® 107 TLC (temperature, level, conductivity) meter. The Solinst® 107 TLC was also used to measure the changing head during the slug testing.

Static groundwater levels where measured as mbgl (meters below ground level) and converted to mamsl (meters above mean sea level). Once converted to mamsl the static water levels were used to determine the groundwater elevation of the study area by Baysian interpolation. Static groundwater levels are also used during the setup of a numerical model.

3.3.3 Water quality sampling

Water quality sampling was conducted on the boreholes in the surrounding areas so as to determine assess the current water quality. The following points summarize the water quality sampling:

- Collection of water samples from boreholes were conducted using a specific sampling bailer designed to capture a water sample at specific depths within the water column. Samples were collected in two litre polyethylene bottles and stored at cool temperatures.
- Water samples were analysed using ICP-MS. Samples were analysed at the North-West University's (NWU) laboratory.
- Concentrations of the various chemical compounds present in the water samples are used to characterise the natural water, using various graphical methods such as Piper plots and STIFF diagrams.
- Natural groundwater quality is also compared to seepage water found at the base of typical gold TSFs. Water quality data of the under-drain water from the Daggafontein and St. Helena TSFs were used for this purpose.

3.3.3 Aquifer testing

Aquifer testing is conducted to determine the hydraulic conductivity. The Bouwer & Rice (1976) method is used to analyse slug tests to determine hydraulic conductivity of an aquifer.

3.4 Data analyses

3.4.1 Seepage estimation

All the components that were considered in the water balance for the case study are shown in Figure 26.

- Typical design split achieved for underflow and overflow from cycloned TSF so as to determine the volumes deposited on the embankment and basin. Designed splits for the case study were taken at 70:30 (overflow / underflow).
- Designed deposition rates (2 100 000 tpm) are used to determine that volume of water that is placed on top of the TSF. From the deposited tonnage water content is derived using slurry densities. Slurry density used was averaged to 1.4 t/m^3.
- Overall footprint of the TSF; also divided into embankment area and basin area respectfully. Total area for the case study is 5 322 000 m^2; the footprint is further divided into an underflow area of 1 113 199 m^2 for the underflow (embankment) section and 4 208 801 m^2 for the overflow (basin) section.
- Volumes of water during deposition are calculated as a flux in m/day.

The water balance calculations are as follows:

$$S_{total} = S_{stored} + S_{infiltrated}$$

$$S_{stored} = \big((Q2 + Q3) - (Q6 + Q7)\big) - Q8$$

$$S_{infiltrated} = Q2 + Q3$$

$$Q6 = \big((Q2 - Q4) \times R\big) + Q5$$

$$Q7 = (Q3 \times R) + Q5$$

$$Q2 = (Q1 \times 0.70) \times 1.2m^3(Water)/ton$$

$$Q3 = (Q1 \times 0.30) \times 1.2m^3(water)/ton$$

$$Q4 = Q2 \times 0.83$$

$$Q5 = P \times R$$

$\Delta S_{overflow}$ = Infiltration rate in m/day

$\Delta S_{underflow}$ = Infiltration rate in m/day

$A_{overflow}$ = Total area covered by the basin in m^2

$A_{undeflow}$ = Total area covered by the embankment in m^2

P = Natural precipitation as a flux in m/day

R = Recharge rate (6% for underflow and 4% for overflow)

Q1= Planned deposition rate in tpm (tons per month)

Q2= Water deposited to the overflow section (basin) of the TSF in m^3

Q3= Water deposited to underflow section (embankment) of the TSF in m^3

Q4= Designed water recovery (Based on cycloned TSF's recovery) in m^3

Q5= Natural precipitation

Q6= Volume of water added to the overflow section i.e. Basin in m^3

Q7= Volume of water added to the underflow section i.e. Embankment in m^3

Q8= Seepage modelled in m^3/day

Infiltration rates where applied as a flux per day. Volumes calculated from the water balance were used to determine the input flux to the seepage modelling software. Fluxes were determined accordingly:

$$S_{overflow} = \left(\frac{Q6}{A_{overflow}}\right) \div 31\ days$$

$$S_{underflow} = \left(\frac{Q7}{A_{underflow}}\right) \div 31\ days$$

During the depositional phase the designed deposition rates remain at 2 100 000 tpm and the infiltration rate will remain constant. The infiltration rates are entered into the Seep/W software package as a flux rate as displayed in Figure 26. Seep/W runs the model under steady state conditions so as to calculate the seepage flux at the base of the TSF.

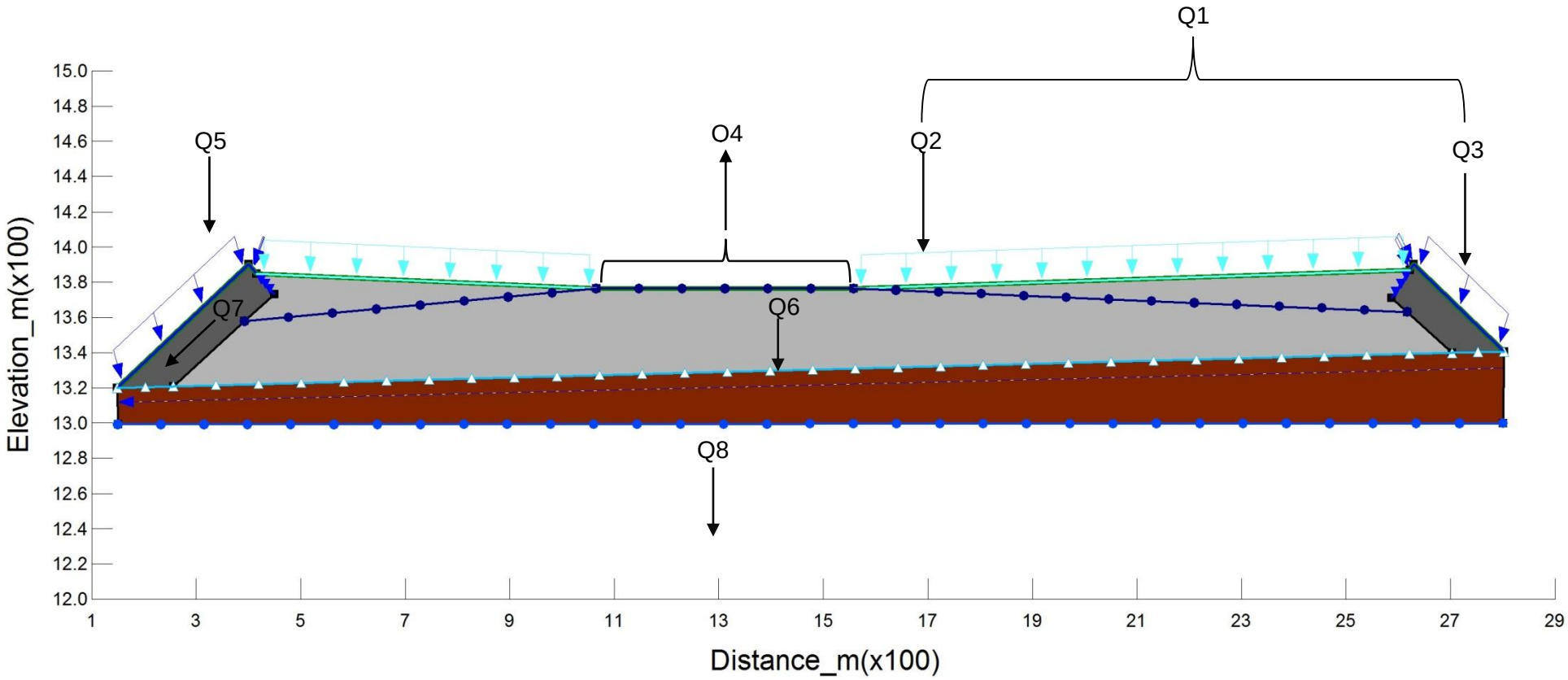

Figure 26: Conceptual model of Mega-tailings used in Seep/W

3.4.3 Groundwater contour mapping

Groundwater contour mapping renders insight as to the flow direction, groundwater gradient and possible pollutant migration within the saturated portion of the subsurface. The goal of any interpolation method is to estimate a variable of interest at an un-sampled location based on direct observations made at known sampling points. The Bayesian interpolation method was chosen to determine the groundwater level for the entire study area.

3.5 Numerical Modelling

3.5.1 Seepage modelling

Seepage is simulated through a 2D section of the TSF with a thickness of 1m (see Figure 27). The entire seepage from the facility is obtained by integrating the seepage flux from the 2D section with the total area of the TSF. Infiltration was applied as a flux on top of the TSF as calculated from the water balance. For the purpose of simulating seepage from the TSF the following materials were considered:

- The underflow will be the annulus of the TSF.
- The overflow will be the core of the facility.

Figure 27: Aerial view of case study illustrating 2D cross-section for seepage modelling

3.5.2 Groundwater flow and mass transport modelling

MODFLOW (using the PMWIN interface) has the ability to perform both steady state and transient modelling and can simulate various boundary conditions. A module in the PMWIN package is MT3DMS which is used for contaminant modelling.

Contaminant mass discharge estimation is used to assess the total of discharge of contaminants into the regional groundwater and surface water bodies at a specific location. Focus is placed on SO_4 as well as Cl that enters the natural groundwater system these contaminants are indicative of gold mine tailings contamination. Transects through the contaminant plume were taken at strategic points identified during the solute transport modelling phase. Transect locations were selected in the directions where the contaminant plume concentrations were the highest and the risk to surface water contamination was the greatest. Mass discharge utilises the groundwater flux across the entire area of the transect; groundwater fluxes were obtained using the water budget calculation in PMWIN. Zones are assigned to the specific transect and a groundwater flux value is obtained.

Once the groundwater flux is determined, the contaminant concentrations established during the solute transport modelling will be multiplied with the total groundwater discharge across the entire transect face for the specified time period and an overall contaminant mass discharge calculated.

3.5.3 Modelling assumptions

Due to the complexity of any natural groundwater system it is necessary to determine several simplifying assumptions so as to simulate groundwater in the most accurate way possible. Assumptions keep the modelling process focussed and support accurate calibration of the numerical model, including:

- Groundwater flow is described using Darcy's law e.g. water with a higher potential moves to a location with a lower potential.
- Aquifer heterogeneity as well as the presence of faults and fracture zones will cause a change in the hydraulic conductivity throughout a study area.
- Recharge from precipitation is spatially uniform.
- Boundary conditions are assumed in the model setup: rivers are considered as fixed head boundaries.
- The base of the TSF is the primary source of contaminants entering the groundwater system through seepage.

- Location of the pool in the centre of the TSF is considered to be a time-variant fixed head boundary as permanent pool conditions prevail on a TSF during depositional phase. The head also varies with time as the facility constantly rises during deposition.
- No pool is simulated once deposition ceases.

2 Chapter 4: Mega tailings investigation

4.1 Background

With pressure from government to rehabilitate old mining operations, reclamation projects such as these are gaining popularity in order to recover any remaining gold/uranium left behind by obsolete mining operations. Reclamation of tailings also has the advantage of rehabilitating mining sites for alternative land use.

It is important to note that the case study is based on data available in the public sector and a hydrocensus and therefore only serves as a demonstration of the developed method. There are a number of short comings in the data including:

- Detailed information regarding lineaments which can lead to uncertainty due to the complexity thereof and the potential impacts on groundwater flow directions and the associated movement of contaminants. A detailed geophysical investigation and study of borehole logs is necessary to address this issue. Unfortunately, no borehole logs were available for this study.
- As the SO_4 concentration of the source is an unknown – only the groundwater flow model was calculated and not the mass transport model. Detailed sampling and leach tests are should be conducted and the results thereof can then be used to calibrate the mass transport model.

4.1.1 Locality

The mega tailings facility is located in the greater Klerksdorp – Orkney – Stilfontein – Hartbeesfontein (KOSH) mining area in the North West Province (Figure 28) in South Africa. The natural topography of the region has a moderate slope in a north east and south west direction (see Figure 29). Elevations range from 1340 mamsl on the eastern border of the study area, flattening to 1300 mamsl in the south. The south western corner of the study area is the lowest point and it is evident that drainage is toward this corner as there is a temporary marsh in the direction of the Vaal River. The property lies quaternary catchments C24A and C24B.

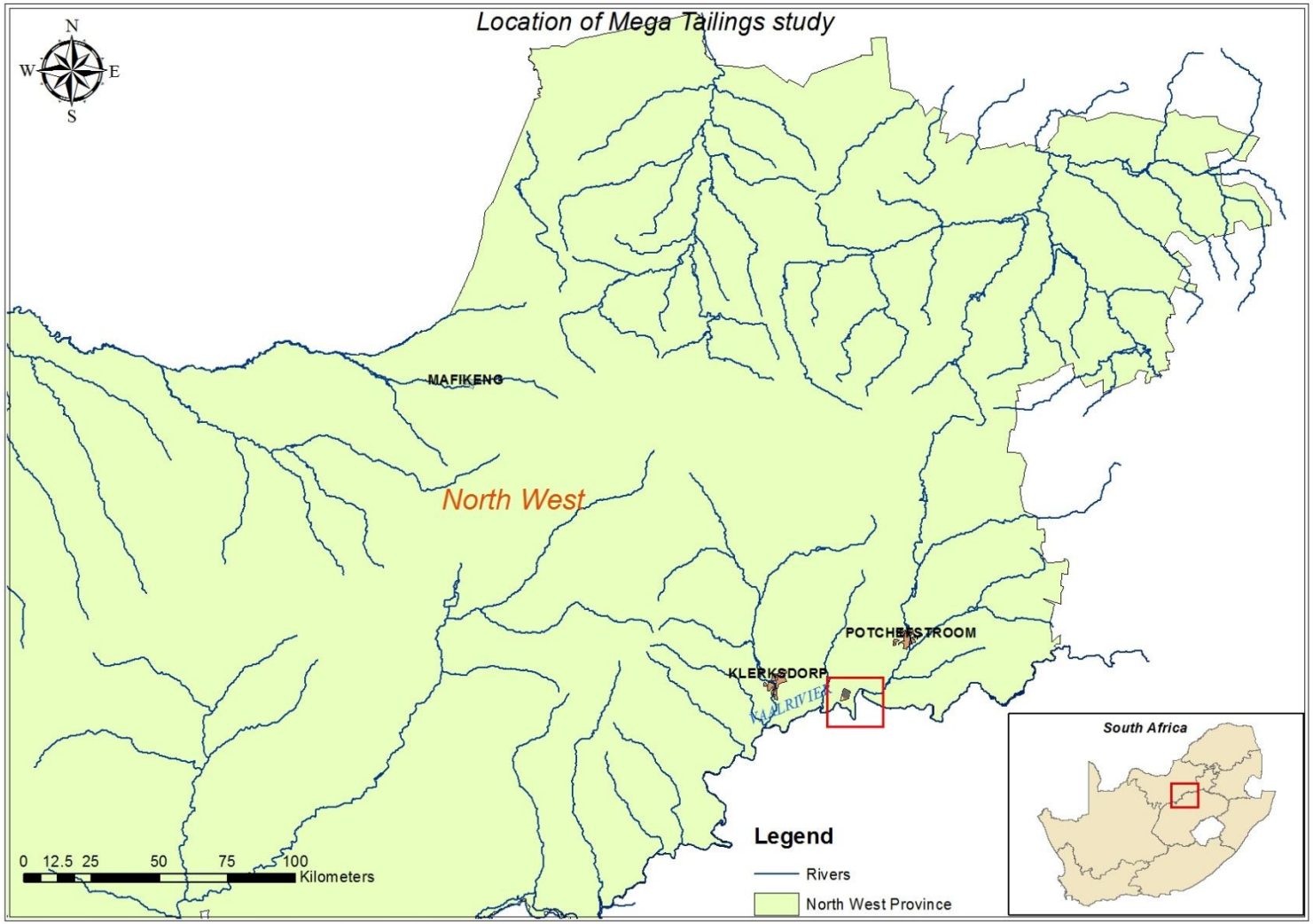

Figure 28: Location of the mega tailings case study

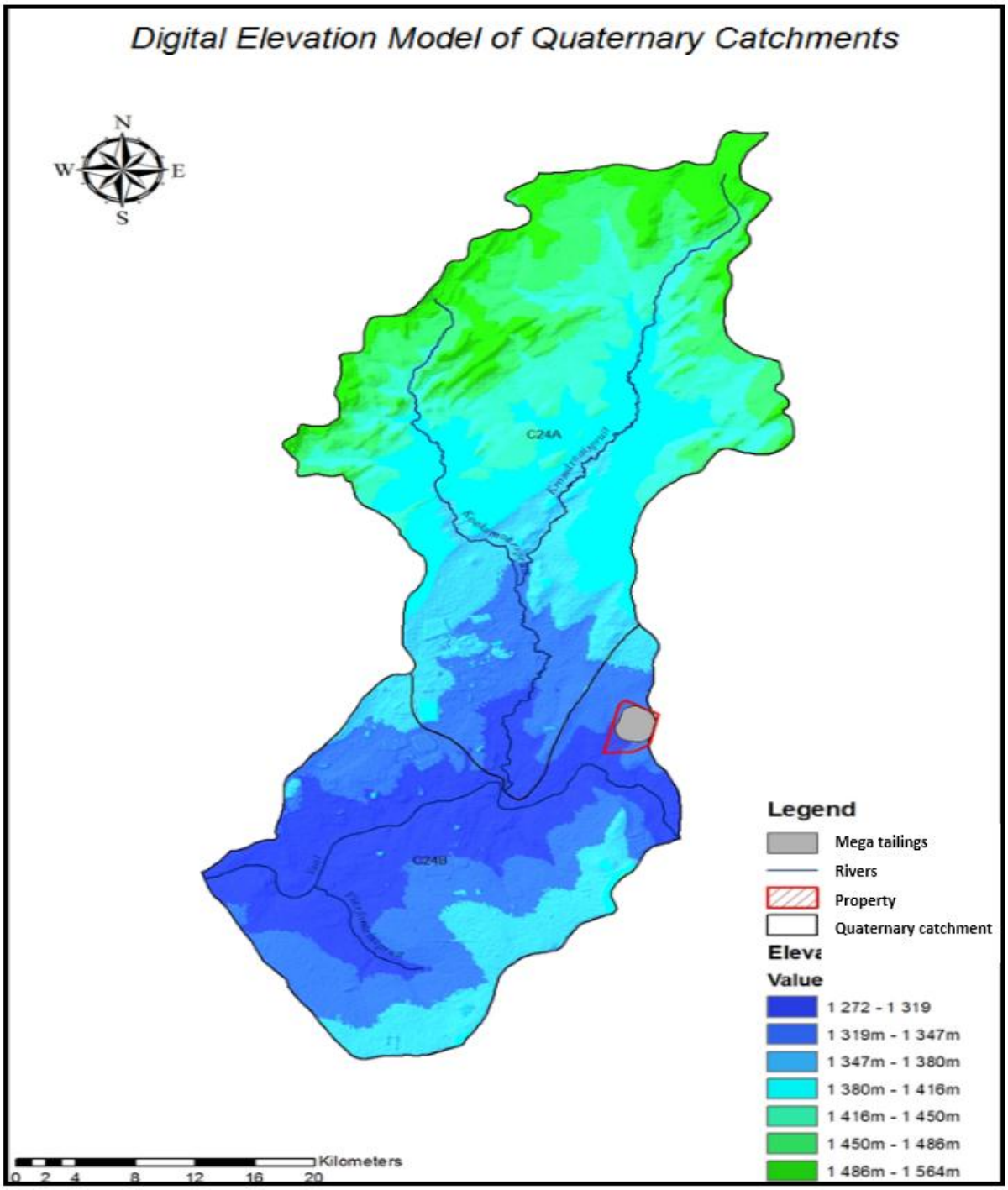

Figure 29: DEM based on the SRTM 90 elevation data for the mega tailings study area (Jarvis et al., 2008).

4.1.2 Vegetation and land use

The natural vegetation in the area is mainly indigenous grasslands unique to a savannah landscape with sparsely spaced acacia trees. The site has been used for game farm and cattle farming because of the grazing potential that the grasslands provide. Crops (mainly maize) are also grown using groundwater driven pivot irrigation.

4.1.3 Climate

The area is mainly a summer rainfall area with high temperatures in the range of the mid thirty degrees during the day. Winters are dry and cold with temperatures below zero during the evenings and day temperatures of mid-teens as cold fronts move over from the south of the country. Precipitation during the winter drops to almost zero, however occasional rain may occur as cold fronts move over. The mean annual precipitation (MAP) of the study area varies between 401mm in drier years and can reach as high as 600mm in a “wet” year (Figure 30).

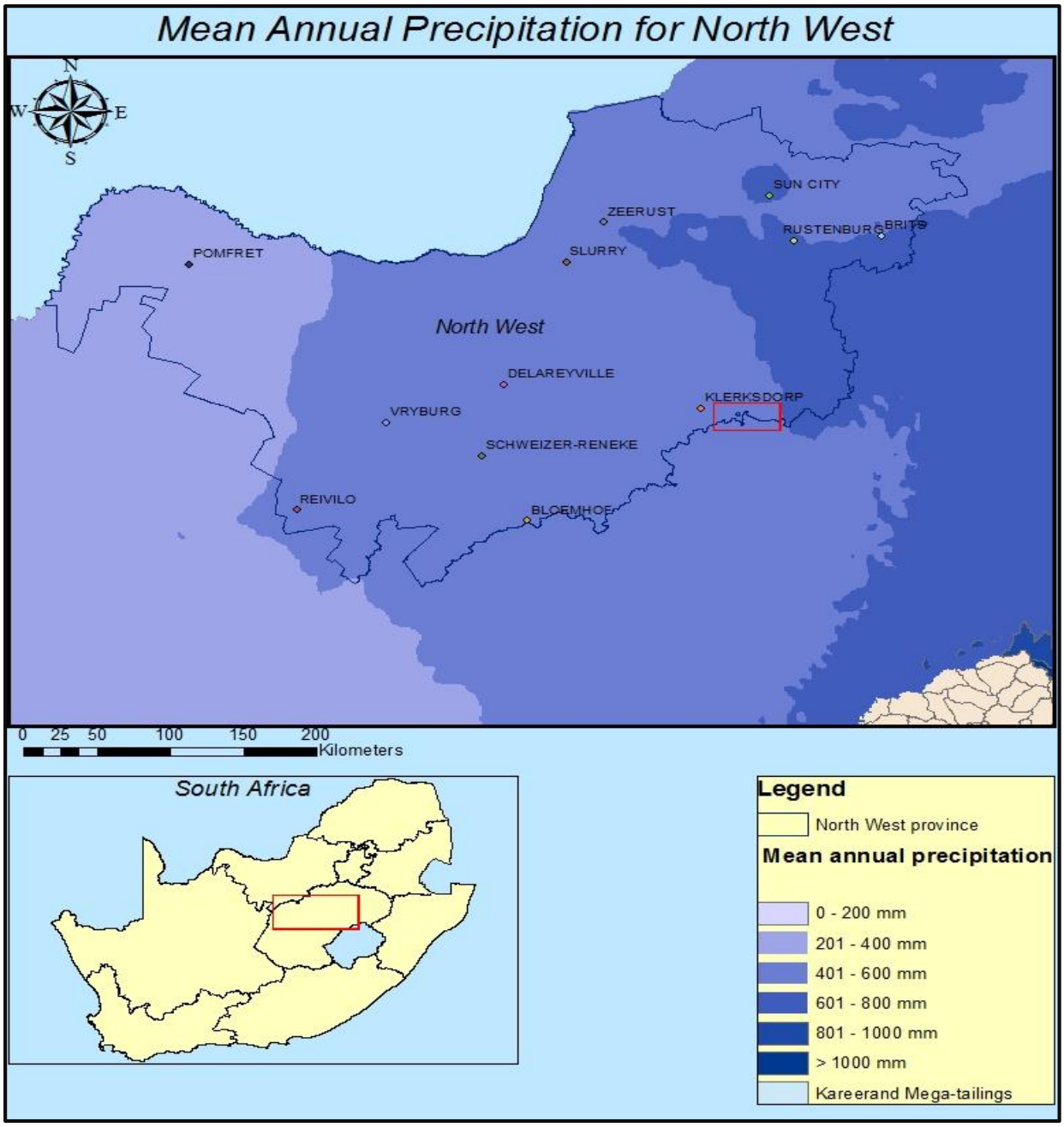

Figure 30: Map of the Mean Annual Precipitation of the North West Province (SAWS, 2001)

The monthly rainfall figures for Potchefstroom, located close to the mega tailings study area are displayed in Figure 31. These figures are representative of the total seasonal rainfall for the greater Potchefstroom area. The seasonal average for this area is at 431mm per year.

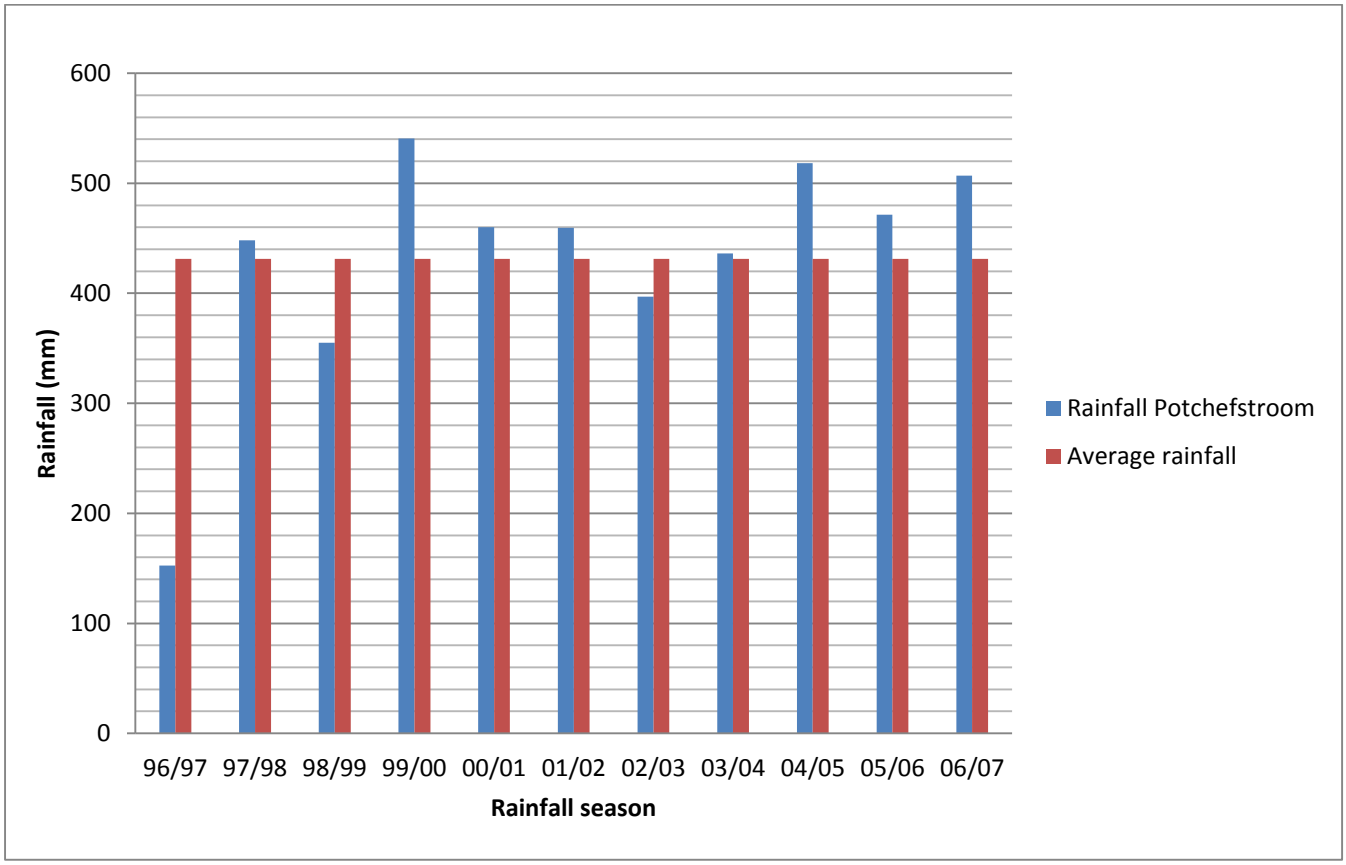

Figure 31: Seasonal rainfall for the Potchefstroom area (SAWS, 2007)

4.2 Tailings construction and recovery

The mega tailings facility is constructed from recovered (re-mined) tailings material from previous mining operations. Tailings are sprayed with high pressure water jets in a sweeping action from top-to-bottom in order to release the consolidated material from the embankments (Figure 32). Once released the slurry flows by means of gravity flow trenches to the metallurgical plant for gold recovery. Once treated at the plant, the remaining tailings are pumped to the facility and deposited using cyclones on the perimeter of the embankment of the tailings facility.

Figure 32: Recovery of mine tailings using high pressure jets in a top-to-bottom sweeping method (Robinson, 2009)

4.2.1 Construction

These mega tailings facilities are constructed using cyclone deposition on the perimeter of the dam so as to classify the residue tailings into two streams. The underflow (coarse material) is used for embankment construction and is placed on the outer perimeter where the fine overflow is pumped from the top the cyclone toward the centre of the dam where it will from the beach (see Figure 33).

The coarser material is used in the embankment as it has superior geotechnical stability therefore fulfilling the role of a containing wall to impound the fine overflow and subsequent supernatant water at the centre of any tailings facility.

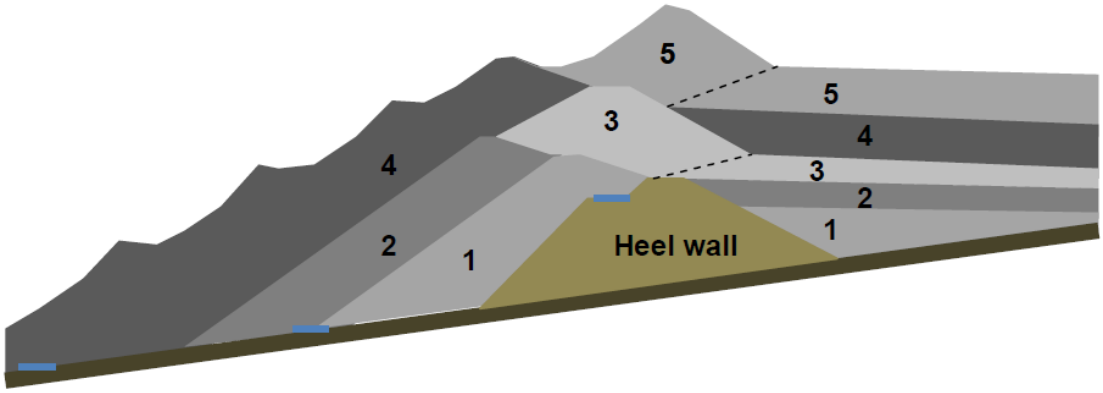

Figure 33: Cross-section of a mega tailings facility depicting the deposition sequence and slope development

The development of the embankment and beach will be combination of downstream and upstream deposition sequences; providing a large stable foundation and sufficient freeboard to accommodate the large tonnages. Initial deposition of the fine overflow has to occur behind an earth starter wall to ensure the stabilisation and formation of a sufficient embankment downstream. Once the overflow has covered the heel wall there will be enough underflow material to support and contain the fine slurry within the embankment. It is for the advantage of stability that the first two deposition phases of the tailings facility will be in the downstream sequence, establishing a wide base where after upstream deposition will form the final slope profile.

4.2.2 Deposition

The study will focus on all the phases of TSFs lifetime e.g. construction phase, operational phase and dormant phase. Therefore, it was decided to conduct simulations on specific time periods that would be indicative of the phase at that time. The simulation will be conducted at six time periods at: 18, 68, 138, 168 (operational phase), 240, and 1200 (post-depositional phase) months after final closure of the facility. An average deposition rate of 2 100 000 tpm was used with a final capacity of 352 000 000 tons, reaching a maximum height of 1390 mamsl (see Figure 34).

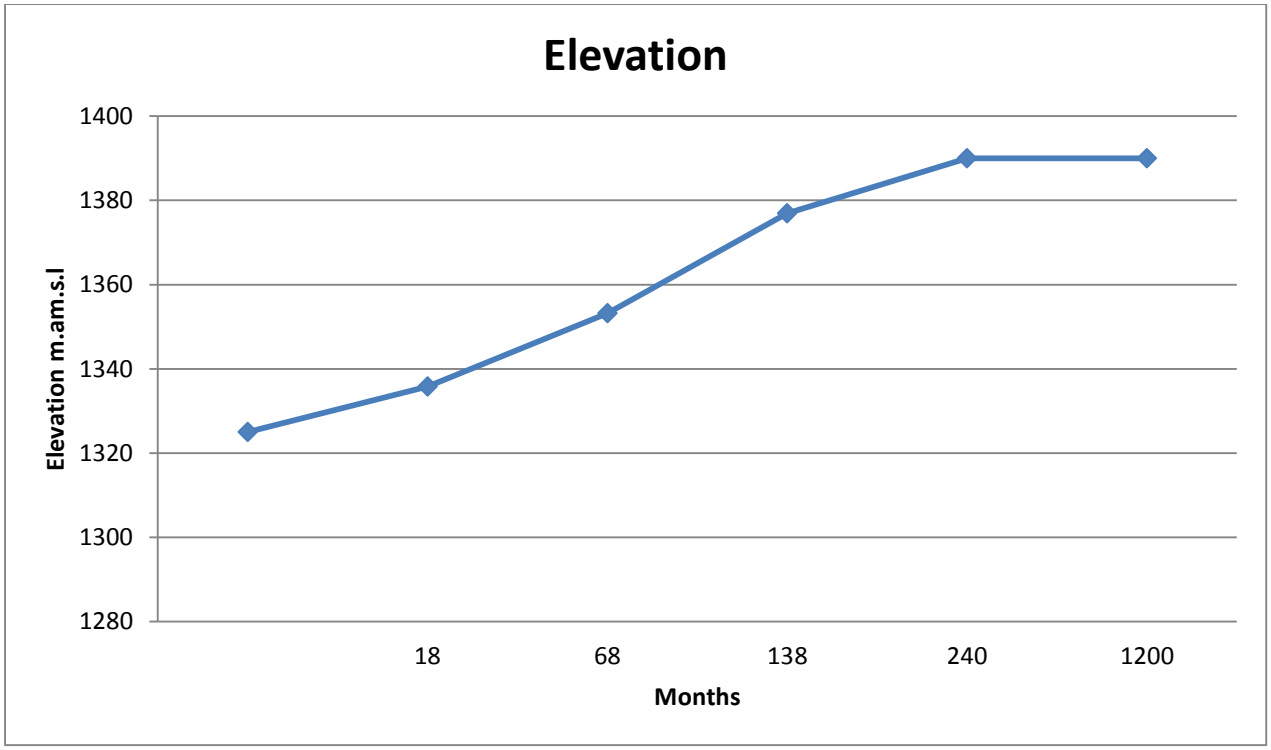

Figure 34: Evolution of the elevation during the lifecycle of TSF

With the targeted deposition rates, an average in-situ dry density of 1.4t/m^3 and the overall footprint of the tailings facility various calculations can be made with regards to the geometry,

capacity, rate of rise and surface area. With the facility being a cyclone operation the designed classification for the cyclones is important, as this will determine the amount of tonnes placed on the embankment (underflow) as well as the amount used for beach formation.

Based on figures from other cyclone operations such as the ERGO (Pty) Ltd. tailings in Brakpan, and the St Helena tailings in Welkom, it was decided to use a 70:30 split or classification capability. Seventy percent of the material being overflow and thirty percent deposited into the embankment as underflow. Figure 35 illustrates the probable growth of the TSF under investigation with the cumulative volume increase as deposition continues throughout the operational lifetime of the facility.

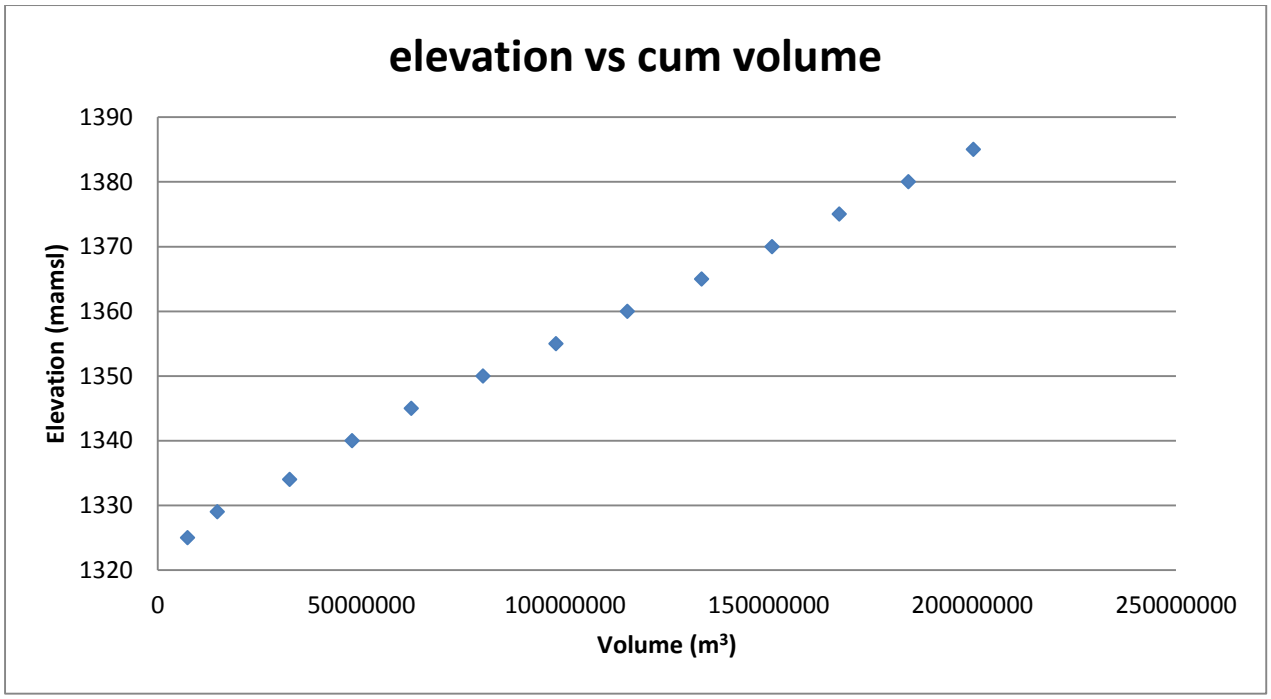

Figure 35: Excel graph illustrating the incremental rise of the TSF with the increase in volume deposited

The shape of the elevation/surface area of the cyclone facility follows much the same trend as conventional ring dyke dams, thus that the surface area will decrease with each “step-in” cycle. However, the initial increase in surface area at the first two cycles of the TSF is indicative of an upstream (brown circle) and downstream (blue circle) cycle indicated in Figure 36. The slight scallop shape of the various deposition cycles can be seen from the graph (green circle). All the design characteristics are representative of the various changes during the lifetime of a tailings facility and should be considered when modelling these phases.

Additional sources of water to the facility will be mainly from the cyclone underflow and overflow. The only sink that is considered from a conservative view (assuming no under drainage systems are installed) is direct seepage to the natural aquifer.

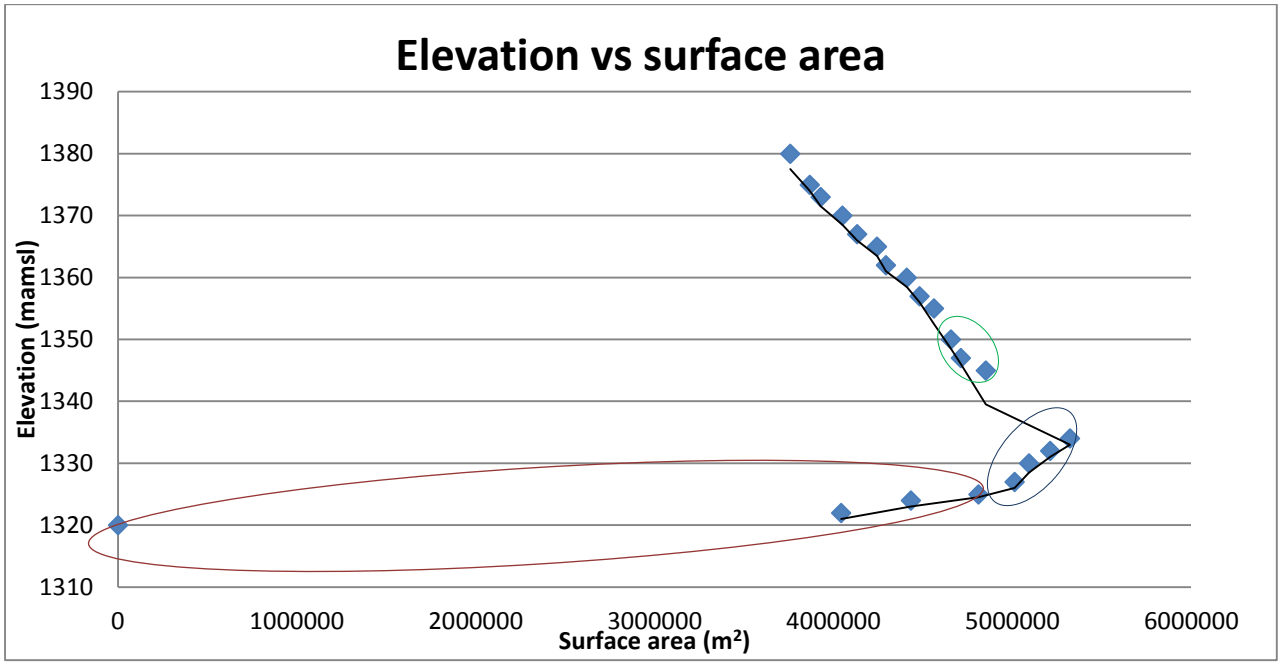

Figure 36: Excel graph illustrating surface area evolution of the TSF with each deposition cycle

4.3 Conceptual model

The model consists of two major factors controlling the overall character of the regional groundwater flow in the study area; the first of which is the natural aquifers system that consists of the geological formations and the second is the mega-tailings facility that will artificially recharge the natural groundwater system as a result of the continual hydraulic deposition of tailings atop the facility.

The VWC and SWCC of the tailings material was derived from the particle size grading tests done on the tailings from the Chemwest no.5 TSF located in Stilfontein (Robinson, 2009). Values from the Chemwest no.5 TSF can be used to estimate the porosity, hydraulic conductivity and permeability of the tailings with acceptable accuracy as the material from Chemwest no.5 will eventually be re-mined to form part of the mega-tailings facility (see Appendix B for grading curves).

Table 2: Hydraulic conductivity calculated from the D_{10} particle size at saturated conditions (Robinson, 2009)

Description	D_{10} (particle size)	Porosity (Saturated VWC)	K_{sat} (mm/sec)	K_{sat} (m/day)	K (m/day)
Underflow material (Coarse)	0.007	0.50000	0.0049	0.42336	0.042
Overflow material (Fine)	0.0022	0.40000	0.000484	0.04182	0.004
Foundation (Alluvium)	0.0001	0.38462	0.000001	0.0000864	0.000009

Hydraulic conductivities for the different zones at saturated conditions were determined using Hazen's formula. Where the hydraulic conductivity $K= (10D_{10})^2$. The D_{10} particle size was taken from the PSD curves developed by Civilab on samples taken from the Chemwest no.5 TSF.

4.3.1 Natural aquifer

The natural groundwater system is controlled by the various lithological units present in the study area. The eastern side of the study area is dominated by a sequence of hard rock aquifers of later magmatic events. To the west, directly below the stream is dominated by the carbonate rocks from the Malmani sequence (see Figure 37). The entire stratigraphy dips in an anticlinical structure toward the east. Each of the lithological units are described separately below as each has different ways of storing and transporting groundwater owing to their unique geological character and mineralogical properties.

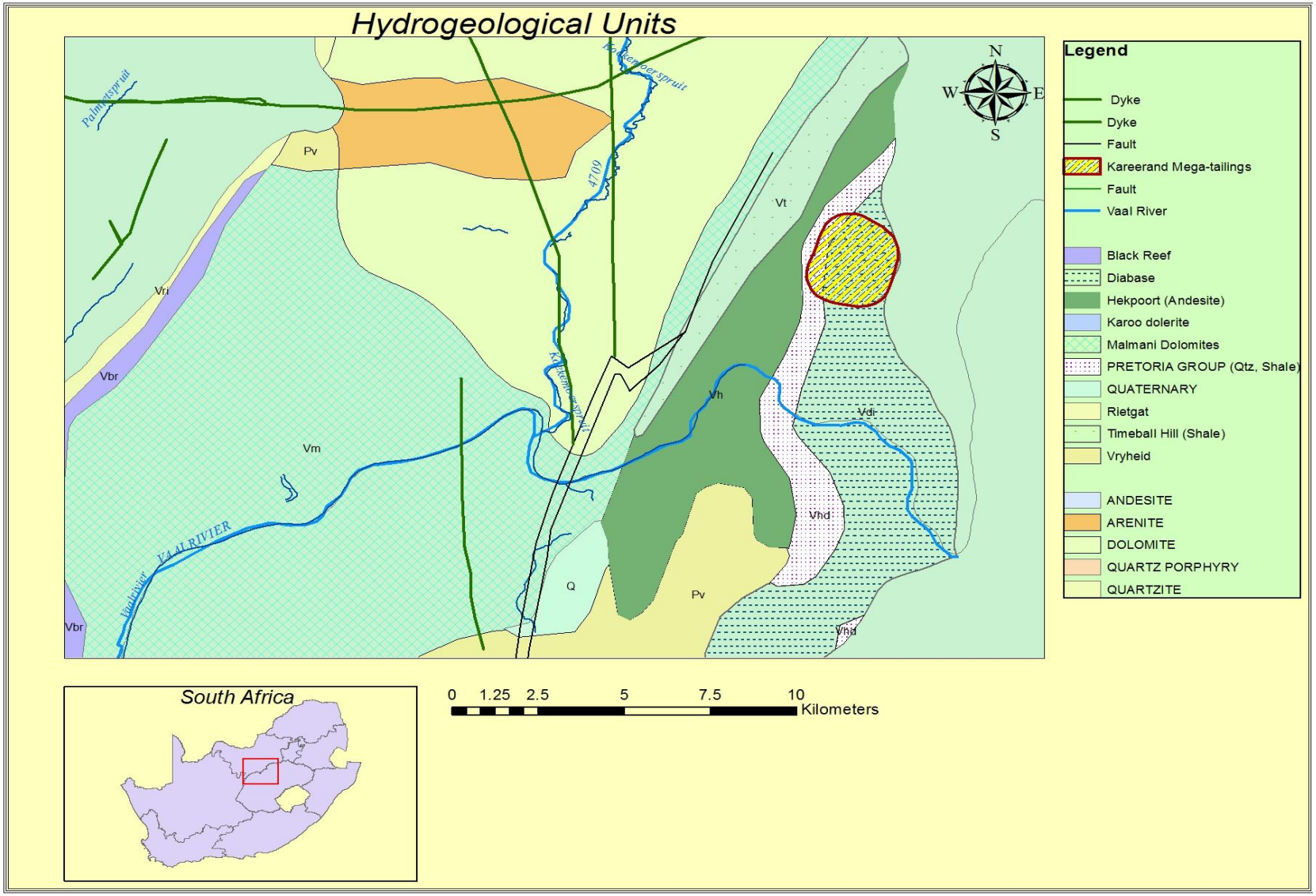

Figure 37: GIS map showing the arrangement of Hydrogeological units encountered at the mega tailings study area (CGS, 2014)

Upper fractured diabase sill: The diabase sill occurs at varying depths from 1mbgl to 120mbgl and consists of weathered and fractured diabase. The formation is a result of an earlier intrusion between the hard andesitic lavas of the Pretoria Group, however unconfined conditions exist and groundwater migration is found to be within internal fractures and contacts between the diabase sill and the host rock (andesites).

Contacts are planes where younger intrusions have caused a discontinuity in the matrix of the host rock. These intrusive bodies crystalize under high pressures and temperature, far greater than the conditions during the time of intrusion, thus resulting in a massive rock matrix that is devoid of primary porosity and a complete difference in mineralogy compared to the host rock. Contacts are smooth planar surfaces between two rocks of different mineralogical character, in much the same way that water and oil would create a contact surface due to the difference in material properties.

Fractured igneous aquifer:

Pretoria Group

The Pretoria Group of the Transvaal sequence has three inter-bedded volcanic formations of importance:

- Bushy Blend Lavas
- Timeball Formation
- Hekpoort formation

The location of the mega tailings is directly underlain by the andesitic basalts of the Hekpoort Formation, Pretoria sequence, Transvaal Supergroup. Andesites are intrusive magmatic events where magma flows or intrudes into the country rock. The rapid cooling of the magma results in a black massive texture that has no clear crystals as part of the matrix apart from amygdales that once was mineral rich gas bubbles. These rocks occur most commonly as large dykes and sills and have virtually no permeability.

A geohydrological assessment by Kruidenier (2010) supports this occurrence. During the assessment boreholes drilled into the Hekpoort andesites of the Pretoria Group were investigated. During aquifer testing, borehole logs were also assessed in order to determine the main water bearing features. The logs revealed that the first 4m were debris typical of hillwash, followed by weathered andesite gravels as well as weathered andesite to the depth of 20m, below 20m hard rock andesite was encountered. The three boreholes tested in the study had water strikes at depths of 13m.

The majority of the Pretoria Group is classified as an inter-granular and fractured aquifer system. For this reason, the water bearing features of the Pretoria Group is regarded as a low to moderate yielding aquifer system consisting of hard rock, with borehole yields ranging from less than 2 l/s to yields exceeding 5 l/s. The majority yields seem to be less than 2 l/s. Aquifer tests conducted by Kruidenier (2010) on boreholes located within the Hekpoort Formation in the Vereeniging area had a mean hydraulic conductivity of 0.032 m/d. The maximum aquifer thickness was approximately 25m. Boreholes located (BH6) in the Hekpoort andesitic lavas at the mega tailings site showed a slightly lower conductivity in the range of 0.077 m/day.

Hard rock aquifers (typically igneous and metamorphic rocks) owe their water bearing properties to fracturing and contact variances in mineralogical character. Igneous rocks such as the lavas found in the Hekpoort andesites are classified as poor aquifers with very low porosity and transmit or store little water within the matrix of the rock formation.

The primary flow of water is confined to anisotropy in mineralogical properties, fractures and joints. Fractures and joints are planes where external forces (tectonic, lithostatic) have caused a partial loss of cohesion in the rock resulting in “cracks” within the matrix (Singhal & Gupta, 1999).

Lower Malmani dolomitic aquifer: The dolomitic aquifer of the West and Far West Rand (FWR) covers an area of roughly 14000km^2. The dolomites of the FWR have been the focus of many studies with regards to dewatering for deep shaft mining operations. Dewatering of the dolomitic compartments started in the late 1950s. During this operation it was noted that the sequence is highly compartmentalised by intersecting dykes and sills. Dolomites are located to the west of the study area, directly below the Koekemoer Spruit. The Malmani sequence has varying quantities of chert and dolomite giving rise to highly heterogeneous water bearing features as a result of preferential weathering.

The quartz rich chert remains almost completely intact in the form of large slabs. Chert mainly breaks up by mechanical action and tectonic stresses as it loses support from the surrounding carbonate rocks that is removed by dissolution.

Natural percolation of acidic rain water through the fractures will lead to larger dissolution karst close to the surface. This continual percolation and neutralisation of dolomite will increase the permeability of the upper sections of the aquifer, reducing gradually with depth as the reaction runs to completion and no more dissolution can occur.

4.3.2 Recharge

Recharge in the KOSH area varies between 6-12% of the mean annual precipitation (L&W Environmental, 1993).

L&W Environmental (1993) have identified three major water tables in the area:

- Perched water table at the interface between soils and weathered rock, which will fluctuate seasonally and has an average depth of 1-3m below surface.
- The fractured rock aquifer of the Malmani dolomite with the natural water level varying between 5-100m below surface.
- The third is a deep, artificial aquifer in the mine void itself and represents the level of controlled flooding in the mine workings.

4.3.3 Borehole investigations

The geographical location of boreholes selected for aquifer testing and investigations are illustrated in Figure 38.

Figure 38: Google earth image depicting the locality of boreholes identified in the hydro census.

Water level monitoring was conducted at the various selected boreholes on the site in order to determine the predominant direction of flow.

Analyses of the borehole tests are attached in Appendix C. A summary of hydraulic conductivities are listed in Table 3 and the associated transmissivities are documented in Table 4.

Table 3: Hydraulic conductivities of boreholes at the mega tailings site

Borehole ID	Depth to water table (mbgl)	Hydraulic conductivity (m/day)
KR1	12.30	0.083
KR2	6.72	0.770
KR3	18.70	0.117
BH5	11.22	0.720
BH7	9.80	0.104
BH8	13.65	0.560

Table 4: Transmissivity values for the various hydrological units

Hydrological unit	Thickness	Transmissivity ($T = k \times d$) ***T*** **=** Transmissivity ***k*** = Hydraulic conductivity ***d*** = Aquifer thickness	Aquifer Type
Vdi = Diabase Sill (magmatic intrusion)	Approx. 120m	9.96 m^2/day	Fractured Rock
Vhd = Residual weathered andesite *(Pretoria Group, Transvaal Sequence*)	Approx. 120m	14.04 m^2/day	Fractured and weathered Rock
Vm = Dolomite (Malmani Dolomites)	>120m	Variable > 100 m^2/d	Carbonate Rock
Contact zones	Approx. 120m	360 m^2/day	

4.4 Water quality results

A total of three boreholes were sampled during the field investigations. Boreholes were predominantly located on the south-eastern of the TSF. Additional monitoring data collected during the EIA process (Menghistu, 2009) for the mega tailings facility were also included so as to gain a comprehensive representation of the groundwater quality in the study area.

Under drains are located at the base of any TSF, with the primary function of improving the drainage of excess water from the centre of the impoundment. These drains are installed at the start of deposition and remain installed for the lifetime of the TSF. Except for drainage these under drains give researchers an opportunity to evaluate the quality of water at the base of the impoundment. Water quality analyses on under drainage water from the Daggafontein TSF are listed in Table 5.

This facility utilises the same deposition method and tailings material therefore it would be the most accurate representation of the seepage water quality.

All the boreholes sampled where compared with the recommended concentrations for domestic use according to the SANS 241 standards (SANS, 2011). This standard classifies water into two major categories:

- Class 1: Acceptable domestic water for lifetime consumption (SANS, 2011).
- Class 2: Can be tolerated for a limited period of use only (SANS, 2011).

Sampled boreholes showed virtually no signs of external contamination except elevated Ca and HCO_3^- concentrations. These elevations are due to the dominant presence of dolomitic rock formations in the immediate area (Chapter 2). Concentrations of cations and anions for the all the boreholes are listed and compared in Table 5. Water quality analyses of boreholes from the mega tailings study site are listed in Table 6.

Table 5: Concentrations of major Cations and Anions from borehole samples at the mega-tailings study site

Sample No.	KR 1	KR2	KR3	BH3	BH5	BH7	BH8	Class 1	Class 2
mg/l									
Ca	63.1	13	16.8	59	59	79	54	150	300
Mg	33.7	30.1	12.4	34	35	38	25	70	100
Na	4.7	10.8	4.9	21	26	15.9	16.9	200	400
K	3.4	10.3	1.2	1.8	2.5	0.9	2.5	50	100
Mn	0.09	0.24	0.04	0.001	0.004	0.001	0.1	0.1	1
Fe	0.17	5.05	0.22	0.007	0.43	0.01	0.19	0.2	2
F	na	na	na	0.1	0.1	0.05	0.1	1	1.5
NO_3	86.1	0.17	1.1	16.7	9	12.9	19.6	44	88
PO_4	0.06	0.17	0.06	na	na	na	na	-	-
Cl	25.28	54.07	7.81	6.1	8.8	10.4	11.3	200	600
SO_4	20.01	0.67	0.66	14.9	2.3	3.5	3.5	400	600
TDS	429	512	179	432	358	486	366	1000	2400
Alk	240	295	132.5	277	275	305	191	-	-
pH	7.31	7.19	7.51	8.7	7.8	8.6	8.3	5.0-9.5	4.0-10.0
EC	67	80	28	64.4	55.9	71.7	54.3	150	370

Green = Class 1

Yellow = Class 2

Red = Exceeds maximum allowable drinking water standard

na - not analysed

Table 6 : Concentrations of Cations and Anions of under drain water from the Daggafontein TSF (Robinson, 2009)

Sample No.	No.2	No.11	No.17a	No.20	No.29	No.33	No.37	Class 1	Class 2
mg/l									
Ca	619	581	645	495	463	486	485	150	300
Mg	50	61	51	82	220	626	126	70	100
Na	295	294	293	316	274	286	296	200	400
K	67	74	67	61	85	99	78	50	100
Mn	9.2	9.4	2.9	14	67	31	30	0.1	1
Fe	3.7	0.03	0.05	0.09	400	300	86	0.2	2
F	0.7	1	0.7	0.8	0.05	0.8	0.5	1	1.5
NO_3	0.2	0.2	0.3	0.2	0.3	0.3	0.3	44	88
PO_4	na	na		na	na	na	na	-	-
Cl	352	373	372	377	358	364	361	200	600
SO_4	1886	1962	1898	1852	4351	4053	2476	400	600
TDS	2850	2900	2860	2810	2580	4250	3210	1000	2400
Alk	25	95	30	136	67	<5	20	-	-
pH	6.5	6.7	8.1	6.4	4.7	5.5	5.7	5.0-9.5	4.0-10.0
EC	4.45	453	447	4.39	4.04	6.64	5.02	1.5	3.7

Green = Class 1

Yellow = Class 2

Red = Exceeds maximum allowable drinking water standard

na - not analysed

Stiff diagrams are graphical representations of chemical analyses of a water sample, first developed by Stiff (1951). This method is widely used by geochemists and hydrologists to analyse the major cation and anion concentrations of a water sample. Stiff diagrams find their use when performing rapid comparison of various water samples to determine a samples origin. Therefore, samples sharing the same origins will most probably have the same polygonal shape when plotted on a Stiff diagram. Stiff diagrams illustrating the balance of major cations and anions found in boreholes at the study area are shown in Figure 39. Stiff diagrams are used as an instant visual tool for the geochemical characterisation of different water types. As expected the samples show extended area occupied by the Ca and HCO_3.

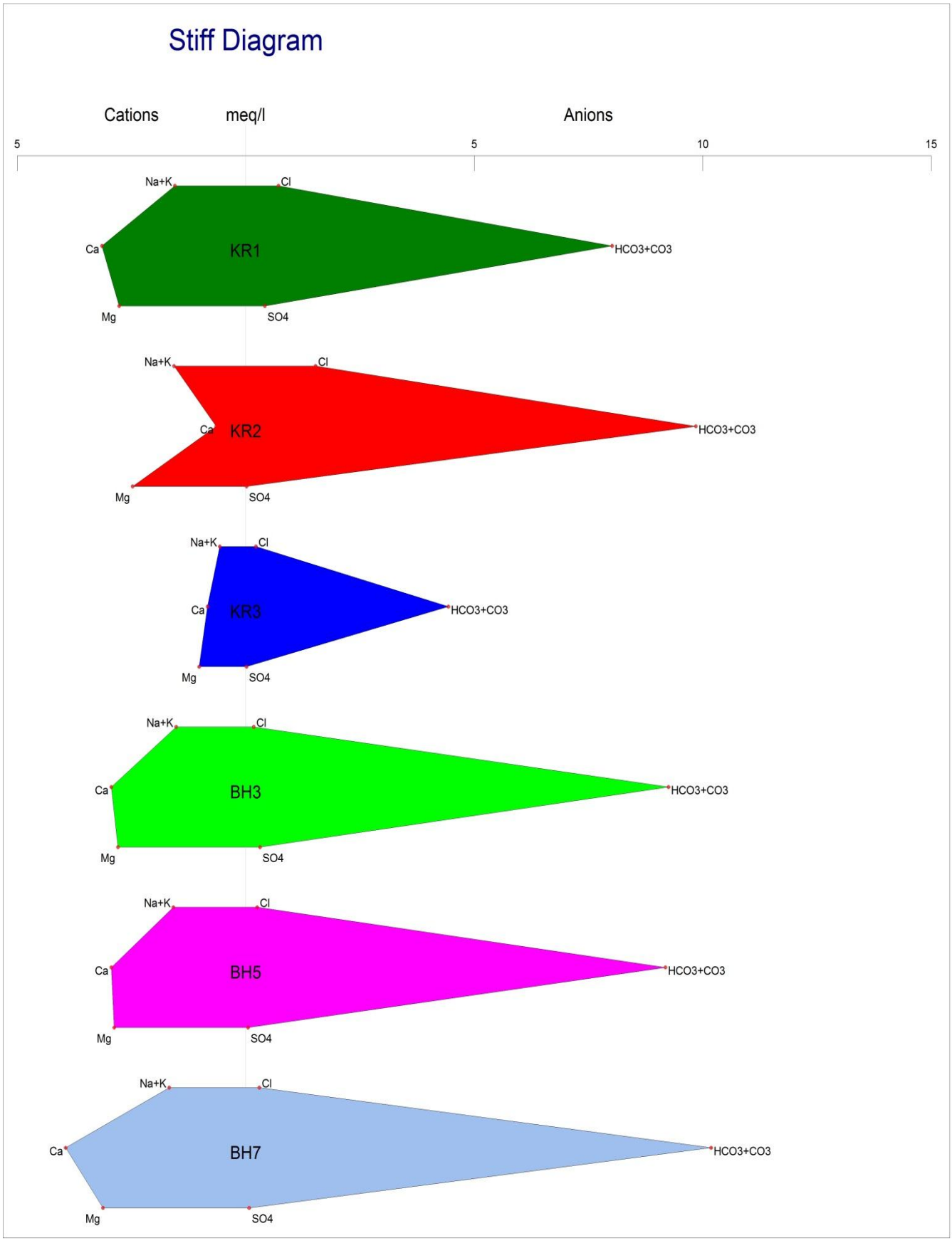

Figure 39: Stiff diagrams for boreholes located in the mega tailings study area.

Scott (1995) used Piper diagrams to characterise two distinct groundwater types in the East Rand. The Piper diagrams of the groundwater samples indicated that there was Ca-Mg-HCO_3 and Ca-MgSO_4 dominance in the major cat- and anions present. Scott (1995) concluded that the samples with a Ca-Mg-HCO_3 dominance is indicative of influenced by the dissolution of carbonate rich mineral i.e. dolomitic aquifers. Scott (1995) also reported that the alkalinity concentration of these groundwater types could exceed groundwater standards.

In contrast groundwater quality dominated by Ca-Mg-SO_4 signature and high levels of TDS are indicative of tailings discharge areas related to the reaction of AMD and dolomite (Palmer, 1992). The anion signature reflects a progressive dominance from HCO_3 toward SO_4 as the oxidation of the sulphate mineral increases.

Rösner (2007) reported that groundwater quality in the immediate vicinity of TSF footprints were found to be dominated by Ca-Mg-SO_4. Groundwater quality improves further downstream of the TSF footprints, however this is attributed to the dilution effect and the strong neutralisation capacity of dolomitic aquifers. Sulphate concentrations in the immediate vicinity of the TSFs still remained above 2000 mg/l.

With reference to the Piper diagram (Figure 40) it is evident that all the water samples fall within the Ca-Mg-HCO_3 dominated water classification type. This is expected from groundwater associated with dolomitic aquifers. Piper diagrams (see Figure 40 and Figure 41) of the dominant cat- and anion concentrations from the mega tailings study site were compared to seepage water from the Daggafontein TSF. The water samples were obtained from boreholes in the vicinity of the mega tailings site as well as the under drains of the Daggafontein TSF.

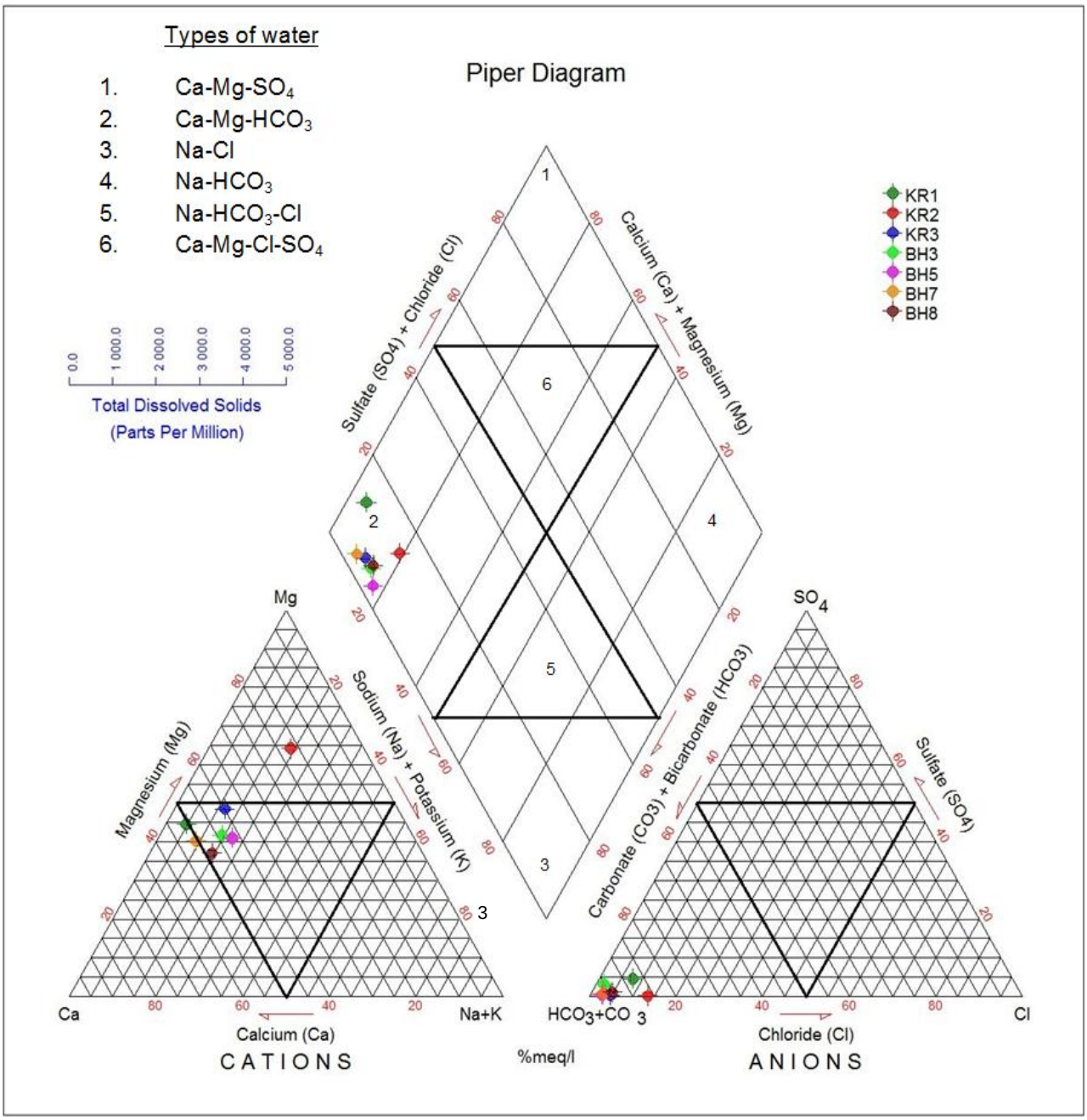

Figure 40: Piper diagram for the water samples taken at the mega tailings study area.

Samples taken of the natural groundwater in the vicinity of the mega tailings study area are relatively low in concentrations when compared to that of the Daggafontein TSF seepage, sampled from the under drains. Also the TSF seepage water is largely SO_4 dominated with a maximum concentration of 4 351 mg/l (See Table 6), therefore it is expected that the introduction of typical TSF seepage water into the natural groundwater system would result in an ultimate change of the geochemical signature of the regional groundwater system. This change would eventually see boreholes at the mega tailings site move from the left (Zone 2) of the Piper diagram, to the right (Zone 1) as the contaminant plume migrates toward these

boreholes, subsequently increasing the concentrations of chemical constituents found in the groundwater.

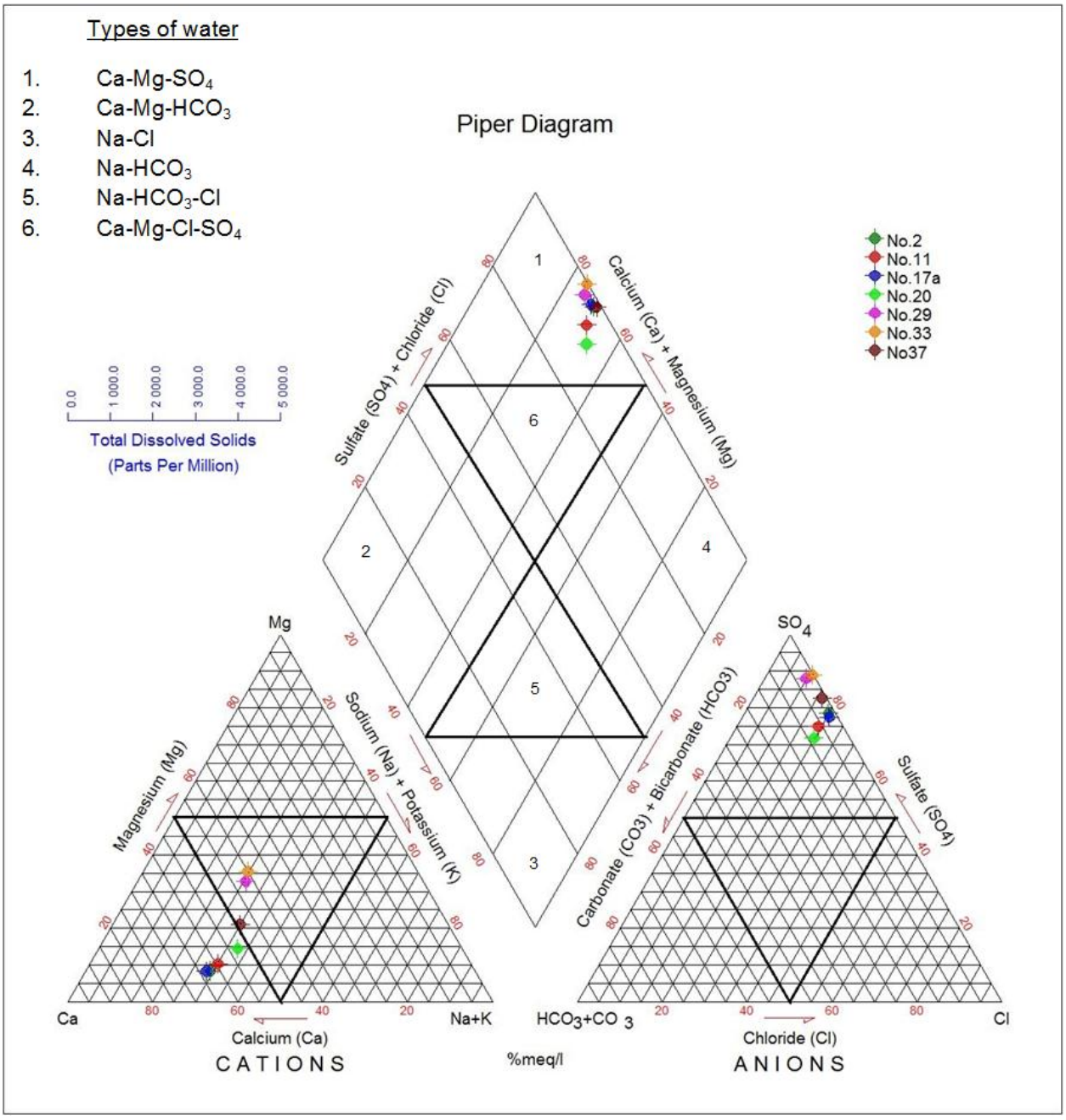

Figure 41: Piper diagram for seepage water taken at the Daggafontein TSF.

4.5 Seepage modelling and artificial recharge flux estimation

SEEP/W is used to simulate seepage in 2D section of a specified thickness (typically 1m). Therefore, a section line through the length of the facility is used to simulate flow through this particular section. The total seepage for the entire footprint is estimated by integrating the profile value with the area of the facility.

A 2D conceptual model across the TSF section must be constructed in the SEEP/W modelling domain so as to assign zone parameters, material properties and boundary conditions prior to simulation.

For the purpose of keeping the simulation focussed and relevant the TSF model comprised of the following materials (Zones) as illustrated in Figure 42:

- Tailings underflow (Zone 1) will be for the annulus around the facility
- Tailings overflow (Zone 2) will be concentrated in the centre where the pool is located.
- Foundation soils (Zone 3) consisting of low permeability colluvium is located at the base of the facility.

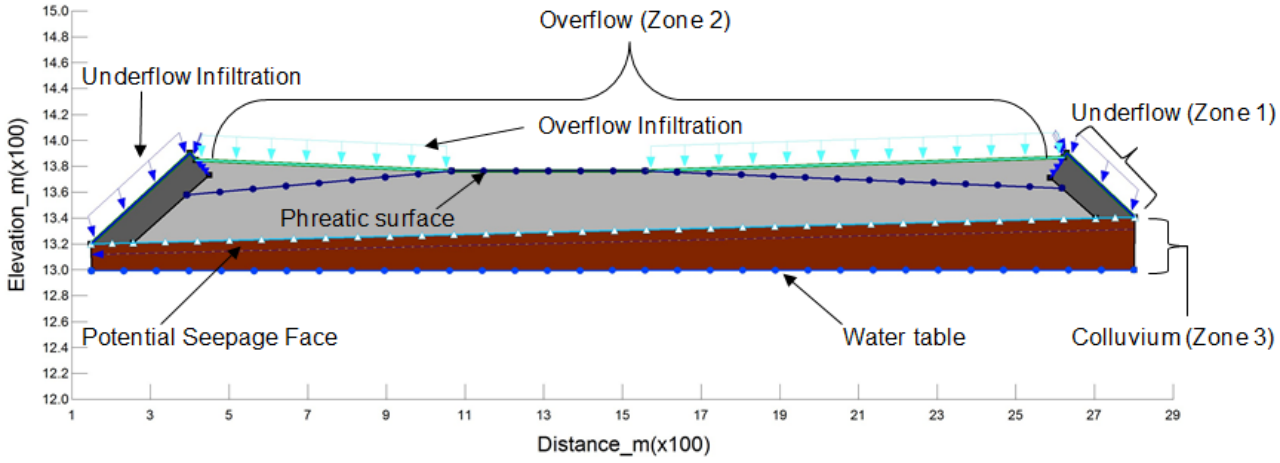

Figure 42: Conceptual of SEEP/W section (operational phase)

4.5.1 Parameter values and assumptions

The regional groundwater is assumed to average at 12m below the natural ground level. The natural groundwater table was assigned a variable head boundary. This condition allows the groundwater table to fluctuate in the proximity of the TSF due to the continual addition of water through seepage. Mean annual rainfall for the area is calculated and added to the water balance once the volume of water from deposition has been determined.

Once the recharge volume is calculated from the deposition tonnages during the operational phase, a recharge flux is calculated by dividing the volume by the area covered. The dimensional parameters are documented in Table 7.

Continual infiltration inflows are assigned to the embankment (Zone 1) and centre (Zone 2) using calculated volumes from a water balance developed for the TSF utilising the method established by Yibas et al. (2011) and documented in Table 8.

Table 7: Dimensional parameters used to estimate the total water flux (m/day)

Zone	Size	Unit
Footprint area	5,322,000	m^2
Underflow area	1,113,199	m^2
Underflow length	250	m
Basin area	4,208,801	m^2
Basin length	2500	m
Total length	2750	m

Lambe & Whitman (1969) estimated recharge values of six percent for underflow and four percent for overflow tailings materials during laboratory test. These values were considered in the seepage modelling phase.

Table 8 Operational water balance for the Mega tailings study

Months	Cumulative tons	Water content (1.2 m^3/t)	Cumulative U/F volume (m^3)	Cumulative O/F volume (m^3)	U/F volume infiltrated	O/F volume recovered	O/F volume infiltrated	U/F Volume remaining	O/F volume remaining
1	2100000	2520000	756000	1764000	45360	1464120	11995.2	710640	1752004.8
18	37800000	45360000	13608000	31752000	816480	22226400	381024	12791520	31370976
68	142800000	171360000	51408000	119952000	3084480	83966400	1439424	48323520	118512576
138	289800000	347760000	104328000	243432000	6259680	170402400	2921184	98068320	240510816
168	352800000	423360000	127008000	296352000	7620480	207446400	3556224	119387520	292795776
O/F Recharge tempo = 8.897e-5m/day									
U/F Recharge tempo = 1.314e-3m/day									

Porosity

The porosity of the various materials is derived from the in-situ dry density and specific gravity of the tailings material as well as the natural soil. The VWC is derived as follows:

$$VWC = n \times S$$

n= porosity of the tailings

S= Degree of saturation

Soils that are fully saturated have a degree of saturation equal to 1.0 which is assigned in the formula. Thus it can be said that the saturated volumetric water content is equal to the porosity. Once the saturated volumetric water content is evaluated, the VWC at various degrees of saturation is evaluated by comparing it to theoretical SWCCs established by van Genuchen. This is done to establish the conductivity of a soil during unsaturated flow conditions. The SWCCs for the natural soil found at the base of the TSF as well as the tailings material is illustrated in Figure 43.

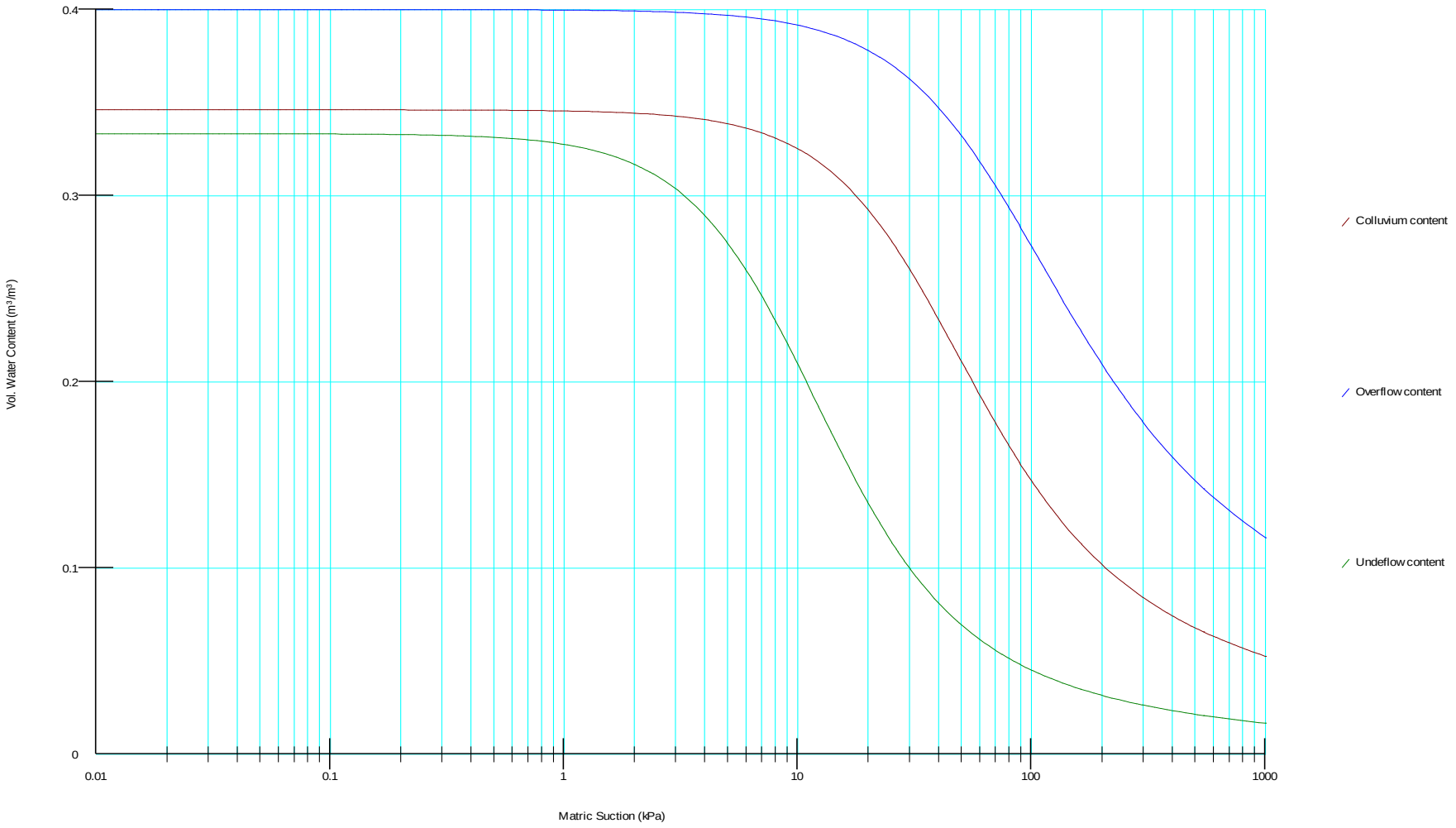

Figure 43: Saturated volumetric water content function estimated from porosity

The Geoslope SEEP/W software package uses the VWC values to estimate the volumetric water content at various degrees of saturation established for different soil types so as to determine a VWC function that is assigned to the various zones.

Tailings material properties are obtained from grading curves derived by Civilab for a TSF that is earmarked for re-mining and will eventually become part of the mega tailings project. The saturated hydraulic conductivity (K_{sat}) for tailings material is calculated using Hazen's formula:

$$K_{sat} = 100 \times D_{10}^2$$

Where K_{sat} is determined by multiplying the degree of saturation, expressed as a percentage with the aperture size D_{10} (mm) through which ten percent of the soil particles can pass. Once the hydraulic conductivity values are, calculated a best fit curve is applied in SEEP/W so as to assign an appropriate conductivity function for the various materials e.g. underflow, overflow and foundation soils (colluvium) as seen in Figure 44.

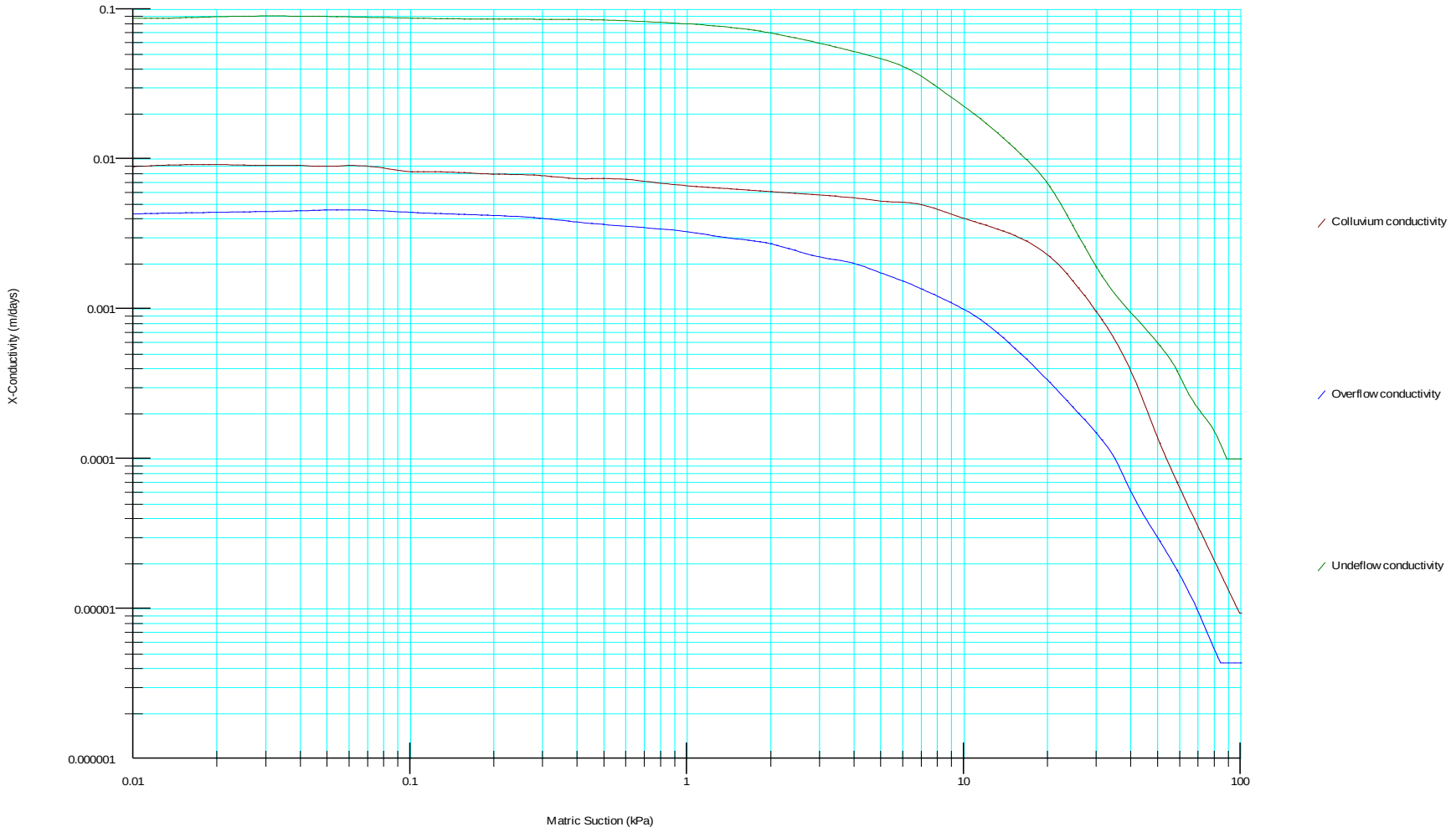

Figure 44: Soil characteristic curves for the various zones

Recharge

The recharge refers to the amount of water that infiltrates the subsurface of the tailings, eventually reporting to the foundation as seepage. During the operational life of the TSF supernatant water is continually deposited during construction. Therefore, water balance calculations from the designed deposition method have to form part of any seepage prediction.

Cyclones classify tailings material into underflow and overflow respectively. The design split is taken at 30:70 under/overflow by mass. Therefore, the total tonnages deposited will be split according to the designed split and so to the volume of water during deposition. These values are also used during the calculation of the water balance.

Given the low permeability of the finer overflow material it must be kept in mind that a large portion of the excess water is drained by means of penstock drains located at the pool. When determining the volume of infiltration, a recovery value is assigned to the water deposited on the beach. Water recovered is subtracted as it is returned to the metallurgical plant for re-use. The recovery value of 83% is used as this is the typical value achieved on similar cyclone facilities. It must be said that the recovery ratio is specific to the method of deposition. These high values of recovery are not practically achievable on conventional paddock facilities as gravitational segregation of tailings particles is not as efficient in separating end removing excess water from the slurry as particles remain relatively uniform reducing the effective porosity of a soil.

Boundary and model discretization

The numerical simulation is conducted on a 2-D section stretching from the NE corner to the SW corner. The total distance is 2800m (horizontal) and 80m (vertical). The domain is discretized into 464 uniform elements of 23m x 23m in size. A constant head boundary is assigned to the pool during the operational life of the TSF as well as the base where the natural groundwater table is located (12 m below natural ground level). A potential seepage face is allocated at the base of the facility and fluid is allowed to flow from the TSF.

Seepage modelling operational and dormant phase

The operational life of the TSF is expected to be about fourteen years. Therefore, steady state simulations are done at various stages throughout the operational life of the TSF. The simulation is conducted in steps of 18, 68, 138, and 168 months into the operation. The noticeable change is the elevation change and the subsequent rise of the phreatic surface within the facility. The modelled phases are presented in the Figure 45 and Figure 46.

For the dormant phase a period of 1200 months is simulated. During this phase there is no infiltration added to the facility other than the natural rainfall. Recharge values are estimated from soils with similar characteristic properties. Therefore, the recharge values for the underflow and overflow materials are 6% and 4% respectively. The phreatic surface in the TSF is also reduced to the base due to the stoppage in deposition.

As the modelling is conducted on a section of 1m wide and is only a 2-D profile, the total volume of seepage still has to be calculated by multiplying the seepage flux of the section by the respective total footprint area covered by the TSF. The parameters used to estimate the entire water flux is listed in Table 9.

The pressure head distribution and seepage flux for the both the operational and dormant phases of the TSF life are presented in Figure 45 to Figure 47.

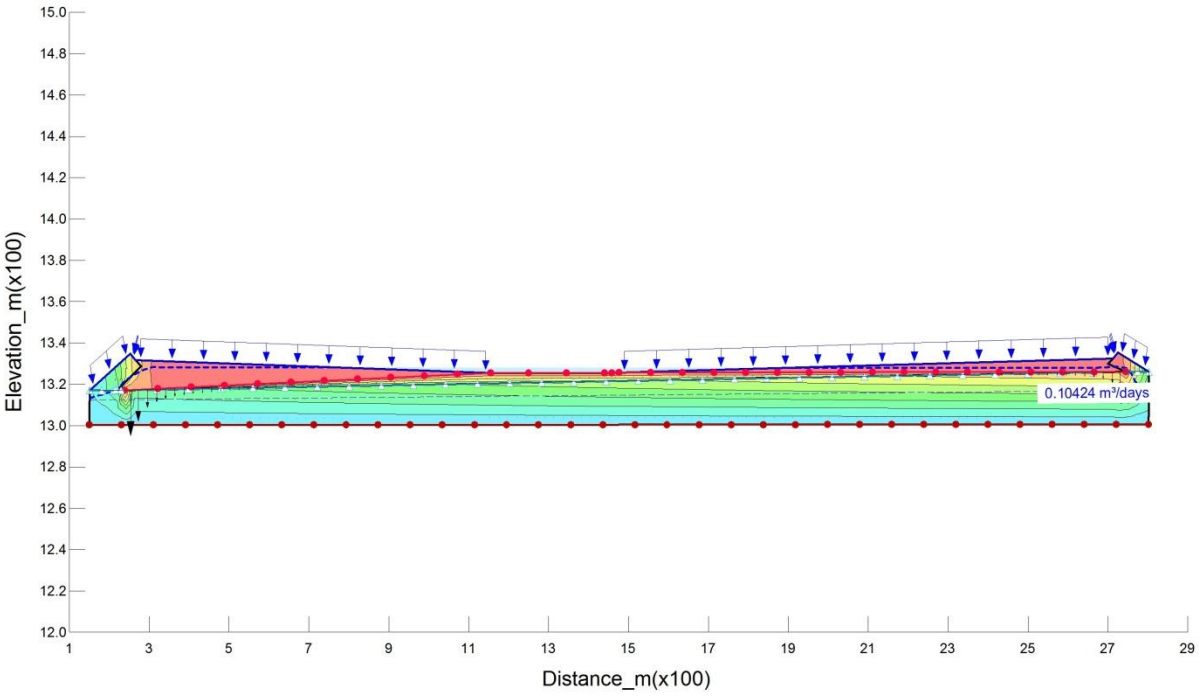

Figure 45: Seepage flux after 18 months

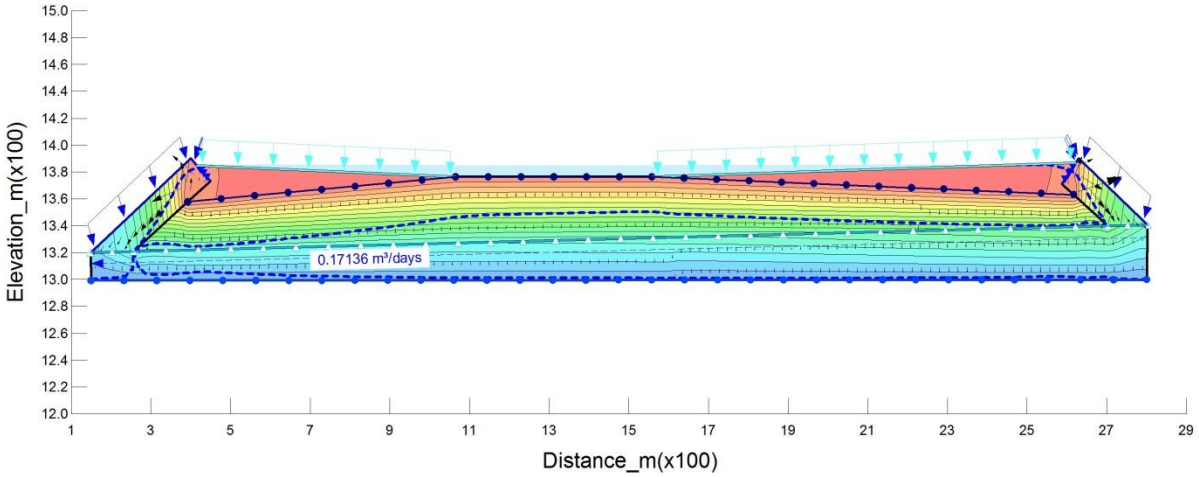

Figure 46: Seepage flux after 68 months

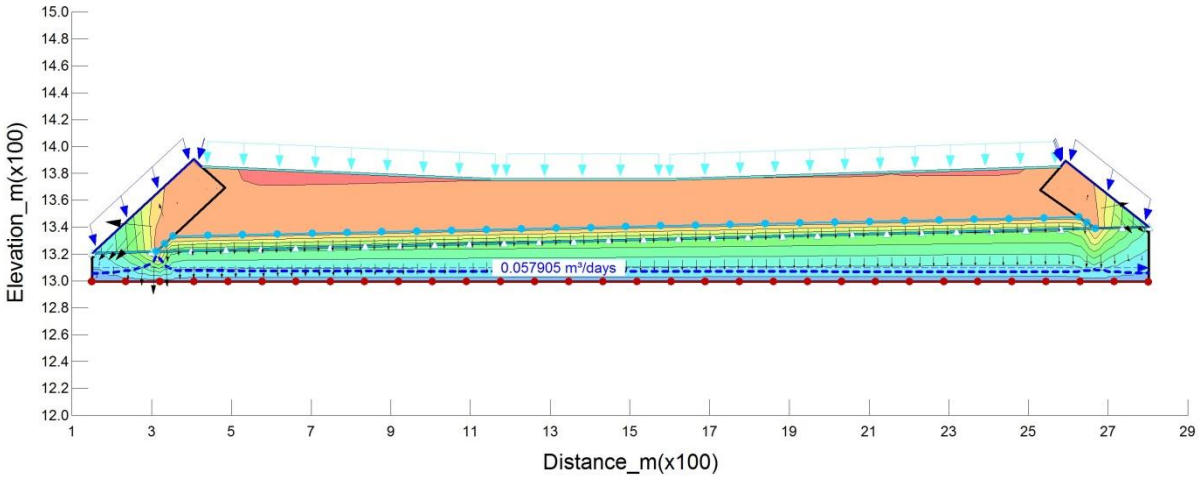

Figure 47: Seepage flux at 1200 months

Table 9: Water flux (m^3/day) for the entire TSF

Time period (months)	Sectional flux (m^3/day)	Total seepage flux (m^3/day)
18	0.10424	201.732
68	0.14963	289.574
138	0.16805	325.222
168	0.17136	331.627
1200	0.057905	112.061

The total amount of seepage estimated from SEEP/W is applied as a rainfall recharge over the area covered by the TSF. The seepage flow rate (mm/y) is given for the entire TSF in Table 10.

Table 10: Total seepage flux in mm/y for the surface area covered by the TSF.

Month	Total Seepage (mm/yr)
18	13.835
68	19.860
138	22.305
168	22.744
1200	7.685

2.1 Numerical modelling and contaminant plume delineation

The aim of this section is to assess the modelled hydrological impact of the mega tailings on the receiving environment. The model will furthermore be used to validate assumptions made about groundwater flow and the resultant contaminant plume. A pre-depositional steady state model will be setup for calibration and the use of steady state heads as an input to the transient depositional and post depositional predictive modelling.

2.1.1 Parameter values and assumptions

The following section discusses the terms used in the setup of the groundwater model, boundaries assigned and assumed initial conditions based of known data and technical aspects.

Groundwater mapping by Bayesian interpolation

Bayesian interpolation requires a strong groundwater elevation vs. topographic correlation in order to produce accurate estimates at un-sampled points within the study area. A strong correlation value indicates that the groundwater level follows the general topography. The correlation for the study area is 94% (Figure 48) indicating that the aquifer is under unconfined to semi-confined conditions.

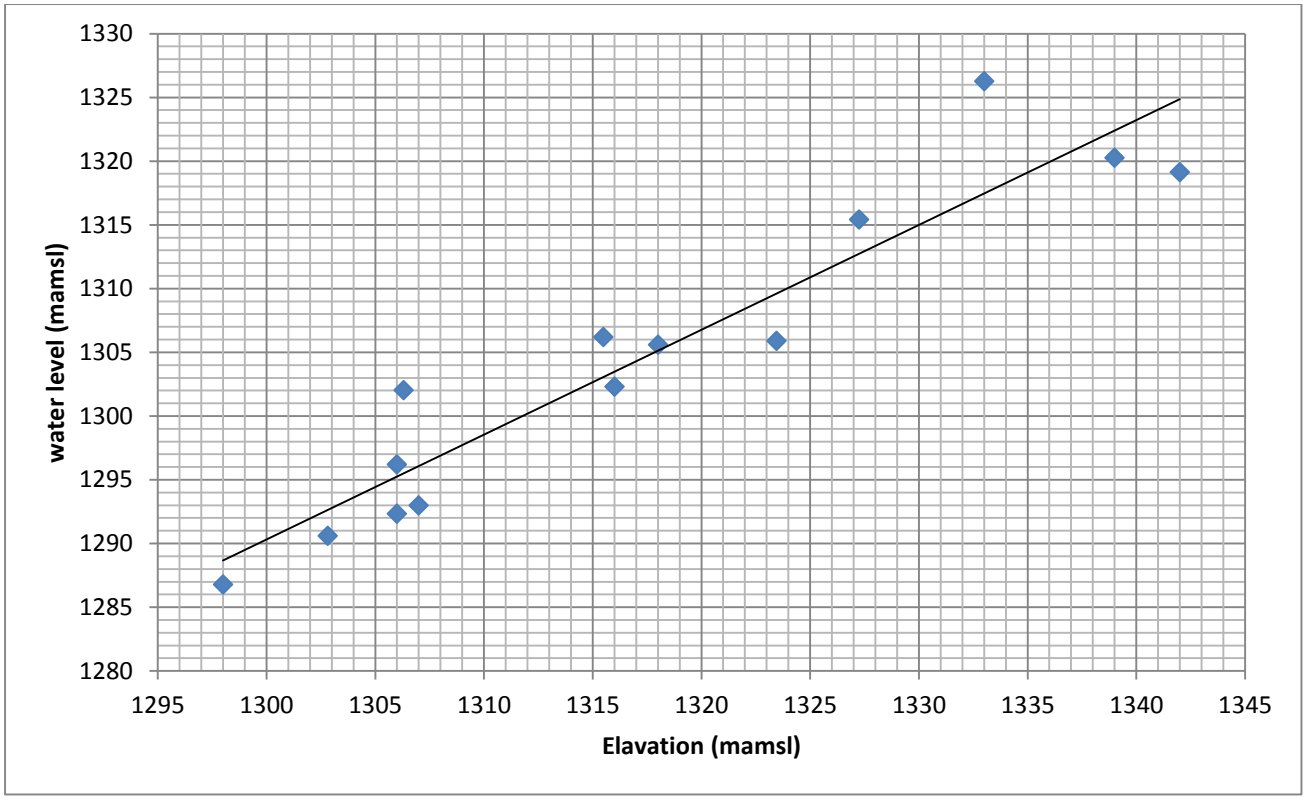

Figure 48: Correlation between groundwater elevation and topographic elevation for the study area

A groundwater level map generated for the area indicates the predominant direction of flow is from north to south where groundwater will flow towards the Vaal River system as seen in Figure 49.

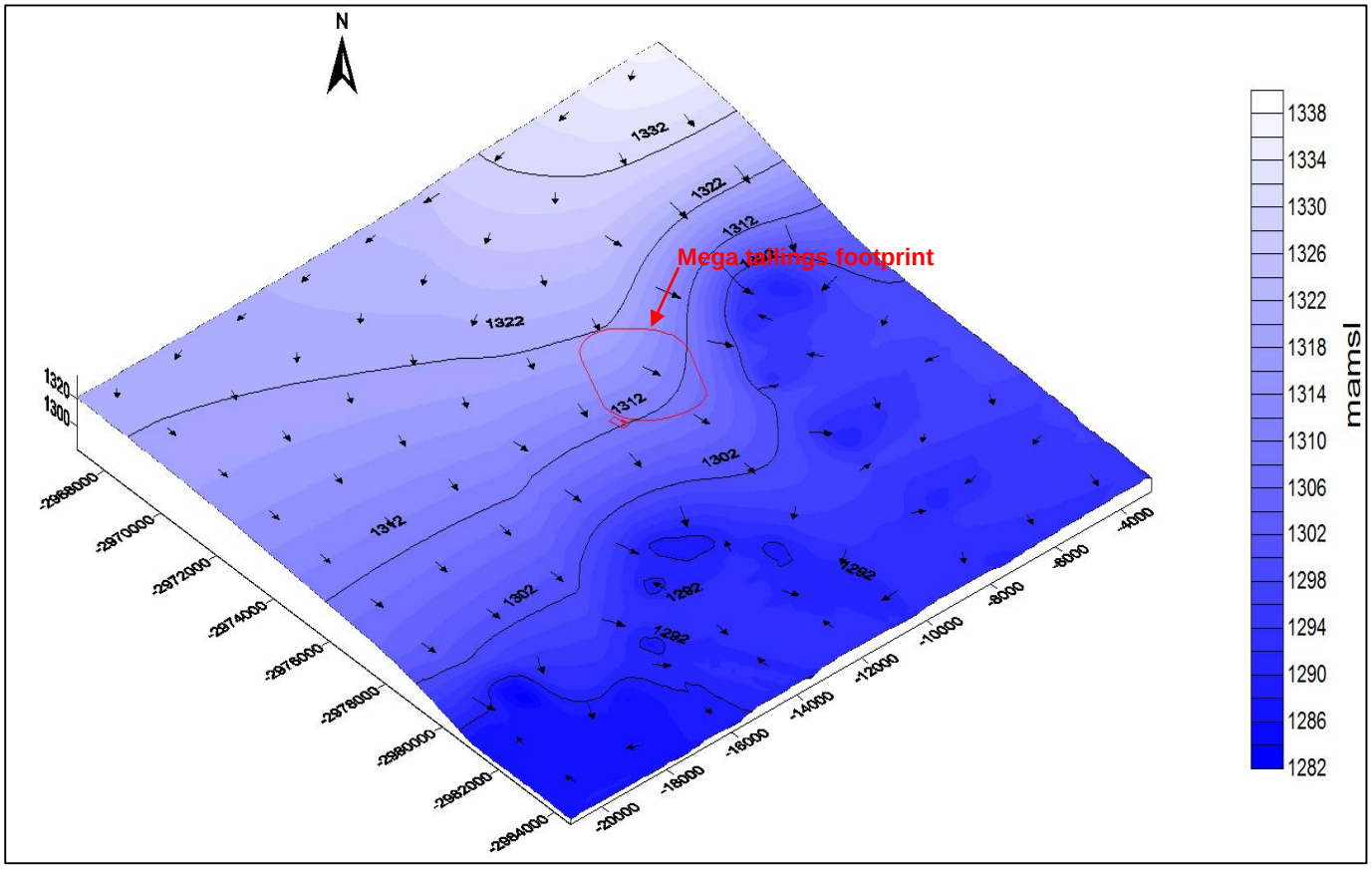

Figure 49: Groundwater contour map

Boundaries

In defining a model domain the model user distinguishes the area investigated from surrounding groundwater systems. Boundaries exist at the edges of the model area as well as locations in the model area where external influences are represented, these are; rivers, and possible water shed (Spitz & Moreno, 1996). Therefore, when using boundaries to delineate the appropriate area of interest it is important to include all the key groundwater mechanisms. Whenever practical the use of topography, surface water bodies and geology are recommended as a guide to the use of boundary conditions.

The Vaal River south of the TSF is set as a constant head boundary. A no-flow boundary is automatically assigned to the north of the modelling domain.

Seepage flux values estimated in Seep/W are assigned as recharge over the footprint area of the TSF. During the depositional phase a rise of the head conditions is expected and should be accounted for as the TSF rises in height. Therefore, a time-variant specified head package is used to account for this phenomenon during transient modelling. The exact height of the

pool is taken at the basin elevation during the selected periods and the basin is assumed to be constantly saturated during the depositional phase. During the dormant phase the specified head is reduced to ground level so as to simulate a declining phreatic level which would be the case once deposition ceases and natural precipitation is the only addition of water to the TSF.

The modelling area is discretised by a grid of 360 rows and 360 columns in the x and y direction, resulting in a cell dimension of 50m x 50m. The subsurface features were modelled in a single layer with a thickness of 120m.

Aquifer parameters

Although the most accurate aquifer parameters are obtained and used for the calibration of the model, a number of parameters have to be calculated or estimated based on both prior knowledge and literature. The following input parameters are calculated/estimated for the model area:

- Recharge: Recharge was calculated as 6% of the MAP (401mm/yr – 601mm/yr) for the KOSH area. This value is based on the studies of L&W Environmental (1993). This relates to a recharge flux of 6.1 x 10^{-10} m/s. The area directly below the TSF has a recharge calculated for the various phases of deposition and post-deposition based on the seepage modelling results. The recharge values for the area covered by the TSF are documented in Table 11.

Table 11: Recharge values assigned to the footprint based on Seep/W results

Months	Recharge flux at base (m/s)
18 months	2.2 x 10^{-9}
68 months	8.5 x 10^{-7}
138 months	4.95 x 10^{-7}
168 months	2.1 x 10^{-7}
1200 months	2.1 x 10^{-8}

- Horizontal hydraulic conductivity: The horizontal hydraulic conductivity for the aquifer is estimated from borehole slug tests and literature was consulted for geological formations which could not be tested during the field investigations. The results from the slug testing are included in Appendix C. These values are used during the initial calibration of the groundwater model, however the final calibrated values for the aquifer parameters are documented in Table 12. The modelling domain as used in PMWIN is displayed in Figure 50.

Table 12: Calibrated hydraulic conductivities of the geological formations at the Mega tailings study area

Hydrogeological formation	Horizontal hydraulic conductivity (m/s)
Diabase	2.43×10^{-6}
Quartzite	1×10^{-4}
Andesite	8.1×10^{-6}
Shale	4.48×10^{-6}
Dolomite	4.05×10^{-6}
Karoo sediments	2.5×10^{-5}

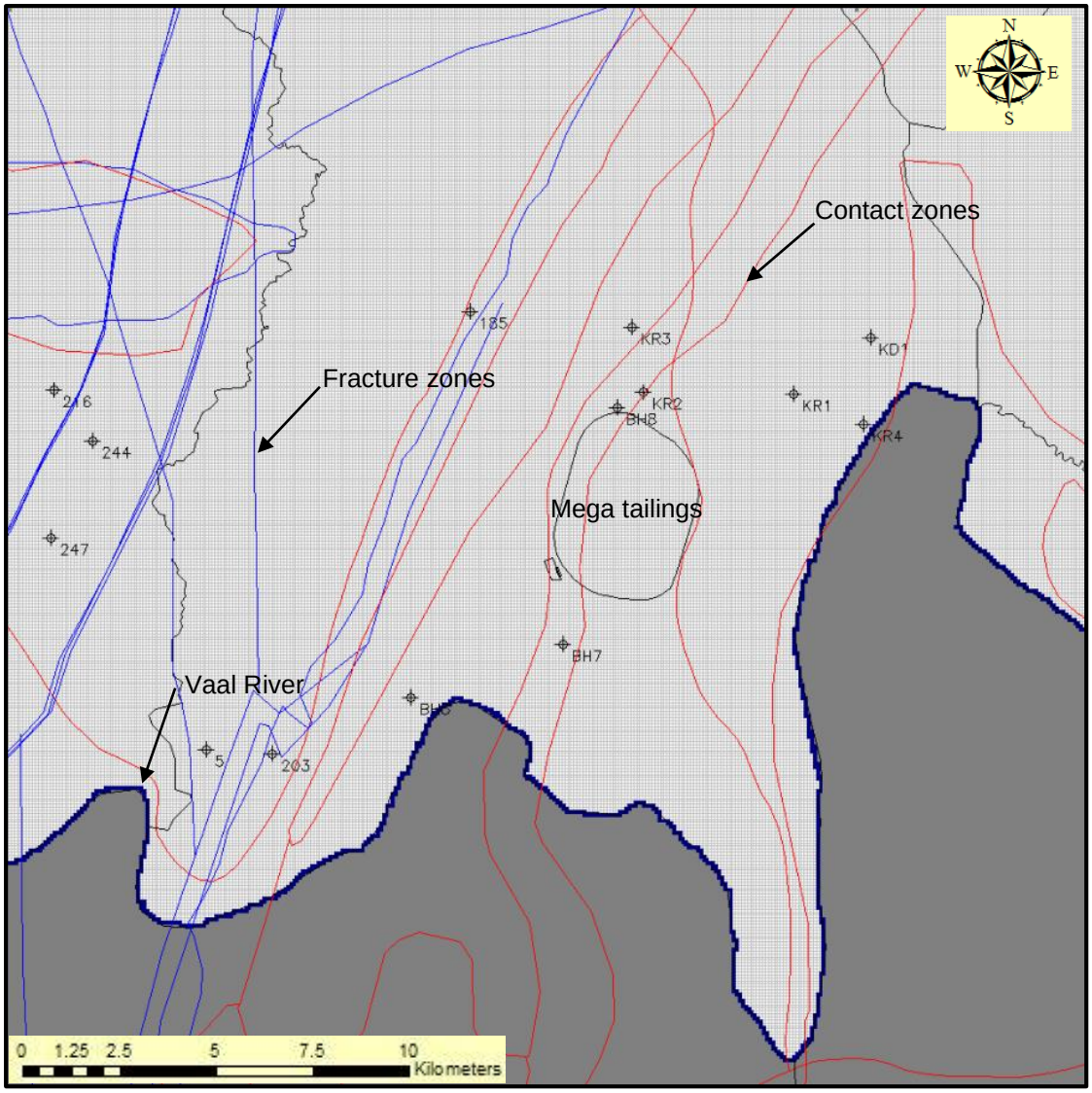

Figure 50: PMWIN model grid for mega tailings study area

4.5.2 Calibration of the model

Groundwater levels for boreholes were obtained during the field investigations, those not visited were obtained from the NGA database. Boreholes are spread evenly across the entire area (including various lithologies), both upstream and downstream producing an adequate representation with which to calibrate the model.

Using the field data, a good fit of simulated and measured groundwater levels was obtained. Calibration of the model was successfully achieved using a trial by error method, making slight changes to the recharge and transmissivity parameters. Transmissivity values were spatially distributed according to the locations of each lithological unit as shown in Figure 51.

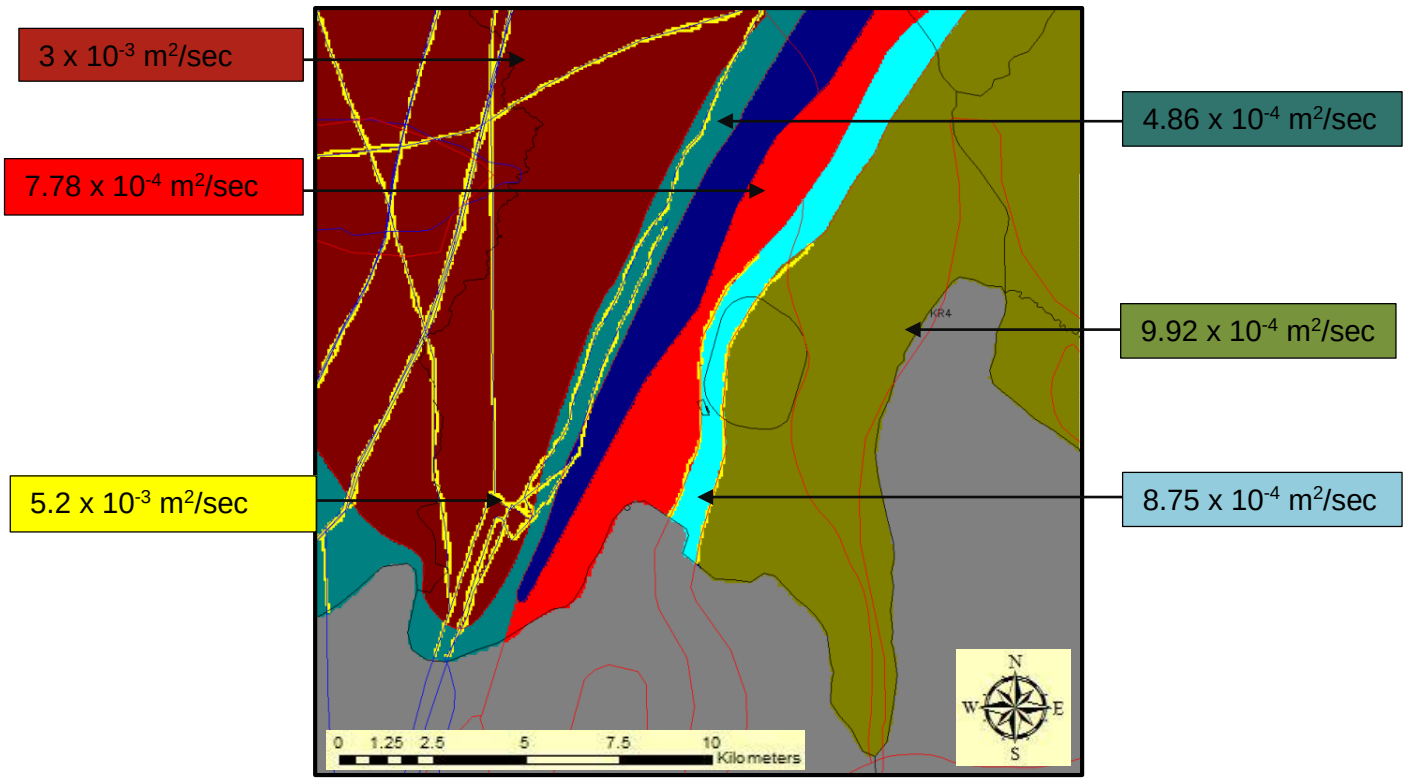

Figure 51: Spatial distribution of aquifer parameters.

A 87.7% correlation is achieved between the modelled and observed heads. Figure 52 illustrates the comparison between the modelled and observed heads. The calibration results are shown in Figure 53.

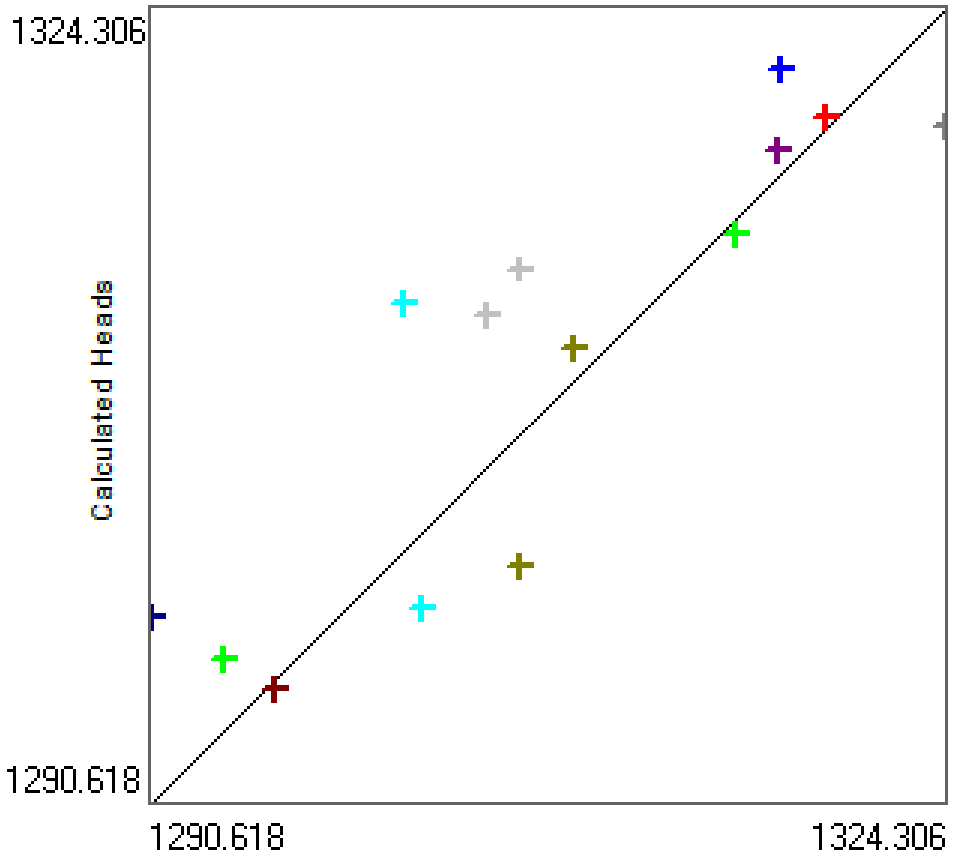

Figure 52: Correlation between calculated and observed heads (in mamsl)

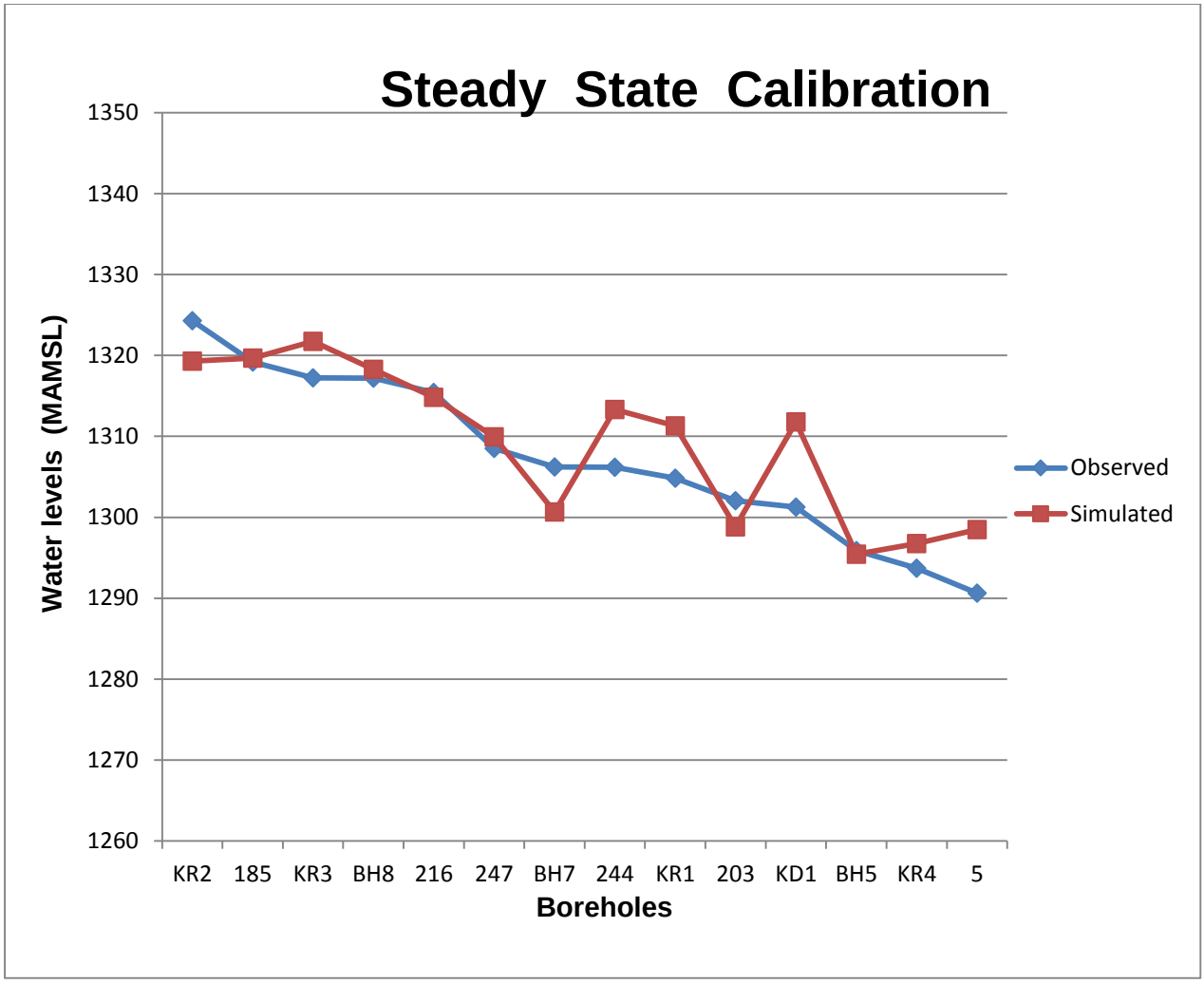

Figure 53: Calibration graph of declining head between observed and simulated head.

The water budget calculator in PMWIN indicates that there is a constant inflow of groundwater into the constant head boundary assigned to the River. Appendix D documents the results from the water budget calculation.

4.5.3 Operational and post operational groundwater levels

The total simulation period is subdivided into a specified amount of time periods. Transient modelling depends on the initial conditions that are usually established during a steady state model. Transient modelling needs additional parameters to be specified (Spitz & Moreno, 1996):

- Storativity of 8.3 x 10^{-6} for fractured rock
- Specific yield of 0.4 for fine sandstone

A transient modelling approach is used to determine the extent of the contaminant concentration and plume throughout the life of the TSF. Specific periods are selected (18, 68,

138, 168, 1200 months) to evaluate both the formation of a groundwater mound and contaminant plume migration. Periods are divided into monthly time steps and recharge assigned on a monthly basis. The groundwater mound for after 68 months and 1200 months are displayed in Figure 54 and Figure 55. Modelling results for 18, 138 and 168 months are documented in Appendix D.

Continual deposition and the resultant seepage increases as the TSF subsequently grows. Seepage rates from SEEP/W are applied as recharge at the base of the facility as this is the point of entry into the natural groundwater system. Time-variant head cells are assigned to the area that is covered by the basin to account for the effect of a constant pool, as is the case during the operational phase. Therefore, maximum seepage is expected from the embankments where the phreatic surface is maintained by controlled seepage.

The modelling revealed the evolution of a localised groundwater mound surrounding the TSF, with a maximum peak at the embankments, declining in a conical fashion. This phenomenon is described by Rösner (1999) and Martin & Koerner (1984) as elevated recharge creates a wetting front.

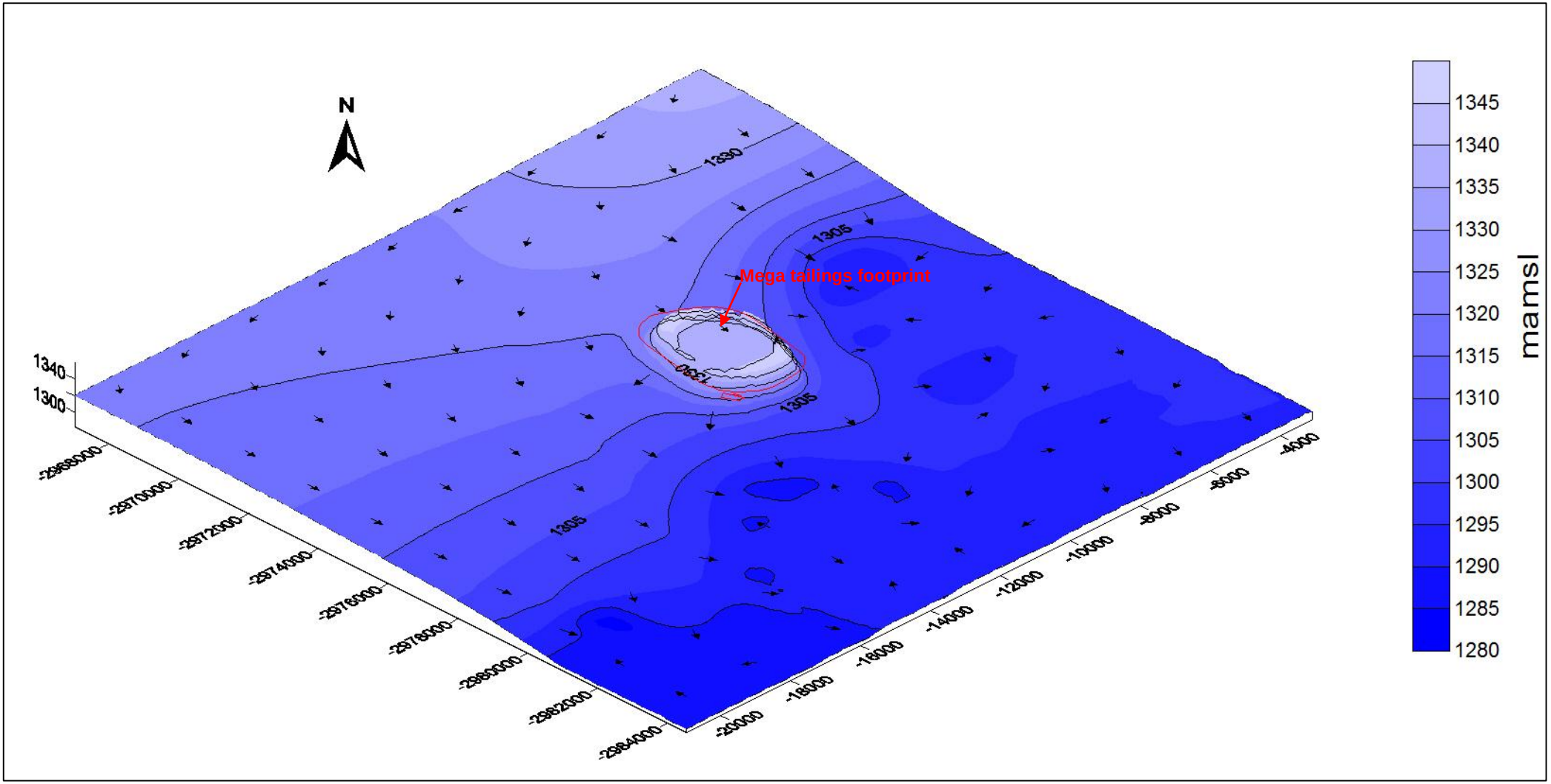

Figure 54: Groundwater mound at 68 months of deposition

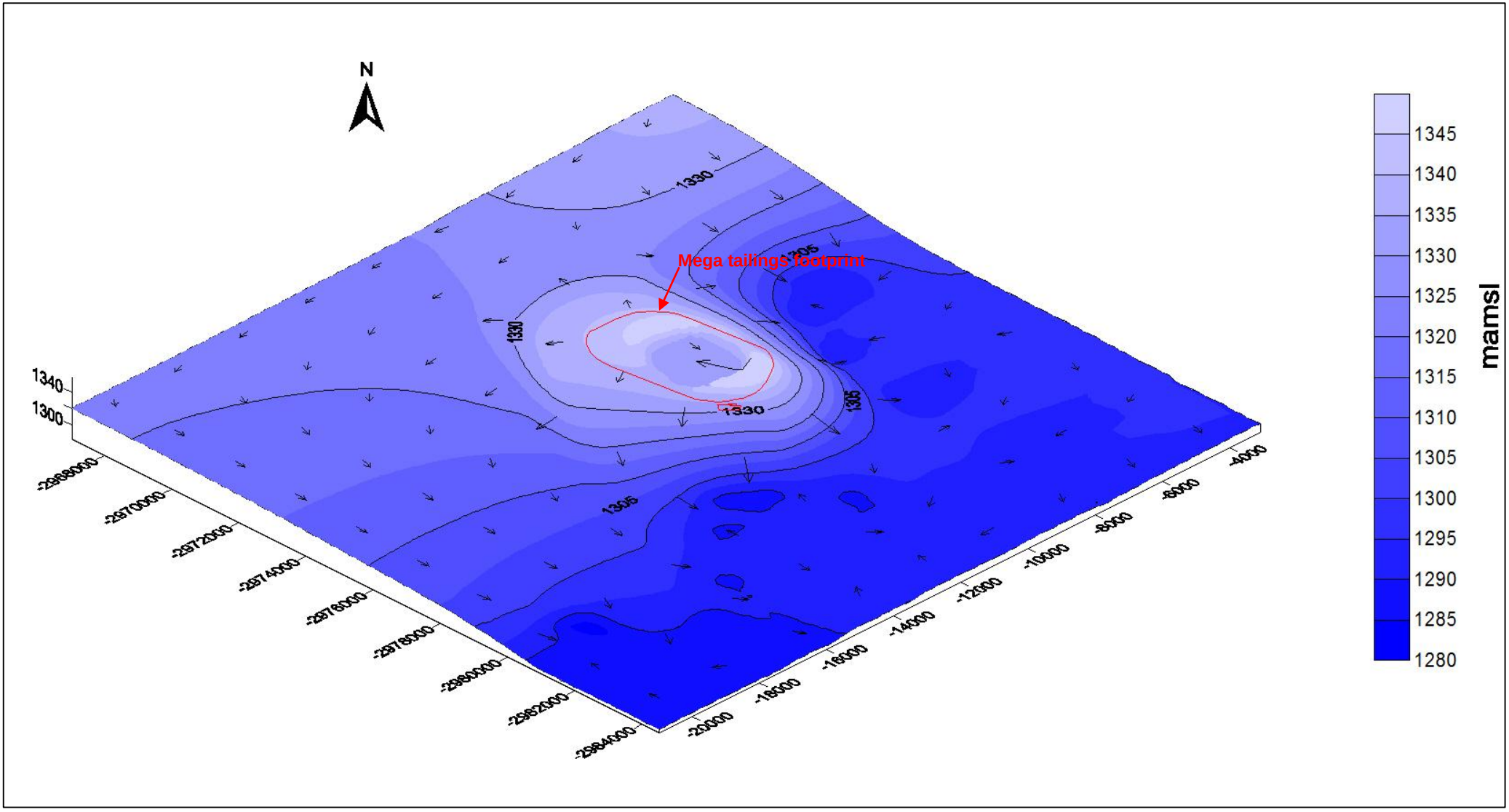

Figure 55: Groundwater mound at 1200 months post deposition

4.5.4 Solute Transport Model

The migration of the contaminant plume is modelled by means of a numerical mass transport package developed MT3DMS developed by Zheng & Wang (1999). The package makes use of hydrodynamic dispersion and advection of contaminant species to calculate the movement of contaminants through a porous medium.

SO_4 and Cl are considered for the solute transport modelling as this was decided to be indicative contaminants specific to gold mine residues. From various studies on gold mine tailings it is evident that sulphates and chlorides are water quality constituents used to identify possible contamination from gold mining activities. The following assumptions are made for the transport modelling of SO_4 and Cl:

- An effective porosity is 0.13 (Spitz & Moreno, 1996)
- Longitudinal dispersivity is 100m.
- The ratio of horizontal transverse dispersivity to longitudinal dispersivity is taken at 0.1 and the effective molecular diffusion coefficient is set to 0 m^2/s.
- An initial concentration of 0 mg/l was assumed for the modelled area, as the natural background values for both SO_4 and Cl are of negligible concentrations as based on groundwater quality samples taken from boreholes surrounding the TSF.
- The contaminant concentrations are introduced to the groundwater through artificial recharge at the base of the TSF. Source concentrations of 3700mg/l for SO_4 and 400mg/l for Cl are selected, based on water samples taken from the Daggafontein TSF. These contaminant concentrations are typical for gold tailings.
- It is assumed that neither sulphate or chloride will decay of be retarded whilst the plume is migrating, thereby simulating a conservative worst-case scenario.
- The calculated water levels from the steady state calibration are used as an initial hydraulic heads in the model.

Predictive modelling

Predictive modelling of the contaminant plume emanating from the TSF represents future estimations of the plume shape and expected concentrations throughout the groundwater system. The continual seepage of contaminated water at the base of the facility will be modelled for a total of 168 months representing the depositional phase of the TSF and 1200 months which is a representation of the post depositional phase i.e. dormant state.

The plume shape and concentrations were evaluated at 18 months, 68 months, 138 months, 168 months and 1200 months.

Worst case scenario

This scenario represents the “worst-case” where there is a constant recharge of seepage with a concentration of 3700mg/l SO_4 and 400 mg/l Cl. No trenches and abstraction boreholes are included in this scenario. As can be seen from the SO_4 simulations in Figure 56 and Figure 57, the plume is expected to spread in the direction of the natural drainage i.e. from north to south towards the river. The breakthrough curves for SO_4 is shown in Figure 58. Note that the complete set of results is included in Appendix D. The following observations can be made:

- The primary plume of SO_4 is likely to reach BH8, KR2, BH7 and KR1 during the depositional phase. KR3 will only be affected by the post depositional phase as continual leaching takes place.
- SO_4 has a much further reach due to the higher concentrations. Cl has a smaller plume shape and lowered concentrations.
- The plume front reaches the Vaal River (approx. 2.5km downgradient) at two distinct locations after 1200 months. The first being in the south west direction (toward BH7), the plume in this direction also has the highest concentration of contaminants. The second location is toward the south east which has a gradual slope toward the river.

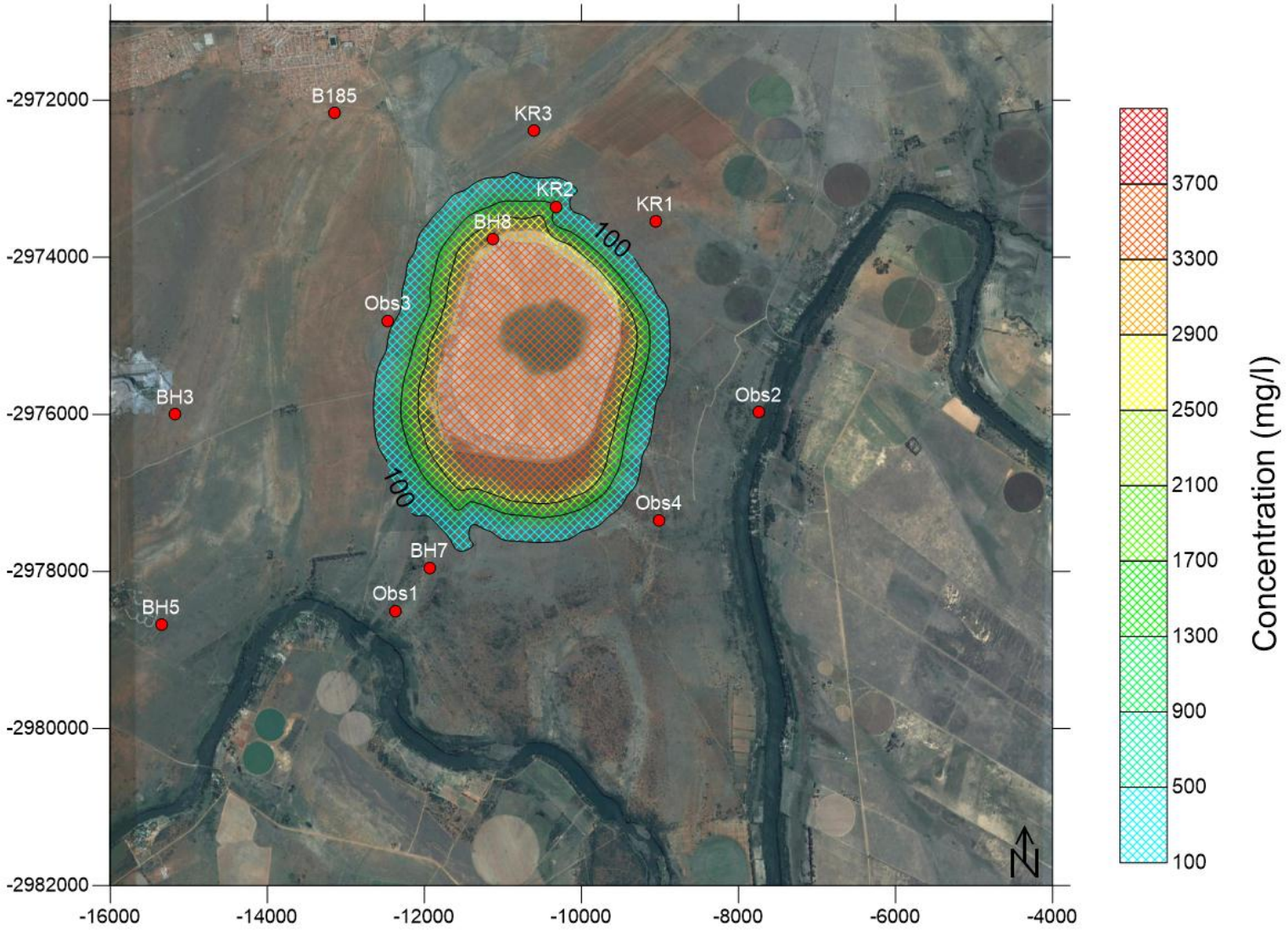

Figure 56: Modelled SO_4 contaminant plume migration for 68 months

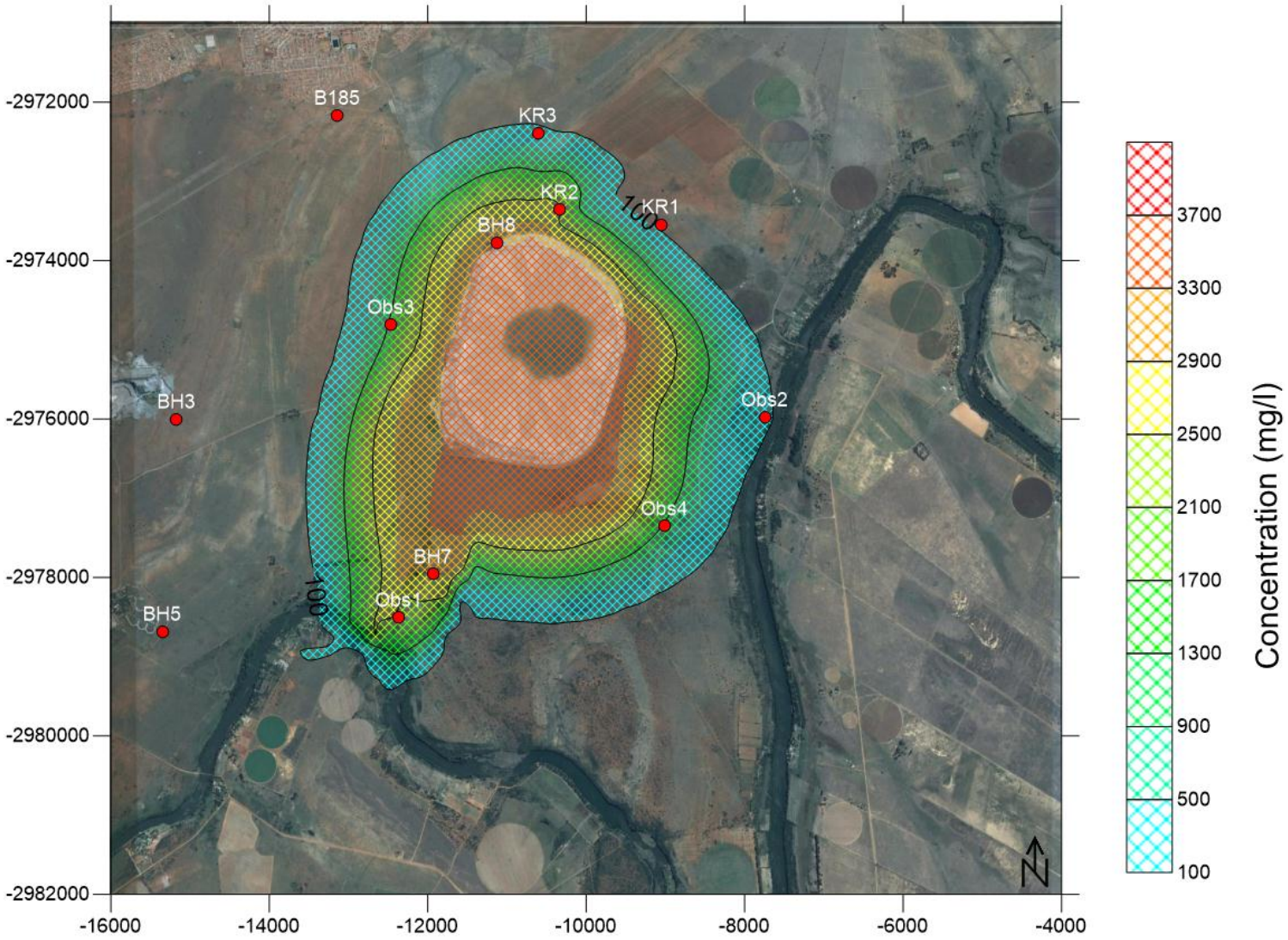

Figure 57: Modelled SO_4 Contaminant plume migration for 1200 months

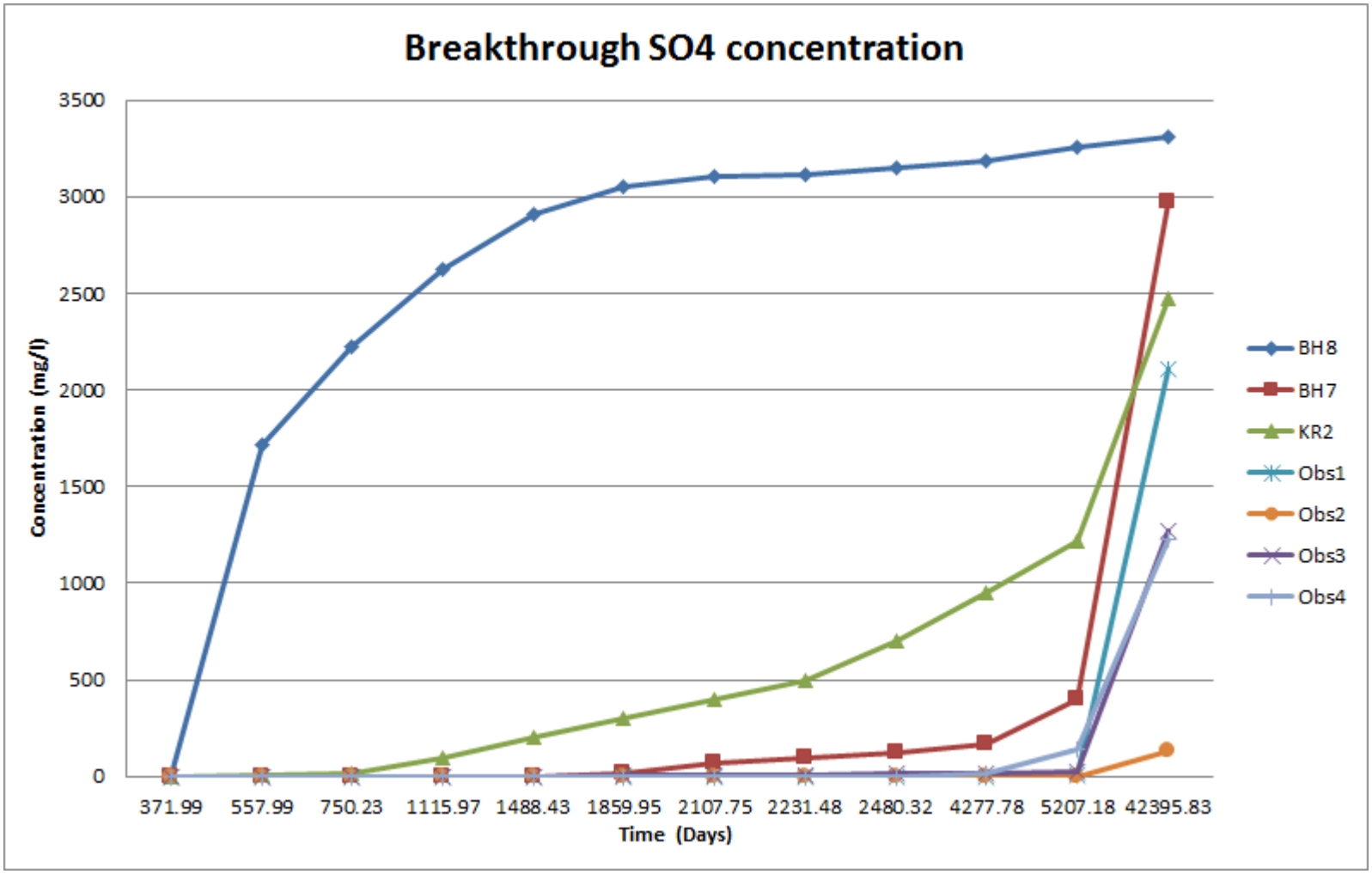

Figure 58: Breakthrough curves for SO_4 concentration

Contaminant load estimation

A zoned water budget calculation in the PMWIN groundwater modelling package is used to determine the total groundwater flux moving across the selected transects. These transects are used to determine the total mass discharge across the entire face of the transect. Five transects are located as to intersect the contaminant plume in the predominant flow direction i.e. toward the Vaal River (Figure 59). An additional transect was placed along the river itself in order to determine the mass discharge into the Vaal River.

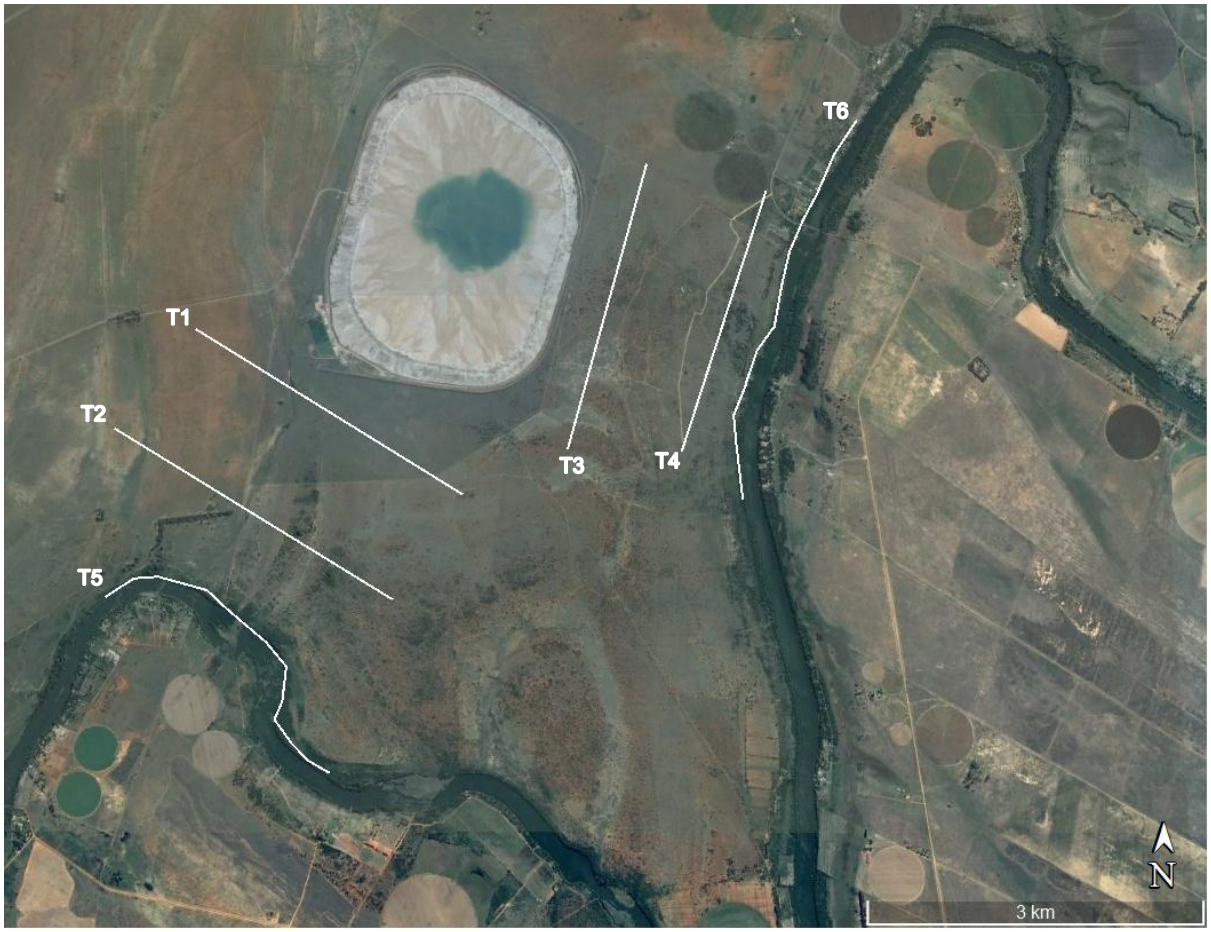

Figure 59: Location of mass discharge transects

The total discharge (Groundwater flow *Q*) from each individual transect is plotted for each modelling time step (18 months, 68 months, 168 months and 1200 months) in Figure 60. The discharge is converted to an overall volume rate (m^3/yr) per time in order to obtain the total contaminant mass discharge rate per year, the total discharge for all six zoned transects as determined in PMWIN is displayed in Table 13.

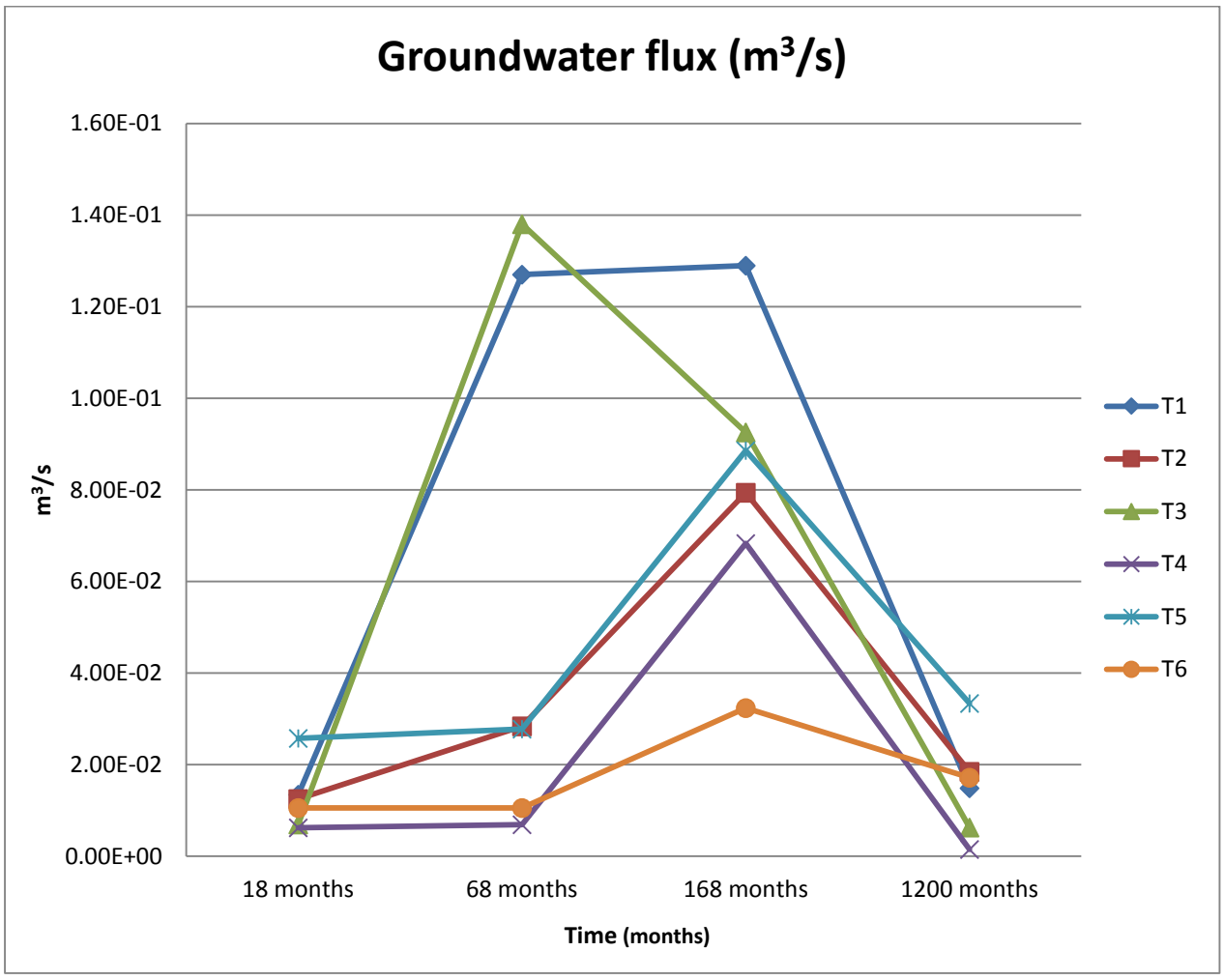

Figure 60: Graph of groundwater flux for the various transects

These discharge rates are then multiplied with the contaminant concentration across the face of the transect, that was modelled using the MT3DMS solute modelling transport package. The results of the contaminant mass discharge for both SO_4 and Cl in kg/yr for 68 months, 168 months and 12000 months is displayed in

Table 14 and Table 15.

Table 13: Groundwater flux through the various transects in m^3/yr

Transect	18 months (Total flow $Q \times t$) m^3/yr	68 months	168 months	1200 months
T1	433900.80	40818812.73	41461648.58	478897.92
T2	401760.00	912798.72	2551980.54	594604.80
T3	224021.37	39602057.11	2976238.10	203451.24
T4	200237.18	222735.74	2195216.65	491754.24
T5	829232.64	893514.24	2847674.88	1073502.72
T6	339728.26	340692.48	1041361.92	552821.76

Table 14: Estimated contaminant mass discharge for SO_4 through the transects in kg/yr

Transect	68 months $M_d = Q \times C$	168 months	1200 months
T1	22858535.13	95361791.73	1543487.99
T2	0	1837425.90	1584027.19
T3	17028884.56	5654852.39	456748.03
T4	0	0	13670.44
T5	0	0	1819587.11
T6	0	0	71314.01

Table 15: Estimated contaminant discharge for Cl through the transects in kg/yr

Transect	68 months $M_d = Q \times C$	168 months	1200 months
T1	5265626.842	15174963.38	199700.43
T2	0	27645.90	230706.66
T3	2534531.66	776798.14	69173.42
T4	0	0	17703.15
T5	0	0	339226.86
T6	0	0	5528.22

Borehole abstraction

One of the accepted practices for mitigation, without removing the source completely, is to try and divert the flow path of subsurface contaminants. This can be achieved by the physical abstraction at a selected number of boreholes. The locations of mitigatory measures such as boreholes can only be determined once the path of contaminants is simulated. The scenario simulates the migration of SO_4 and Cl from the TSF whilst abstraction is taking place.

Three existing boreholes (BH7, BH8, KR2) are selected as boreholes to be pumped. Low pumping rates are used to prevent dewatering of the aquifer. An initial pumping rate of 8.64 m^3/d is used. The three boreholes are pumped for 24 hours per day. The contaminant plume continues to migrate outward and downstream, however once the boreholes are reached the contamination decreases in the vicinity (Figure 61 and Figure 62).

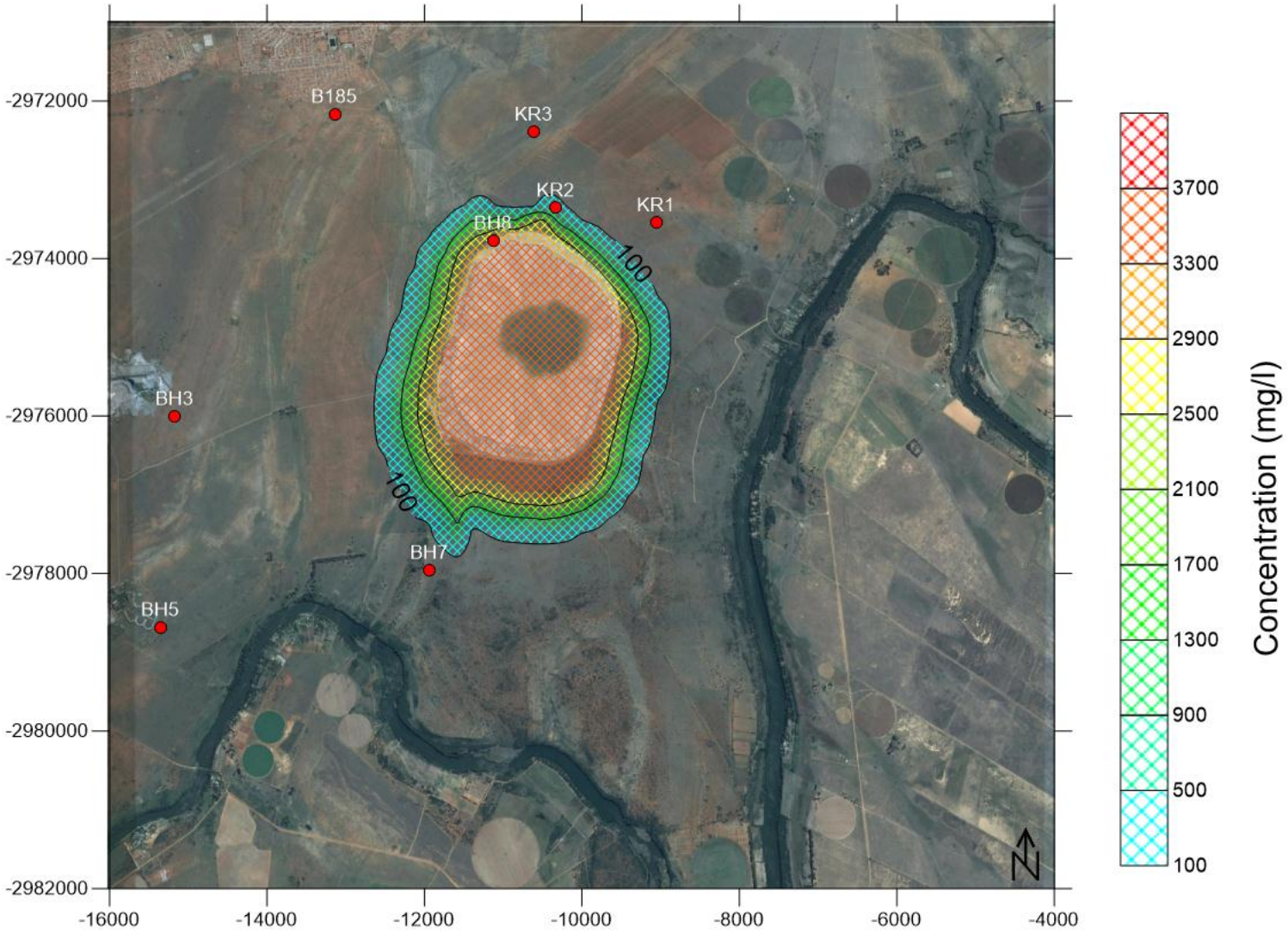

Figure 61: Modelled SO_4 contaminant plume at 68 months during abstraction of 0.1l/s

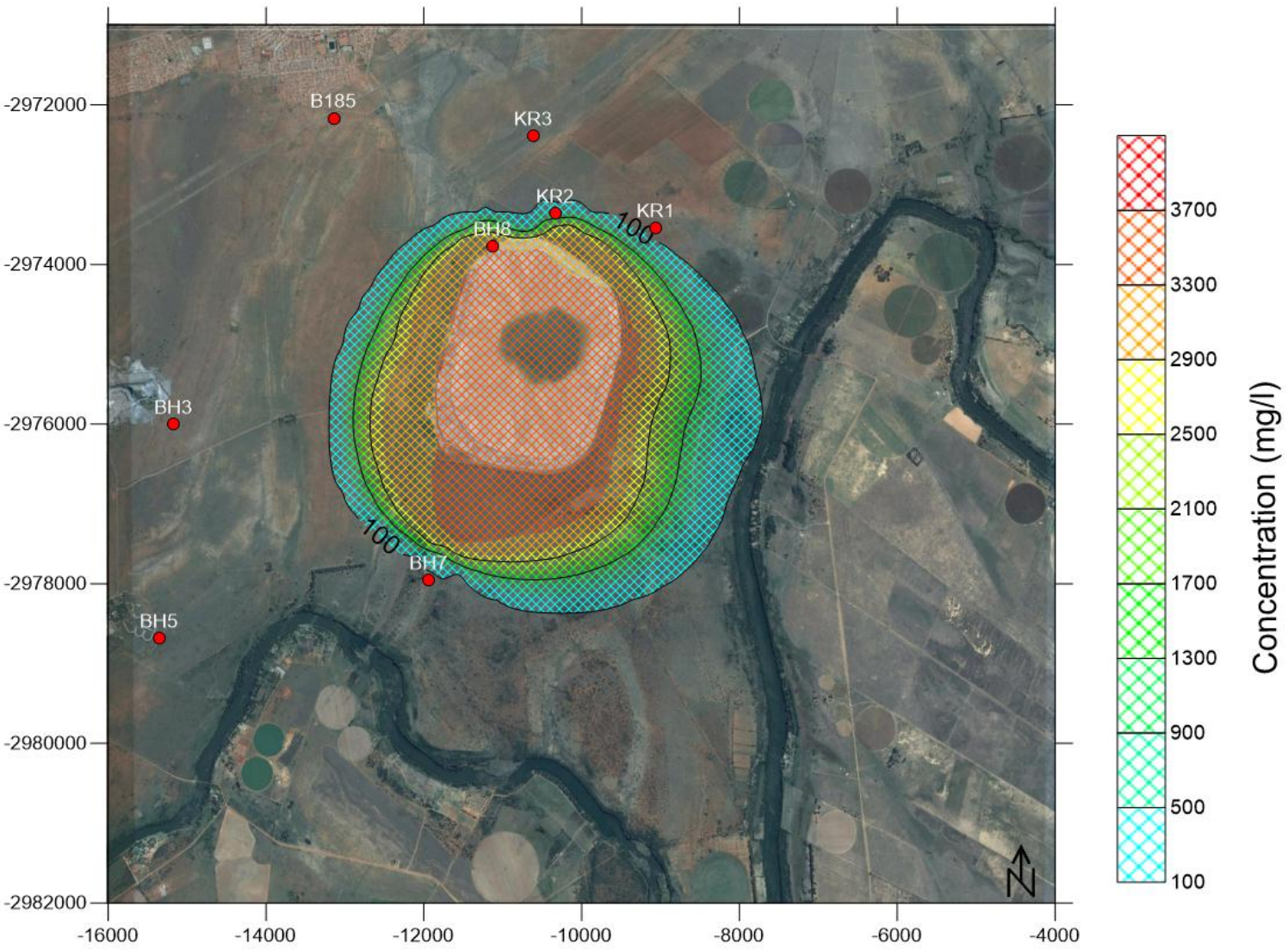

Figure 62: Modelled SO_4 contaminant plume at 1200 months with an abstraction rate of 0.1 l/s

Figure 63 illustrates an increased pumping rate of the on-site boreholes to 25.92 m^3/day. The scenario with the elevated abstraction rate has a smaller contaminant plume when compared to the previous scenario. However, the plume migration still moves downstream toward the southern portion toward the river (Figure 64).

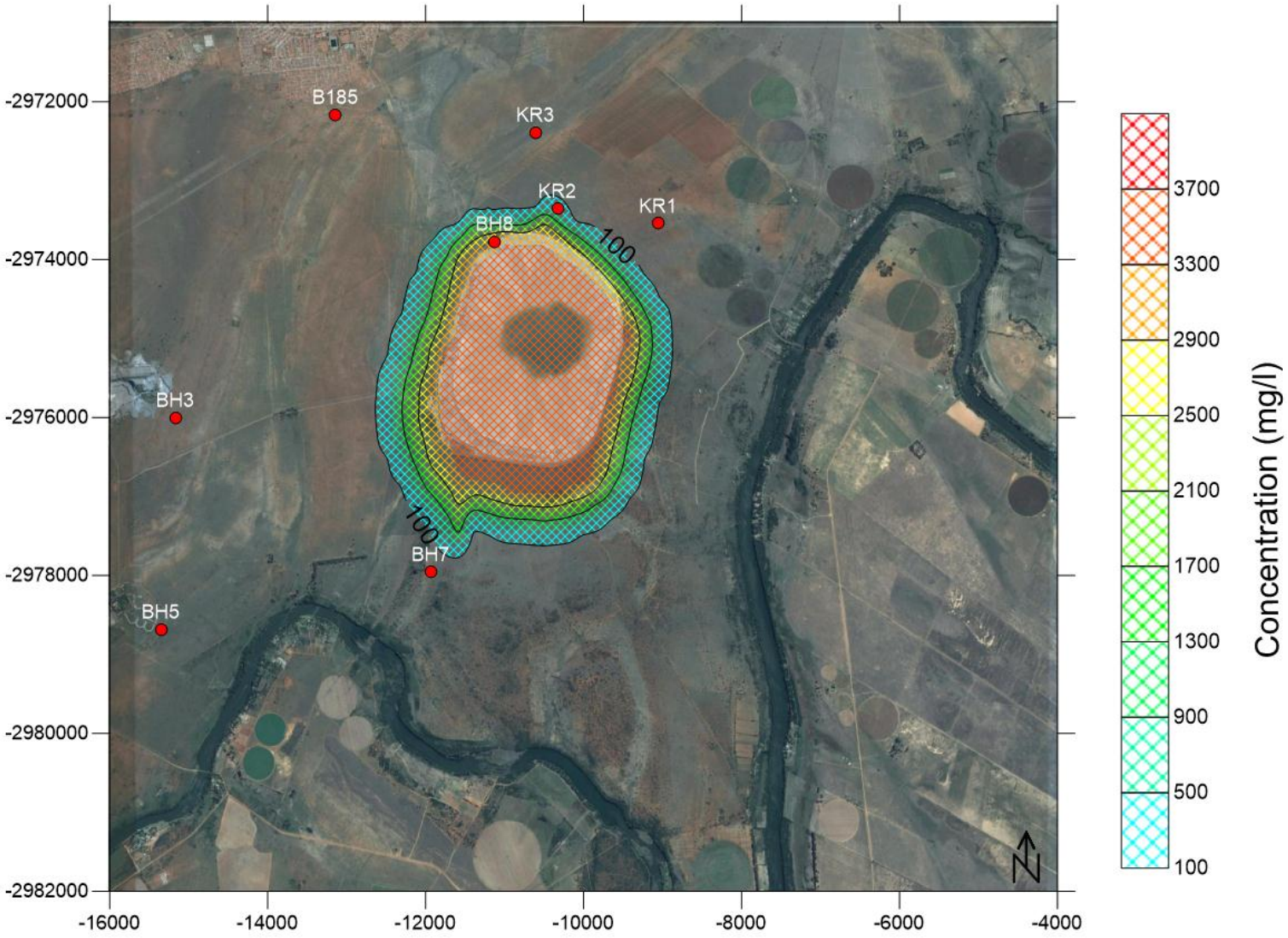

Figure 63: Modelled SO_4 contaminant plume at 68 months with an abstraction rate of 0.2 l/s

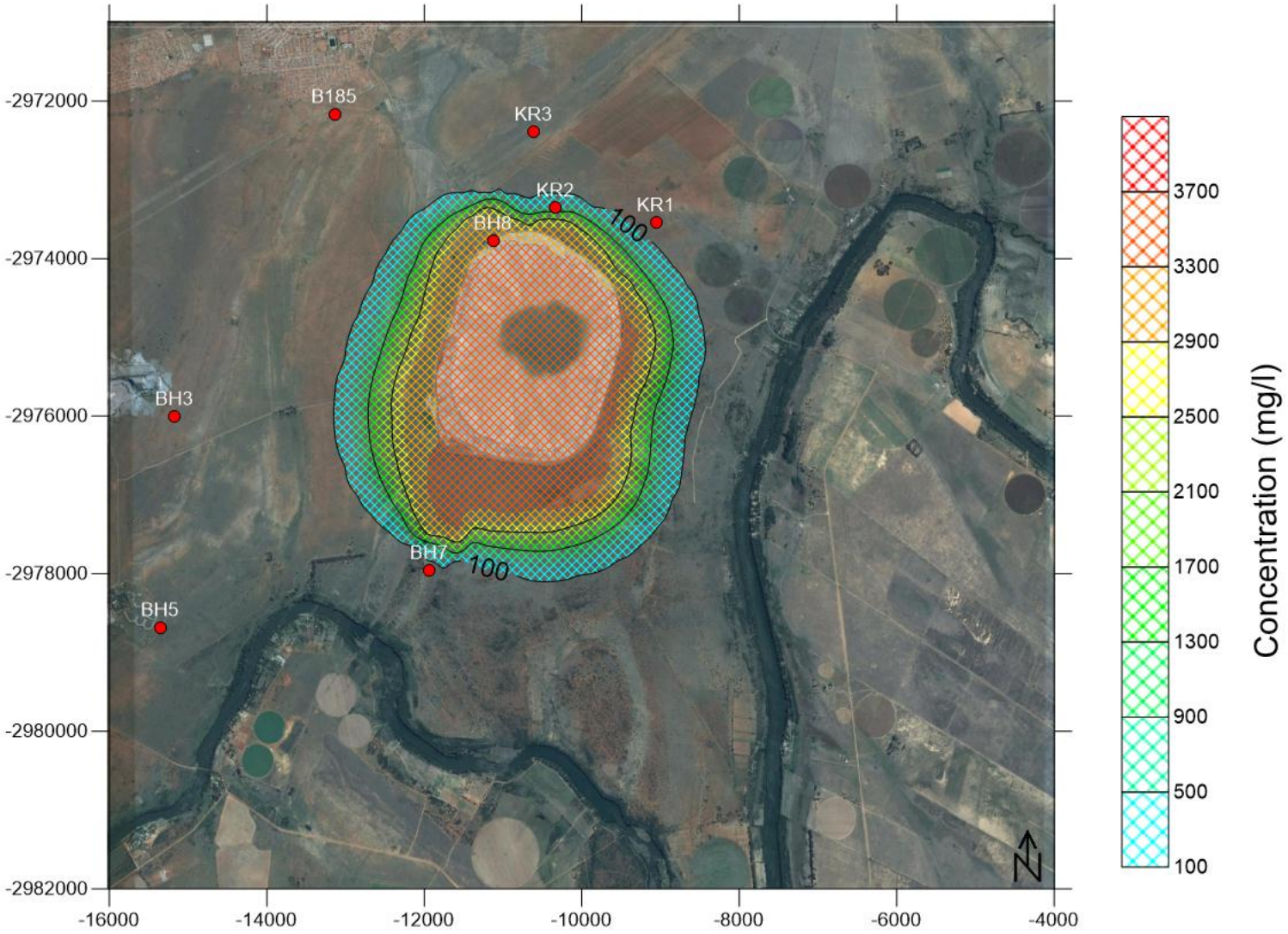

Figure 64: Modelled SO_4 contaminant plume at 1200 months with an abstraction rate of 0.2 l/s

In addition to the model results, the following observations can be made:

- As anticipated the pumping of certain strategic boreholes would inhibit the plume migration to some extent. Therefore, the contaminant concentrations downstream have decreased as a result.
- The plume has an inverted shape downstream where especially BH7 has managed to divert the contaminant path.
- The effectiveness of a higher abstraction rate (0.2 l/s) can be seen. The plume has a reduced shape when comparing to a pump rate of 0.1 l/s.
- Therefore, the effect of such a scenario (pumping at 0.2 l/s) would prove more successful in reducing the contaminant plume, however the viability of such a strategy would most likely depend on a feasibility study of whether the operating company of the TSF could consume the contaminated water abstracted.

Trench drain

The scenario represents the inclusion of two L-shaped trench drains on the eastern and western flanks of the TSF. The French drain design requires the excavation of a trench to a depth below the groundwater level so as to encourage the natural flow toward the trench. Once the area is excavated, a drainage system (commonly perforated PVC pipes) is installed at the base and covered with a highly permeable material e.g. course (see Figure 65).

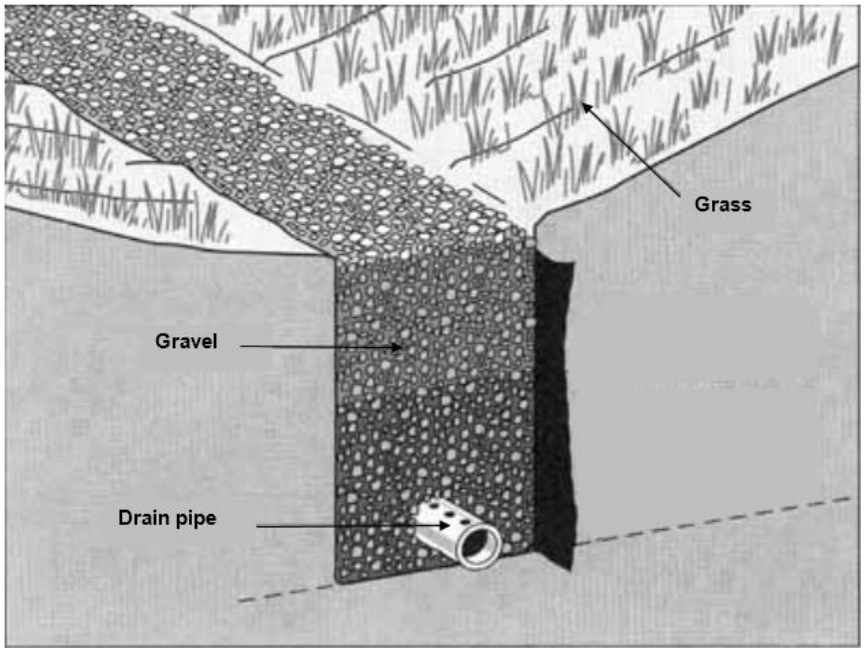

Figure 65: Cross section of a typical trench drain using a perforated underdrain pipe (CDOT, 2004)

The modelling results illustrate the effect of installing a trench drain without any additional abstraction from boreholes surrounding the TSF (see Figure 66 and Figure 67).

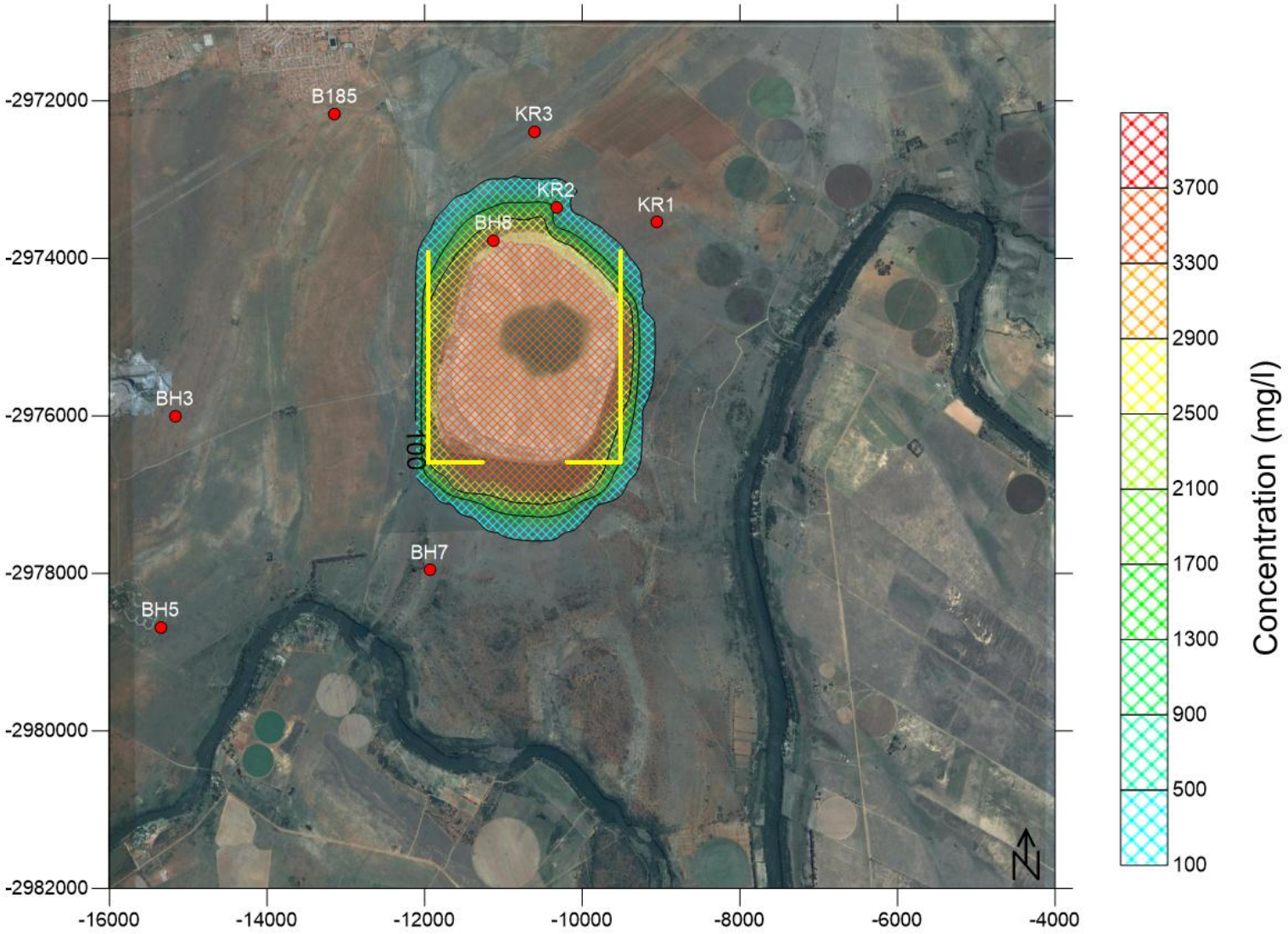

Figure 66: Modelling results for SO_4 plume with trench-drain at 68 months

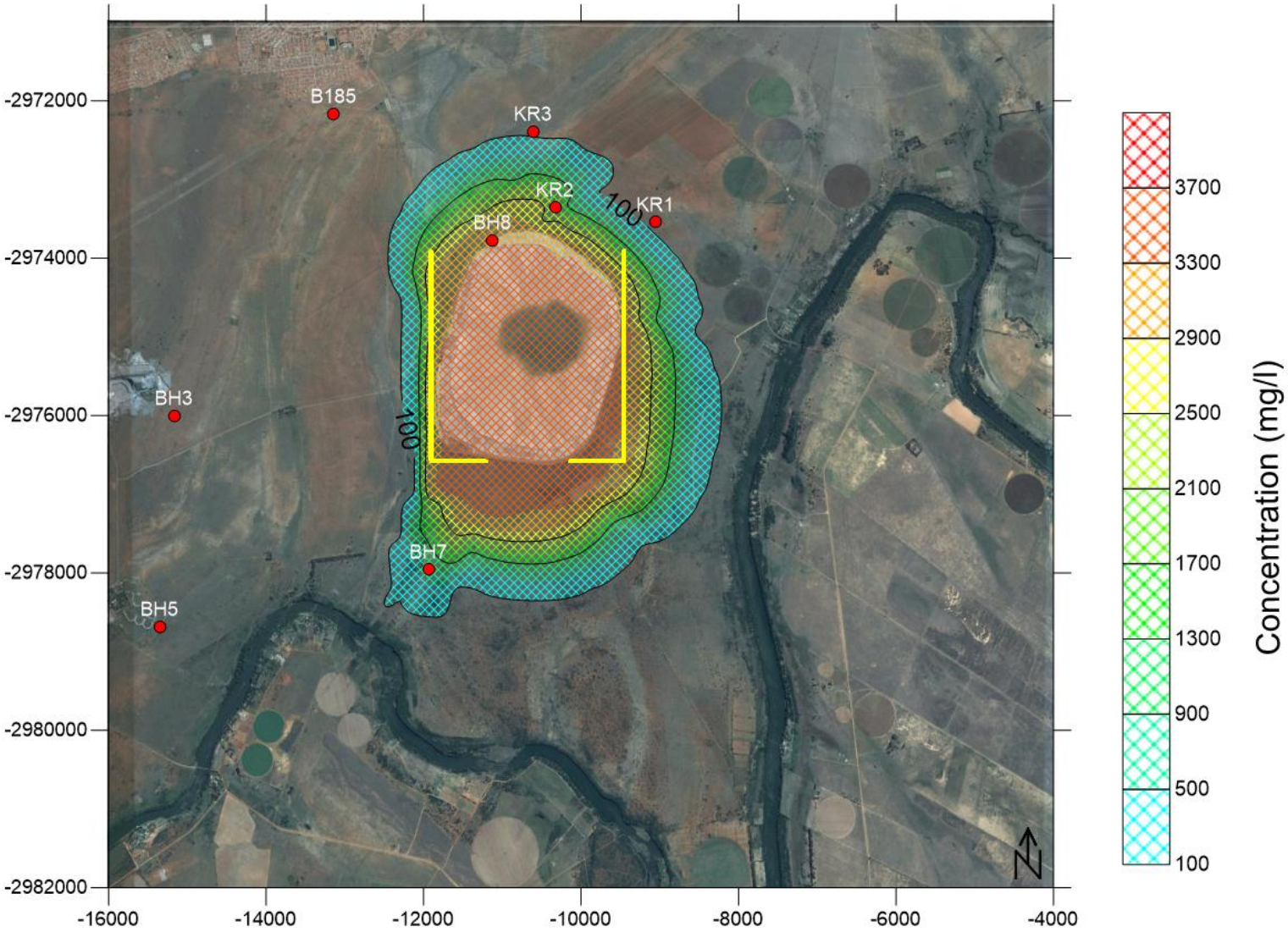

Figure 67: Modelling results for SO_4 plume with trench-drain at 1200 months

Combination of borehole abstraction and trench drains

This scenario represents the construction of two L-shaped trench drains on the eastern and western sides of the TSF.

For trench drains to be effective the groundwater table must be at a higher elevation than that of the trench itself as groundwater moves from a higher potential to a lower potential according to Darcy's law for groundwater movement. Therefore, to obtain a maximum efficiency from the trench-drain, three boreholes (BH7, BH8, KR2) are pumped at 0.1 l/s.

With reference to Figure 68 and Figure 69, it can be seen that the plume has decreased to such an extent that the river is now unaffected by the contaminated groundwater. Elevated concentrations are found around the immediate vicinity of the TSF and the combination of a trench drain and abstraction has reduced the overall contaminant plume.

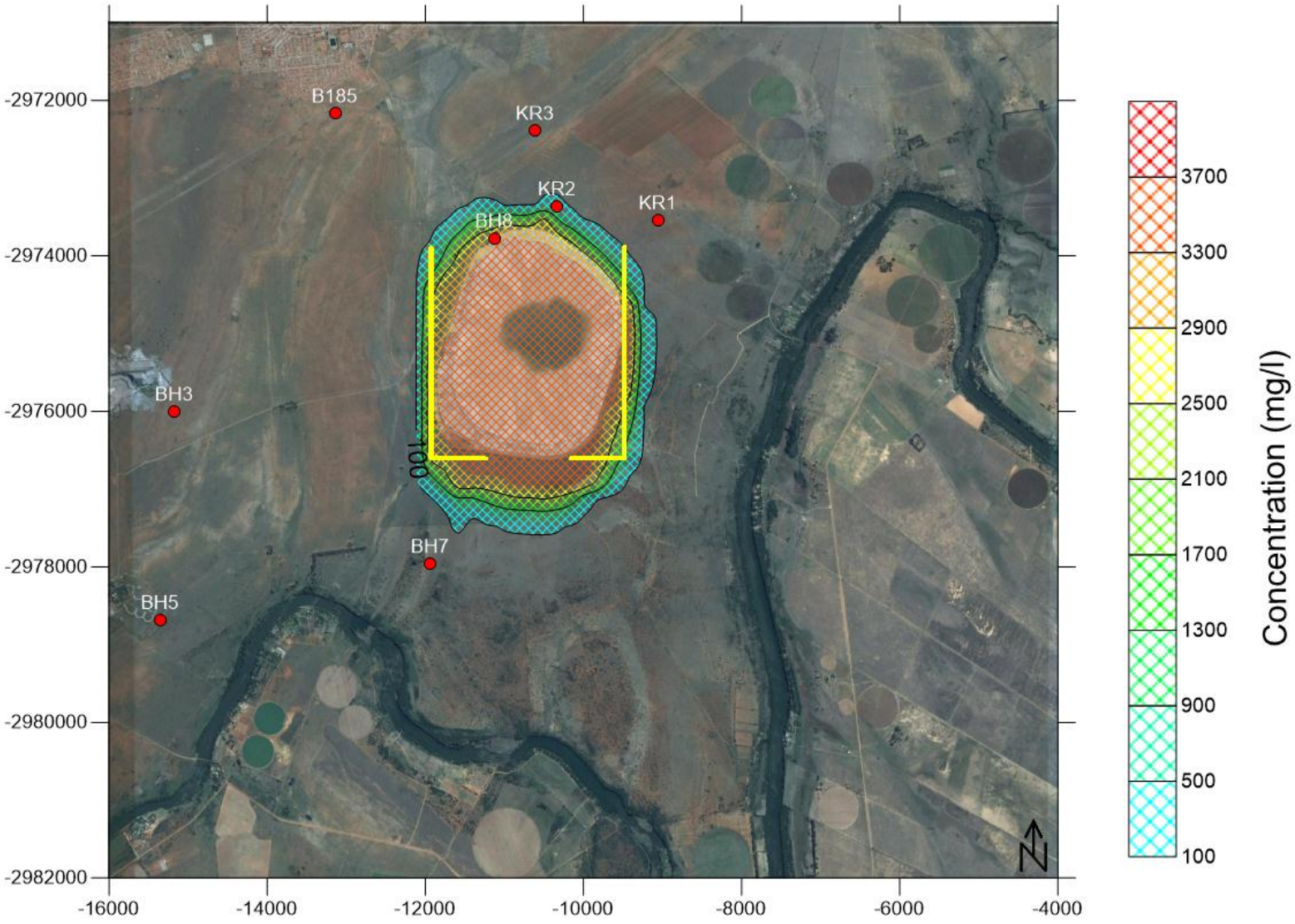

Figure 68: Modelled results for SO_4 plume with a trench drain and abstraction of 0.1l/s at 68 months

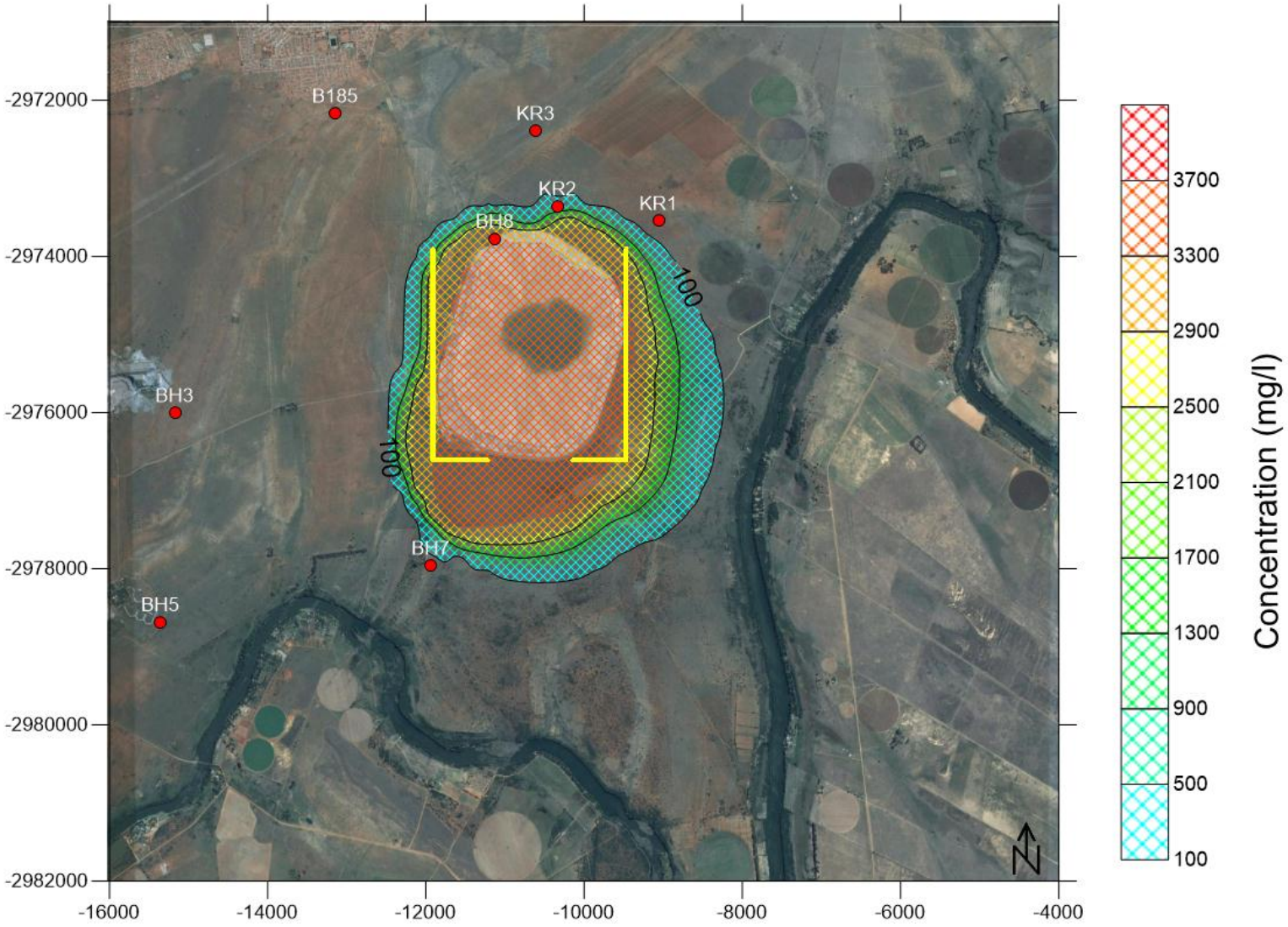

Figure 69: Modelled results for SO_4 plume with a trench drain and abstraction of 0.1l/s at 1200 months

Chapter 5: Discussion

Continual seepage from TSFs has been long identified as the source of large scale contamination of groundwater. High levels of sulphate and chloride water are contaminants closely related to gold and coal mining industry. Many studies on the gold bearing conglomerates of the Witwatersrand Group have confirmed that the high levels of sulphate are a direct result of high levels of sulphide bearing minerals present in the ore body. The sulphide rich tailings are prone to generate AMD which in turn mobilises heavy metals due to the low pH condition of the water released from these TSFs. To date more than 270 TSFs have been constructed in the greater Johannesburg and Far West Rand (Rösner, 2007), most of which are unlined. Only once that tailings material has been completely removed from an area will the continual seepage of contaminants cease. Continual seepage of water with excessive concentrations of contaminants ultimately leads to an increase of the dissolved solids found in natural groundwater. These activities render the groundwater unsafe for both domestic and agricultural use.

For this reason, it is imperative to be able to predict the transport of such contaminants so as to have any chance in reducing the impacts of TSFs on groundwater quality. The source-pathway-receiver framework is a proven methodology to use as a precursor to numerical transport modelling. Numerical models are only a tool that is user guided in order replicate hydrological flow processes. In other words, the accuracy of a numerical model is only as accurate as the data used as input, therefore conceptualising and collection of data is the core of any predictive modelling practice.

The numerical modelling conducted on the mega tailings study area showed that the continual seepage from the TSF produced a localised groundwater mound. This elevated groundwater table is the driving process for contaminants to enter the natural groundwater system below. The TSF has no form of lining and is directly linked to the natural aquifers. Elevated head conditions only occur from 68 months, reaching a peak at 168 months when seepage flow is also at its highest. Once deposition ceases there is a subsidence of the groundwater table and the TSF moves into a dormant state.

The contaminant plume modelled for the mega tailings moves in two distinct directions, the first portion moves slightly faster toward the south west as contaminants move with groundwater in the contact zone between the dolerite and quartzite zones. This location is also a low lying marsh where the water table is close to the surface and directly drains into the Vaal River. The second plume travels slightly slower as transmissivity of the sill is much lower

toward the south east. The contaminant plume front only reaches the Vaal River after a period of 1200 months, which would be a result of the lower transmissivities.

Contaminant concentrations for the boreholes BH8, KR2 and BH7 rise almost exponentially once the plume front enters these boreholes. The same trend is noticed with the Cl concentration.

Contaminant mass discharge calculations for the site revealed that during the initial depositional phase of the TSF contaminant concentrations do not spread any further that the footprint of the TSF. From 68 months the various transects started recording elevated concentrations with an increase in groundwater discharge. This increase in discharge can be attributed to the addition of seepage water from the base of the TSF into the surrounding aquifer. Contaminant mass discharge rates for SO_4 ranged between 7.13×10^4 kg/yr and 9.95×10^7 kg.yr. These high values where found at transects T1 and T3 which where adjacent to the TSF, which was expected as the highest groundwater discharge and contaminant concentrations are found closer to the TSF footprint. However, a greater emphasis was placed on transects T5 and T6 which recorded flow into the Vaal River and the SO_4 concentrations where for T5 1.18×10^6 kg/yr and T6 7.13×10^4 kg/yr respectively.

Mass discharges for Cl across the various transects ranged between 1.52×10^3 kg/yr and 1.52×10^7 kg/yr. The transects T5 and T6 recorded mass discharge rates of 3.39×10^5 kg/yr and 1.52×10^3 respectively. The transects showed a gradual increase in contaminant mass discharge as the contaminant plume moved across the various transects.

An overall reduction in contaminant concentration is noticed in both hypothetical and existing boreholes for all mitigation scenarios. However, abstracting boreholes still saw an increase in contaminant concentration especially BH8. Both KR2 and BH7 saw increases in concentrations, however to a lesser extent than the worst case scenario. During the abstraction scenarios it took less time for contaminants to reach the abstraction boreholes, with BH8 showing an almost instant increase. This reduction in time proves the effect of borehole abstraction as contaminants are drawn toward the borehole where it can be removed from the aquifer system, thus reducing any downstream contaminant transport. The combination of the trench drains and abstraction boreholes (pumping at 0.1 l/s) proved the more effective. Low pumping rates don't cause a significant drop in the groundwater level and therefore the trench drains can operate effectively. The combination of trench drains and abstraction reduced the contaminant plume to such an extent that contaminants do not reach the Vaal River within the time period of the simulation.

5.1 Limitations of the modelling exercise

The modelling was completed to an accuracy level permitted by the amount of data available. It was assumed that the aquifer system where horizontal flow is dominant. Contaminants (SO_4 and Cl) were assumed to act as conservative un-reactive tracers. Although all efforts were considered to produce a model as accurate as possible it must be considered in accordance with the assumptions made for data that was not obtainable. The most important of which is that a fractured aquifer will behave as a porous medium, which could lead to some uncertainty. Due to the complexity of the subsurface mechanisms controlling physical chemical reactions an exact concentration of contaminants.

Chapter 6: Conclusions and Recommendations

4.1 Conclusions

From the information discussed in the preceding sections the following conclusions can be made:

- The primary source of water introduced to the TSF is both from the deposition of tailings as well as natural precipitation. During the operational phase of a TSF supernatant water creates constant pool condition where it is removed for reuse in the metallurgical plant. Once deposition ceases a rapid decrease in the phreatic surface takes place as precipitation is the only source of water atop the TSF. Therefore it is necessary to calculate a water balance upon which to base estimates of volumes and available to seepage from within the facility. Additional modelling (SEEP/W) improves accuracy in determining a flux volume of water that reaches the base of the facility contributing to the regional groundwater.
- The continual deposition of slurry and constant pool conditions introduced by the TSF resulted in a localised rise in groundwater level during the flow modelling. Therefore, the existence of a groundwater mound around a tailings facility of this nature is supported as described by Rösner (1999). This mound would form the link between the natural groundwater and the interstitial water within the TSF.
- The elevated concentrations of specific contaminants e.g. SO_4 and associated heavy metals would ultimately lead to a localised increase in contaminant concentrations found in the natural groundwater. Continuous seepage from the TSF will see a change in the overall groundwater chemistry to a SO_4 dominated water as seen in the Piper diagrams of typical TSF seepage water. Acidic conditions can also have an added threat of mobilising heavy metals, effectively raising concentrations.
- Contaminated seepage flux increases throughout the depositional life, reaching its peak flux between 138 and 168 months. Continuous deposition of supersaturated slurry and the vertical rise of the TSF will cause a rise in the phreatic surface, which in turn would make result in a larger volume of water available to seep downward.

Numerical modelling is used to support and evaluate groundwater transport mechanisms described in the conceptual model. The predictive modelling scenarios that were simulated found the following:

- The contaminant plume simulated during “worst case” scenario produced the largest contaminant plume. The area affected by the contaminant migration far exceeds the area covered by the TSF.

- Contaminant transport is greater downstream and follows the general slope of topography toward the Vaal River. Two key areas toward the south east and south west of the TSF were identified by the modelling as potential seepage locations into the river. Once the plume front reaches the river contaminants will contribute to the overall salt load through base flow.
- The construction of TSFs on low permeability volcanic rock such as diabase does slow down the transport of contaminants, however from the transport modelling the extend of the contamination plume still manages to far exceed the bounds of the TSF and additional mitigation measures must be considered in an attempt to reduce the impacts of these activities of the natural groundwater.
- The reduction in artificial recharge from the TSF does slow down the plume migration.
- Seepage rates that have been determined from the operational water balance i.e. depositional phase of the TSF were 8.897 x 10^{-5} m/day for the overflow section and 1.314 x 10^{-3} m/day for the underflow section respectively. The dramatic increase in seepage rate between the two sections is due to the increase difference in material properties such as permeability.
- The SO_4 contaminant transport plume has the same shape and extent than that of Cl plume, however the C concentrations are lower.
- Groundwater abstraction from strategic boreholes (BH8, KR2 and BH7) managed to contain the contaminant plume to an extent at the constant pumping rate of 0.1 l/s. Increasing the pumping rate to 0.2 l/s showed a reduction in the size of the contaminant plume. However, the increased groundwater abstraction from long periods of time could have an adverse effect on the availability of groundwater as a resource due to the formation of large cones of depression around the abstracting boreholes.
- Abstraction also only proved effective at localised spots with the downstream borehole BH7 having the greatest impact; borehole abstraction seemed to have almost no effect toward the south east and north west of the TSF where no boreholes where located. The plume still migrated toward the Vaal River.
- The addition of L-shaped trench drains to the west and east of the TSF showed a reduction in the overall footprint of the TSF. The most noticeable reduction of the contaminant plume is seen during the depositional phase of the TSF. Lowering of the pumping rate to 0.1 l/s during this scenario improved the drain efficiency as there is a slight rise in the groundwater table. Thus when introducing trenches as a passive drainage solution it must be kept in mind that the groundwater level must always remain at a higher level than that of the drain. The combination of abstraction boreholes and trench drains has the greatest reduction in the contaminant plume. Reducing pumping

rates and supplementing drainage capacity with passive systems such as drains have the added benefit of reducing costs and maintenance. The risk of large scale dewatering is also reduced as smaller volumes of water are abstracted over the long term.

Contaminant mass discharge calculations are based on the “worst case” scenario utilising outputs from groundwater modelling and solute transport modelling practices. The calculations revealed the following:

- Initially contaminant mass discharge rate across the various transects showed no contaminant discharge at all. This is as a result of the contaminant plume formation, there is a delayed transport of contaminants as groundwater discharge gradually increases from the base of the TSF and a groundwater mound forms creating a direct linkage between TSF seepage water natural groundwater.
- Increases in groundwater flux showed an increase in contaminant mass discharge across the transects.
- Transect T1 showed the highest contaminant mass discharge for both SO_4 and Cl at 9.54×10^7 kg/yr and 5.27×10^7 kg/yr respectively. This would be expected as transect T1 is in the closest proximity to the TSF footprint.
- Elevated contaminant discharges from transects T2 and T5 for both SO_4 and Cl indicates that the contaminant plume is more inclined to move toward the south westerly direction. Contaminant concentrations are also higher in this region.
- Contaminant mass discharge along transect T5, located along the Vaal River had mass discharge rates for SO_4 at 1.82×10^6 kg/yr and Cl at 3.39×10^5 kg/yr. These load estimates would eventually be contributed to the Vaal River system, adding to the rivers overall dissolved salt load.

The methodology presented in this document incorporates a water balance approach with numerical models to bridge the gap between two well established approaches. The methodology attempts to deliver an acceptable level of accuracy for contaminant migration and mass flux determination whilst remaining as simple and cost effective. Most often the “black box” water balance approach to determine seepages at the base of the TSF does not take into account the physical properties of the TSF itself. This can lead to an underestimation of the rates of water retention within the TSF. The seepage modelling proposed by this methodology accounts for those shortfalls. Modelling various phases of the depositional life of the TSF will also improve seepage modelling accuracy as deposition plans change throughout this period of a TSFs lifetime.

Fluxes modelled by the seepage modelling are then incorporated into an established numerical groundwater model that could determine the potential fate of contaminants from seepage. The key to this methodology is to take volumes determined from an operational and post-operational water balance and introduce it as seepage in a numerical groundwater model in order to evaluate contaminant migration from a TSF into the natural groundwater system.

4.2 Recommendations

The numerical model used water balance based on preliminary deposition data that was established during the design phase of the TSF. The accuracy of the water balance could be improved by using current depositional data. Tailings material properties of specifically the compacted material closer to the base of the TSF could be determined and used to improve seepage modelling inputs.

Furthermore, seepage estimates could be used as an input for geochemical modelling. This approach is can be used to simulate individual chemical species throughout the entire TSF and associated groundwater system.

Lastly contaminant mass discharge rates can be calibrated if boreholes are monitored regularly. Additional monitoring boreholes can also be drilled to ensure accurate input data for the model. It must be noted that the boreholes must be constructed to facilitate the monitoring of the potential mound and the water levels and quality of the shallow and deeper fractured aquifers.

References

Abiye, T.A. no date. Hydrogeochemical footprint as a result of mining activities in the Johannesburg area. Johannesburg: Wits.

Abiye, T.A. 2011. Provenance of groundwater in the crystalline aquifer of the Johannesburg area, South Africa. *International Journal of Physical Science,* 6(1).

Abiye, T.A., Mengistu, H. & Demlie, M.B. (2011) Groundwater resource in the crystalline rocks of the Johannesburg area, South Africa. *Journal of Water Resources and Protection,* 3(4).

AQTESOLV. 1998. *Solutions, Hantush & Jacob r/B solution for Leaky Confined Aquifers.* Available from http://www.aqtesolv.com/hantush-jacob.htm. [Accessed: 25 January 2015].

Blight,G.E. 1988. Some less familiar aspects of hydraulic fill structures. Hydraulic Fill Structures. ASCE Geotechnical Special Publication No. 21.

Blowes, D.W., Ptacek, C.J., Benner, S.G., Waybrant, K.R. & Bain, J.G. 1998. Permeable reactive barrier for the treatment of mine tailings drainage water. In: Merkel, B., Helling, C. (Eds.), Proceedings of International Conference and Workshop Uranium Mining and Hydrogeology. Vol. 2. Freiburg, Germany.

Bouwer, H. & Rice, C. 1976. A slug test for determining hydraulic conductivity of unconfined aquifers with completely or partially penetrating wells. *Water Resources Research,* (12).

Brixel, B., Caldwell, J.A. & Wels, C. 2012. Groundwater issues in the Design, Operation, and closure of Tailings, Waste rock and Heap leach facilities. *Tailings & Mine waste proceedings of the 16th International Conference.* Colorado, USA. Available from: www.rgc.ca/?page=publications [Accessed: 20 August 2014]

Brooks, R.H. & Corey, A.T. 1964. Hydraulic properties of porous media. *Colorado State University Hydrology Paper.* Fort Collins. Vol. 27

Cobb, P.M., McElwee, C.D. & Butt, M.A. 1982. Analysis of Leaky Aquifer Pumping Test Data: Using Sensitivity Analysis. *Groundwater,* 20 (3).

Coetzee, H., Kotoane, M., Atanasova, M. & Roelofse, F. 2013. Interactions between dolomite and acid mine drainage in the Witwatersrand – Results of field and laboratory studies and the implications of natural attenuation in the West Rand Goldfield. (*In:* Brown, A.,

Figueroa, L. & Wolkersdorfer, eds. Ch*:* Reliable Mine Water Technology. Denver: USA.)

Cooper, H.H. 1946. A generalised graphical method for evaluating formation constants and summarizing well field history. *Transactions American Geophysical Union,* (27).

Council for Geoscience (CGS). 2014. GEODE/GIS spatial database. Pretoria, South Africa.

Duane, M.J., Pigozzi, G. & Harris, C. 1997. Geochemistry of some deep gold mine waters from the western portion of the Witwatersrand basin, South Africa. *Journal for African Earth Science*, 24(1/2).

Einarson, M.D. 2001. Flux based Corrective Action. Princeton Groundwater Remediation course. Denver, Colorado.

Enslin, J.F. & Kriel, J.P. 1968. The assessment and possible future use of dolomitic groundwater resources of the Far West Rand, Transvaal, Republic of South Africa. *Papers of the International Conference on Water for Peace. 1967 May 23 – 31. Washington DC. Vol2.* Washington. US Government Printing Office.

Fabbri, P., Ortombina, M. & Piccinini, L. 2012. Estimation of hydraulic conductivity using the slug test method in a shallow aquifer in the Venetian Plain. *AQUA Mundi*. Available from: www.acquesotterranee.it/sites/default/files/am06045. [Date accessed: 12 December 2015].

Fisher, S. 1983. Coal Development. (*In*: Dave Brooks., *ed*. L. Branch & C. Fisher, Papers presented at coal development workshops in Grand Juction, Colorado and Casper, Wyoming.)

Fredlund, D.G., Xing, A., & Huang, S. 1994. Predicting the permeability function for unsaturated soils using the Soil-Water Characteristic Curve. *Canadian Geotech Journal*, (31).

Fredlund, M.D., Ward Wilson, G., & Fredlund G. 1997. Estimation of hydraulic properties of unsaturated soil using a Knowledge-Based system. *Proceedings of characterisation and measurement of the hydraulic properties of porous media.* Riverside, California. 22 – 24 October 1997.

Garrick, H., Digges La Touche, G., Plimmer, B. & Hybert, D. 2014. Assessing the hydraulic performance of tailings management facilities. (*In* Hunger, E., Brown, T.J. & Lucas, G

Ed. Proceedings of the 17th Extractive Industry Geology Conference, EIG conferences Ltd.)

Gauteng Department of Agriculture, Environment, and Conservation (GDACE). 2008. Mining and Environmental Impact Guide. Johannesburg, South Africa.

Geoslope. 2012. Seep/W software, Geoslope International Ltd. Calgary, Canada.

Govender, K., Bezuidenhoud, N., Van Zyl, A, & Rousseau, P. 2009. Prediction of seepage emanating from a TSF in an Arid climate. *Abstracts of the International Mine Water Conference*. Pretoria, South Africa. 19 – 23 October 2009. Available at: www.imwa.info/docs/imwa_2009/IMWA2009_Govender.pdf. [Accessed: 20 January 2015]

Gunn, J. 1986. A conceptual model for conduit flow dominated karst aquifers. *Proceedings of the international symposium.* Anarkara, Turkey.

Hantush, M.S. & Jacob, C.E. 1955. Non-steady radial flow in an infinite leaky aquifer. *Transactions American Geophysical Union*, (36)1.

Harbaugh, A.W & McDonald, M.G. 1996. User's documentation for MODFLOW-96, an update to the U.S. Geological Survey modular finite-difference ground-water flow model. S.l.: U.S. Geological Survey.

Hatfield, K., Rao, S., Annable, M. & Campbell, T. 2002. Device and Method for measuring fluid and solute fluxes in Flow systems. (Patent: US 6401547B1).

Hattingh, R.P., Lake, J., Boer, R.H., Aucamp, P. & Viljoen, C. 2003. Rehabilitation of contaminated gold tailings dam footprints. Water Research Commission (WRC). WRC report No. 1001/1/03. Pretoria, South Africa.

Hazen, A. 1892. Some physical properties of sands and gravels. Massachusetts State Board of Health. Annual Report.

Hearne, C.L. & Bush, R.A. 1996. Investigation into the impact of diffuse seepage from gold mines in the Klerksdorp region on water quality in the Vaal River, Phase1. Report no. CED/011/96 for the Klerksdorp Mine Managers Association (KMMA). Johannesburg. (Unpublished).

Hemond, H.F. & Fechner – Levy, E.J. 2000. Chemical fate and Transport in the Environment. SD: Academic Press.

Hölting, B.H. 1996. Hydrogeologie. Stuttgart: Enke.

Interstate Technology & Regulatory Council (ITRC). 2010. Use and Management of Mass Flux and Mass Discharge. *MASSFLUX-1*. Interstate Technology & Regulatory Council, Integrated DNAPL site strategy team. Washington, D.C.

Jarvis, A., H.I. Reuter, A. Nelson & E. Guevara. 2008. Hole-filled SRTM for the globe Version 4. Available from the CGIAR-CSI SRTM 90m Database (http://srtm.csi.cgiar.org).

Johnson, B.D. & Hallberg, K.B. 2005. Acid Mine Drainage remediation options: a review. *Science of the Total Environment*, (338). Available at: www.sciencedirect.com. [Accessed: 13 July 2014]

Jones, G.A., Brierly, S.E. & Geldenhuis, S.J.J. Howard. 1998. Research on the Contribution of Mine Dumps to the Mineral Pollution Load at the Vaal Barrage. Water Research Commission (WRC). WRC report no. 136/1/89. Pretoria, South Africa.

Kozeny, J. 1927. Uber kapillare leitung des wassers im Boder Sitzunger Akademie Wiss, Wien. 136(2a).

Kresić, N. 2007. Hydrogeology and groundwater modelling 2nd ed. CRC press, Taylor & Francis.

Krumbein, W.C. & Monk, G.D. 1942. Permeability as a function of the size parameters of unconsolidated sand. *Transactions of American Institute of Mining and Metallurgical Engineering (151) 165 – 183.*

Lambe, W.T. & Whitman, W.V. 1969. Soil Mechanics. Massachusetts Institute of Technology. NY: John Wiley & Sons.

L&W Consulting Environmentalists. 1993. Klerksdorp regional groundwater baseline study. Report no. 2562/623/1/E. Marshaltown, L & W Environmental. (Unpublished).

Labuschagne, P.F. & Human, C. 2009. Estimating the impact of site Hydrogeology on Groundwater Liability, Closure and Rehabilitation. *Abstracts of the International Mine Water Conference*. Pretoria, South Africa, 19 – 23 October 2009. Available at: www.imwa.info/docs/imwa_2009/IMWA2009. [Accessed: 21 January 2015].

Marino, M.A. & Luthin, J.N. 1982. Seepage and Groundwater. NY: Elsivier Scientific Publishing Company.

Martin, J.P. & Koerner, R.M. 1984. The influence of vadose zone conditions on groundwater pollution – Part 1: Basic principles of static conditions. *Journal of Hazardous Materials*, (8).

Martin, J.P. & Koerner, R.M. 1984. The influence of vadose zone conditions on groundwater pollution – Part 2: Fluid movement. *Journal of Hazardous Materials,* (9).

McPhail, G.I. & Wagener, J.C. 1987. Disposal of Residues. (*In:* Stanley, G.G., *ed.* The Extractive Metallurgy of Gold in South Africa. Johannesburg: The South African Institute of Mining and Metallurgy).

Menghistu, M.T. 2009. Frist Uranium – Chemwest Project Chemwest Tailings Disposal Facility (TDF) Estimation Of Water Flux and Water Volume Expected to Seep From The TDF. Project No. RI301-00204/01. Knight Piésold Consulting. Rivonia, South Africa.

Morgan, D.J.T. & Brink, A.B.A. 1984. The Far West Rad dolomites. *Proceedings of the International Conference Groundwater Technology*, 1984. Johannesburg, South Africa.

Naicker, K., Cukrowska, E. & McCarthy, T.S. 2003. Acid Mine Drainage arising from gold mining activity in Johannesburg, South Africa and environs. *Environmental Pollution,* (122). Available at: http://www.elsivier.com/locate/envpol. [Accessed 05 October 2014]

Nichols, E. & Roth, T. 2004. Flux Redux: Using mass flux to improve clean up decisions. *L.U.S.T. Line.* New England Interstate Water Pollution Control Commission. Lowell, Massachusetts.

Nininger, R.D. 1954. The Uranium Ore Minerals: A Guide to Exploration of Uranium, Thorium and Beryllium. NY: Van Nastrand Company.

Oxtobee, J.P.A. & Novakowski, K. 2002. A field investigation of Groundwater/ Surface water interaction in a fractured bedrock environment. *Journal of Hydrology*, 269(3). Available at: www.sciencedirect.com/science/article [Accessed: 25 September 2014]

Palmer, A.N. 1991. Origin and morphology of limestone caves. *Geological Society of America Bulletin,* (103).

Penman, A.D.M. 1994. Tailings dams, some aspects of their design and construction. Geotechnical Engineering: Emerging trends in Design and Practice. K.R. Saxena Edition.

Pourbaix, M. 1988. Atlas of Electrochemical Equilibria in Aqueous Solution. *International NACE Cebelcor*. Brussels.

Pulles, W., Howie, D., Otto, D. & Easton, J. 1995. A manual on mine water treatment & Management Practices in South Africa. Chamber of Mines of South Africa, Environmental Services. Document prepared for the Water Research Commission, WRC report no. TT 80/96. Pretoria, South Africa.

Ripley, E.A, Redman, R.E. & Maxwell, J. 1982. Environmental impact of mining in Canada. *Environmental impact of mining series,* (2)

Robinson, B.C.S. 2009. Concept design report for the chemwest Mega Tailings dam. Rept no. FA/BR/019/2009. Fraser Alexander. (Unpublished).

Rosberg, J. 2010. Well testing, methods & applicability. Lund: LU. (Thesis – PhD)

Rose, A. W. 2010. Advances in Passive Treatment of Coal Mine Drainage. PA: Penn State University.

Rösner, T. 1999. The environmental impact of seepage from gold mine tailings dams near Johannesburg, South Africa. Pretoria: Pret. (Thesis – PhD).

Rubridge, B.S. 1995. Biostratigraphy of the Beaufort Group, South African Commission on Stratigraphy*. Biostratigraphy Series,* (1)

SANS (South African National Standards). 2011. Drinking Water, Part 1: Microbiological, physical, aesthetic and chemical determinants. Pretoria: SABS, Standards Division. (SANS 241- 1:2011).

Sánchez Espana, J., Lopez Pamo, E., Santofimia Pastor, E., Reyes Andrés, J. & Mertin Rubi Juan, A. 2005. A geochemical and mineralogical study on the impact of acid mine drainage on the water quality of the Odiel River. *9th International Mine Water Congress*. Available at: www.imwa.info/docs/imwa_2005/IMWA2005 [Date accessed: 17 June 2014]

Scott, R. 1995. Flooding of Central East Rand Gold Mines: An investigation into controls over flow rate, water quality and predicted impacts of flooded mines. Water Research Commission (WRC). WRC Report no. 486/1/95. Pretoria, South Africa.

Sheppard, M.I., Thibault, D.H. & Mitchell, J.H. 1987. Element leaching and capillary rise in sandy soil cores, experimental results. *Journal of Environmental Quality,* (16).

Smith, M.E., Bentel, D.L. & Robertze, J.B. 1987. Management guidelines for the construction of gold tailings dams. *Proceedings, International Conference on Mining and Industrial Waste Management*. Johannesburg, South Africa.

Department of Water Affairs and Forestry (DWAF). 2006. Rivers database systems for DWAF. Pretoria.

South Africa. 2001. South African Weather Services Act 8 of 2001.

Spitz, K. & Moreno, J. 1996. A Practical Guide to Groundwater and Solute Transport Modelling. NY: John Wiley & Sons.

Stanley, G.G. 1987 The Extractive Metallurgy of Gold in South Africa. *The S.A. Institute of Mining and Metallurgy Monograph Series M7*. Johannesburg: The Chamber of Mines South Africa.

Stiff, H.A. 1951. The interpretation of chemical water analysis by means of patterns. *Journal Petroleum Technology,* (3).

Taylor, C.J. & Greene, E.A. 2008. Hydrogeologic Characterization and Methods Used in the Investigation of Karst Hydrology. (*In*: Rosenberry, D.O. & LaBaugh, J.W. *ed.* Field Techniques for Estimating Water Fluxes Between Surface Water and Ground Water. U.S. Geological Survey.)

The International Network for Acid Prevention (INAP). 2009. Global Acid Rock Guide (GARD Guide). Available at: www.gardguide.com/. [Date accessed: 03 December 2015].

Theis, C.V. 1935. The relation between the lowering of the piezometric surface and the rate and duration of discharge of a well using groundwater storage. *Transactions American Geophysical Union*, (16).

Tutu, H., McCarthy, J.S. & Curkrowska, E. 2008. The chemical characteristics of acid mine drainage with particular reference to sources, distribution and remediation: The Witwatersrand Basin, South Africa as a case study. *Applied Geochemistry,* (23). Available from: www.elsivier.com/locate/apgeochem [Date Accessed: 23 June 2013]

United States of America. Colorado Department of Transportation (CDOT). 2004. Drainage Design Manual. Colorado.

Van Genuchten, M. Th. 1980. A closed-form equation for predicting the hydraulic conductivity of unsaturated soils. *Soil Science Society of America Journal*, (44).

Van Tonder, G., Harald, K. & Yongxin, X. 2001. FC-Program. Institute for Groundwater Studies (IGS). Bloemfontein: UFS.

Van Zyl, D. 1993. Mine Waste Disposal. *Geotechnical Practice for Waste Disposal*. London: Chapman & Hall.

Vermeulen, N.J. 2001. The Composition and State of Gold Tailings. Pretoria: Pret. (Thesis – PhD) Available from: www. repository.up.ac.za/bitstream/handle/2263/23079/00front.pdf?sequence=1 [Accessed: 15 May 2013].

Vick, S.G. 1990. Planning, Design and Analysis of Tailings dams. Richmond: BiTech Publishers.

Wagener, F von M., Crain, H.J., Blight, G., McPhail, G., Williams, A.A.B., & Strydom, J.H. 1997. The Merriespruit dam failure- A review. *SAICE 2nd International Conference on mining and Industrial Waste Management*. Johannesburg, South Africa.

Wang, B. & Murry, L. 2011. An unsaturated soil seepage analyses for design of a soil cover system to reduce oxidation of a mine tailings deposit. *Geological Survey of Canada.*

Winde, F. & Sandham, L.A. 2004. Uranium pollution of South African streams an overview of the situation in gold mining areas of the Witwatersrand. *Geological Journal*, (61).

Winde, F. 2002. Slimes dams as a source of uranium-contamination of streams – The Koekemoerspruit (Klerksdorp-Goldfield) as a case study. *Conference on environmentally responsible mining in Southern Africa*. Johannesburg: Chamber of Mines of South Africa.

Yibas, B., Pulles, W., Lorentz, S. & Maiyana, B. 2011 Development of water balances for operational and post-closure situations for gold mine residue deposits to be used as input to pollution prediction studies for such facilities. Water Research Commission (WRC). WRC Report no: 1460/1/11. Pretoria, South Africa.

Zheng, C. & Wang, P.P. 1999. MT3DMS, A modular three-dimensional multi-species transport model for simulation of advection, dispersion and chemical reactions of contaminants in groundwater systems (Version 5.3) [Computer program] Available at http://www.hydro.geo.ua.edu/mt3d.

Appendix A: Pump test solutions

- Theis (1935). The Theis solution was specifically developed for the determination of storativity and transmissivity for confined aquifers during a transient drawdown measurement of head using a pump. Assumptions that are made used when unsteady state conditions are accepted are:
    - Water removed from storage is discharged instantaneously with the decline in head
    - The diameter of the borehole is so small that storage in the borehole itself can be ignored.

  This method takes into account, a two-dimensional radial flow to a borehole from an infinite homogeneous aquifer source. The Theis solution is referred to as a curve fit method where the measured pumping data is plotted on a log-log axis and matched to the Theis curve as illustrated in Figure 70. This curve is expressed as:

$$s = \frac{Q}{4\pi T} W(u)$$

$$u = \frac{r^2 S}{4Tt}$$

  Where:

  S = Drawdown

  Q = Pumping rate

  T = Transmissivity

  t = Time

  W(u) = Well function

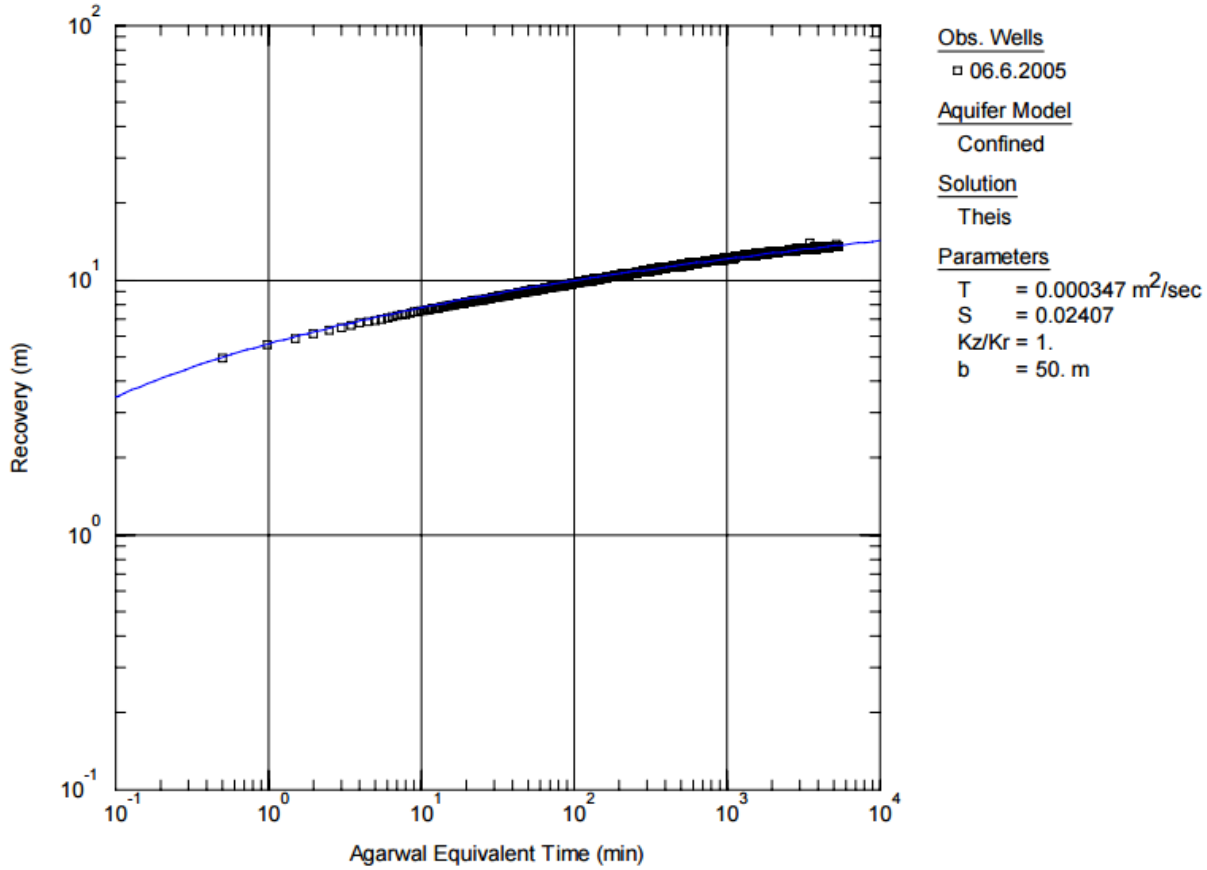

Figure 70: Tramsmissivity determined by means of the Theis recovery method (1935) (Rosberg, 2010)

- Cooper & Jacob (1946). The Cooper & Jacob method or straight line Time-Drawdown method is an approximation based on the Theis method and is applicable when the *u* < 0.05. A semi-log graph is used to plot the field drawdown data (linear scale) against time (log scale). The data is then joined using a straight line that is projected back through zero. The time where the straight line intercepts zero is marked t_0 The value for drawdown per log cycle is obtained by the slope of the graph $\Delta(h_0\text{-}h)$ (See Figure 71). The values for transmissivity and storativity is then calculated using the following equations (Zhang, no date):

$$T = \frac{2.3Q}{4\pi\Delta(h_0 - h)}$$

$$S = \frac{2.25\,Tt_0}{r^2}$$

Where:

T = Transmissivity

S = Storativity

t = Time

r = Radial distance to the pumping borehole

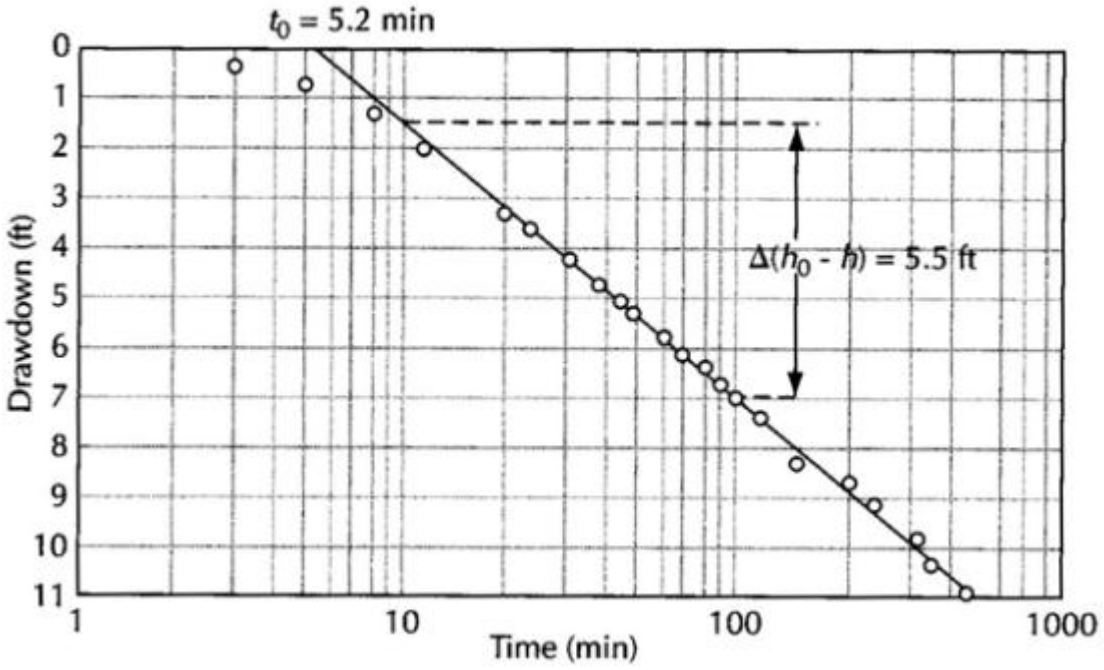

Figure 71: Cooper-Jacob straight line time-drawdown method (Zhang, no date)

- Hantush & Jacob (1955). Reffered to as the Hantush – Jacob (1955) solution this methodology is another time drawdown curve-fitting technique. This method however is applicable to a leaky aquifer system. The aquifer system described by this solution is composed of an isotropic, homogeneous, porous medium that is infinite in areal extent. However, as this equation deals with a leaky aquifer the following assumptions are applicable:
    - Flow to the control borehole is horizontal if it fully penetrates the aquifer
    - The aquifer is leaky confined
    - The aquitards have infinite areal extent
    - Flow in the aquitard is vertical and storage within them are negligible
    - Water that is released from storage results in an instant decline of head

  The aquifer system described by this solution is illustrated in Figure 72.

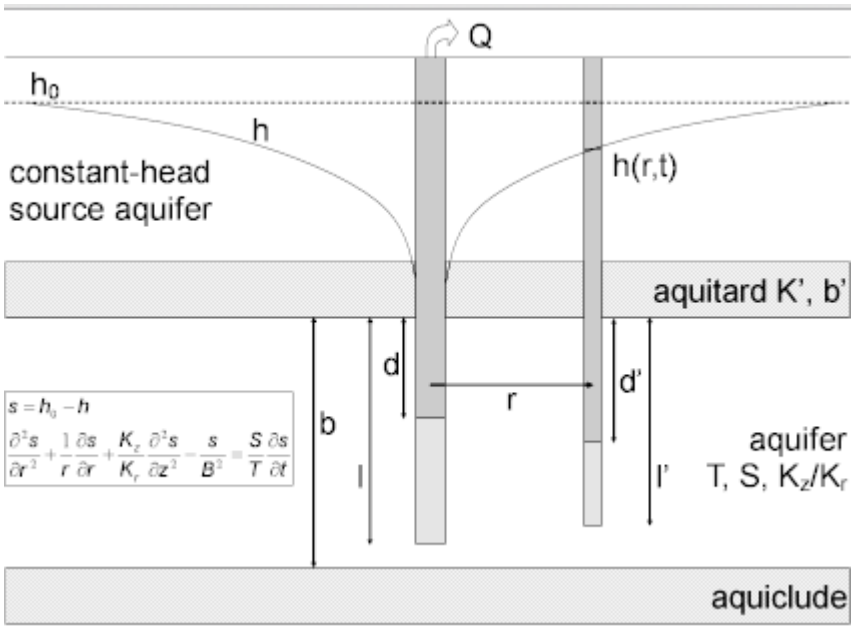

Figure 72: Leaky confined aquifer described by Hantush & Jacob, 1955 (AQTESOLV, 1998)

The Hantush – Jacob (1955) equation can be expressed as:

$$s = \frac{Q}{4\pi T} w(\frac{u, r}{B})$$

Where:

S = Drawdown

Q = Discharge

T = Transmissivity

r = Radial distance from the pumping borehole to the observation borehole

$B = \sqrt{\frac{T_{b'}}{K'}}$

K' = Vertical hydraulic conductivity

b' = Aquitard thickness

The equation is used to describe a theoretical straight head drawdown curve that is used to best fit the plotted observation data as illustrated in Figure 73.

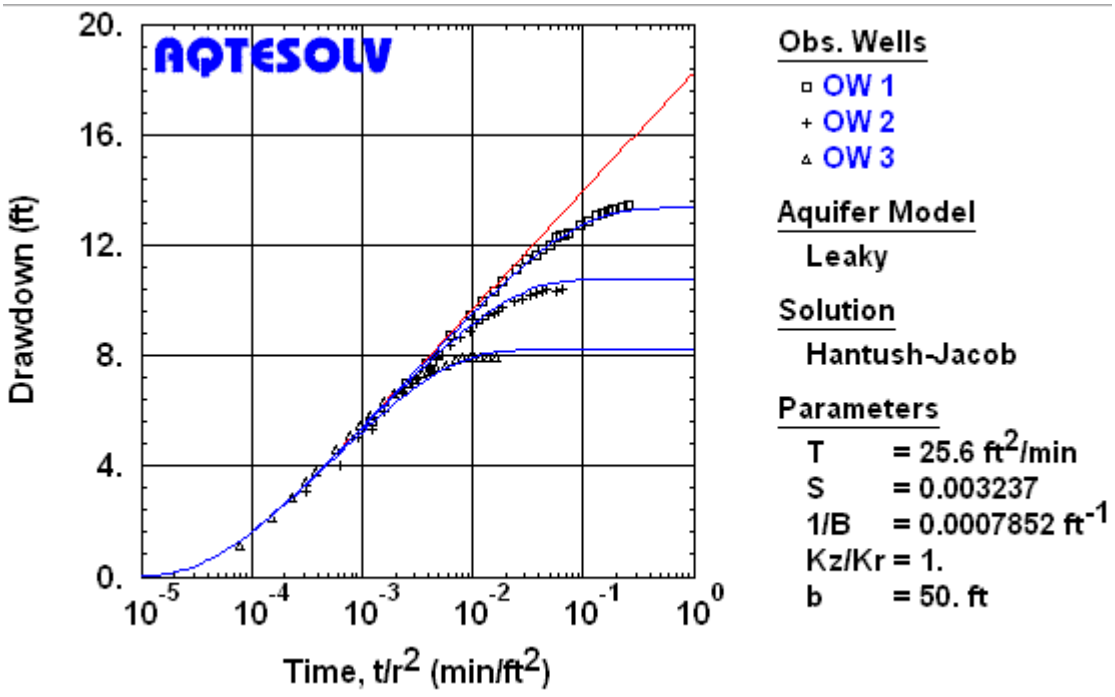

Figure 73: Example of the Hantush - Jacob (1955) drawdown curve fit (AQTESOLV, 1998).

Appendix B: Grading curves

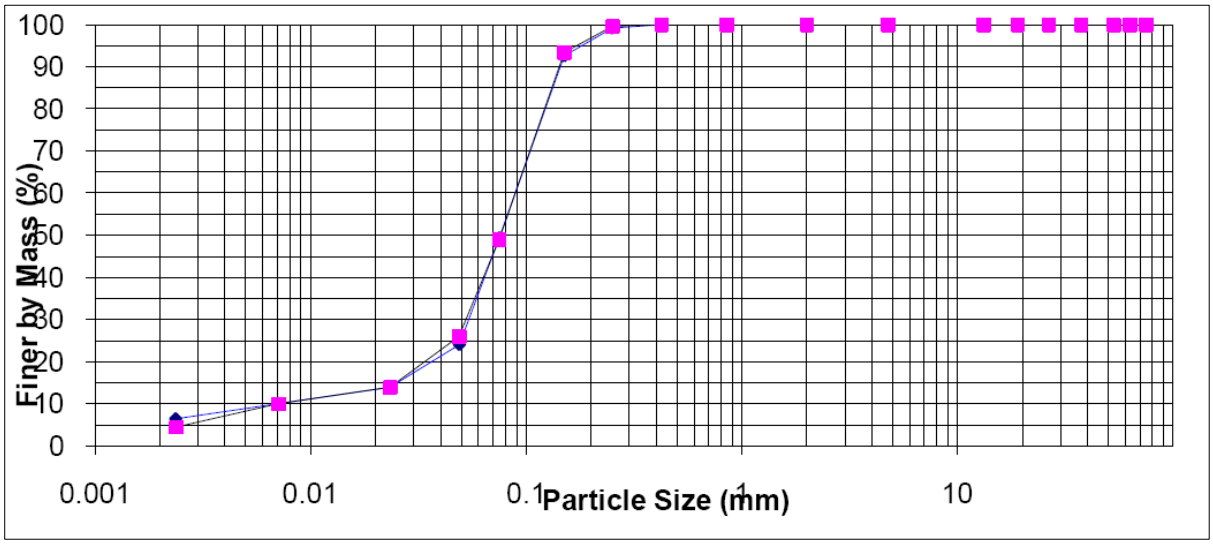

Figure 74: Grading curves for Underflow material

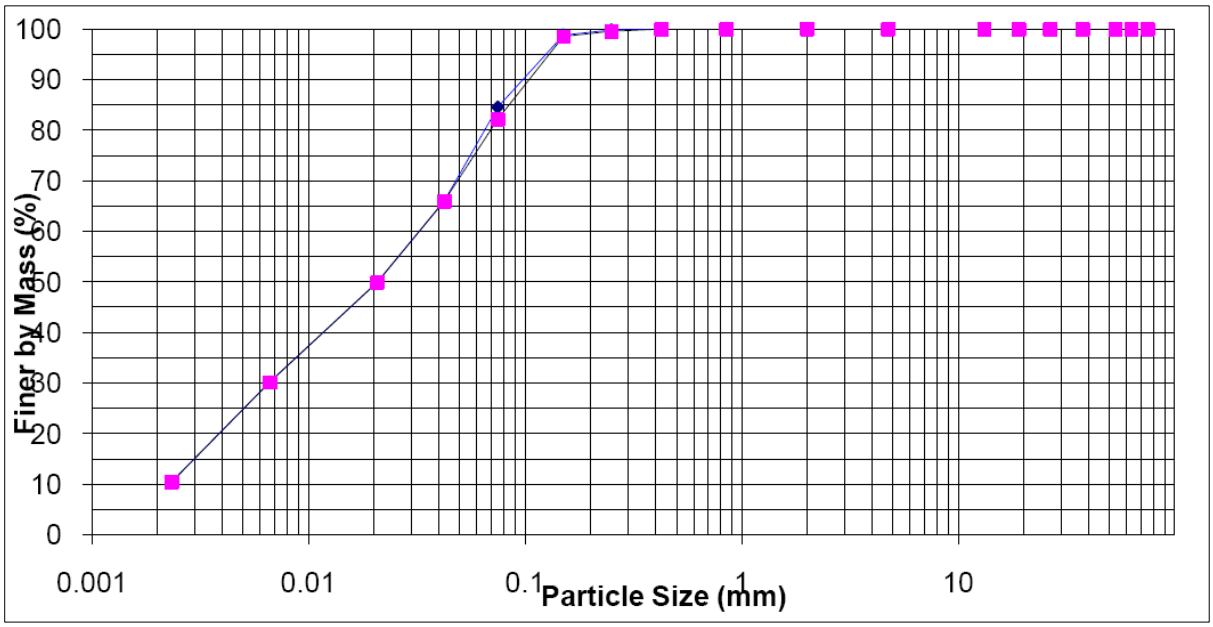

Figure 75: Grading curve for Overflow material

Appendix C: Analyses of borehole tests

Slug Test | Main | KR1

H0 (m)=	0.2	r_w(m) =	0.106	d(m) =	50	d/rw =	471.7	C =	9.9045253	ln(Re/rw)=	5.077401
		b (m) =	55	K (m/d)=	0.083						

t(s)	h(m)
0	0.2
5	0.198
10	0.194
15	0.19
20	0.187
25	0.184
30	0.179
35	0.172
40	0.165
45	0.163
50	0.159
55	0.153
60	0.149
65	0.145
70	0.141
75	0.137
80	0.135
90	0.129
100	0.122
120	0.117
140	0.11
160	0.104
180	0.101
200	0.097
240	0.092
280	0.086
500	0.08

x0	0
x1	500
y0	0.2
y1	0.086

1/t*ln(h0/ht)= 145.8380281

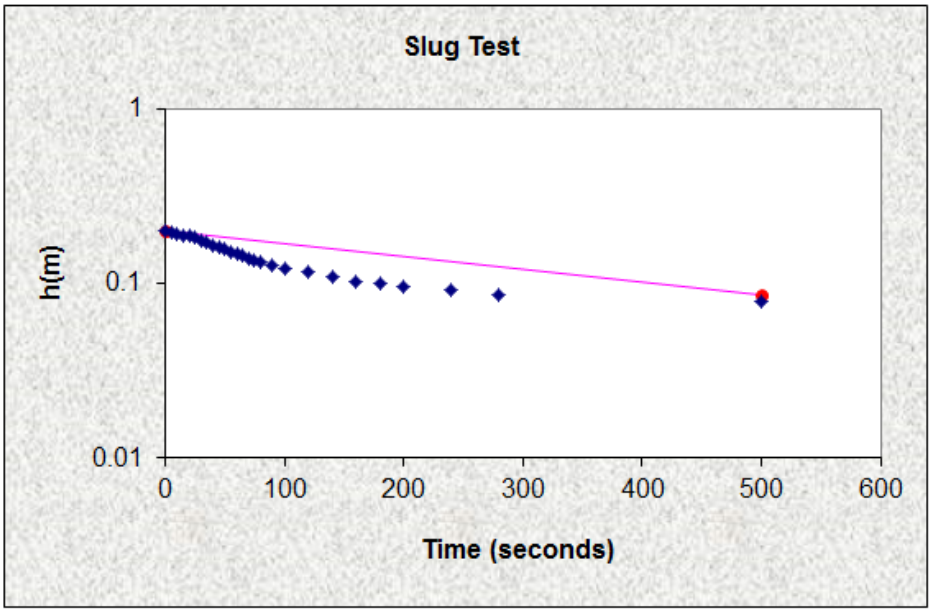

Figure 76: Slug test for KR1

Slug Test | Main | KR2

H0 (m)=	0.1	r_w(m) =	0.106	d(m) =	80	d/rw =	754.72	C =	10.830478	ln(Re/rw)=	5.505107
t(s)	h(m)	b (m) =	76	K (m/d)=	0.164						
0	0.07										
5	0.12										
15	0.105										
30	0.1										
45	0.085										
60	0.08										
75	0.065										
90	0.06										
105	0.05										
120	0.045										
135	0.04										
150	0.039										
180	0.036										
210	0.031										
240	0.028										
270	0.026										
300	0.021										
330	0.018										
360	0.016										
390	0.013										
420	0.01										
450	0.009										
480	0.008										
500	0.007										
550	0.0065										

x0 0
x1 540
y0 0.1
y1 0.007

1/t*ln(h0/ht)= 425.4816059

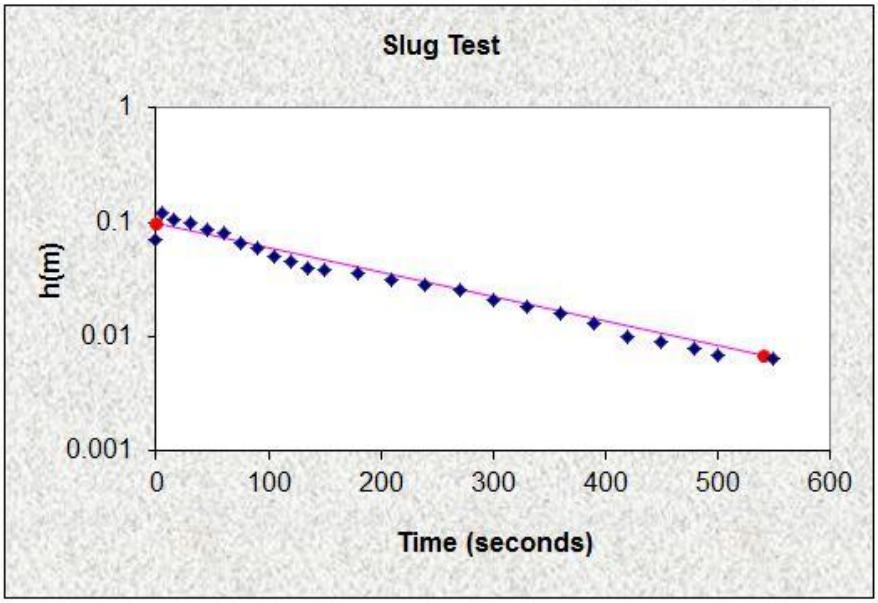

Figure 77: Slug test for KR2

Slug Test | Main | KR3

H0 (m)=	0.083	r_w(m) =	0.106	d(m) =	37	d/rw =	349.06	C =	8.5082633	ln(Re/rw)=	4.78442
		b (m) =	40.99			K (m/d)=	0.117				

t(s)	h(m)
0	0.083
15	0.08
30	0.078
45	0.075
60	0.07
75	0.068
90	0.065
105	0.064
120	0.061
135	0.06
150	0.058
165	0.056
180	0.055
240	0.049
300	0.043
360	0.039
420	0.036
480	0.032
540	0.029
600	0.025
720	0.022
840	0.019
960	0.016
1080	0.014
1200	0.012
1320	0.01

x0	0
x1	850
y0	0.083
y1	0.017

1/t*ln(h0/ht)= 161.1743477

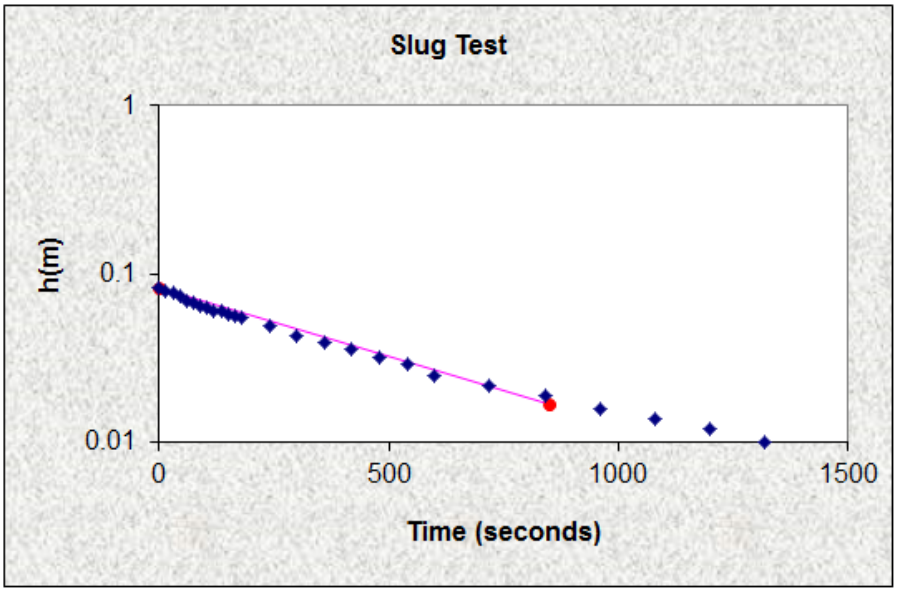

Figure 78: Slug test for KR3

Appendix D: Results of water budget calculation

```
PMWBLF (SUBREGIONAL WATER BUDGET) RUN RECORD
FLOWS ARE CONSIDERED "IN" IF THEY ARE ENTERING A SUBREGION
THE UNIT OF THE FLOWS IS [L^3/T]

TIME STEP    1 OF STRESS PERIOD    1

============================================================
 WATER BUDGET OF ZONES WITHIN EACH INDIVIDUAL LAYER
============================================================

 ZONE    1   IN LAYER    1
------------------------------------------------
        FLOW TERM                IN                OUT            IN-OUT
          STORAGE   0.0000000E+00   0.0000000E+00   0.0000000E+00
    CONSTANT HEAD   7.6959664E-03   1.4444791E-01  -1.3675193E-01
  HORIZ. EXCHANGE   1.4696145E-01   1.0264229E-02   1.3669722E-01
EXCHANGE (UPPER)    0.0000000E+00   0.0000000E+00   0.0000000E+00
EXCHANGE (LOWER)    0.0000000E+00   0.0000000E+00   0.0000000E+00
           WELLS    0.0000000E+00   0.0000000E+00   0.0000000E+00
          DRAINS    0.0000000E+00   0.0000000E+00   0.0000000E+00
        RECHARGE   5.4900014E-05   0.0000000E+00   5.4900014E-05
              ET    0.0000000E+00   0.0000000E+00   0.0000000E+00
    RIVER LEAKAGE   0.0000000E+00   0.0000000E+00   0.0000000E+00
  HEAD DEP BOUNDS   0.0000000E+00   0.0000000E+00   0.0000000E+00
   STREAM LEAKAGE   0.0000000E+00   0.0000000E+00   0.0000000E+00
INTERBED STORAGE    0.0000000E+00   0.0000000E+00   0.0000000E+00
MULTI-AQIFR WELL    0.0000000E+00   0.0000000E+00   0.0000000E+00
SUM OF THE LAYER    1.5471232E-01   1.5471214E-01   1.7881393E-07
  DISCREPANCY [%]   0.00

------------------------------------------------------------

============================================================
WATER BUDGET OF ZONES OVER THE ENTIRE MODEL
============================================================

ZONE: 1
------------------------------------------------
                         IN                OUT            IN-OUT
          STORAGE   0.0000000E+00   0.0000000E+00   0.0000000E+00
    CONSTANT HEAD   7.6959664E-03   1.4444791E-01  -1.3675193E-01
  HORIZ. EXCHANGE   1.4696145E-01   1.0264229E-02   1.3669723E-01
EXCHANGE (UPPER)    0.0000000E+00   0.0000000E+00   0.0000000E+00
EXCHANGE (LOWER)    0.0000000E+00   0.0000000E+00   0.0000000E+00
           WELLS    0.0000000E+00   0.0000000E+00   0.0000000E+00
          DRAINS    0.0000000E+00   0.0000000E+00   0.0000000E+00
        RECHARGE   5.4900014E-05   0.0000000E+00   5.4900014E-05
              ET    0.0000000E+00   0.0000000E+00   0.0000000E+00
    RIVER LEAKAGE   0.0000000E+00   0.0000000E+00   0.0000000E+00
  HEAD DEP BOUNDS   0.0000000E+00   0.0000000E+00   0.0000000E+00
   STREAM LEAKAGE   0.0000000E+00   0.0000000E+00   0.0000000E+00
INTERBED STORAGE    0.0000000E+00   0.0000000E+00   0.0000000E+00
MULTI-AQIFR WELL    0.0000000E+00   0.0000000E+00   0.0000000E+00
SUM OF ZONE(   1)   1.5471232E-01   1.5471214E-01   1.7881393E-07
  DISCREPANCY [%]   0.00


============================================================
WATER BUDGET OF THE WHOLE MODEL DOMAIN:
============================================================

        FLOW TERM                IN                OUT            IN-OUT
          STORAGE   0.0000000E+00   0.0000000E+00   0.0000000E+00
    CONSTANT HEAD   7.6959664E-03   1.4444791E-01  -1.3675193E-01
           WELLS    0.0000000E+00   0.0000000E+00   0.0000000E+00
          DRAINS    0.0000000E+00   0.0000000E+00   0.0000000E+00
        RECHARGE   1.3680552E-01   0.0000000E+00   1.3680552E-01
              ET    0.0000000E+00   0.0000000E+00   0.0000000E+00
    RIVER LEAKAGE   0.0000000E+00   0.0000000E+00   0.0000000E+00
  HEAD DEP BOUNDS   0.0000000E+00   0.0000000E+00   0.0000000E+00
   STREAM LEAKAGE   0.0000000E+00   0.0000000E+00   0.0000000E+00
INTERBED STORAGE    0.0000000E+00   0.0000000E+00   0.0000000E+00
MULTI-AQIFR WELL    0.0000000E+00   0.0000000E+00   0.0000000E+00
------------------------------------------------------------
              SUM   1.4450149E-01   1.4444791E-01   5.3584576E-05
  DISCREPANCY [%]   0.04
```

Appendix E: Modelling results

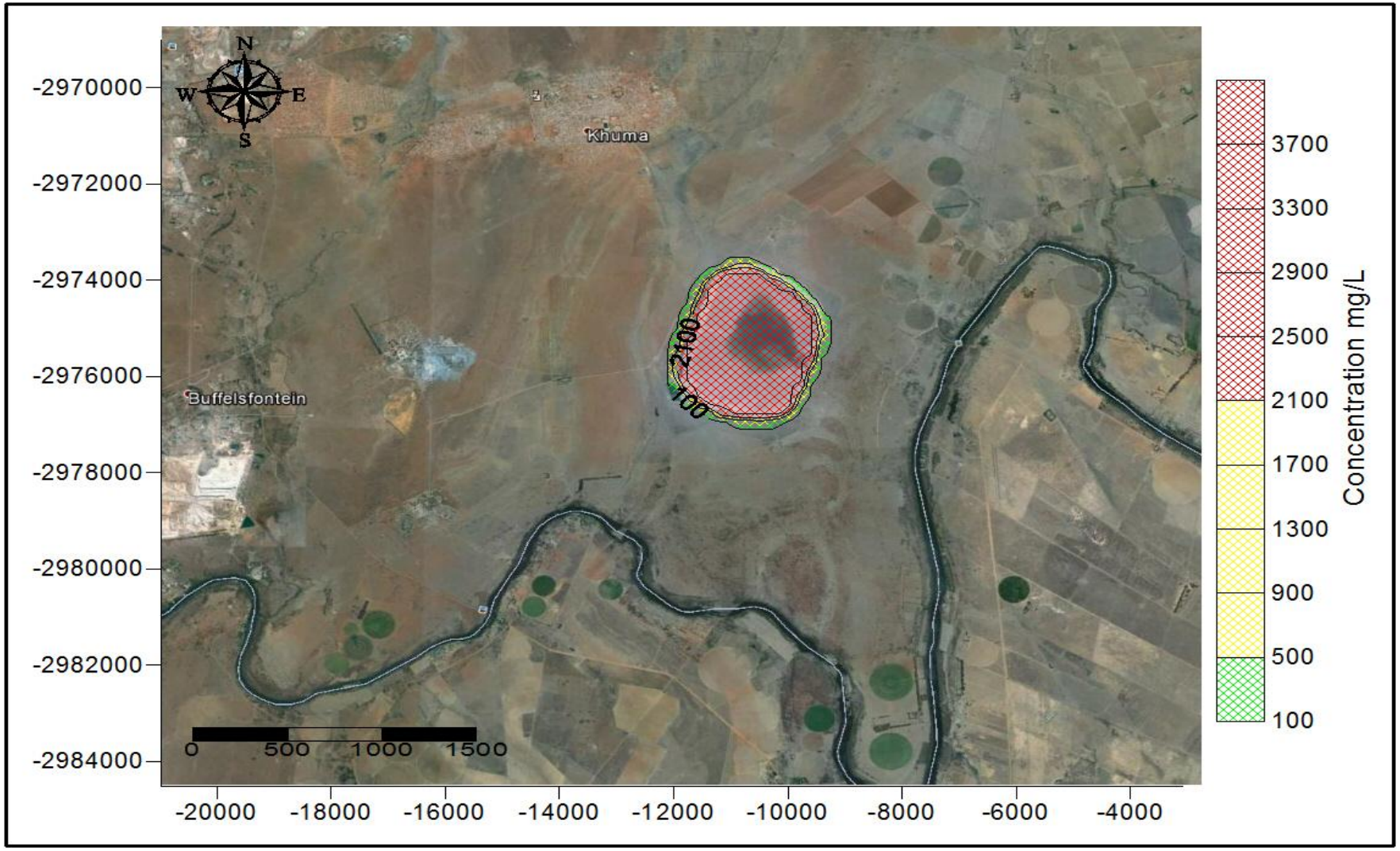

Figure 79: Modelled SO_4 plume at 18 months

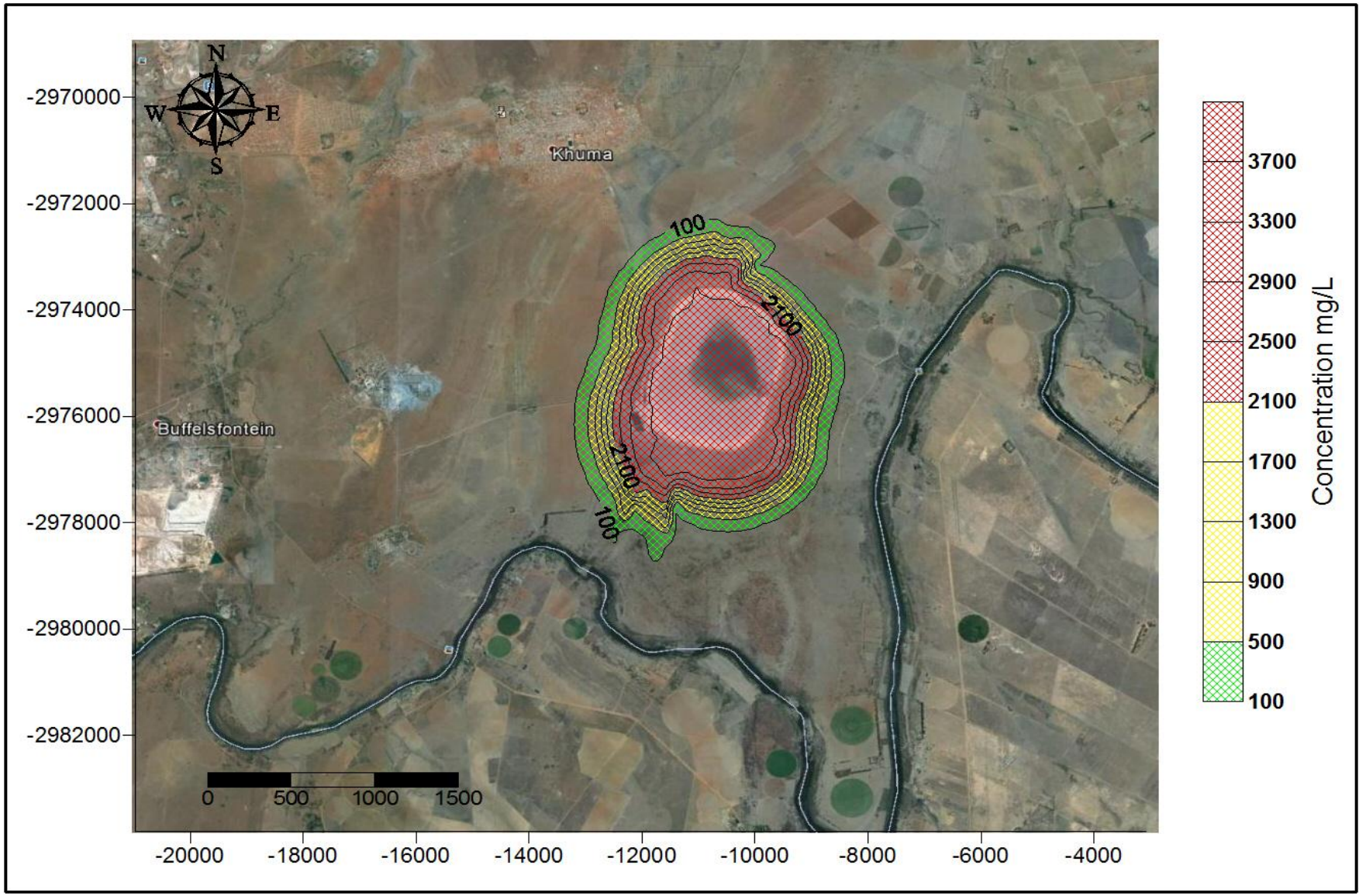

Figure 80: Modelled SO_4 plume at 168 months

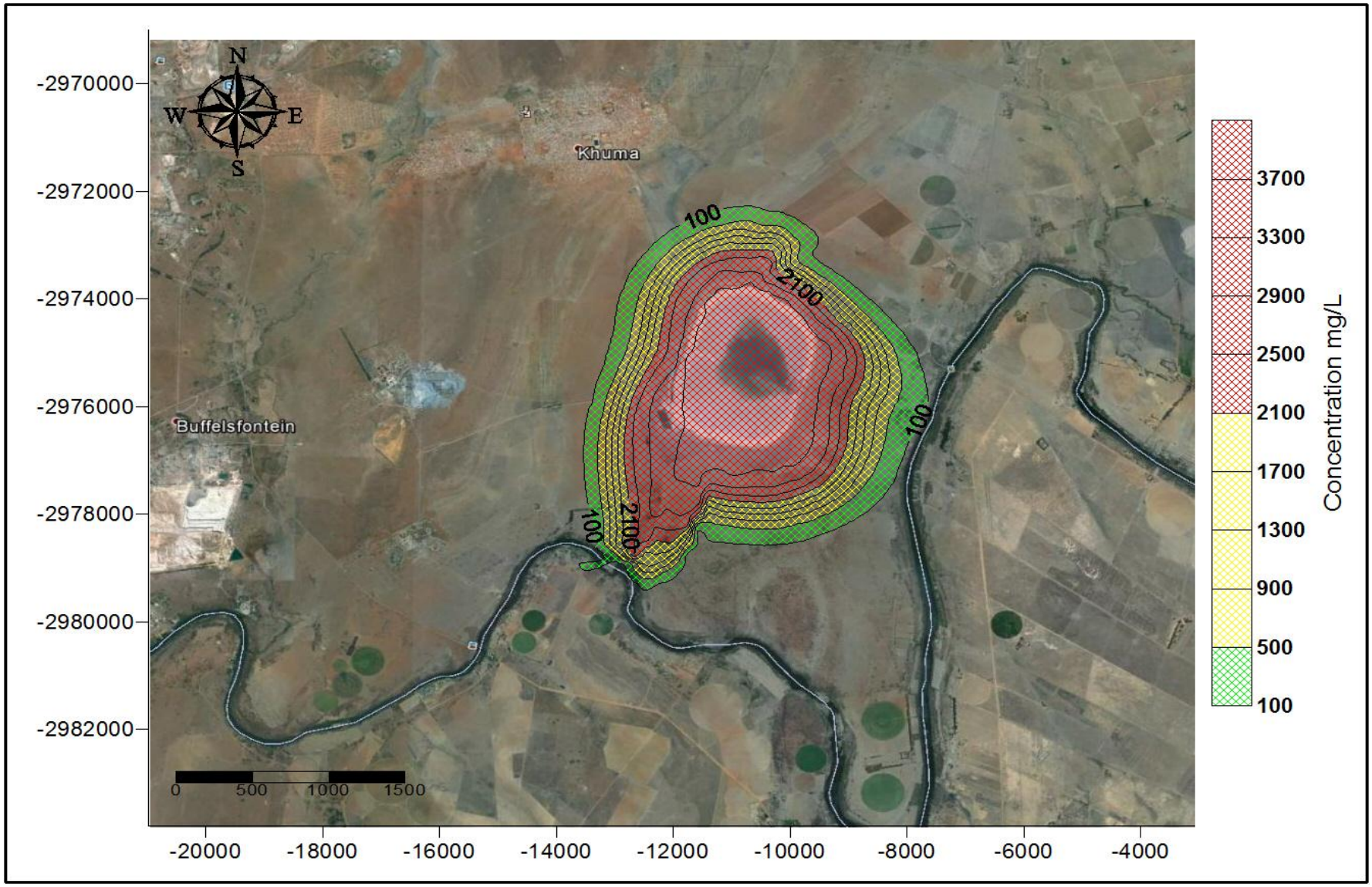

Figure 81: Modelled SO_4 plume at 1200 months

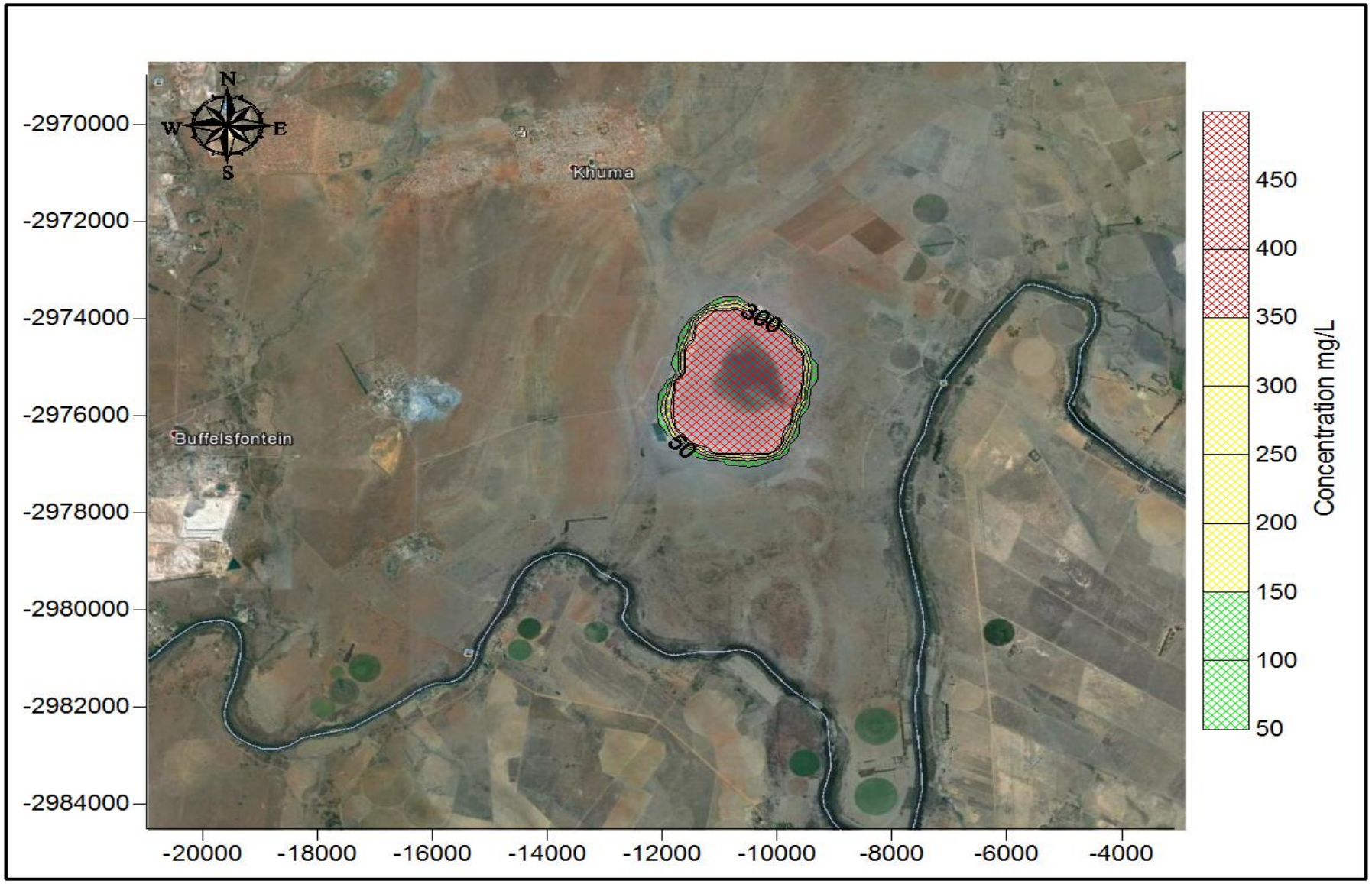

Figure 82: Modelled Cl plume at 18 months

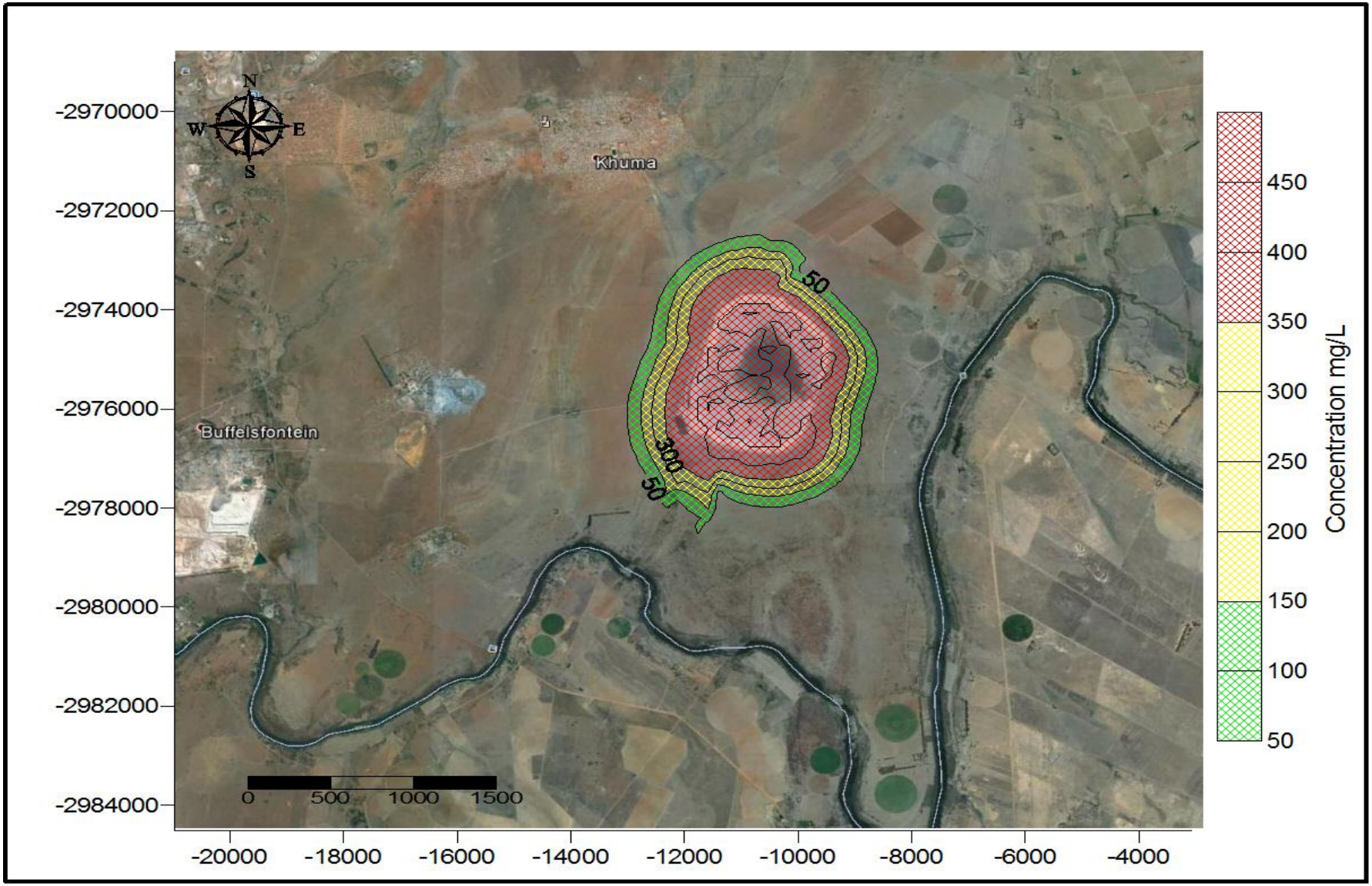

Figure 83: Modelled Cl plume at 168 months

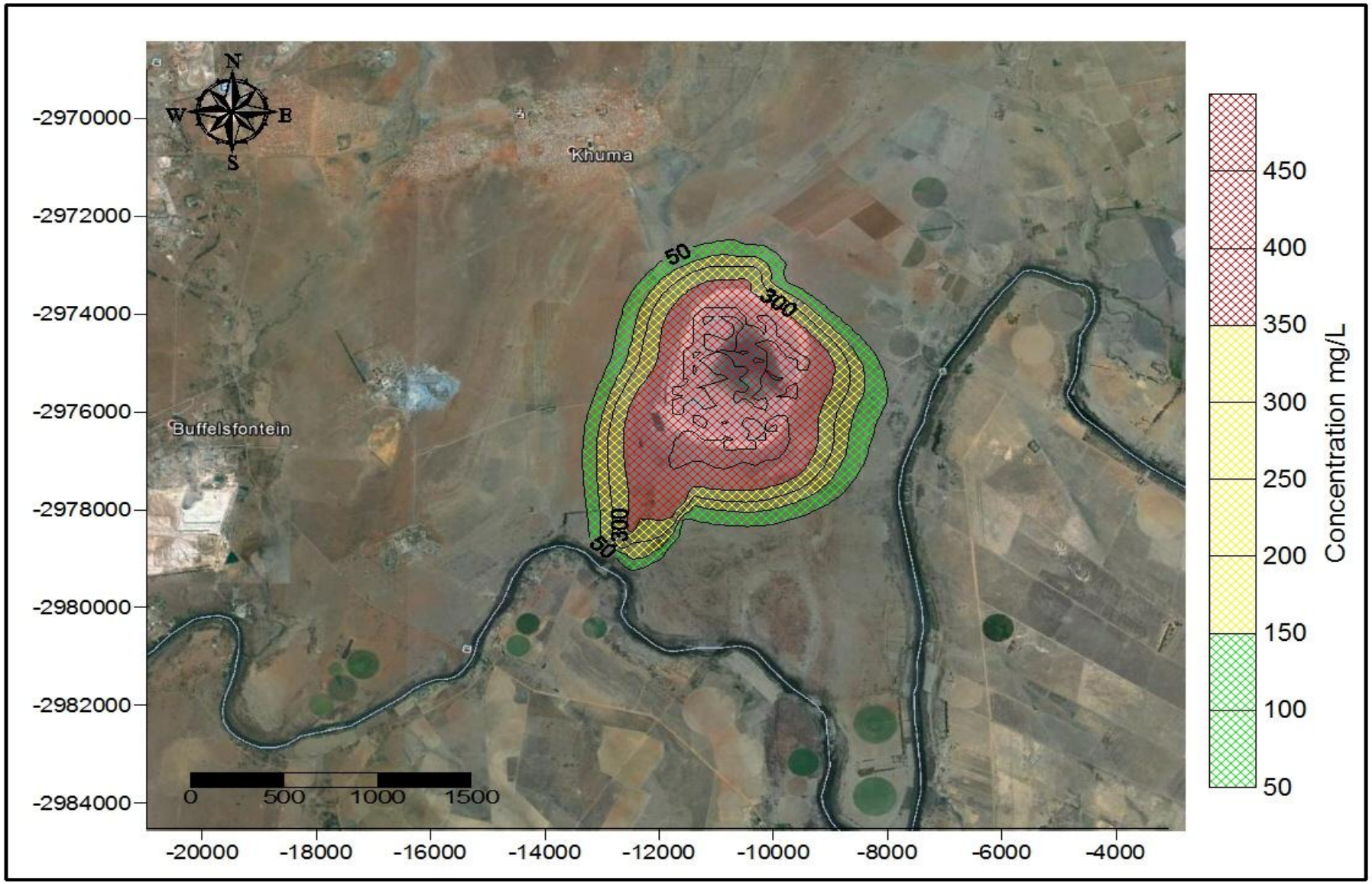

Figure 84: Modelled Cl plume at 1200 months

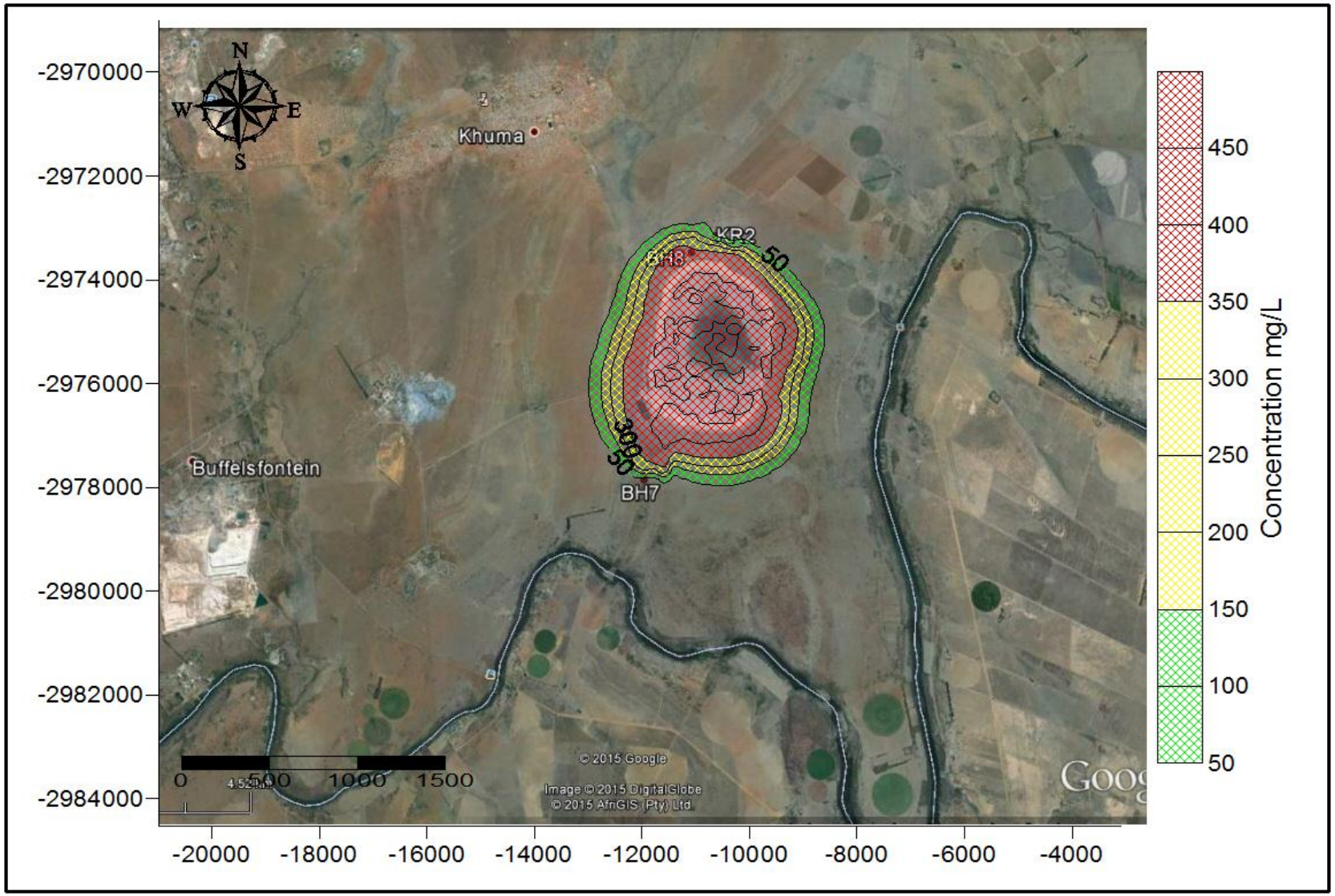

Figure 85: Modelled Cl plume at abstraction of 0.1 l/s (168 months)

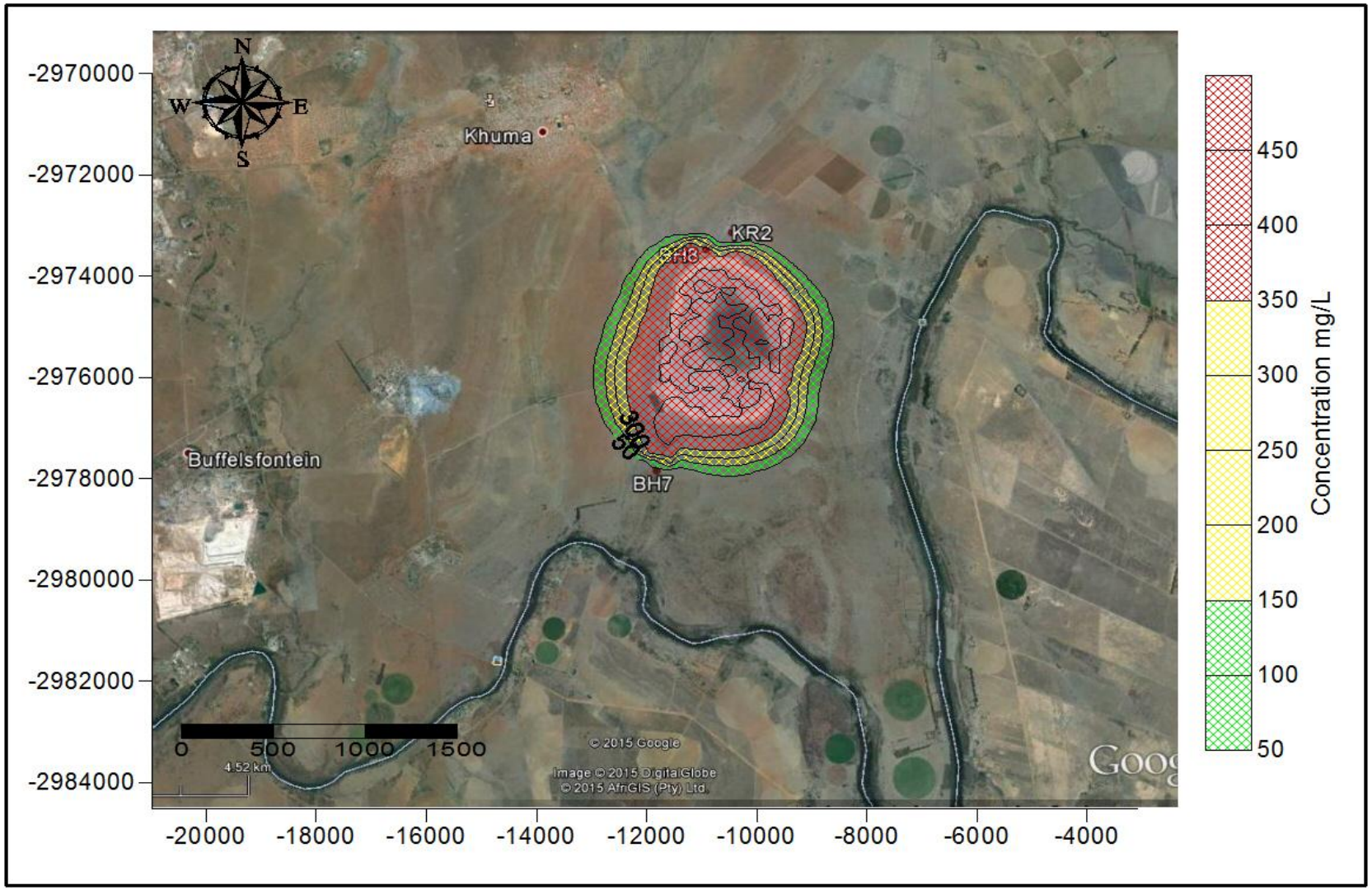

Figure 86: Modelled Cl plume at abstraction rate of 0.2 l/s (168 months)

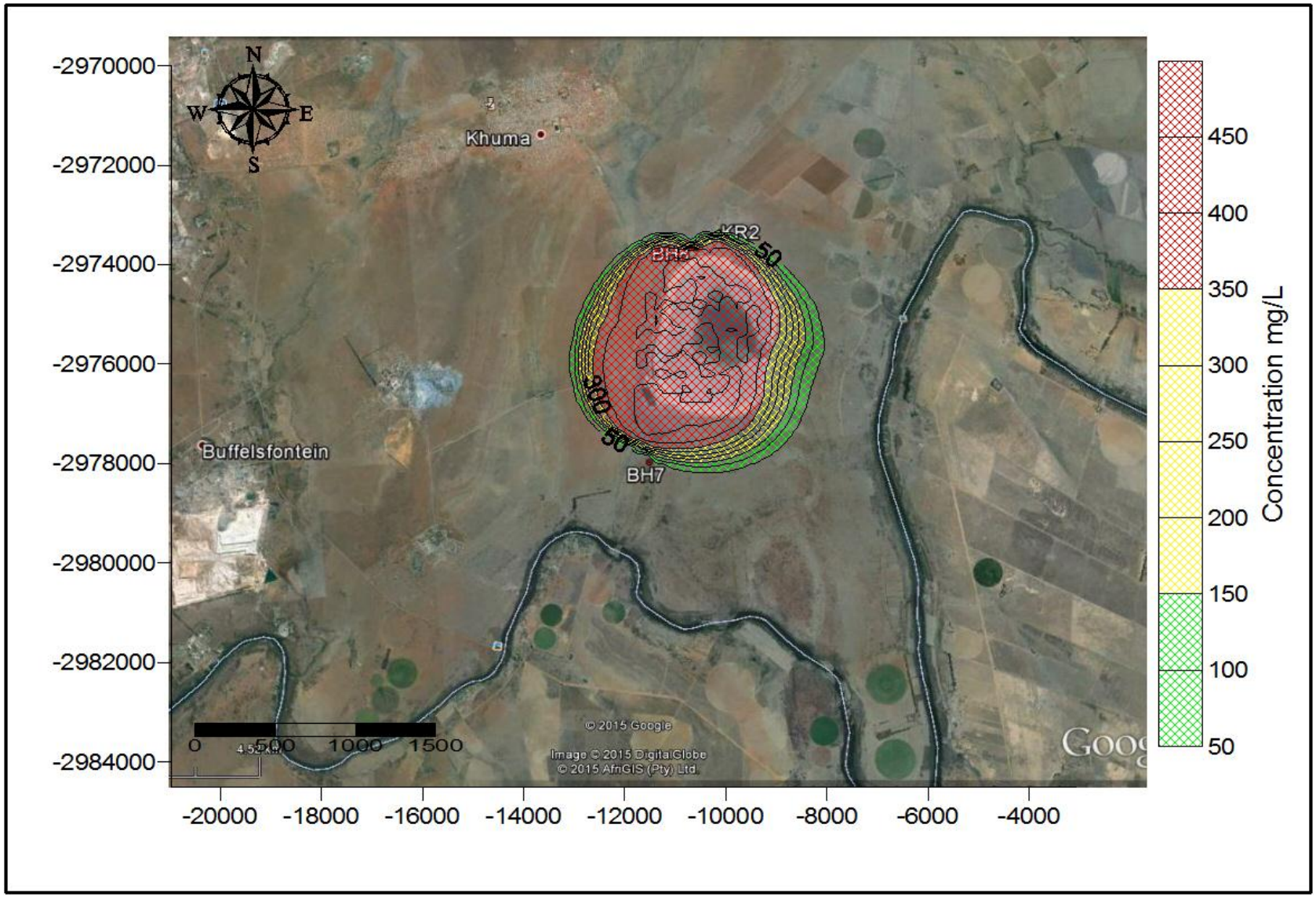

Figure 87: Modelled Cl plume at abstraction of 0.1 l/s (1200 months)

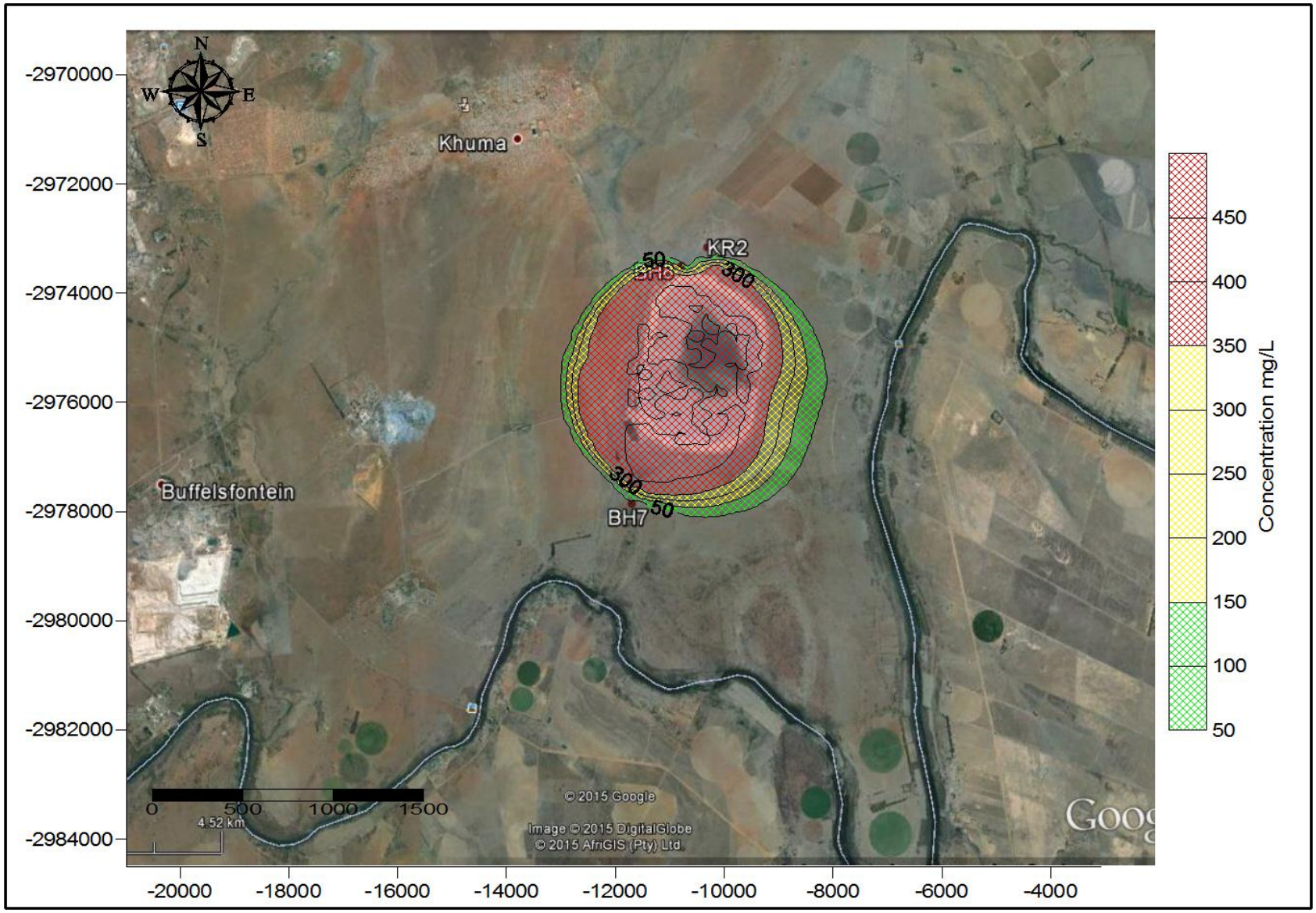

Figure 88: Modelled Cl plume at abstraction of 0.2 l/s (1200 months)

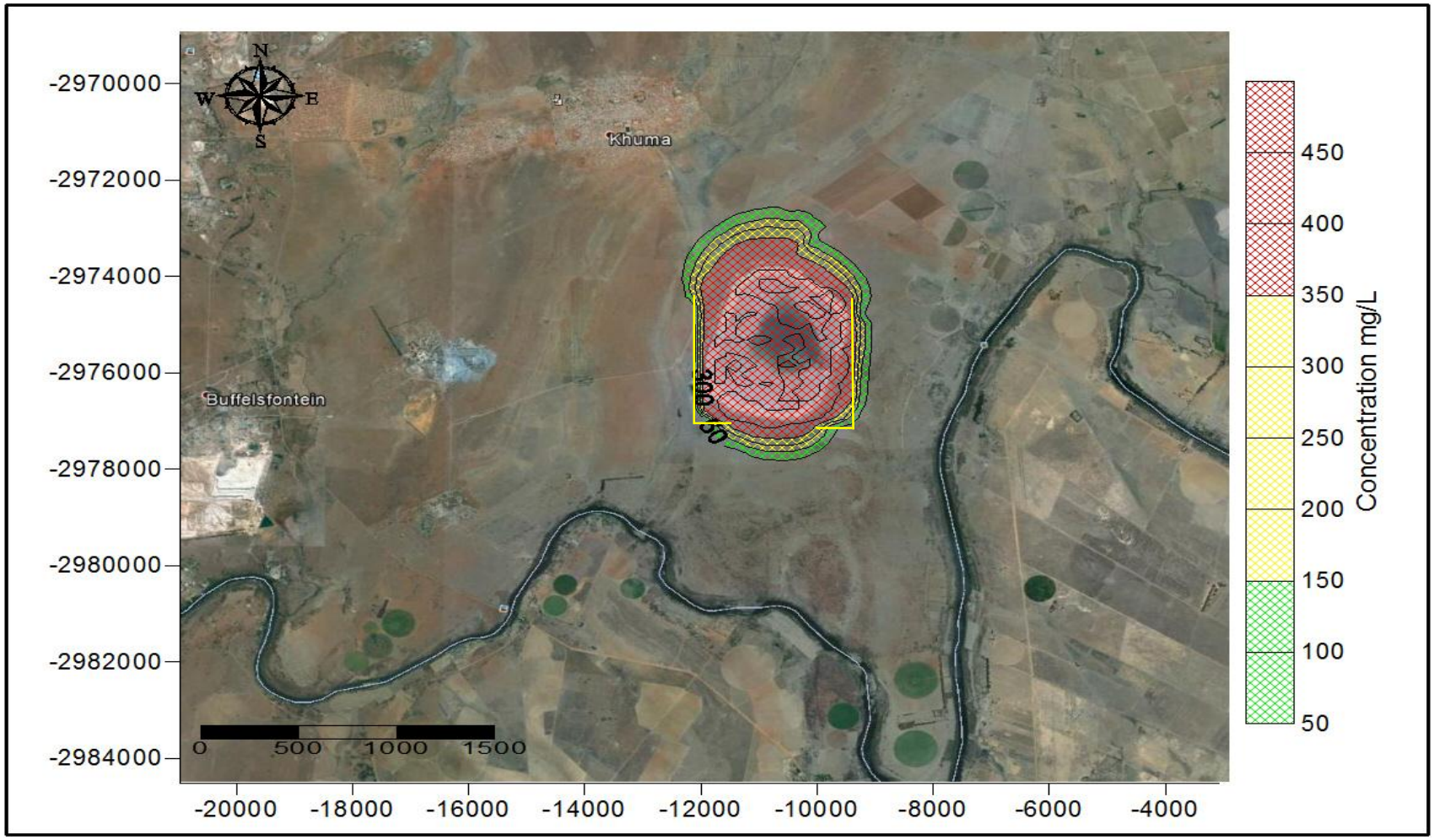

Figure 89: Modelled Cl plume with trench drain installed (168 months)

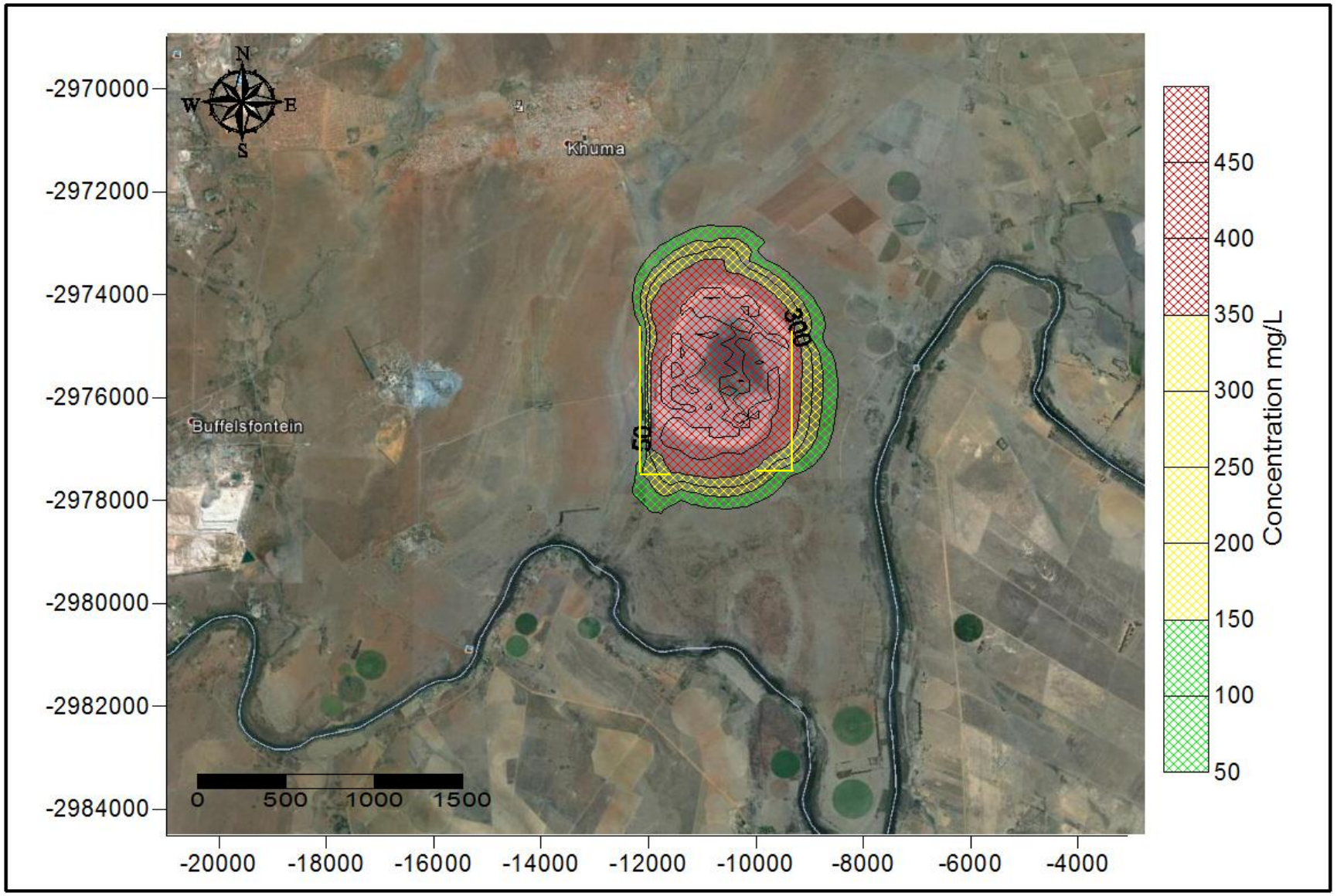

Figure 90: Modelled Cl plume with trench drain installed (1200 months)

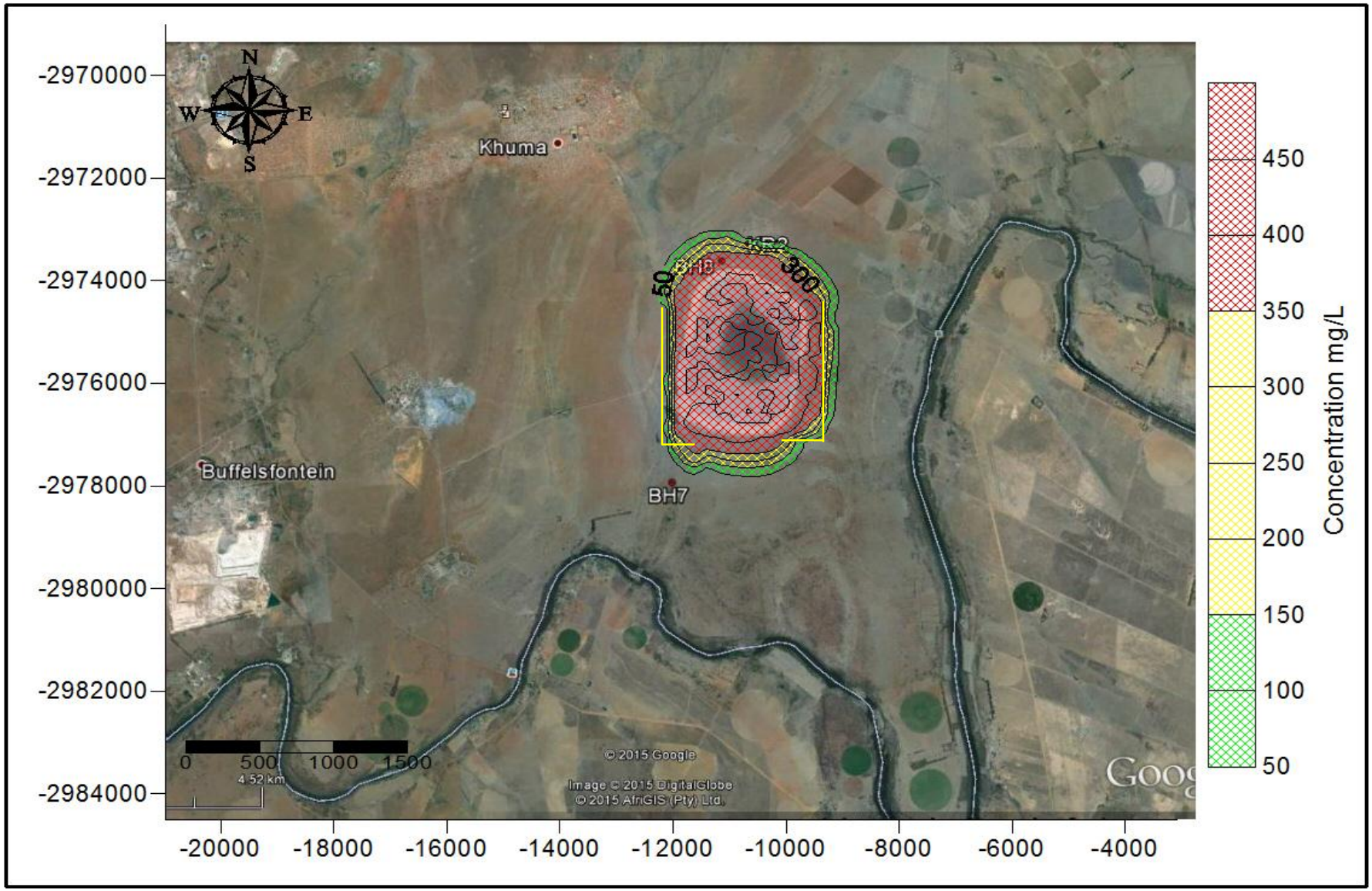

Figure 91: Modelled Cl plume at 168 months with combination of abstraction and trench drain

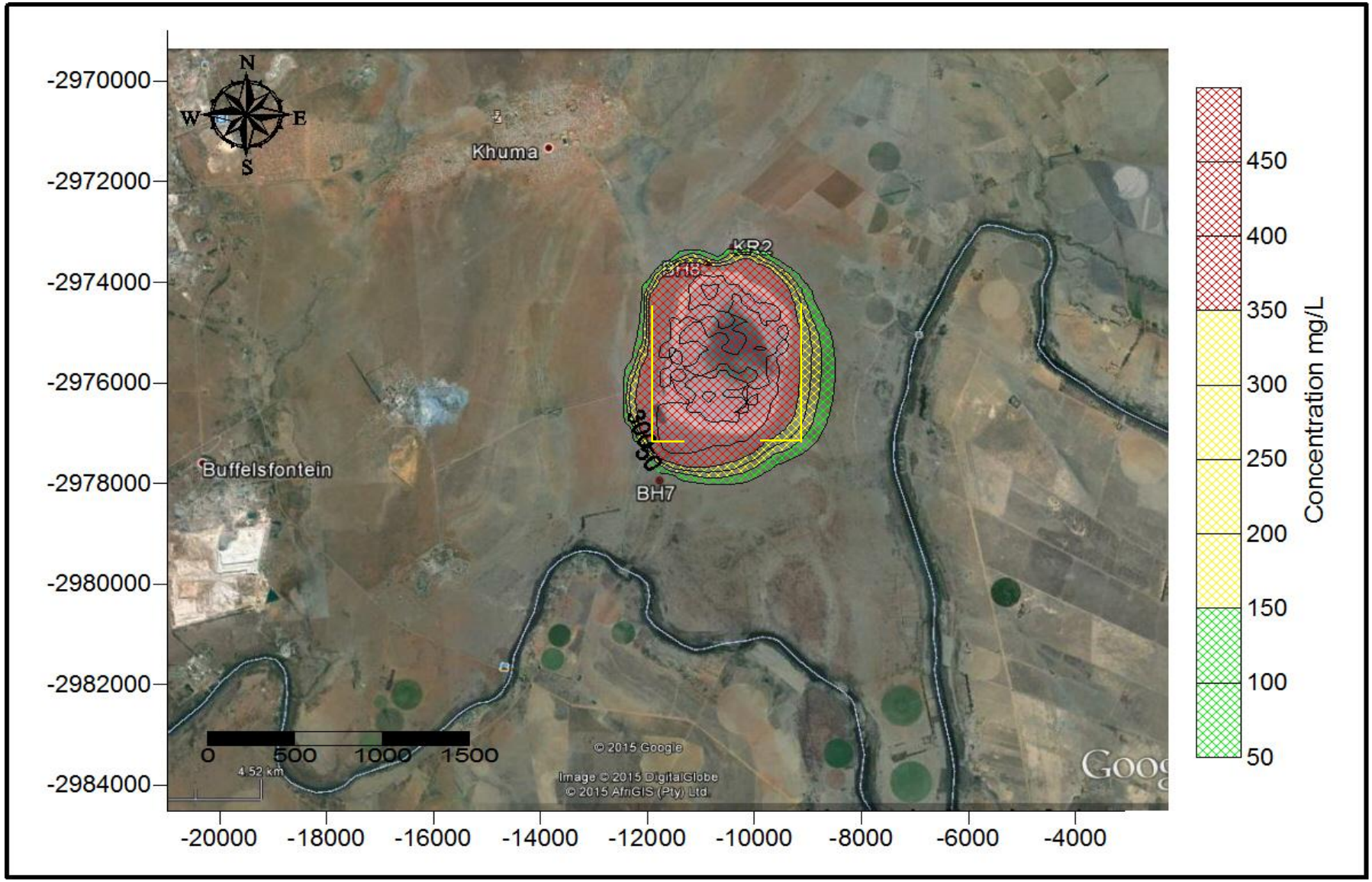

Figure 92: Modelled Cl plume at 1200 months with combination of abstraction and trench drain